Technical Report Documentation Page

1. Report No.	2. Government Accession No.	3. Recipient's Catalog No.
FHWA/VA-91-R22		

4. Title and Subtitle	5. Report Date
A Geophysical System Combining Electrical Resistivity and Spontaneous Potential for Detecting Delineating and Monitoring Slope Stability	June 1991
	6. Performing Organization Code: 2671-059-940
7. Author(s): Ronald A. Erchul & David F. Noble	8. Performing Organization Report No.: VTRC 91-R22
9. Performing Organization Name and Address: Virginia Transportation Research Council, P. O. Box 3817, University Station, Charlottesville, Virginia 22903	10. Work Unit No. (TRAIS)
	11. Contract or Grant No.
12. Sponsoring Agency Name and Address: Virginia Department of Transportation, 1221 E. Broad Street, Richmond, Virginia 23219	13. Type of Report and Period Covered: FINAL REPORT, March 1988 - January 1991
	14. Sponsoring Agency Code

15. Supplementary Notes

In Cooperation with the U.S. Department of Transportation
Federal Highway Administration

16. Abstract

Various geophysical electrical measuring techniques, i.e., spontaneous potential (SP), terrain conductivity meter (TCM), and conventional electrical resistivity/conductivity (ER), were tested to determine their effectiveness in detecting, delineating, and monitoring weak zones and layers along three slopes in western Virginia. In addition, the SP technique in conjunction with an automatic measuring system (AMS) were used to monitor two slopes in real time in order to determine their stability with regard to environmental factors, such as heavy precipitation. Novel techniques were employed to determine electrical properties. In addition to the AMS, a unique resistivity/conductivity sensor was fabricated, tested, and deployed with the use of a small penetrometer. The special sensor cone penetrometer system was able to obtain depth profiles of conductivity and soil strength on steep slopes where conventional penetrometers would be unsafe to operate. The data collected by these various electrical measuring techniques were then compared with each other as well as with environmental and geotechnical data collected as part of this study and in previous investigations.

17. Key Words	18. Distribution Statement
Monitoring slopes, spontaneous potential, terrain conductivity, electrical resistivity, automatic measuring system, portable cone penetrometer	No restrictions. This document is available to the public through the National Technical Information Service, Springfield, Va. 22161

19. Security Classif. (of this report)	20. Security Classif. (of this page)	21. No. of Pages	22. Price
Unclassified	Unclassified		

FINAL REPORT

A GEOPHYSICAL SYSTEM COMBINING ELECTRICAL RESISTIVITY AND SPONTANEOUS POTENTIAL FOR DETECTING, DELINEATING, AND MONITORING SLOPE STABILITY

Ronald A. Erchul
Professor
Department of Civil Engineering
Virginia Military Institute

David F. Noble
Research Scientist

(The opinions, findings, and conclusions expressed in this report are those of the author and not necessarily those of the sponsoring agencies.)

Virginia Transportation Research Council
(A Cooperative Organization Sponsored Jointly by the Virginia Department of Transportation and the University of Virginia)

In Cooperation with the U.S. Department of Transportation
Federal Highway Administration

Charlottesville, Virginia

June 1991
VTRC 91-R22

1856

ACKNOWLEDGMENTS

The work described herein was performed during the period April 1988 through June 1990 by Ronald A. Erchul of the Department of Civil Engineering, Virginia Military Institute (VMI), and David F. Noble, Research Scientist, of the Virginia Transportation Research Council. Assisting these investigators during the summer of 1989 was Jose Gomez of the Department of Civil Engineering, VMI, who helped install the Automatic Measuring System at Site III.

Throughout this investigation period, cadet assistants (Bruce English, John Gillespie, Raymond Marsh, and Terry Plunk) were involved in conducting data analysis and field testing for extended periods of time. Numerous other cadets assisted in the project for short periods of time taking field data. The VMI technical staff (Joseph Wheeling, James Glass, and Donald Aliff) were helpful in providing continuity, especially in maintenance and operation of test equipment. The investigators greatly appreciate the technical knowledge, professional competence, and assistance of Dave Woolley, Geologist, Lynchburg District, Virginia Department of Transportation, and his staff. With their cooperation, much of the data were taken and historical records and previous technical data provided. Also to be thanked is Edward Dinwiddie, who faithfully provided meteorological data for Sites I and II.

1858

TABLE OF CONTENTS

1860

ABSTRACT

Various geophysical electrical measuring techniques, i.e., spontaneous potential (SP), terrain conductivity meter (TCM), and conventional electrical resistivity/conductivity (ER), were tested to determine their effectiveness in detecting, delineating, and monitoring weak zones and layers along three slopes in western Virginia. In addition, the SP technique in conjunction with an automatic measuring system (AMS) were used to monitor two slopes in real time in order to determine their stability with regard to environmental factors, such as heavy precipitation. Novel techniques were employed to determine electrical properties. In addition to the AMS, a unique resistivity/conductivity sensor was fabricated, tested, and deployed with the use of a small penetrometer. The special sensor cone penetrometer system was able to obtain depth profiles of conductivity and soil strength on steep slopes where conventional penetrometers would be unsafe to operate. The data collected by these various electrical measuring techniques were then compared with each other as well as with environmental and geotechnical data collected as part of this study and in previous investigations.

The findings of this study could lead to procedures for the following:

1. the detection of preferred subsurface flow paths along a slope and the location of areas of high hydraulic gradients in order to locate horizontal drains better and prevent slope bulge and eventually slope failure

2. the detection and determination of the thickness of weak layers in order to stabilize such layers better and prevent possible slope failures along them

3. the rapid and economical establishment of the depth of bedrock over the slope area, and thus the bedrock surface, to help determine if the area could be a failure plane

4. the monitoring of a slope in real time to establish slope saturation conditions and determine if a slope is in jeopardy of failure in order that warning may be sent and appropriate road closure action taken.

1862

FINAL REPORT

A GEOPHYSICAL SYSTEM COMBINING ELECTRICAL RESISTIVITY AND SPONTANEOUS POTENTIAL FOR DETECTING, DELINEATING, AND MONITORING SLOPE STABILITY

Ronald A. Erchul
Professor
Department of Civil Engineering
Virginia Military Institute

INTRODUCTION

The purpose of this research was to test and evaluate the use of both active (electrical resistivity and terrain conductivity) and passive (spontaneous potential) electrical measuring techniques on selected unconsolidated slopes and determine if these methods would be effective in detecting, delineating, and monitoring the stability of the slopes over time.

The specific objectives of the research were as follows:

- to evaluate the effectiveness of the combined spontaneous potential, electrical resistivity, and terrain conductivity measuring systems for detecting and delineating weak zones associated with slope instability
- to develop and field test instrumentation for assessing vertical, in situ characteristics of weak zones in unconsolidated slopes using a penetrometer fitted with a special resistivity sensor
- to develop and implement a long-term, real-time monitoring system using spontaneous potential electrodes and an automated data collection system to function as an early detection and alarm system at potential slope failure sites.

A variety of instruments and novel measurement systems were tested in order to carry out these objectives, and this report describes the measuring systems, measuring techniques, sites, and results.

Spontaneous Potential (SP) Technique

The flow of fluids through a porous soil on rock generates electrical voltages (potentials) through a process known as electrokinesis. These potentials are called spontaneous, streaming, or self potentials by various writers. The SP technique is a passive, electrical measuring technique in that only naturally induced currents and potentials are measured. The magnitude of the SP depends on the electrical resistivity (ER), dielectric constant, and viscosity of the fluid; a coupling constant between the fluid and the soil/rock; and the pressure drop, or hydraulic gradient, along the flow path. The SP anomaly caused by the flow can be measured on the surface above the flow path, and this is the basis of the SP method for seepage detection and mapping.

SP techniques have traditionally been used for well logging and mineral prospecting. In recent years, however, they have been applied to a number of novel geotechnical and hydrogeological uses: exploring for geothermal resources (Anderson & Johnson, 1976; Corwin & Hoover, 1978), tracking underground coal fires (Corwin & Hoover, 1978; Rodriguez, 1984), and studying anomalies in SP induced by water diffusion prior to earthquakes (Fitterman, 1978).

The greatest recent use of SP has been for detection of seepage zones in dams, drainage structures, and landslide masses (Bogoslovsky & Ogilvy, 1972; Butler, 1984; Cooper, 1982, 1983; Cooper & Koester, 1984; Corwin, 1984; Koester et al., 1984; Ogilvy et al., 1969). Ernston and Sherer (1986) concluded that the SP technique may become a valuable and standard technique in hydrogeology.

The U.S. Army Corps of Engineer's Waterways Experiment Station (WES) has successfully applied the SP and other geophysical methods to detect, map, and monitor anomalous seepage conditions at water retention and hazardous waste disposal sites throughout the United States. The keystone of this successful method is the SP method, which has been applied using permanent arrays of inexpensive copper-clad steel (CCS) electrodes, cut from common grounding rod stock. Use of the metallic electrodes for SP measurements is contrary to commonly accepted geophysical practice; however, cost, ease of installation and maintenance, and general success considerations seemed to outweigh other factors.

In this study, three slopes in Western Virginia were instrumented to allow SP measurements to be taken. As with the WES, 71 CCS electrodes 2 ft in length and 5/8 inch in diameter were used. Electrodes were placed in an array pattern of rows and columns along each of the slopes. These arrays of spaced electrodes would cover the slope area and in most cases consisted of 6 to 8 electrodes in each row and two to four rows, depending on the size of the slope area to be monitored. The electrodes were driven approximately 18 inches into the soil, and a No. 18 AWG stranded-copper, plastic, Teflon-insulated wire was soldered to the exposed CCS elec-

trode. The wire was then tied to the electrode for an additional mechanical bond. All electrodes were connected to the wire in this manner, and the terminus wire end was marked to designate the specific electrode. Each wire was taken to a central location for ease in data collection. A CCS common ground or reference electrode was also installed in the same manner, some distance away from the electrode array on the study slope. In some instances, 2 reference electrodes were installed.

Initial SP measurements were obtained by using a high-impedance, digital voltmeter. The meter was connected between the wire from the reference electrode and the terminus wire from a specific slope electrode, thus completing the measurement half of the circuit (the earth being the other half), and a measurement was taken. On recording this reading, the investigator would take another wire from another electrode and record the reading. This procedure was repeated until all SP values were measured.

Usually, data were initially collected daily, then biweekly, and then monthly at the three slopes for a period of 3 months. In addition to the manual collection of data with voltmeters, automated measuring systems (AMS) were used at two of the slopes. These systems, in addition to the electrode array, consisted of a battery power source, a portable computer, an analog/digital signal converter interface, and air and ground temperature sensors. The AMS was housed in a weatherproof case and could be left in the field and programmed to gather data at any desired frequency. The metal electrodes were wired directly to the signal inputs of the analog/digital signal converter interface. The AMS was used for two tasks: (1) to monitor the effects of environmental variables on SP over time; and (2) to monitor SP changes resulting from a possible slope failure, thus providing valuable precursor-to-failure data. If the SP data could reflect a slope failure in real time, then use of the SP/AMS measuring technique would prove to be an effective slope failure alarm system.

Areal Conductivity/Resistivity Technique

ER measurements have been used by many investigators to map geological and geotechnical features. Making an ER measurement is an active electrical measuring technique in that a known electrical current is induced into the ground. Although there are many advantages and disadvantages of using conventional ER measuring techniques, one of the major disadvantages has been the time and thus the cost required to conduct an effective survey over a large area. It is because of this that use of the electromagnetic terrain conductivity meter (TCM) is fast becoming the preferred active electrical survey technique by many engineers and geologists.

Conductivity is the reciprocal of resistivity, and therefore the terrain conductivity is just the inverse of the terrain resistivity. The application of electromagnetic techniques to the measurement of terrain conductivity is not new, and excellent descriptions of this technique are given by Keller and Frischknecht (1966) and Wait (1962).

A TCM measures the ground conductivity and operates under the following principles: a transmitter coil energized with an alternating current at an audio frequency is placed on the earth and a receiver coil is located a short distance away. The time-varying magnetic field arising from the alternating current in the transmitter coil induces very small currents in the earth. These currents generate a secondary magnetic field that is sensed, together with the primary field, by the receiver coil. If one assumes a uniform earth, then the conductivity will be directly proportional to the ratio of the secondary magnetic field to the primary magnetic field and inversely proportional to the electromagnetic frequency and the spacing between coils. The ratio is measured by the TCM, and the coil spacing and frequency are operator controlled. In addition, as the coil spacing is increased, the volume of terrain or earth measured is also increased; thus TCM can stepwise select depths ranging from 7.5 to 60 meters. The major advantage of using the TCM is its portability. Two people can easily operate the TCM over steep and rugged terrain, taking numerous measurements as rapidly as they can walk. By taking numerous measurements at various coil spacings and plotting contours of equal conductivity, the depth to the water table and bedrock can be inferred.

The TCM used in this study was recently acquired by the Virginia Military Institute (VMI) and was therefore used at only one of the sites at penetration depths of 24.6 ft and 49.2 ft. A conventional ER survey was conducted at all of the sites using only the installed SP electrodes having equal spacings of 32.8 ft. Other electrode spacings using conventional ER equipment were not attempted at these sites since running wires and installing other electrodes would have been too time-consuming.

Vertical Conductivity/Resistivity Technique

In 1988, a conductivity/resistivity sensor cone probe (see Figure 1) was developed for the VMI Dinastar penetrometer (see Figure 2). The Dinastar penetrometer is a lightweight, portable, static-dynamic penetrometer developed to test soils in situ at locations where it would be difficult or impossible for conventional boring rigs or sounding trucks to reach or work. This combined system is unique and provides both geotechnical and electrical data with regard to the unconsolidated soil material with depth. The VMI penetrometer allows data to be taken on slopes and other confined areas where larger penetrometer measuring systems would be prohibited or unsafe to operate.

The sensor cone probe consists of four brass ring electrodes spaced 2 cm apart and separated by a nonconducting hard plastic called agaldite. The electrodes are in a Wenner configuration (i.e., are equally spaced), with the upper and bottom brass electrodes being current electrodes and the inner two electrodes being potential electrodes. The end of the sensor cone probe is a hardened steel, standard cone 10 cm^2 in area. The sensor cone probe is screwed onto a standard penetrometer rod, and the electronic cable is threaded through the annulus of the penetrometer rods. The other end of the electrical cable is attached to a signal conditioner. The signal

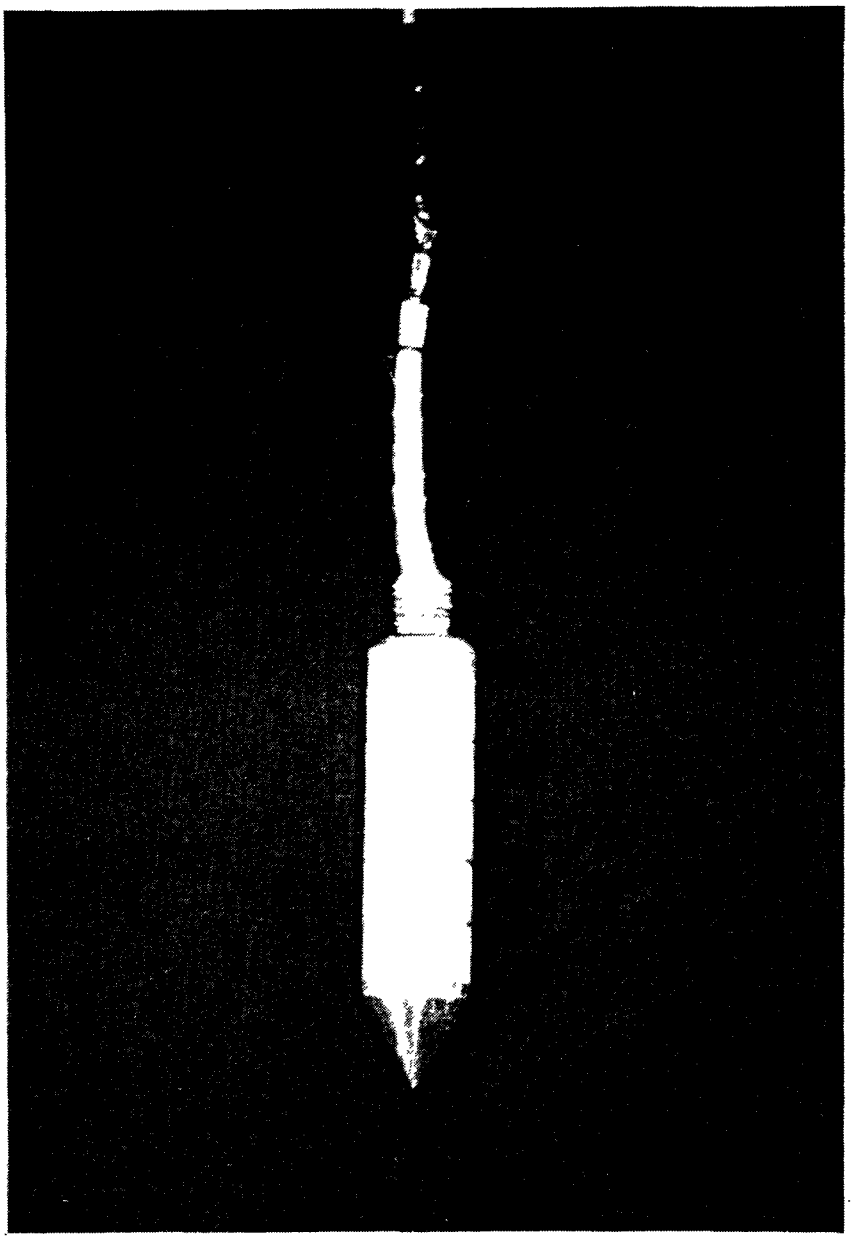

Figure 1. Sensor Cone Probe.

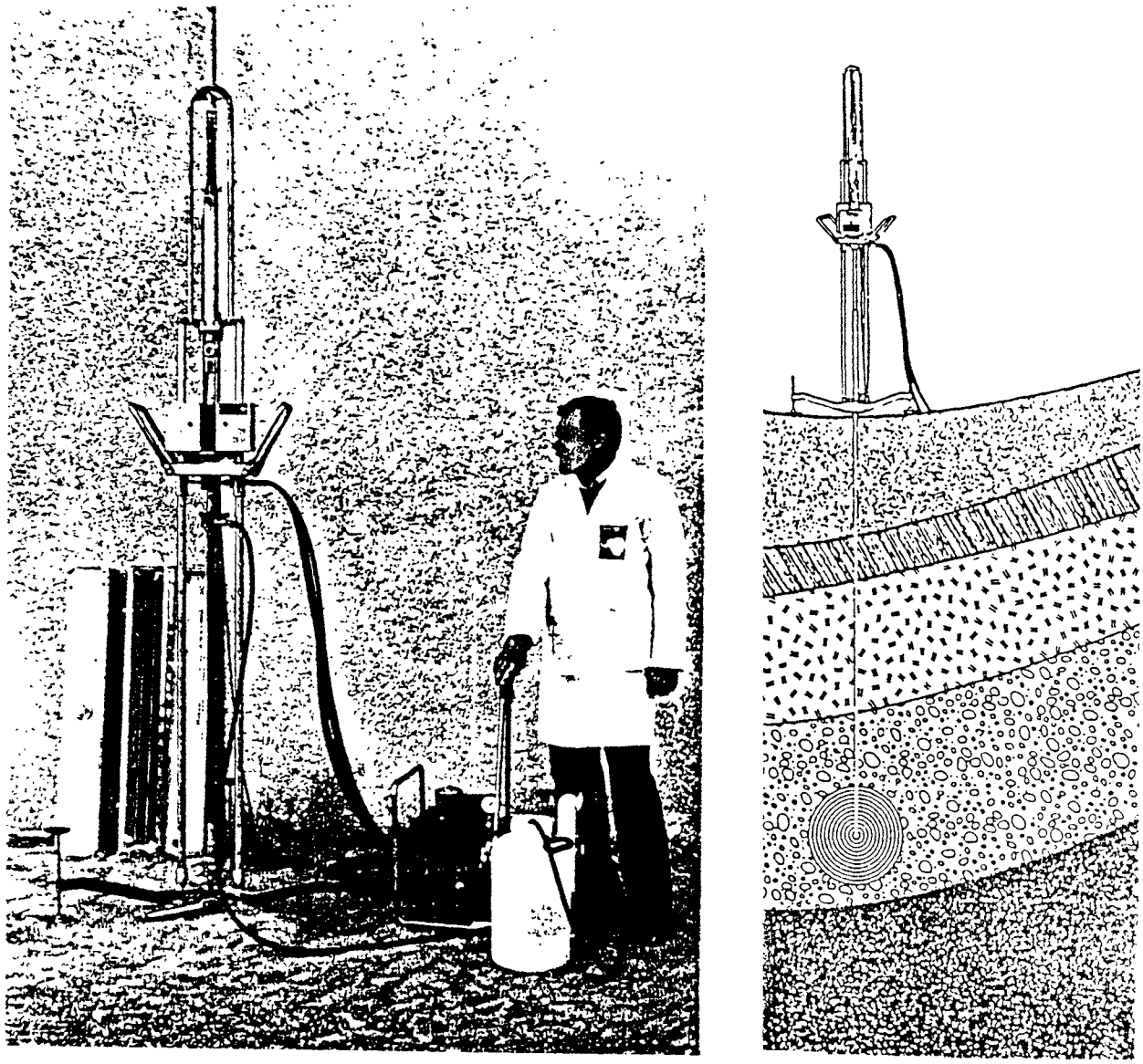

A B

Figure 2. VMI Dinastar Penetrometer (*A*) and Concept of Operation (*B*).

conditioner sends a 1,000-Hz current signal to the current electrodes and receives the voltage signal from the potential electrodes. "Knowing" the current and the received voltage, the signal conditioner can electronically process signals to provide an output voltage that is proportional to the conductivity of the effective media in the vicinity of the sensor cone probe.

The sensor cone probe was calibrated in the laboratory and then attached to the penetrometer and tested on the parade field at VMI. Upon completion of these tests, the penetrometer was used to obtain geotechnical and electrical data with depth at various locations along a selected slope site. The vertical geotechnical and conductivity data were then used to determine the thickness of weak layers located at this slope, the location of saturated zones, and the depth of bedrock.

SITE DESCRIPTIONS

Sites I and II

The slopes designated sites I and II are located within one-half mile of each other, approximately 0.4 miles and 0.3 miles respectively, northwest of the entrance to the Wintergreen Ski Resort on Route 664 in Nelson County, Virginia. The specific location for these sites (using Virginia Department of Transportation [VDOT] maps) are between baseline stations 40 + 00 to 41 + 00 and baseline stations 42 + 00 to 43 + 25, respectively, for sites I and II.

These sites are located near the Blue Ridge Parkway, and the geology of this area was well defined by Bartholomew (1971). Specifically, the sites are underlain by the Catoctin formation. The Catoctin greenstones at these sites are dark green, fine-grained schist and gneiss of the pre-Cambrian period and have a prominent southeast dipping cleavage. Therefore, at these two sites on Route 664, the slopes are in the general direction of dipping cleavage. These sites are not natural slopes since the construction of this road was a cut and fill operation. The slope material is fill consisting of a mixture of compacted excavated rock debris, saprolite, and other residual soils.

There is evidence of slope movement at these sites in that tension cracks exist in the pavement of Route 664 and resurfacing work also exists. Most of the cracks and resurfacing work exist over the roadway nearest the downhill fill slope. VDOT has installed inclinometer casings to monitor slope movement and has taken numerous soil borings at site I.

In the spring of 1988, a total of 39 CCS electrodes were installed at sites I and II. The electrodes were installed in array patterns and labeled with 28 and 11 electrodes at sites I and II, respectively. The elevation of each electrode was deter-

mined at site I, and a slope topographic and surface plot was developed. A resistivity survey was also conducted at sites I and II (with electrodes spaced 32.8 ft apart). SP measurements commenced in May 1988 and were taken manually until late August 1988, at which time an AMS was installed and commenced taking SP measurements hourly on 14 selected electrodes. Only 14 SP electrodes were monitored since the AMS system used at this site was limited to 14 data channels. These hourly measurements were taken until the middle of November 1988, after which time no further data were taken at these two sites. Meteorological data obtained at these sites were provided by Edward Dinwiddie, a member of the Central Virginia Society of the American Meteorological Society, who is the official weather data collector for the Wintergreen area of Virginia.

Site III

Site III is located near Route 670, 1 mile west of the junction of Route 670 and Route 501 in Campbell County near Lynchburg, Virginia. The specific location is between baseline stations 206 + 00 and 207 + 99 along the old Route 670. The road is at an elevation of about 790 ft near this site.

The slope at this site has actually failed and is well documented by aerial photographs. Failure commenced in 1962. By 1967, the crown of the slope had already reached within 10 ft of Route 670. This slope failure is a classical slump-earth flow as described by Varnes (1978). The distance from the crown to the tip of the toe is approximately 300 ft (see Figure 3). The distance between the right and left flanks is 225 ft. The entire slope relief is approximately 125 ft; however, the relief of the exposed main scarp is 46 ft.

The foot of this slope failure extends into a quarry. The Blue Ridge Stone Corporation opened the quarry in 1956. The stone mined from this quarry (Arch marble formation) was used mainly for road metal and concrete aggregate. The thickness of the Arch marble formation at this site is approximately 400 ft, and due to this thinness, Route 670 is actually located on a different formation, called the Pelier schist. The Arch marble formation underlies the Pelier schist. The contact between these two formations is very steep at this site (50 to 60 degrees) and dips toward the southeast. A geological cross section has been developed that cuts through this specific site. The general geology of the area, along with a cross-section map, was provided by Brown (1958).

It appears that failure was initiated when the quarry operation cut through the underlying Arch marble foundation into the weathered Pelier schist. By this loss of support, the exposed weathered schist, saprolite, and residual micaceous silts and clays became unstable when moisture contents became excessively high and flowed into the quarry through the breach in the Arch marble. Subsequent quarry operations cut one or more benches but left intact the bench supporting the toe of the slope failure.

Between 1972 and 1973, the quarry operation stopped, and by 1973, the water level rose in the quarry. The water covered the foot and part of the main body of

Figure 3. Site III Slope Failure Extending into Quarry. The dashed line designates the current water level in the quarry.

Figure 4. Site III Slope Failure (Enclosed in Box) with Water-Filled Quarry.

the slope, creating a bay (see Figure 4). The elevation of the water in the quarry has remained fairly constant at 715 ft. Since that time, some erosion has occurred along the flanks and main scarp. In 1984, VDOT installed two inclinometer casings, one on each side of Route 670 near the center line of the slope failure to monitor any slope movement since the main scarp of the slope was so close to Route 670 and any further progression of slope failure would endanger the road. On September 9, 1987, a 1-in displacement was detected after a 5-in rainfall in the inclinometer casing nearest the slope at a depth of 26 ft. This movement stimulated plans to reroute Route 670 100 ft to the northwest, up gradient from the existing road. Construction was completed on this rerouted section of Route 670 in 1989. The new road exists on a solid inclusion of quartz within the Pelier schist and appears to be in no danger from the existing slope failure. It was hoped that this slope would continue to fail during the period of monitoring, possibly even engulfing the old road, and that the SP monitoring system would capture the failure.

In the spring of 1988, a total of 32 CCS electrodes were installed at site III. The electrodes were installed in a four-by-eight array pattern centrally located over the slope failure from the old Route 670 to the quarry water line and covering both slope flanks. The elevation of each electrode location was measured in May 1988 and again in June 1990 at the completion of the work. From this elevation data, a topographic and surface plot of the area measured was prepared. A terrain conductivity survey at coil spacings of 24.6 ft and 49.2 ft was conducted at this site, and an ER survey using an electrode spacing of 32.8 ft was also conducted.

All electrodes were initially monitored manually for SP using a high-impedance voltmeter, and it had been planned to monitor all 32 electrodes at this site with a new AMS starting in the fall of 1988. However, due to delays in procurement, difficulties in laboratory testing and calibration, and an inadequate field testing power supply, the new AMS did not start to monitor the electrodes until September 1989. SP measurements were taken every 15 min using the new AMS, and all SP data were stored on disc for analysis. SP data were collected through April 1990 using the new AMS.

During the summer of 1990, the VMI Dinastar penetrometer with a conductivity sensor cone probe was used to obtain a depth profile of geotechnical and electrical data along the center line of the slope and also from the center line laterally to the left flank of the slope. In addition, water table data were obtained along the center line of the slope, and soil and rock samples were collected. In-place shear strength measurements were taken at the lower face of the main scarp. Meteorological data for this site were obtained from the National Oceanographic and Atmospheric Agency (NOAA) located at the Lynchburg Airport.

RESULTS AND DISCUSSION

The majority of the data and results of this research is presented in the appendices. However, certain key descriptive data and results are presented here.

Site I

Site Preparation

Site I was installed with 28 CCS SP electrodes on May 3, 1988. An array pattern was established for the electrodes. Each row was numbered 0 to 3, and each column was lettered A through H; therefore, each electrode was labeled C0 through H3. Row 0 is the highest elevation row and row 3 is the lowest elevation row, located at the crown and the toe of the slope, respectively. The distance between columns was 32.8 ft, and the distance between rows 0 and 1 was 20 ft; the distance between all other rows was 32.8 ft. Electrodes A0, A3, B0, and H0 were not installed due to the road curvature or rock at the site. The shorter distance between row 0 and 1 was due to the area of the slope—confined between the road, Route 664, and rock outcrops at the toe of the slope. The array pattern, showing the position and labels of each electrode, is illustrated in Figure 5.

An elevation of each electrode position was obtained, and a topographic and surface relief map of the area developed. This topographic map and a three-dimensional surface map of the elevation data are presented in Figure 6. The elevation is between 2,278 ft and 2,300 ft across the top of the array at site I. From the closely spaced contour lines, the slope is steepest along column D and less steep along column A.

Electrical Resistivity Survey

An ER survey of site I was conducted on June 10, 1988, using in-place SP electrodes. With the SP electrode spacing, the effective depth of penetration of the resistivity study was approximately 30 ft (see Figure 7). The lower ER values are near the crown of the slope. The higher ER values are near the toe of the slope. The ER values at this site below 1,000 ohm-ft are indicative of well-to-moderately-fractured bedrock with moist, filled cracks. ER values above 1,000 ohm-ft would be indicative of low-fractured bedrock. From this ER survey, it would appear that the water would more easily flow through the high-to-moderately-fractured bedrock, whereas the subsurface flow would be impeded by the low-fractured, more intact, or massive bedrock.

Spontaneous Potential Measurements

At site I, SP measurements were collected manually on May 4, 5, 6, 9, 11, 13, 20, 23, and 31; June 10, 16, and 29; and July 1, 1988. By using these SP data and computer software, SP contour maps were plotted for each day data were collected. The SP data are presented in Appendix A. Although SP data varied somewhat during the measurement period, the following general pattern can be discerned from this initial SP data:

1. The more negative SP values are in the up-gradient or higher-elevation electrode rows near the crown of the slope.

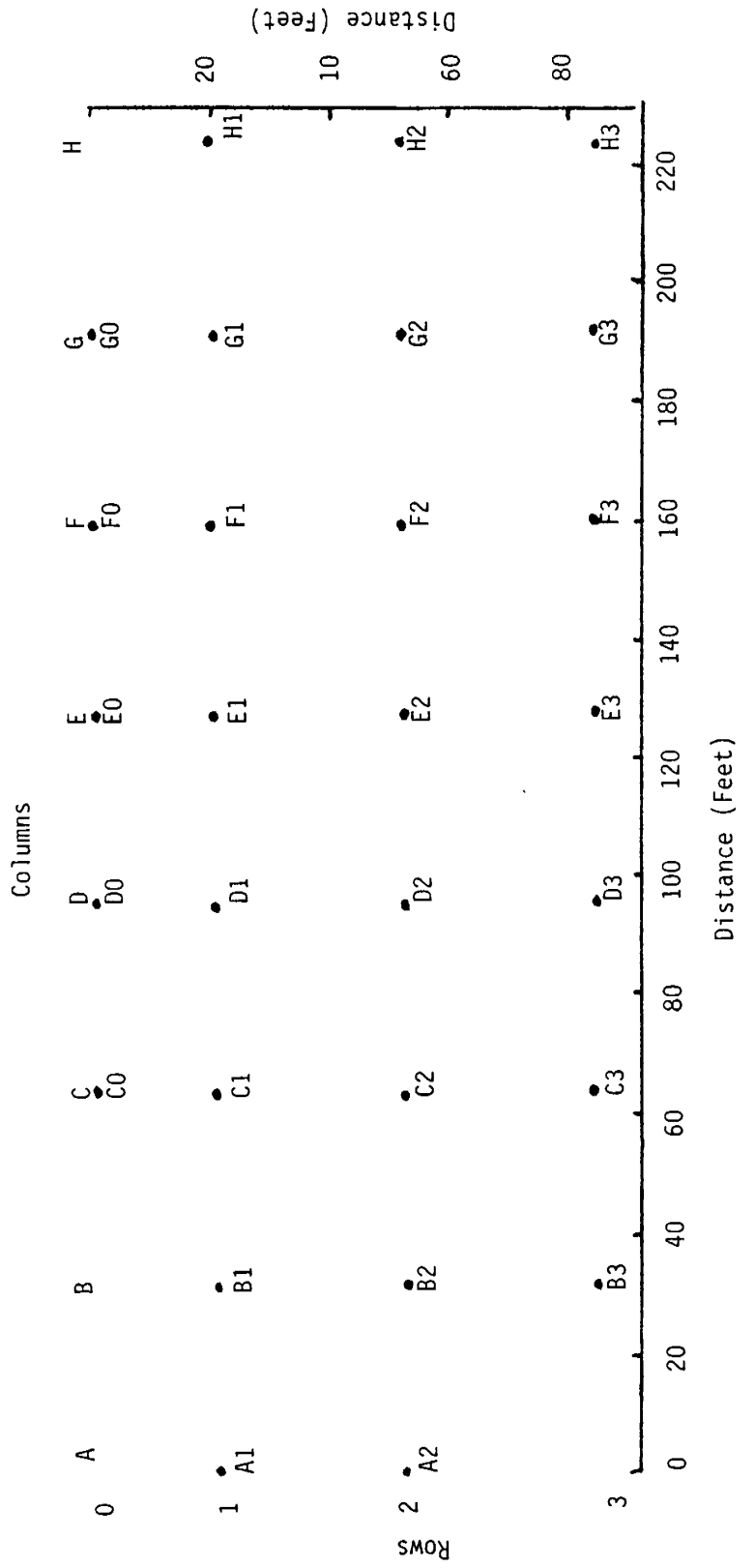

Figure 5. Spontaneous Potential Electrode Array Pattern at Site I. The 28 installed electrodes are labeled C0 through H3.

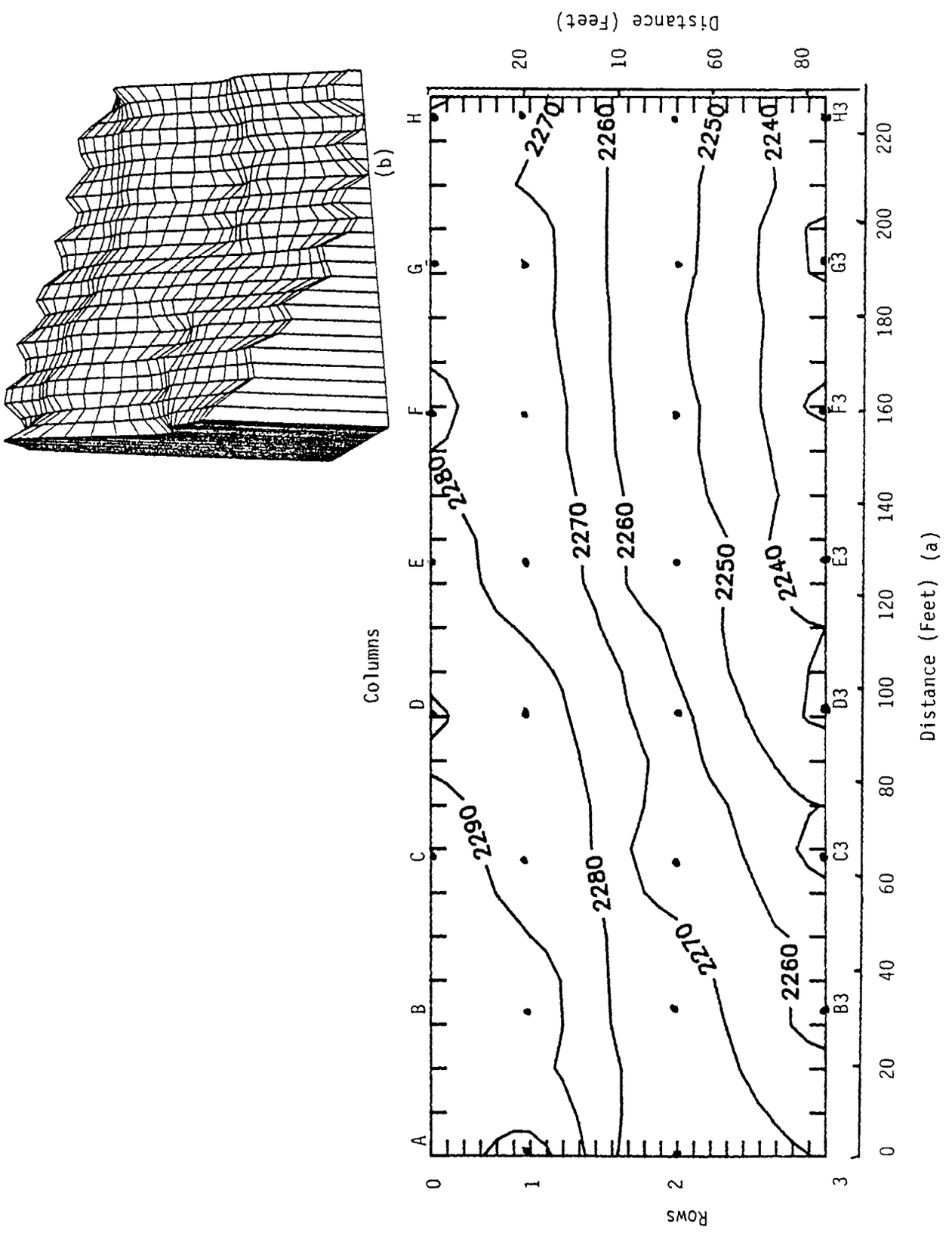

Figure 6. Elevation Contour (*A*) and Surface (*B*) Maps of Site I. The contour interval is 10 ft.

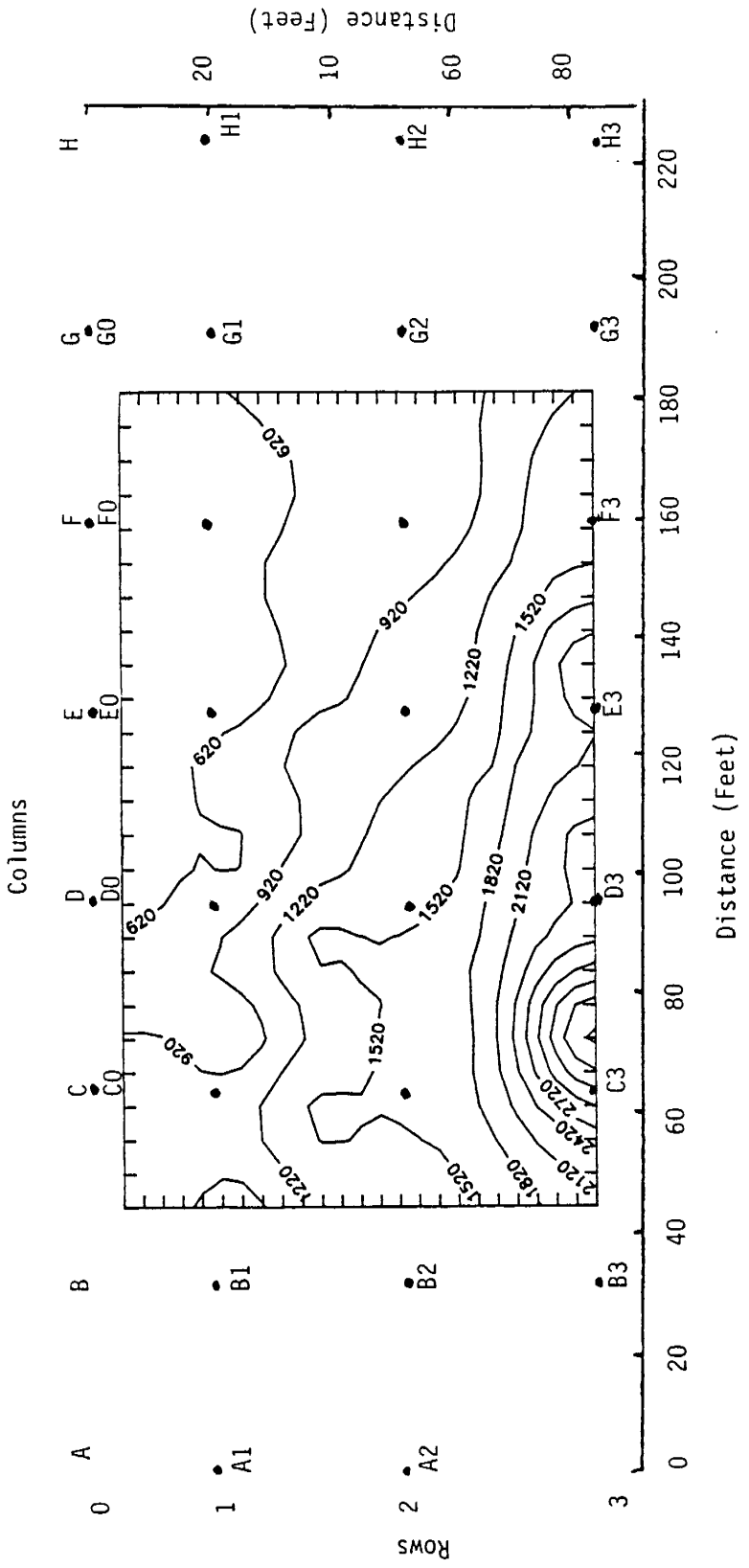

Figure 7. Electrical Resistivity Contour Map for Site I. The contour interval is 300 ohm-ft.

2. The more positive SP values are near the toe of the slope.
3. Anomalous to this general trend are two electrodes: the negative lower-trend-gradient SP electrode is consistently F2, and the most positive up-gradient electrode is C0.

SP gradients are easily seen in the May 11, 1988, SP contour maps (see Figure 8). The gradients are indicative of high hydraulic gradients on preferential flow patterns. To normalize SP data, a technique used by the investigators was to take the most positive SP value in any given array of data, subtract the value from all of the SP values in the array, and then take the absolute value of the number; thus, all SP values will be positive. The most positive SP value will be 0, and the most negative SP value will be the largest value in the array. An SP contours and surface plot was developed using this normalized technique (see Figure 9). Figure 9 is similar to Figure 8 except for the values. However, when looking at Figure 9 and discussing it in light of recent findings by Corwin (1989), one can infer the following:

1. Subsurface seepage flow paths or areas of high hydraulic gradient are in the areas of high-normalized SP values.
2. Seepage outflow areas or areas of low hydraulic gradient are in the areas of low-normalized SP values.

Therefore, at site I, high hydraulic gradients exist in the general direction of electrode F2 and low hydraulic gradients or seepage outflow exists at electrodes C0, B2, D3, and H3. This would indicate that a seepage outflow exists in the vicinity of electrode C0 and that the highest subsurface flow is in the general direction of electrode F2. The anomaly at electrode F2, being a high hydraulic gradient area, may merit additional monitoring and possible installation of horizontal drains to reduce the unusually high hydraulic gradient and prevent a slope bulge and eventual slope failure at the area. The response of electrode C0 could be caused by the location of a black, plastic, corrugated drainpipe that discharges water from a spring located under Route 664.

Fourteen SP electrodes were monitored continually at site I using an AMS acquired for a research project supported by the U.S. Army Corps of Engineers. This AMS was limited to 14 channels; therefore, those SP electrodes that had the most positive and negative values were connected to the AMS. Also, all SP electrodes in row 1 were connected to allow a row profile to be developed over time. The SP electrodes monitored were C0, D0, F0, G0, A1, B1, C1, D1, E1, F1, G1, H1, and F2. The monitoring frequency was hourly, and the monitoring period was from August 25 until November 16, 1988. The hourly readings at site I for the period of August 25 until September 4, 1988, are presented in Appendix A. Also in Appendix A are the daily averages for the same electrodes for the entire monitoring period.

Effect of Air Temperature and Precipitation on SP Values

During this monitoring period, the air temperature and precipitation were recorded at nearby Wintergreen. The daily average temperature and daily

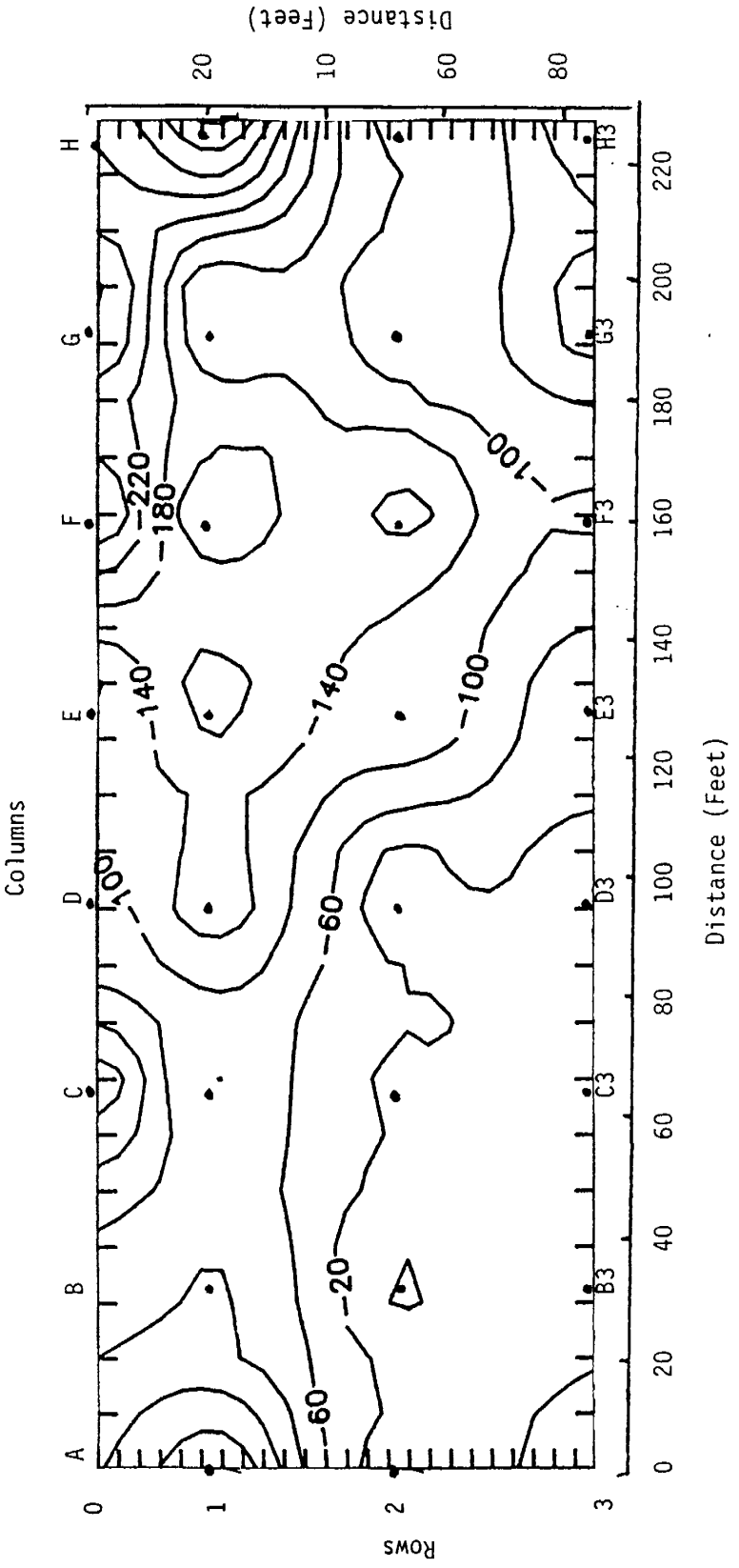

Figure 8. Spontaneous Potential Contour Map for Site I on May 11, 1988. The contour interval is 40 mv.

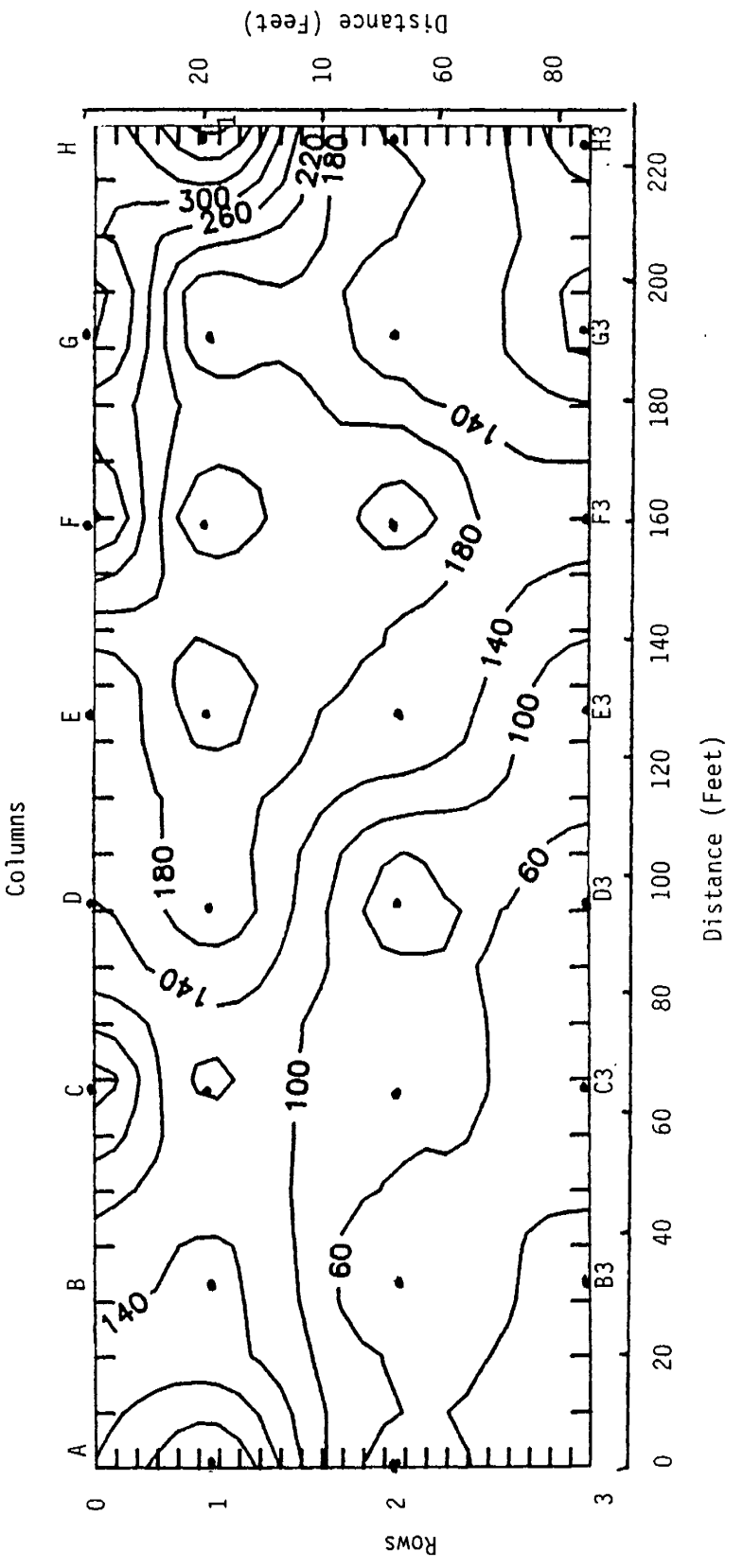

Figure 9. Normalized Spontaneous Potential Contour Map for Site I on May 11, 1988. The contour interval is 40 mv.

precipitation are shown in Figure 10. An example of hourly temperature effects can be seen by the hourly SP values at electrode H1 (see Figure 11). For the period August 25 to August 28, warm temperatures, those occurring during the heat of the day, resulted in reduced SP values whereas cooler evening temperatures resulted in increased SP values. These changes in SP are the result of the electrodes heating and cooling during the day. It is interesting to note that certain shaded electrodes did not register this diurnal thermal response. Also, if the weather was overcast and the variation between maximum and minimum temperature was small, very little thermal response was recorded. This is shown during a wet and overcast period at site I (see Figure 11).

The effects of temperature fluctuation on SP values were studied by Corwin and Hoover (1978). They noted a coupling effect and described a decrease in SP values over geothermal areas (where temperature extremes are high). In this study area, as surface temperatures decrease in the cooler months, a thermal couple develops between the cool surface and warmer ground at depth. This thermal difference may approximate the effects of geothermal areas, and thus SP values decrease as surface temperature decreases. This is observed in the daily average SP values of each electrode (see Appendix A) where SP values generally decrease as the daily average temperature decreases.

The other major environmental factor affecting SP values is precipitation. Precipitation generally has two effects on SP values: (1) as the slope becomes saturated with moisture, the SP values will increase; and (2) as the slope drains, high rates of subsurface flow and high hydraulic gradients will lead to reduced SP values. This was especially evident during the period August 28 to September 4, 1988, when nearly 5 in of rainfall was recorded.

During the period August 28 to September 4, 1988, all SP electrodes monitored peaked or had their highest SP value (400 mv) at 5 p.m. on August 29 (see Appendix A and Figure 11). These high SP values occurred after the heavy rainfall of August 28 and 29. This would be indicative of a saturated slope condition, and although failure did not occur, it would be at such a condition that one might expect failure. Had more rainfall occurred and high positive values continued on all electrodes, the stability of this slope would probably be in extremis. Twelve hours or more after significant precipitation, the values of SP decreased as subsurface water flows and hydraulic gradients increased due to slope drainage. Another aspect of the change in SP values as a result of precipitation can be seen in Figure 12. In Figure 12, the daily average SP values for August 29 and September 1 are plotted for row 1, electrodes A1 through H1. After the high rainfall of August 28, all electrodes in this row increased in SP value. Then, when slope drainage occurred (September 1), there was a significant decrease in SP values. This shows how SP can be used to monitor a slope and "see" the slope expand as it saturates and contract as it drains during precipitation. Since most slope failures in Virginia are triggered by precipitation, a measuring system that could monitor and indicate an extremis situation would be extremely valuable.

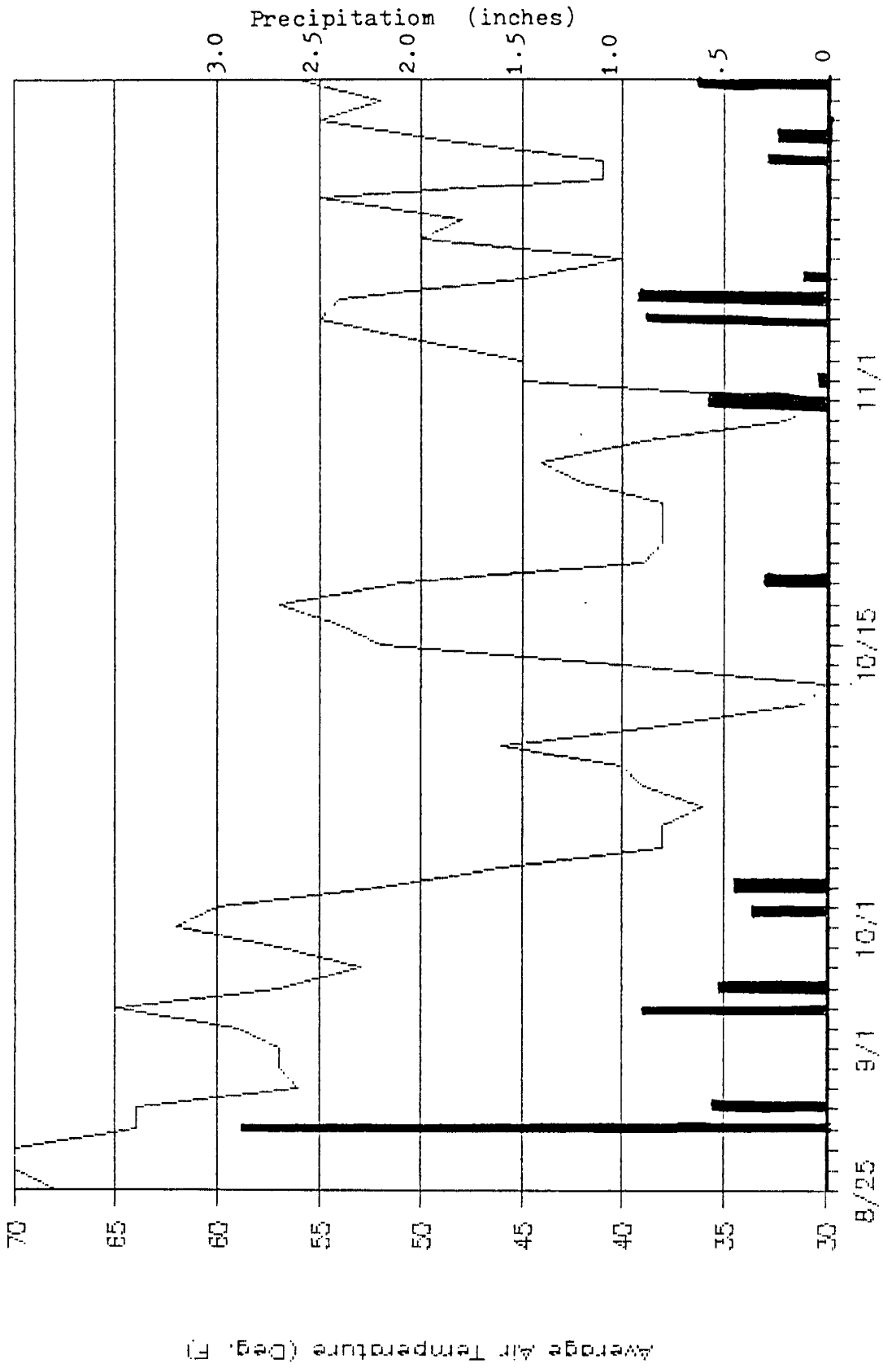

Figure 10. Temperature and Precipitation at Sites I and II from August through November 1988.

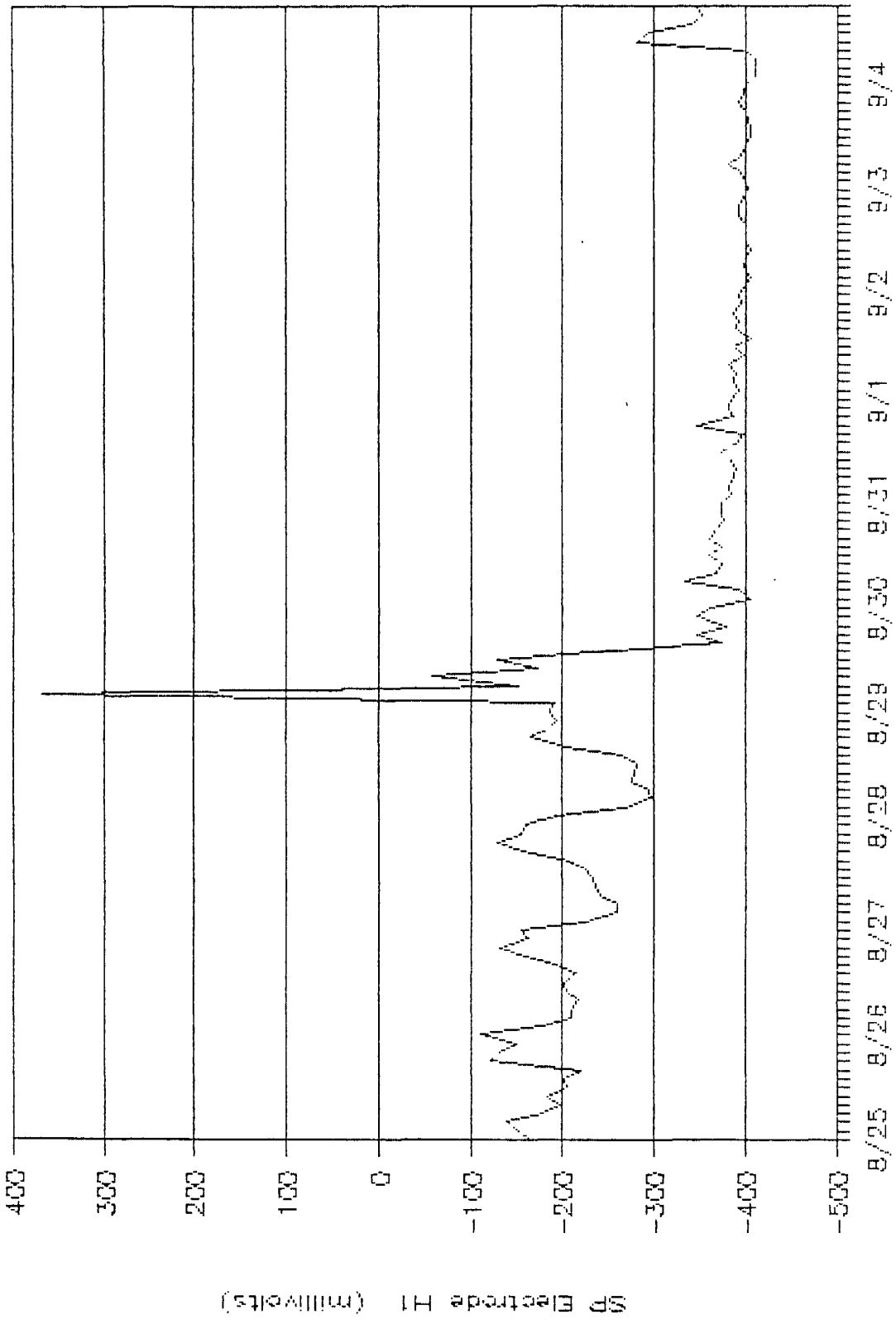

Figure 11. Hourly Spontaneous Potential Measured at Electrode H1 versus Time for the Period August 25 through September 4, 1988.

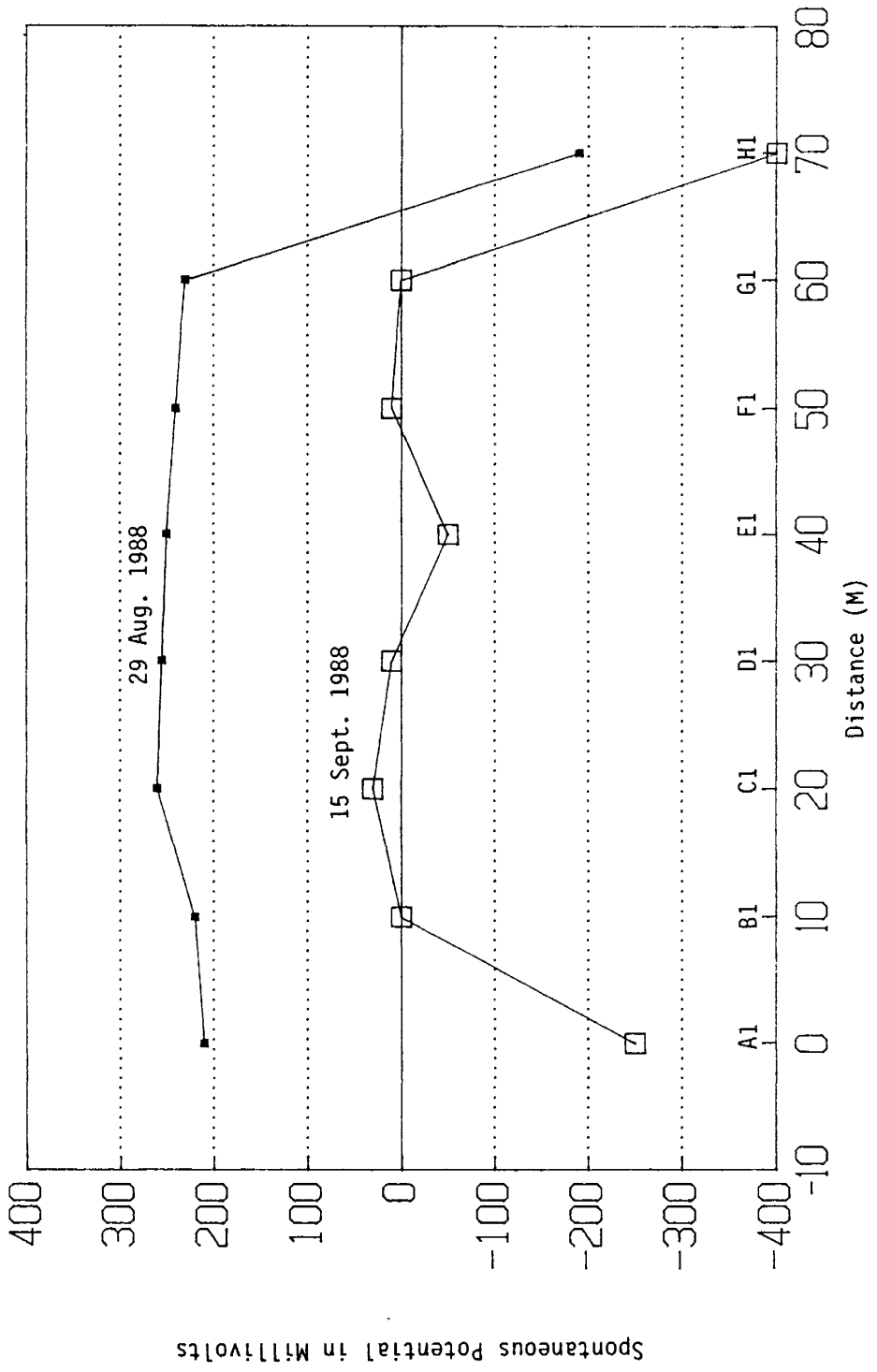

Figure 12. Daily Average of Spontaneous Potential Values Along Row 1 at Site I during August 29 and September 1, 1988.

The inclinometer data confirmed the SP data in that the slope at this site appeared to breathe, i.e., expand and contract, with rainfall. In addition, the inclinometer data showed that soil contractions do not quite return the slope to its original position, and therefore a slight downhill creep results after each cycle. The expansion and contraction are most likely due to the saprolite and residual soils mixed in with the slope fill material becoming saturated and then expanding and then, during the moisture drainage periods, the fill contracting. These expansions and contractions are correlated with the amount of rainfall (i.e., high rainfall, major expansion; low rainfall, smaller expansion). Inclinometer and SP data appear to confirm each other relative to the effects of rainfall on slope stability.

Real-Time Warning System

A real-time system for issuing warnings of landslides during major storms is being developed for the San Francisco Bay region, California, by Keefer et al. (1987). The system is based on empirical and theoretical relations between rainfall and landslide initiation, geologic determination of areas susceptible to landslides, real-time monitoring of a regional network of telemetering rain gages, and National Weather Service precipitation forecasts. This system was used to issue warnings during the storms of February 12 to 21, 1986, which produced 31.5 in of rainfall in the region. Although analysis after the storms suggested that modifications and additional developments were needed, the system successfully predicted the times of major landslides. This system, coupled with a real-time SP monitoring system on specific trouble slopes, could be used effectively as a warning system for road closures in landslide-prone regions, such as western Virginia.

Site II

Site Preparation

Site II was installed with 11 CCS SP electrodes and 1 reference electrode in May 1988. Only two rows were used: the upper gradient row (row 1) located below the crown of the slope had 6 SP electrodes, and the low gradient row (row 2) had 5. All SP electrodes were separated by 32.8 ft, and an array was configured, with each electrode labeled as shown in Figure 13.

Electrical Resistivity Survey

The elevations of the SP electrodes at Site II were not measured; however, an ER survey was conducted. The ER survey consisted of only five measurements due to the 11 SP electrodes installed. The effective depth of the ER survey was 32.8 ft, and the survey covered an approximate area encompassed by the following 4 corner SP electrodes: B1, E1, E2, and B2 (see Figure 14). In this survey area, ER values did not vary significantly at 575 to 742 ohm-ft. These ER values would indicate that the underlying materials at the depths surveyed consisted predominantly of high-to-moderately-fractured bedrock with moist, filled cracks.

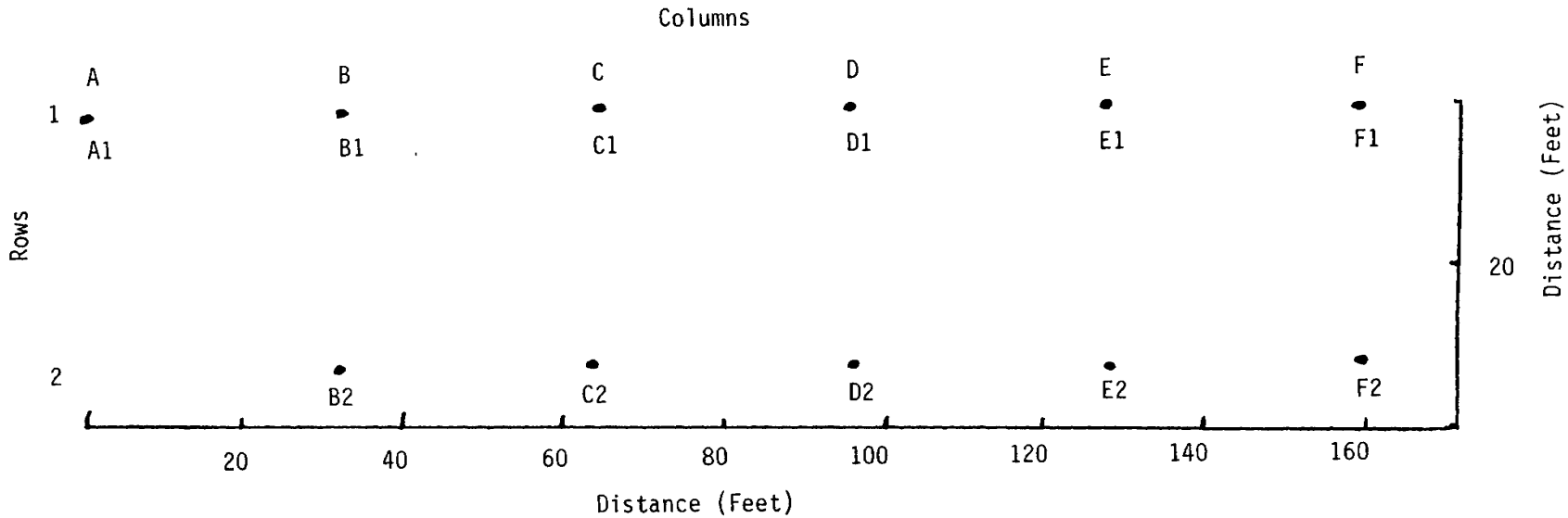

Figure 13. Spontaneous Potential Electrode Array Pattern at Site II.

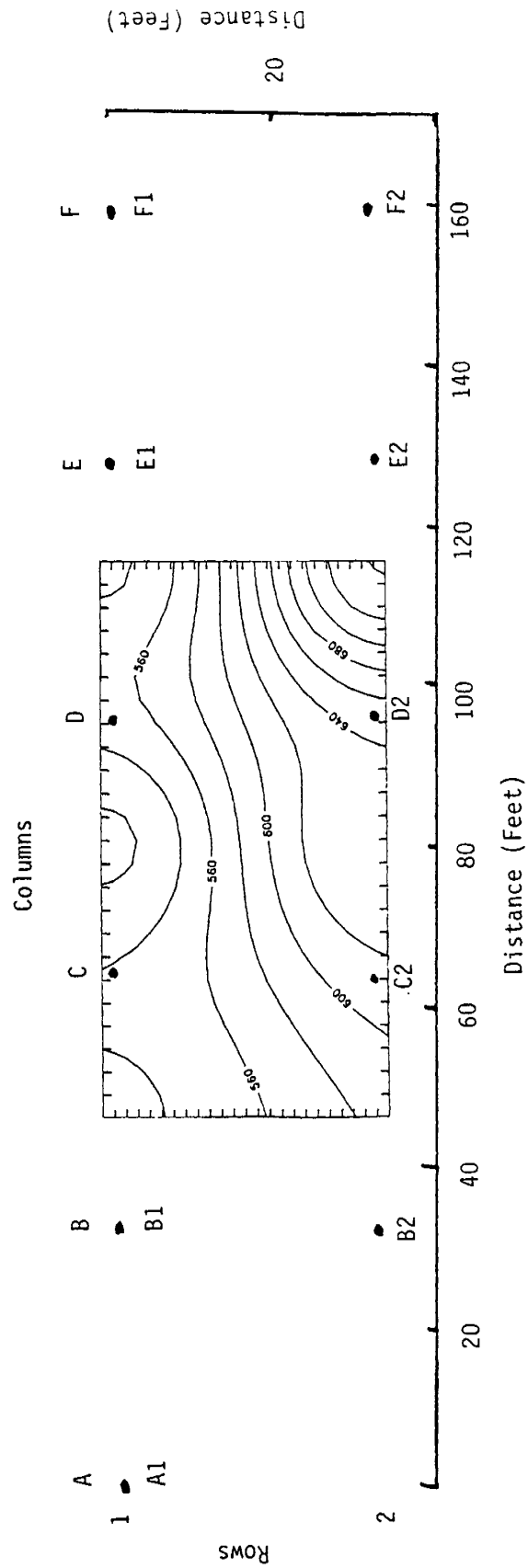

Figure 14. Electrical Resistivity Contour Map for Site II. The contour interval is 20 ohm-ft.

Spontaneous Potential Measurements

At site II, SP measurements were collected manually on May 4, 5, 6, 9, 15, 20, 23, and 31; June 10, 16, and 29; July 1 and 26; August 12; September 8, 15, 20, 25, and 26; October 7, 13, 18, 20, 24, 27, and 31; and November 3, 7, 10, 14, and 22, 1988. SP contour maps were plotted for each day's data and are presented in Appendix B. Although SP values varied significantly during the 7-month (May to November 1988) testing period for individual electrodes, the ranking values between electrodes were consistent. Those electrodes having the higher SP values always remained the highest electrodes, and those electrodes having the lower SP values always remained the lowest, even though in the case of electrode B2 and F1 the SP value varied between +333 mv and +458 mv and –1 mv and –93 mv, respectively. Therefore, the general contour map of equal SP values have relatively the same pattern (see Appendix B). In general, the SP values in the up-gradient row (row 1) are lower than those in the lower-gradient row (row 2). In row 1, SP electrodes at the flanks of the slope A1, E1, and F1 have the lowest SP values in that row. In row 2, SP electrode D2 consistently has the lowest SP value in the row.

Effect of Drainpipe

Using the same rationale of analysis of SP data proposed for site I, it is evident that this slope is draining at the toe and that a flow path or high hydraulic gradient exists between electrodes F1 and D2. This site also has a 30-in drainpipe between electrode columns D and E. The pipe collects water from a ditch on the opposite side of Route 664 and diverts it under the road. The water exits the pipe approximately 25 ft below electrode E2. The pipe or the method of installation and the soil around this pipe may have a significant influence on the SP values and the general flow toward electrode D2 and the resulting high hydraulic gradient in that direction. In addition, there is an 8-in, plastic, corrugated drainpipe between column C and D, near row 1 at this site. This pipe is connected to a spring box located under the road. Site II, during a recent inspection (1990), appeared to be failing between rows 1 and 2 and columns C through E. The slope in this area was observed to be humucky, with small scarps, absent of any ground cover. These features were not evident in 1988; however, SP values during that time indicated that electrode D2 was associated with high subsurface flow rates.

Site III

Site Preparation

Site III, the slope that extends into a water-filled quarry, was installed with 32 CCS SP electrodes and 2 reference electrodes in May 1988. A grid pattern was established for this array of electrodes. Each row was numbered 1 to 4, and each column was lettered A through H. The distance between columns was 32.8 ft, and the distance between rows was 32.8 ft. Each row of the array was long enough to

cover from the right to the left flank of the slope, and each column ran from the crown of the slope to within 20 ft of the quarry water line. This is a failed slope, and the foot of the slope extends into the quarry approximately 150 ft and is completely covered by water. The array pattern of electrodes does encompass the majority of the main body of the slope, including the main and minor scarps. A grid pattern showing the position and labels of each electrode is illustrated in Figure 15.

An elevation of each electrode position was obtained initially upon installation of all the electrodes in May 1988 and again on completion of the project in June 1990. A topographic map and surface plot for the 1988 and 1990 elevations are shown in Figures 16 and 17, respectively. Cross-sectional profiles along columns A though H have been prepared and are in good agreement with VDOT cross-sectional profiles prepared in 1987. The cross sections for columns A through H are shown in Figures 18 and 19. In these figures, the 1988 profile is plotted as a solid line, with the 1990 elevation data plotted as a point value to allow visualization of any change in elevation over the 2-year period. Both the major and minor scarps are evident from the surface plots of Figures 16 and 17. No major changes in elevation are seen from the profiles in Figures 18 and 19; however, erosion has reduced the elevation slightly in profile H, and material accumulation is observed in the lower slope elevation, particularly in profiles D and F. From site observation, profiles D and F appear to be the result of erosion of surfacial water runoff from the road elevation down to the quarry. Also evident in the profile are the columns that mark the slope flanks. Columns A and H are profiles of the right and left flanks, respectively. All other columns, B through G, are profiles along the main body of the slope.

Electrical Resistivity Survey

An ER survey was conducted on May 9, 1988. A TCM survey of site III was conducted on April 11 and 14, 1988. The ER survey was conducted using the in-place SP electrodes, and thus the effective depth of penetration of this survey was approximately 30 ft (Figure 20). The TCM survey was conducted prior to installation of SP electrodes in order to prevent any electrode interference with the TCM and its sensitivity to detect ferromagnetic objects. The TCM survey was conducted at coil spacings of 24.6 ft and 49.2 ft, and therefore depths of penetration would be approximately 25 ft to 50 ft, respectively. The TCM survey data were plotted in contours of equal conductivity for the survey area and are presented in Figures 21 and 22. In these figures, the entire array field (including all electrode rows) is shown, along with a smaller field including only electrode rows 2 through 4. The reason for this is that the TCM operator was concerned that the guardrail along Route 670 was very close to row 1 and caused electromagnetic interference, resulting in erratic and high conductivity readings. In the TCM data, the higher conductivity values are along the center line of the slope and they decrease proceeding away from the center line toward the flanks. This might be expected, as the flanks are held up by consolidated weathered bedrock. Therefore, the TCM surveys conducted at site III provide a general indication of the underlying bedrock relief, as expected from

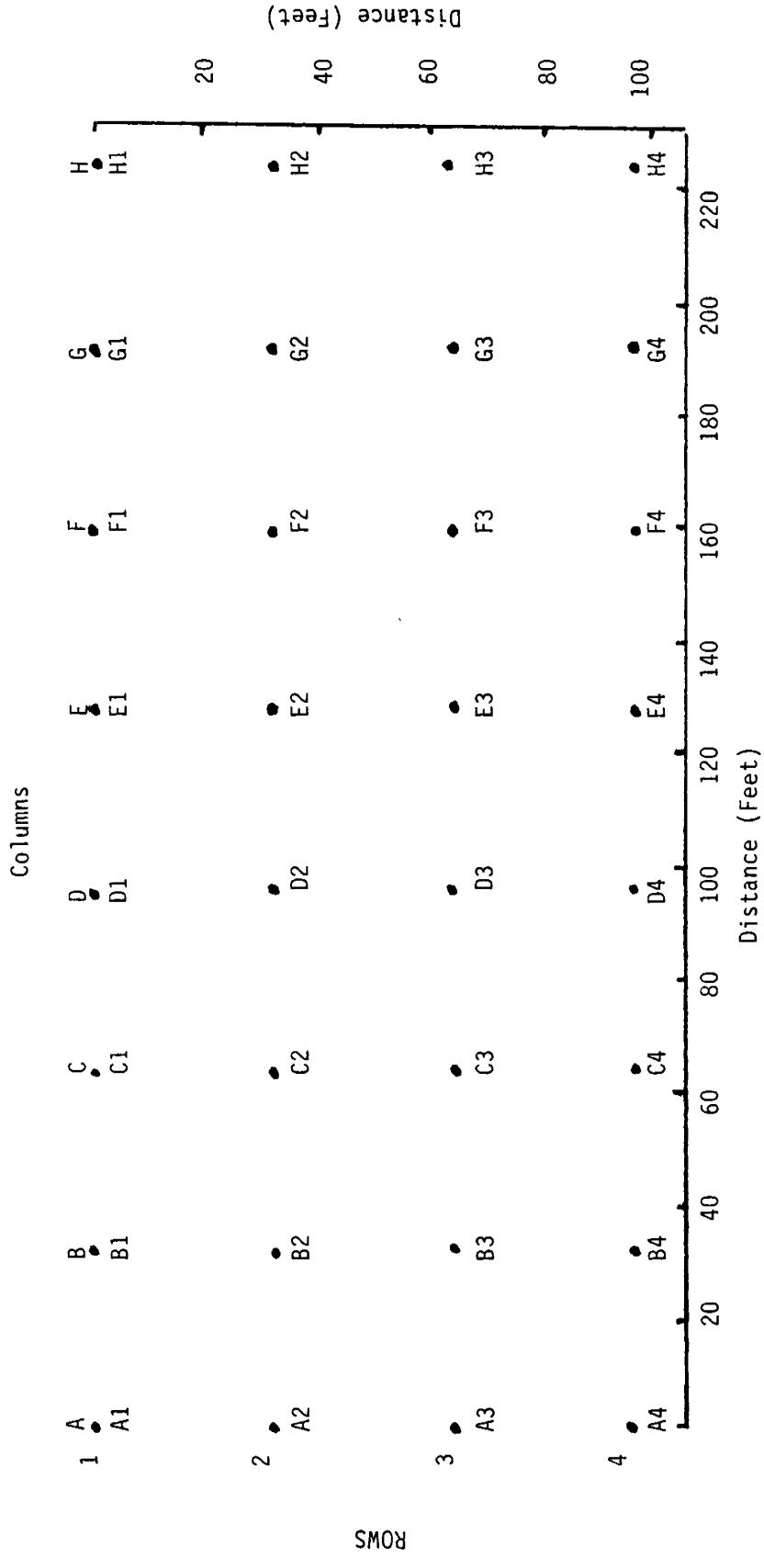

Figure 15. Spontaneous Potential Electrode Array Pattern at Site III.

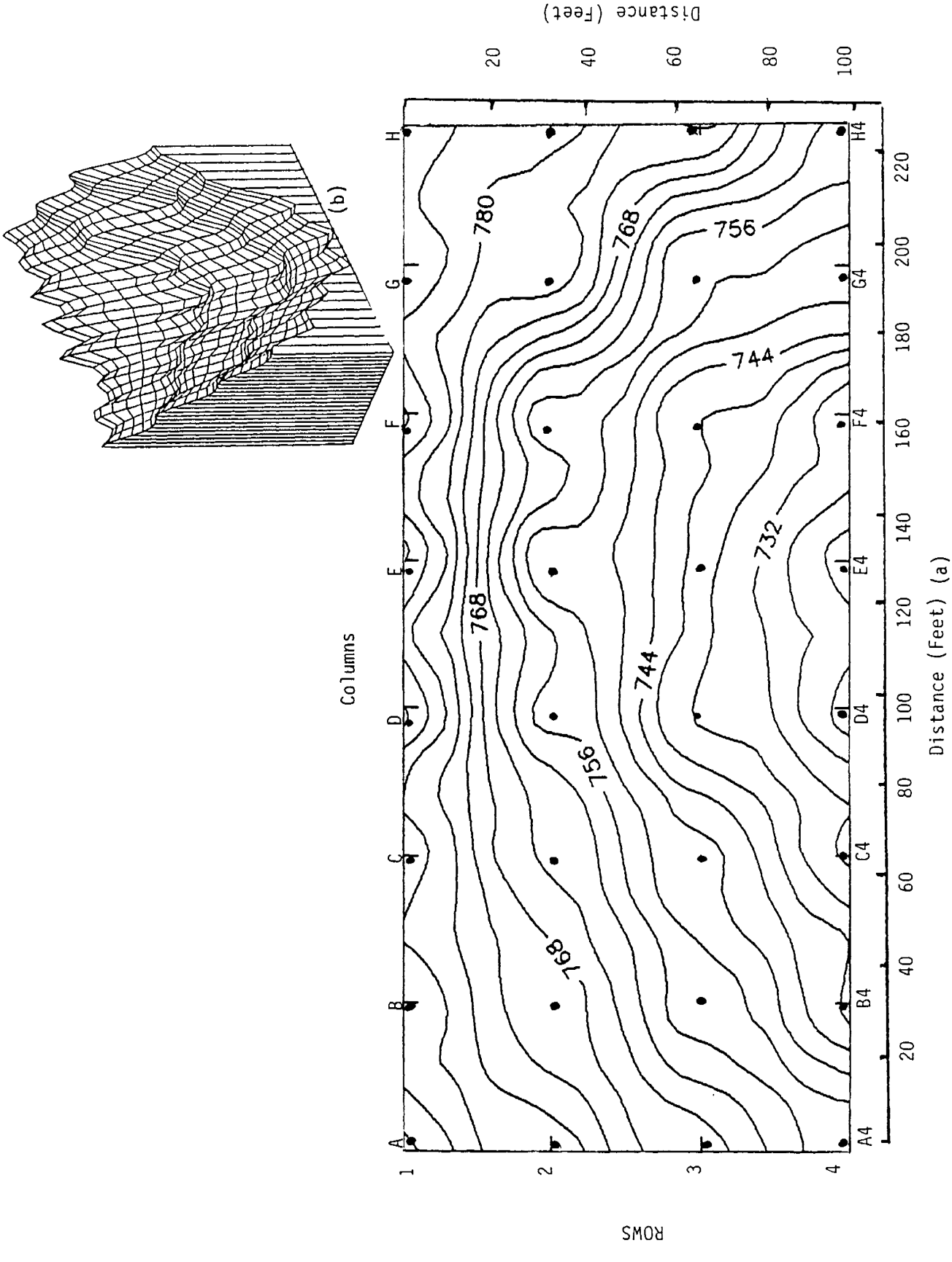

Figure 16. Contour (*A*) and Surface (*B*) Maps of 1988 Elevation Data at Site III. The contour interval is 4 ft.

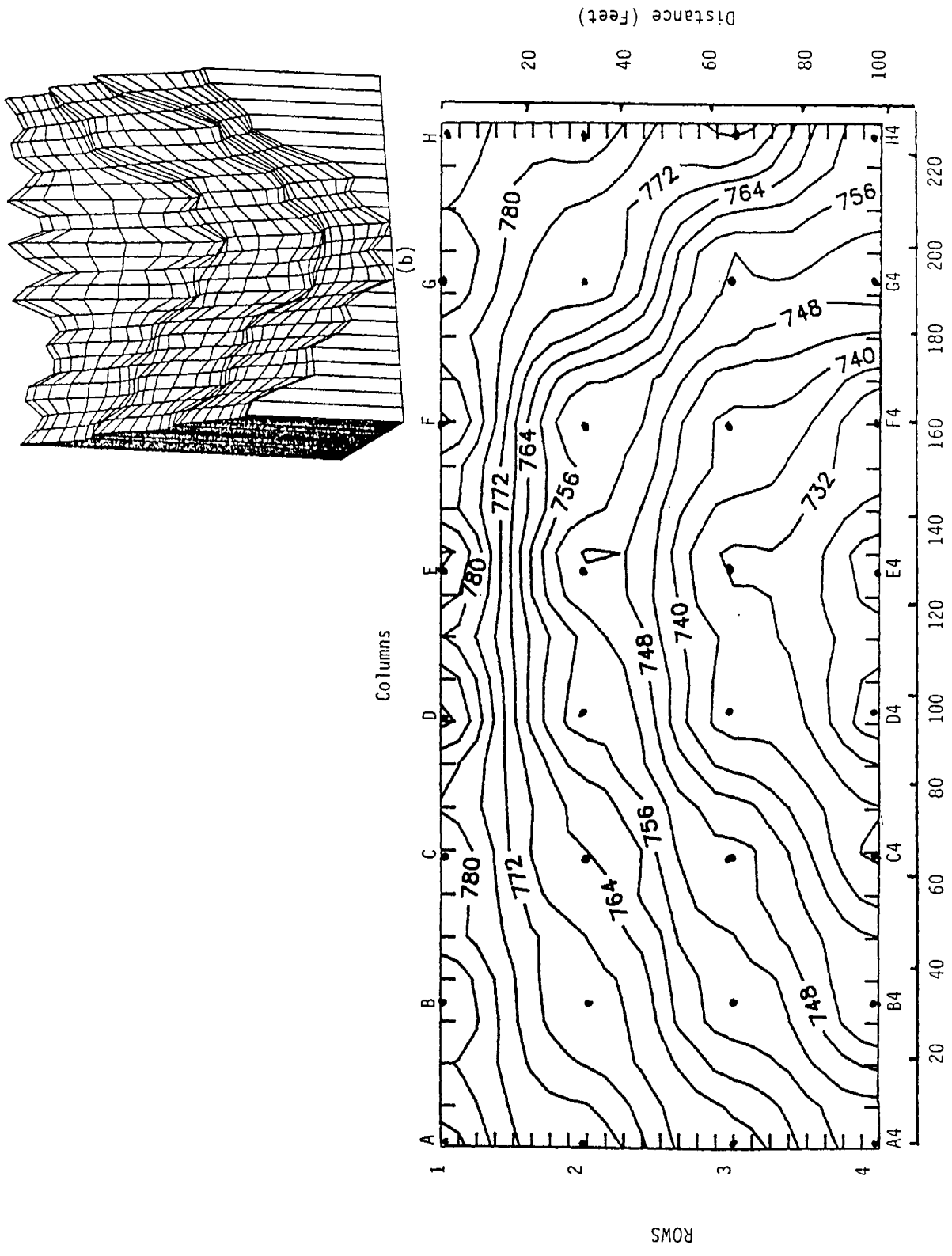

Figure 17. Contour (*A*) and Surface (*B*) Maps of 1990 Elevation Data at Site III. The contour interval is 4 ft.

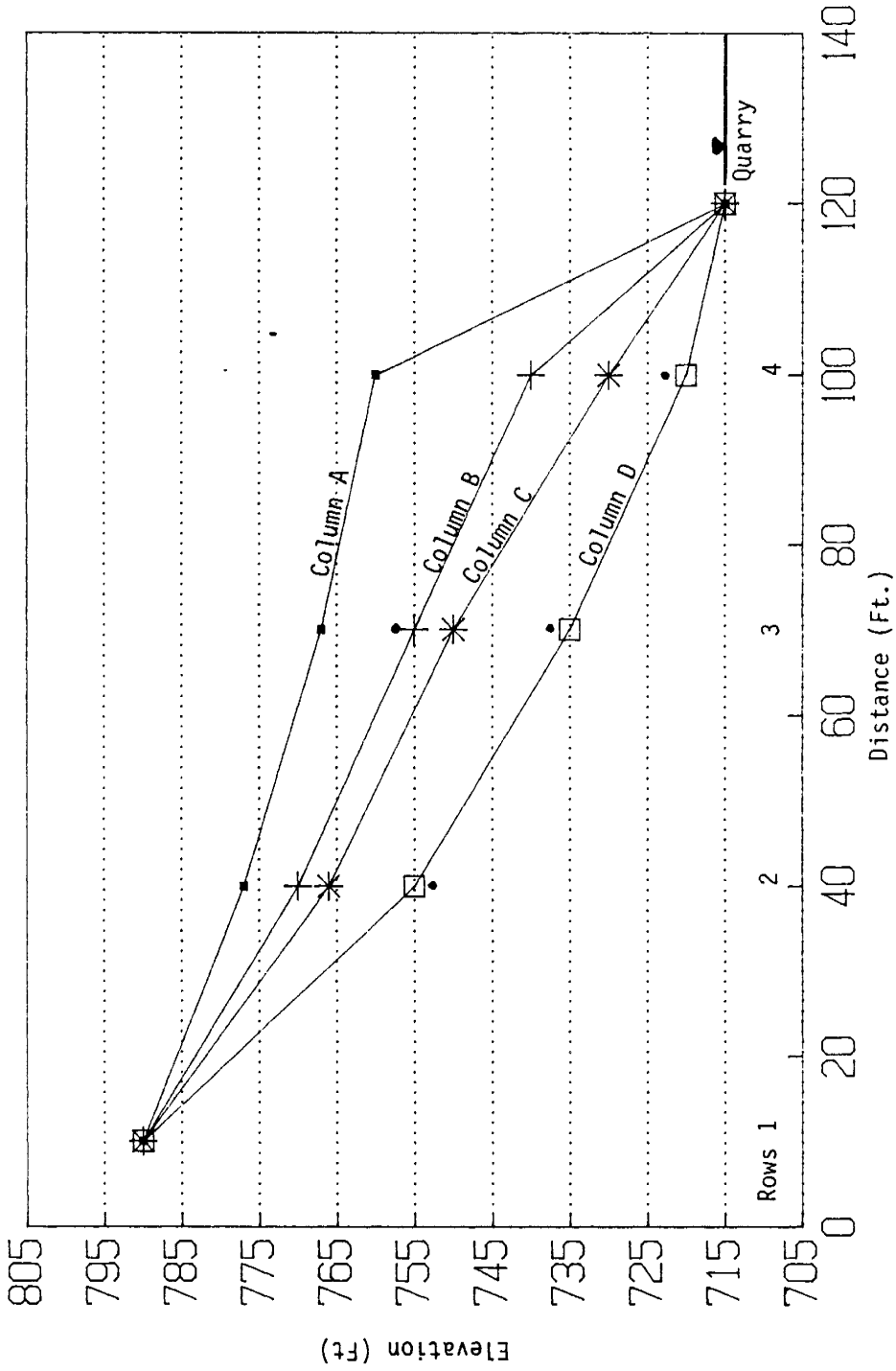

Figure 18. 1988 Elevation Profiles Along Columns A, B, C, and D. The 1990 changes are indicated with a dot (•) for Site III.

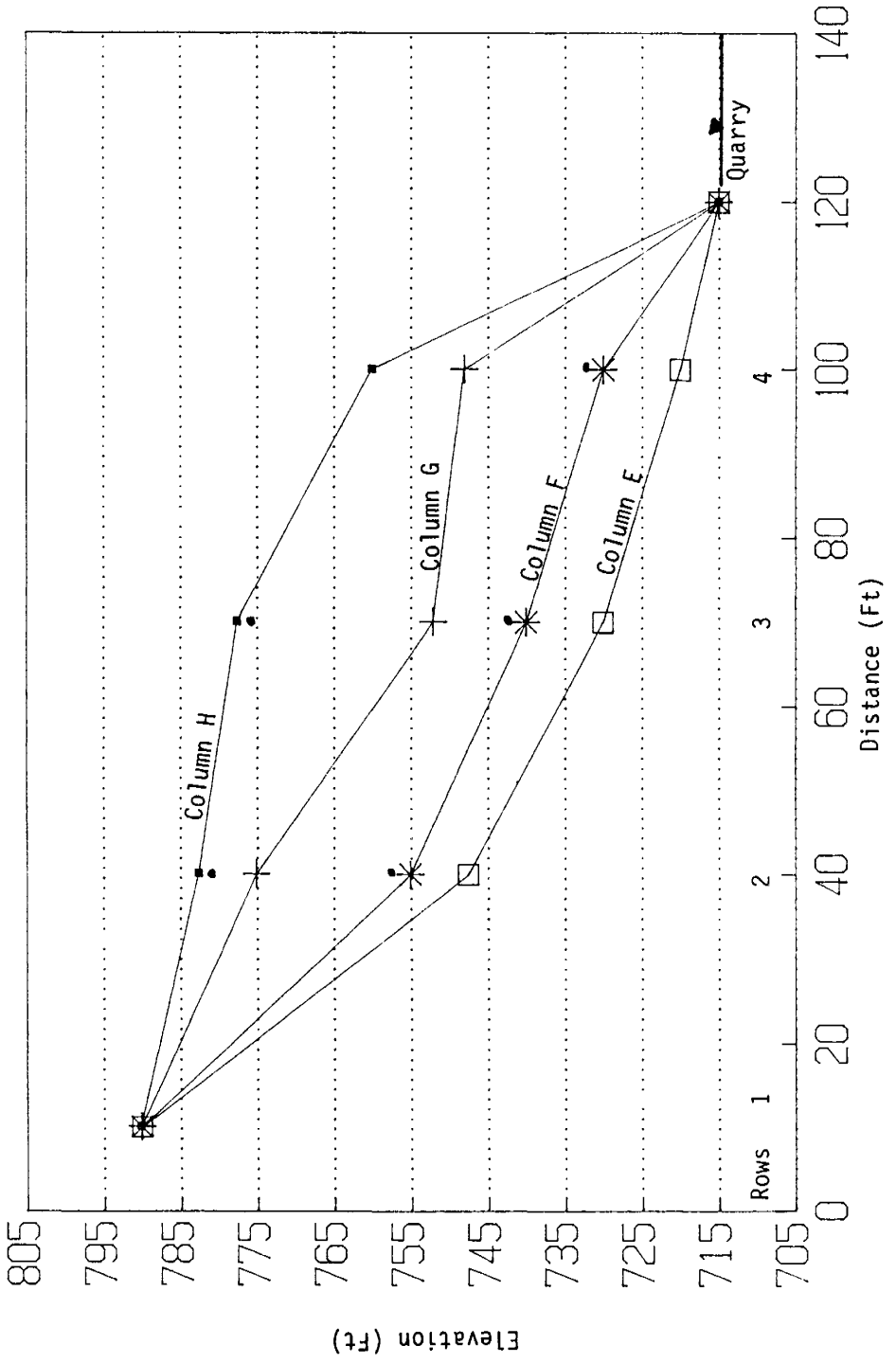

Figure 19. 1988 Elevation Profiles Along Columns E, F, G, and H. The 1990 changes are indicated with a dot (•) for Site III.

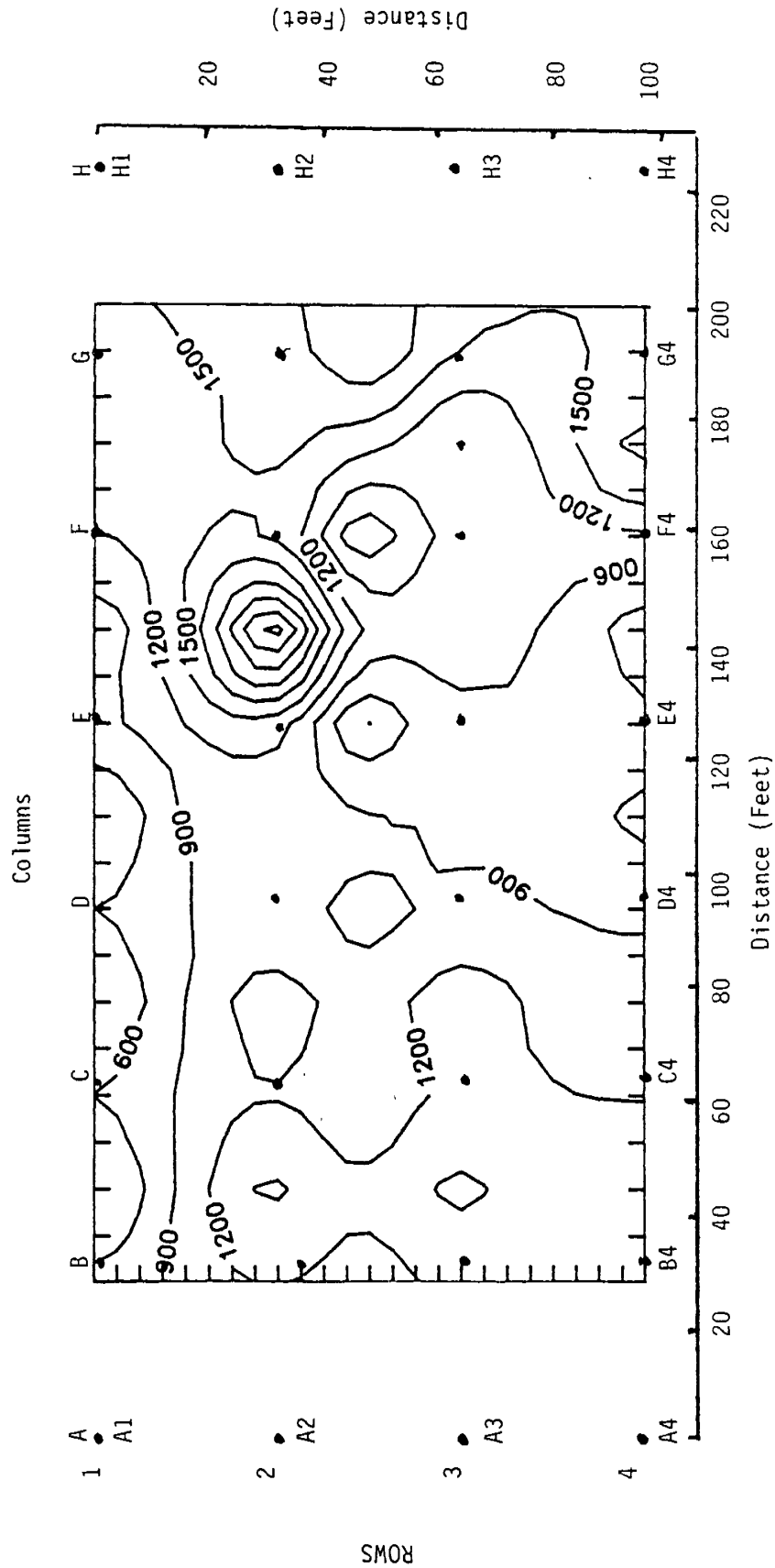

Figure 20. Electrical Resistivity Contour Map for Site III. The contour interval is 300 ohm-ft.

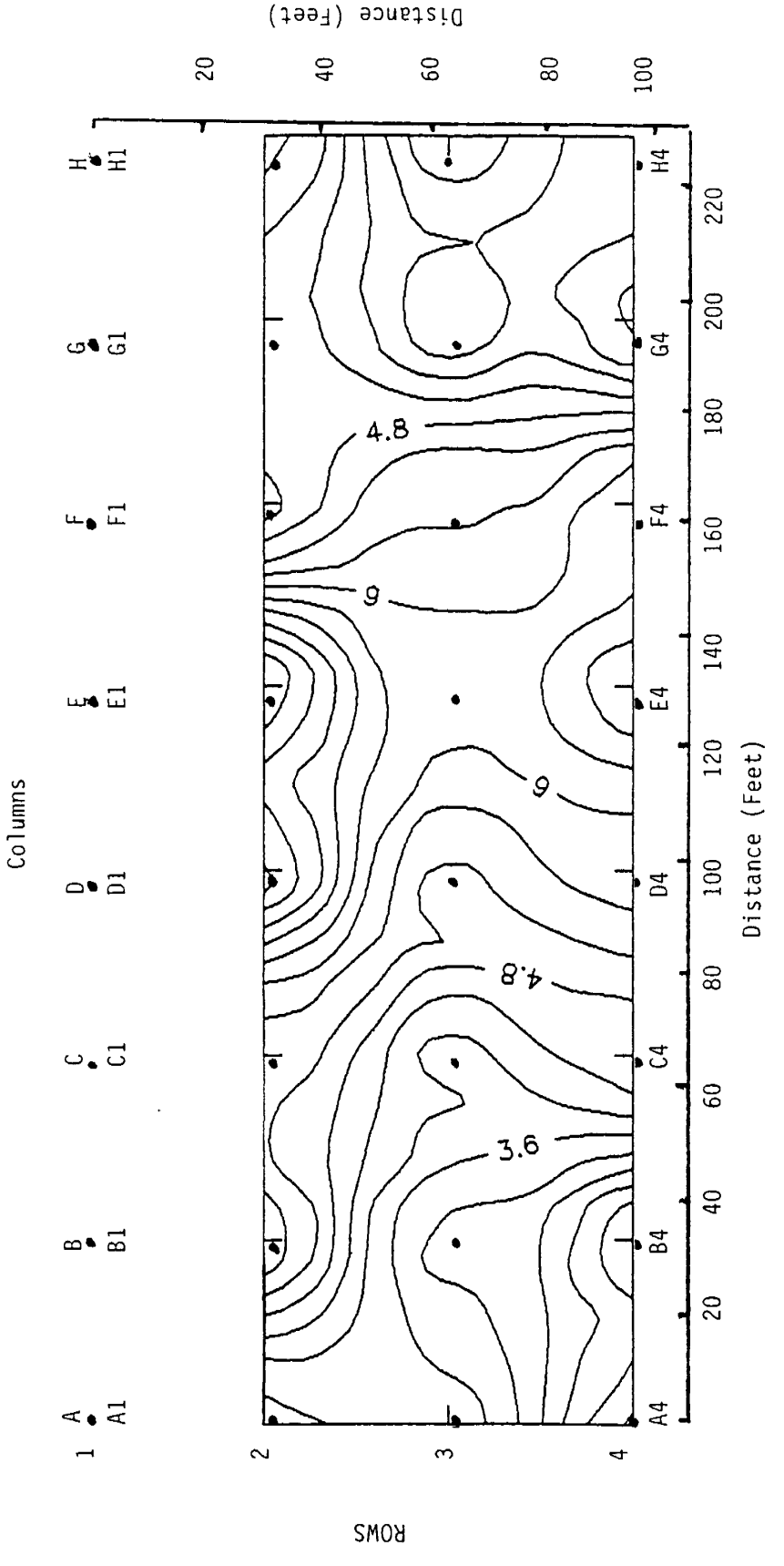

Figure 21. Conductivity Contour Map to a Depth of 24.6 ft at Site III Using the Terrain Conductivity Meter. The contour interval is 0.4 milliSieman per meter (mS/M).

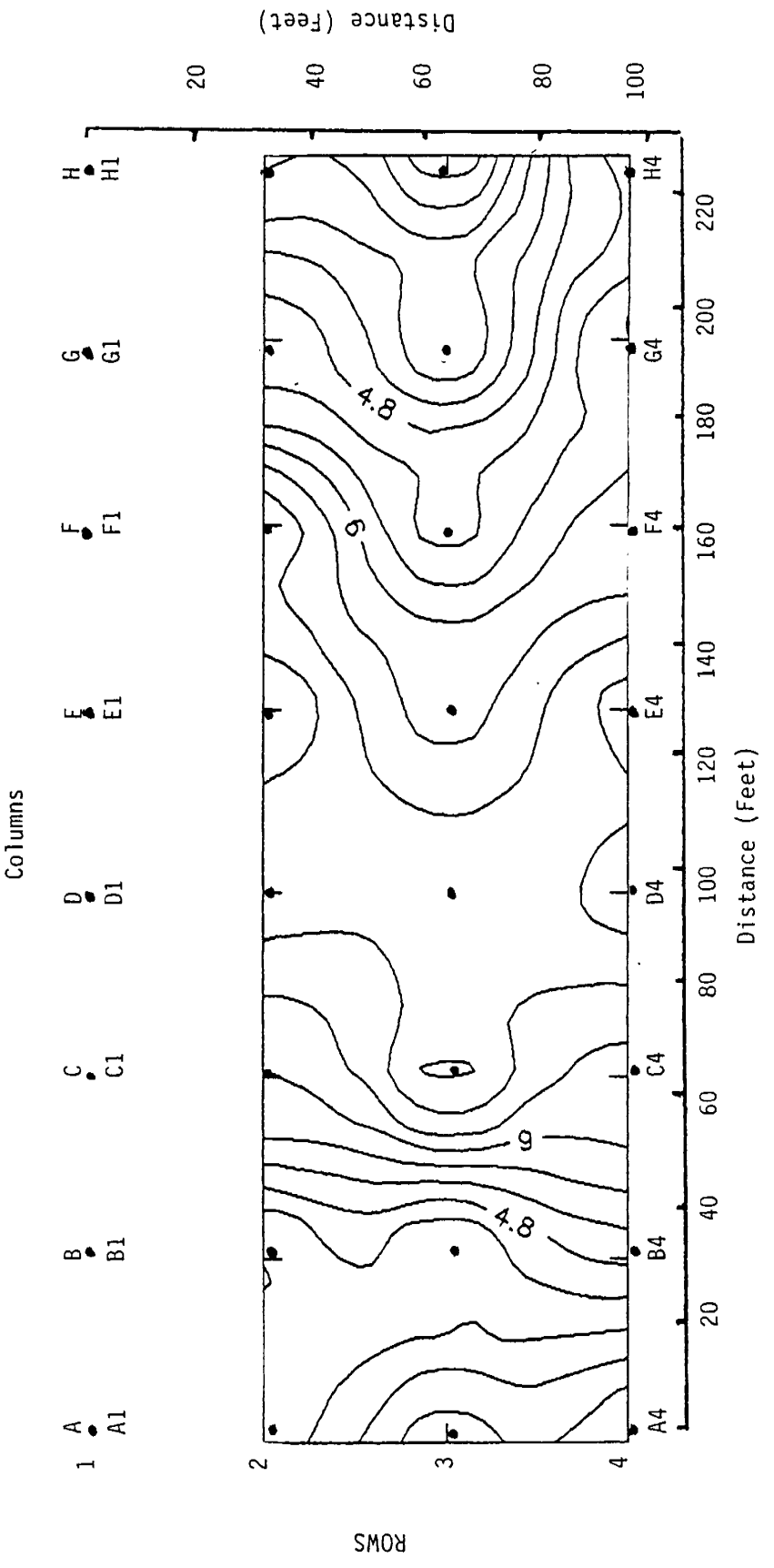

Figure 22. Conductivity Contour Map to a Depth of 49.2 ft at Site III Using the Terrain Conductivity Meter. The contour interval is 0.4 milliSieman per meter (mS/M).

geological studies in this area. In addition, since water is generally the conducting medium in an unconsolidated material, the central failed area of the slope should be closer to the water table and should be associated with higher conductivity values. The ER survey is shown in Figure 20 and confirms the TCM survey.

Spontaneous Potential Measurements

At site III, SP measurements were collected manually using two reference electrodes. Reference electrode 1 was located along row 1, 50 ft west of column A. Reference electrode 2 was located directly down gradient from the central measuring site in the quarry and covered by water. Data were obtained using reference electrode 1 on May 4, 5, 6, 9, 13, 17, and 23, and August 25, 1988. Data were obtained using reference electrode 2 on May 17 and 23; June 10; July 11 and 19; August 25 and 30; September 13 and 20; and November 22, 1988, and on May 19 and June 8, 1989. Using these SP data and computer software, SP contour maps were plotted for each day's data and are presented in Appendix C. The following information can be discerned from these SP data:

1. The low SP values are located in the up gradient, or row 1, near the crown of the slope.
2. The high positive SP values are located in row 4, nearest the water line of the quarry.
3. The greatest gradient of SP is located between G1 and F2 and D1 and E2.
4. The gradient between D1 and E2 on August 30, 1988, and on June 8, 1989, disappears. During those two dates, data were taken after a wet period. This is also the path of the most significant surface runoff and erosion along the crown of this slope.
5. SP measurements are independent of the reference electrode used. For example, on May 17 and 23, 1988, SP data were collected using both reference electrode 1 and 2. The SP contour maps are similar; they vary only in SP value.

Breakdown of Equipment

On September 1, 1989, all 32 SP electrodes were connected to the newly procured AMS, and SP readings, along with air and ground temperatures, were automatically and continuously taken every 15 min. The AMS used reference electrode 2 and was located at the central measuring site, along with a solar powered battery pack to provide continuous power to the system. The data disc was periodically removed and a new disc inserted by VDOT personnel. Readings were taken through April 1990 at this site. Due to equipment difficulties, solar power failure, and disc overload, there are gaps in the record. However, most discouraging was the breakage of the electrical wires going to the electrodes. Originally, this new AMS was to be installed during the fall of 1988, but procurement delays and laboratory testing and calibration postponed the installation until September 1989. During this

16-month period, breaks in electrode wires occurred. These breaks were not obvious since all electrodes when checked still had the wire securely attached to the CCS electrode. In addition, each electrode was giving a signal reading other than 0 volts, which would have been indicative of an open circuit. A possible reason for this was that all wires were covered and intertwined with the Kudzu vines that grew prolifically along this slope, which could have grounded the broken wire ends and therefore indicated a completed circuit. When the AMS electrodes and wires were recovered, breaks in 26 of the wires were discovered. Wire breakage at this site could have resulted from the following:

1. There are numerous groundhog holes along the slope. If a wire crossed the pathway of a groundhog and the animal considered it a nuisance, the groundhog with its powerful incisor teeth would have little difficulty breaking the wire.
2. Falling debris could have broken wires. The site has been used for illegal disposal of trash, with refrigerators and other large objects thrown over the slope during the period of investigation.
3. Erosion and failing of upper slope material could have resulted in wire breakage.
4. People on the measuring team could have tripped on the wires and broken them while inspecting electrodes.
5. Vandals could have broken wires.

Analysis of Spontaneous Potential Data

Those electrodes that remained intact during the AMS measuring period were A3, A4, B2, B3, and D2. The data for these electrodes are presented graphically in Appendix C. The data collection rate was every 15 min. Data for the first 6 days at this sampling rate (September 1 to 6, 1989) are shown unfiltered for electrode A3 in Figure 23. The AMS or electromagnetic air and ground signals could have caused spurious readings. In Figure 24, the obviously spurious readings were filtered. Also shown in Appendix C is the filtered signal for each electrode during this 6-day period. In Figures 25 and 26 are the 15-min sampling rates for air and ground temperatures taken at site III. The temperature of the surface of the ground lags slightly behind the air temperature, as would be expected. Also noted is the inverse effect temperature has on the SP value of each electrode; i.e., as temperatures increase and warm the SP electrode, the SP value decreases, and as temperatures decrease, the SP value increases.

To eliminate the diurnal temperature effects, all SP values were averaged and this daily average SP value was plotted for all these electrodes for the entire AMS measuring period (September 1989 to April 1990) and are shown in Appendix C. The breaks in the record are the result of equipment difficulties, lack of solar power supply, disc overloading, or an oversight in installing and programming a new disc to record data. An example of an electrode plot over the entire AMS

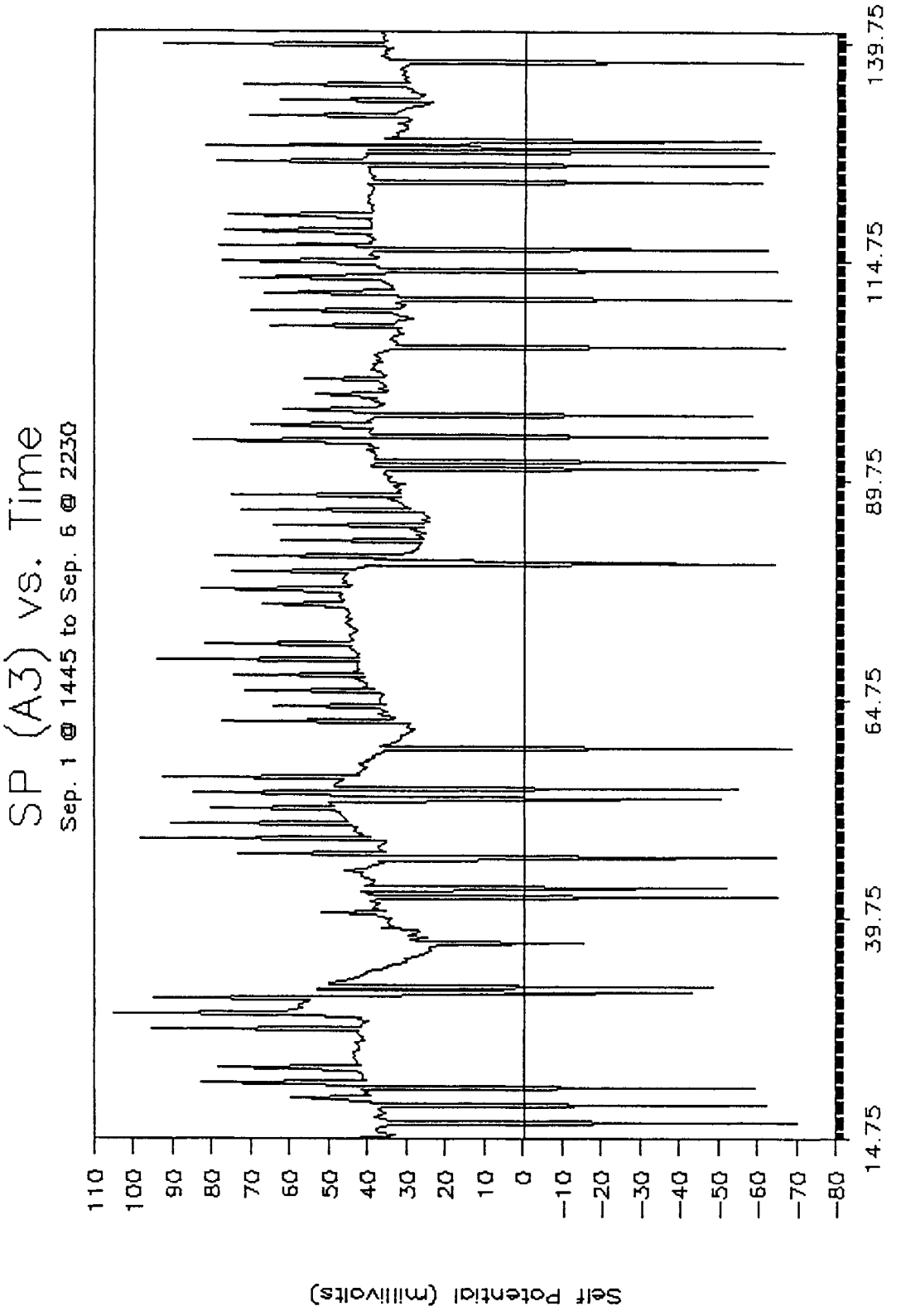

Figure 23. Spontaneous Potential Data for Electrode A3 at Site III.

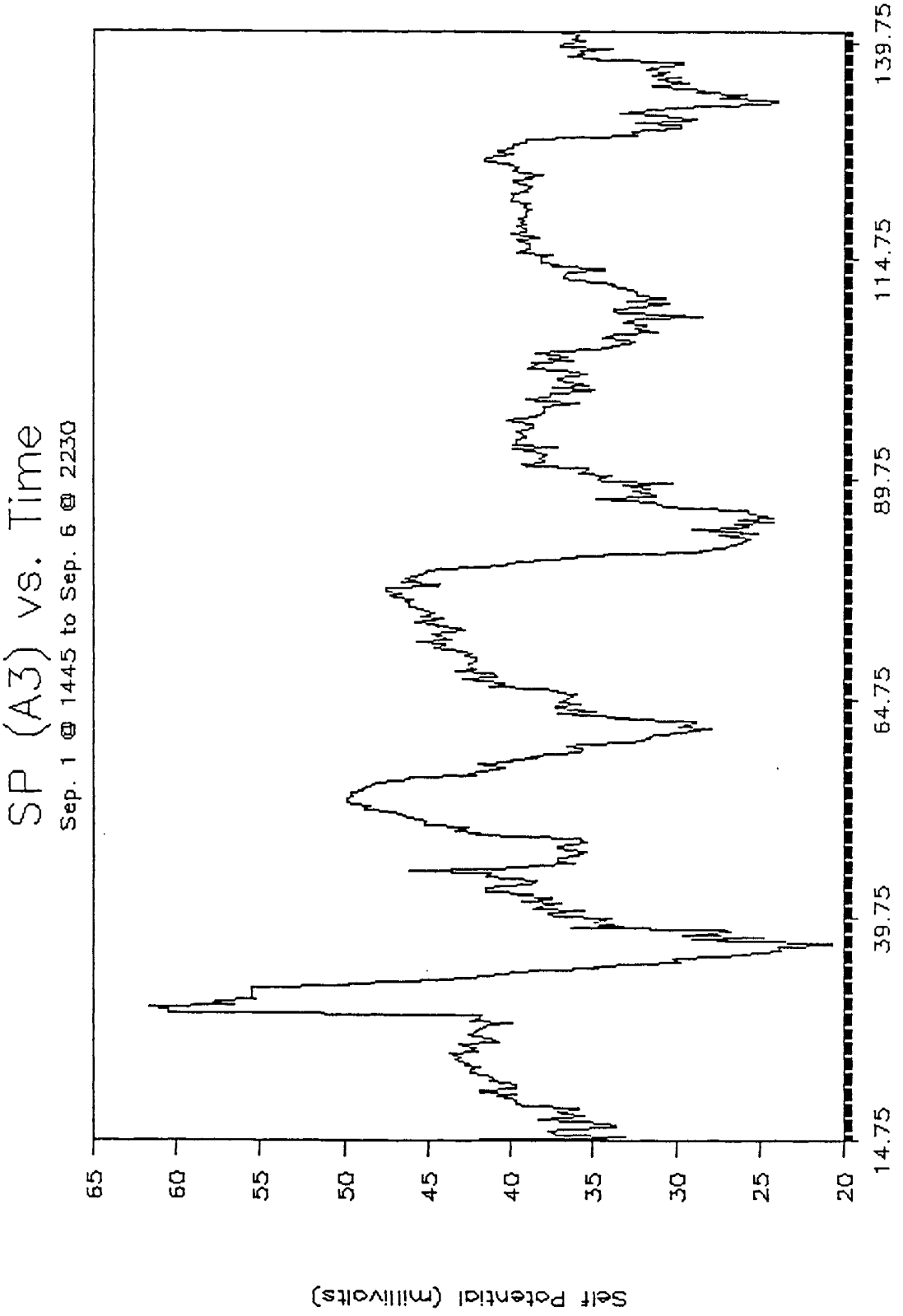

Figure 24. Filtered Spontaneous Potential Data versus Time for Electrode A3 at Site III.

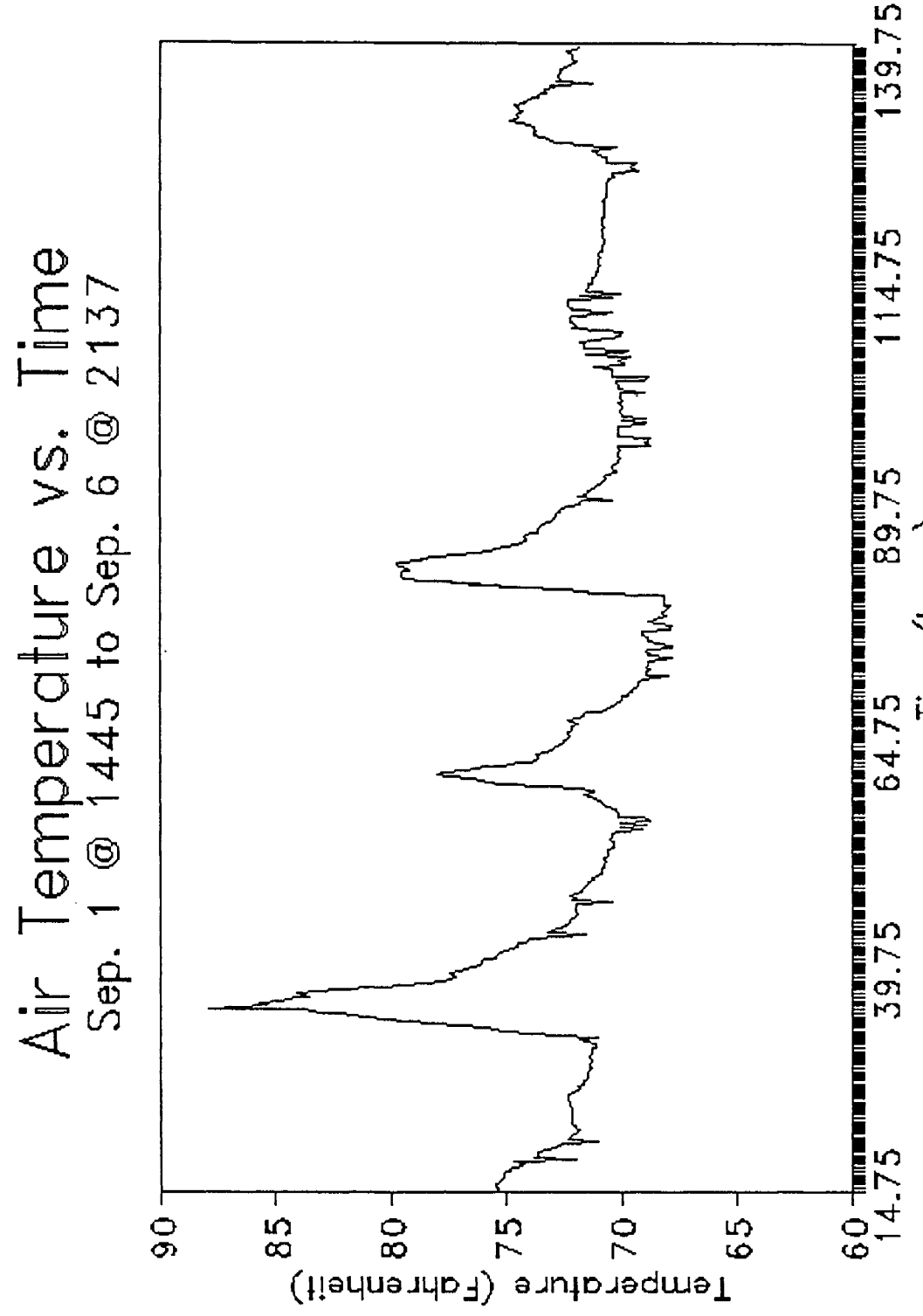

Figure 25. Air Temperature versus Time at Site III.

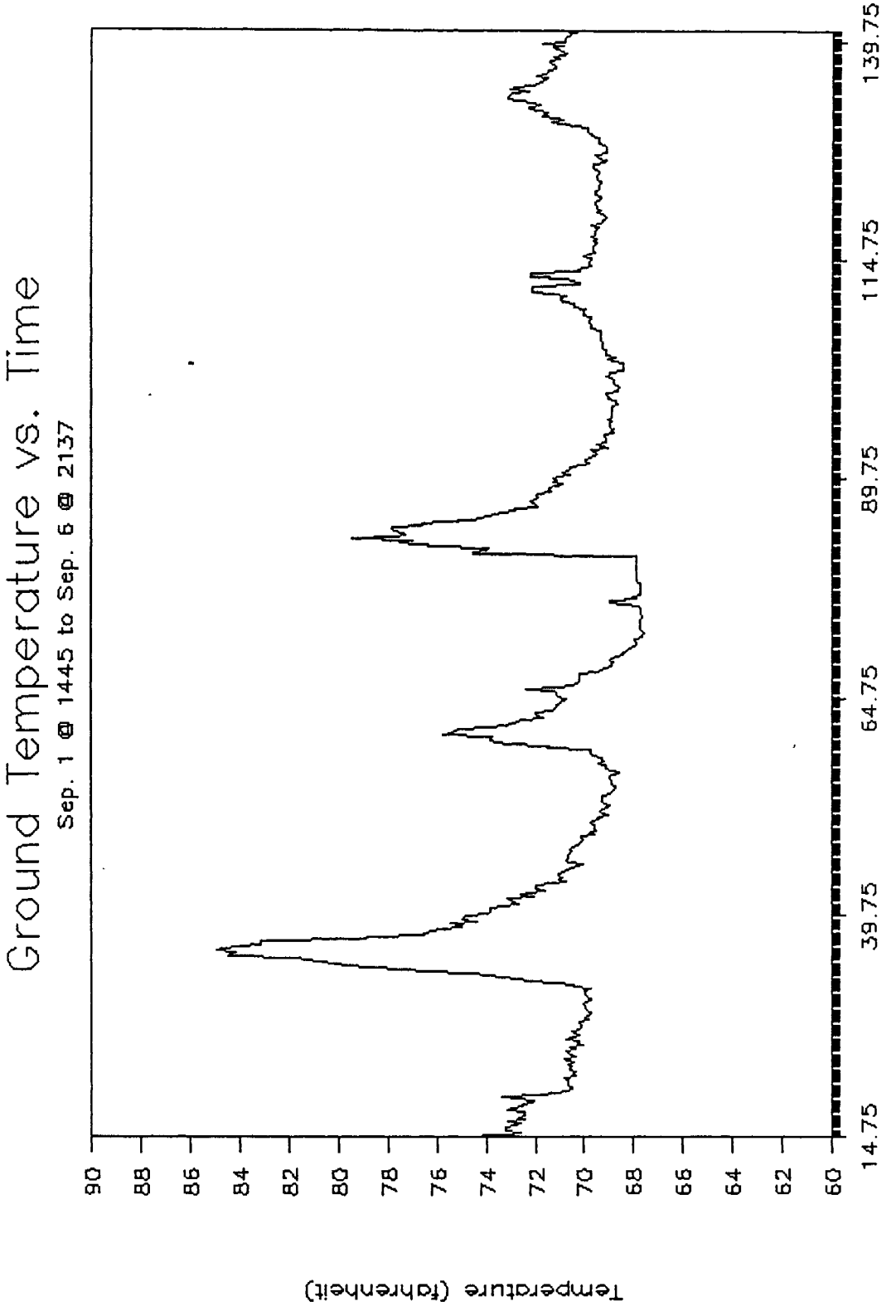

Figure 26. Ground Temperature versus Time at Site III.

measuring period is shown in Figure 27. Figure 28 shows the average daily air temperature and precipitation for the entire AMS measuring period. This record is continuous. Since the air temperature at the site correlated well with the temperature at the Lynchburg airport, the airport's record of temperature and precipitation is presented in this figure.

The VMI Dinastar penetrometer configured with a conductivity sensor cone was used to obtain geotechnical and electrical data along a center line profile down line of the slope at electrodes E1, E2, E3, and E4 and a profile outward from the center line toward the left flank at electrodes E3, D3, C3, and B3. The resistance and conductivity results of these seven penetration holes are presented in Appendix C. Since the unconsolidated soil was a cohesive clayey silt, the dynamic mode of penetration was used. The dynamic cone resistance was calculated using the Dutch formula, which considers only the theoretical potential energy (Triggs & Liana, 1988). Although this resistance is not so precise as the static cone resistance, the operation is faster and for this study provides sufficient accuracy, especially for the depth to bedrock and location of weak layers. Penetrometer refusal depth is considered 50 blows with less than 10 cm of penetration using a 30-kg hammer falling 20 cm. This is equivalent to a dynamic cone resistance of 70 kg/cm^2, or 70 ton/ft^2. Although this value may not be the actual resistance of the bedrock, the penetrometer is encountering regolith or material of significant strength.

In general, cone penetration resistance usually increases with depth. This is seen most descriptively in SP electrode bore hole sites E3 and E4. However, sometimes, very little resistance is encountered in the upper layers (see electrode E2 or B3) whereas at another site a hard surface layer exists below which softer material is encountered (see electrode E1). The softer or harder layers could be the result of the following: (1) a recently deposited loose unconsolidated material; (2) at site E2, located very close to the base of the main scarp, possibly a filled transverse crack; (3) at site E1, punching through the compacted road shoulder into weaker soils below; and (4) in some cases, after a recent rainfall, a soft surface layer that would not support the weight of the penetrometer (B3). In all cone resistance verse depth profiles, the importance of low cone resistance is an indicator of a weak seam or layers. It is along these weak layers that progressive failure of this slope is most likely to occur. In addition, the determination of penetration refusal as an indication of the depth of bedrock is extremely important. For example, depending on the environmental and geological conditions, the unconsolidated soil material may become saturated and simply slide off the bedrock surface.

The conductivity in micro mhos per cm versus depth profiles at the same location is also presented in Appendix C. In general, conductivity increases where cone resistance decreases. This would be indicative of moist, soft seams. It is along these moist seams that most water flow occurs. As the sensing cone probe enters into the regolith or approaches bedrock, the conductivity usually decreases. Conductivity values were lower on the crown of the slope, near site E1, and higher as the quarry water line was approached, at site E4. At site E4, conductivity values as high as 700 micro mhos per cm were recorded. At site E4, the water table is 2 ft below the surface, whereas at site E1, the water table is nearly 40 ft below the surface

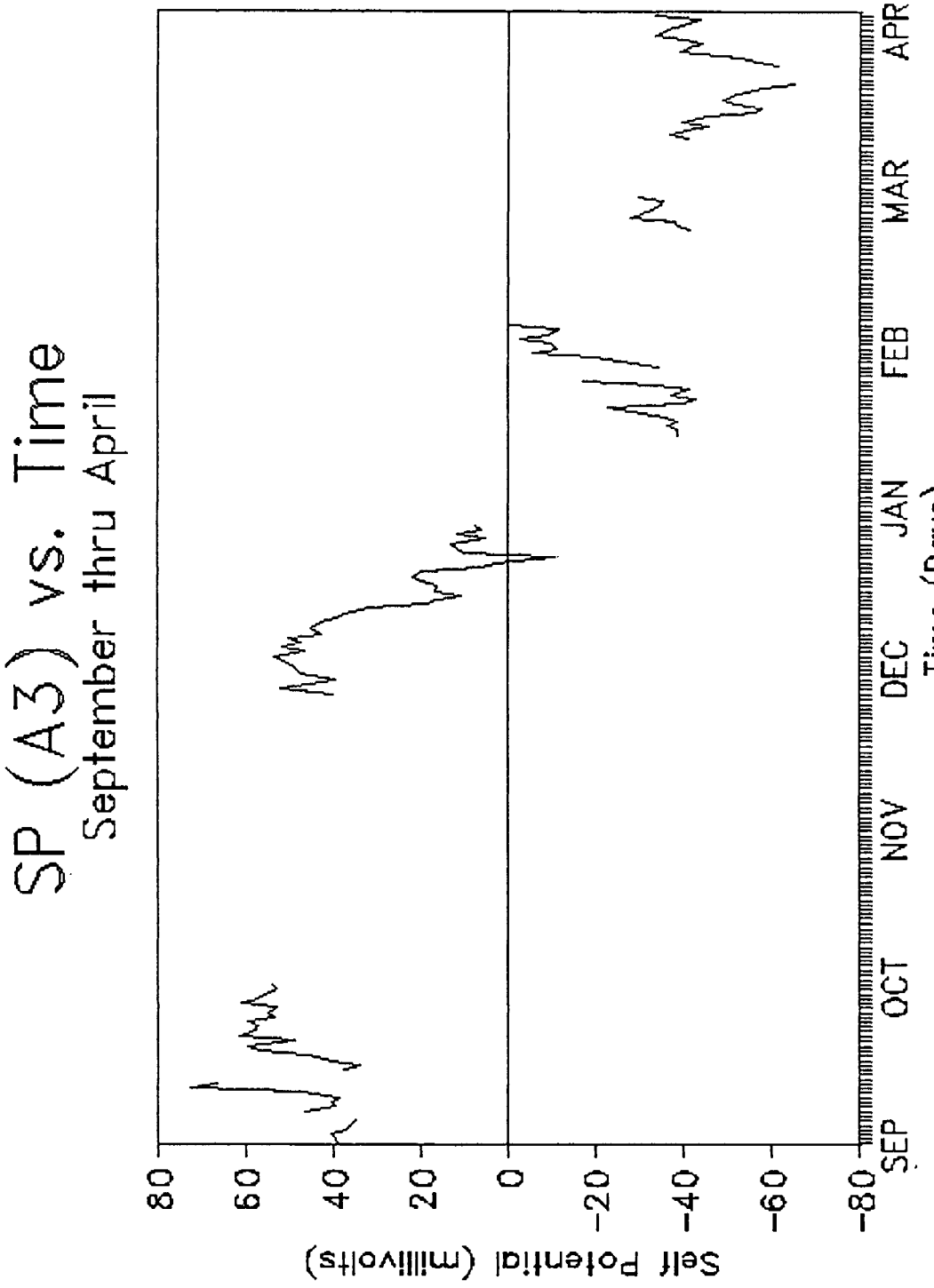

Figure 27. Filtered and Daily Averaged Spontaneous Potential Data versus Time for Electrode A3 at Site III for the Entire Automatic Measuring Period of Data Collection.

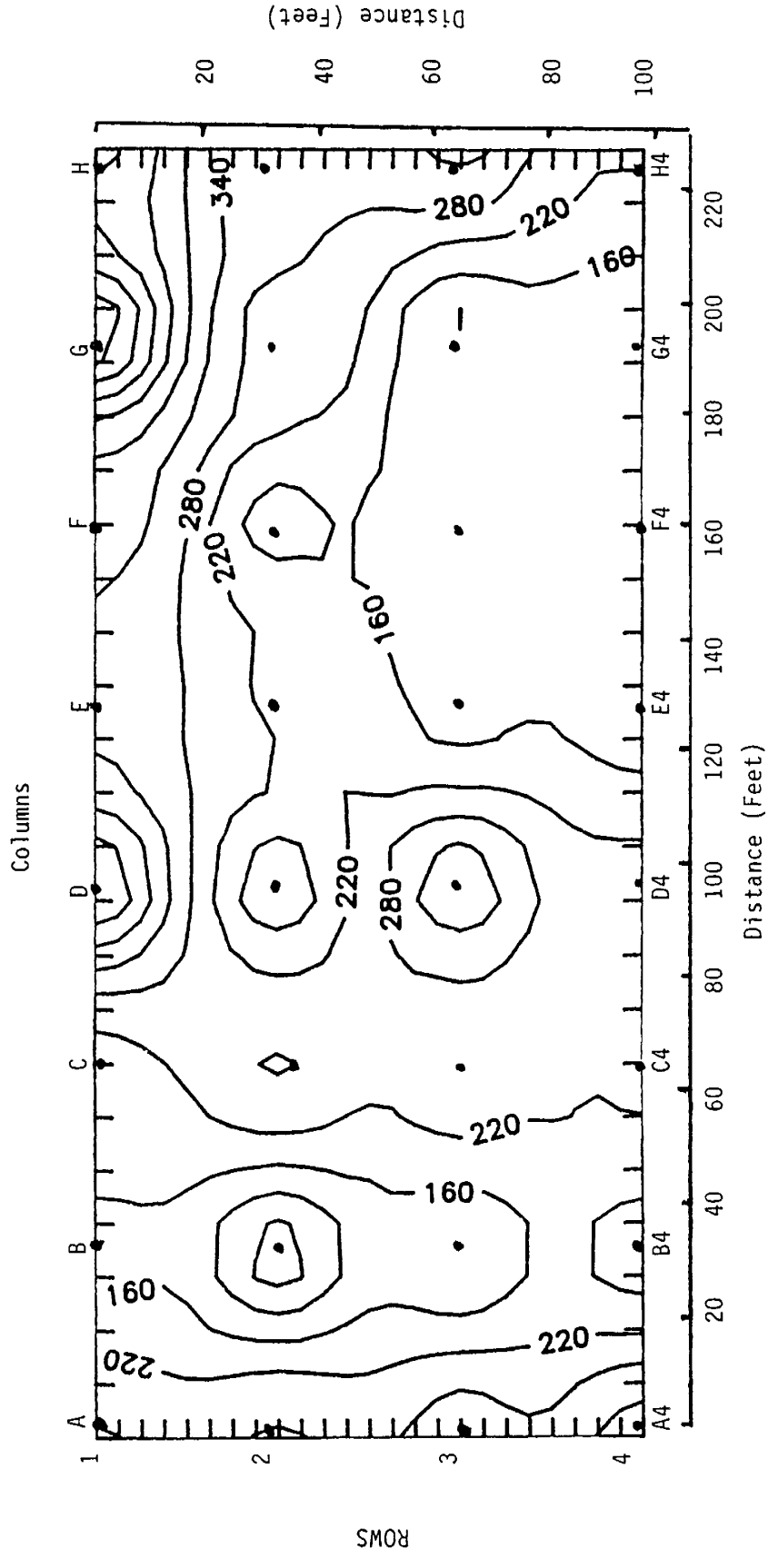

Figure 28. Normalized Spontaneous Potential Data at Site III for May 4, 1988. The contour interval is 60 mv.

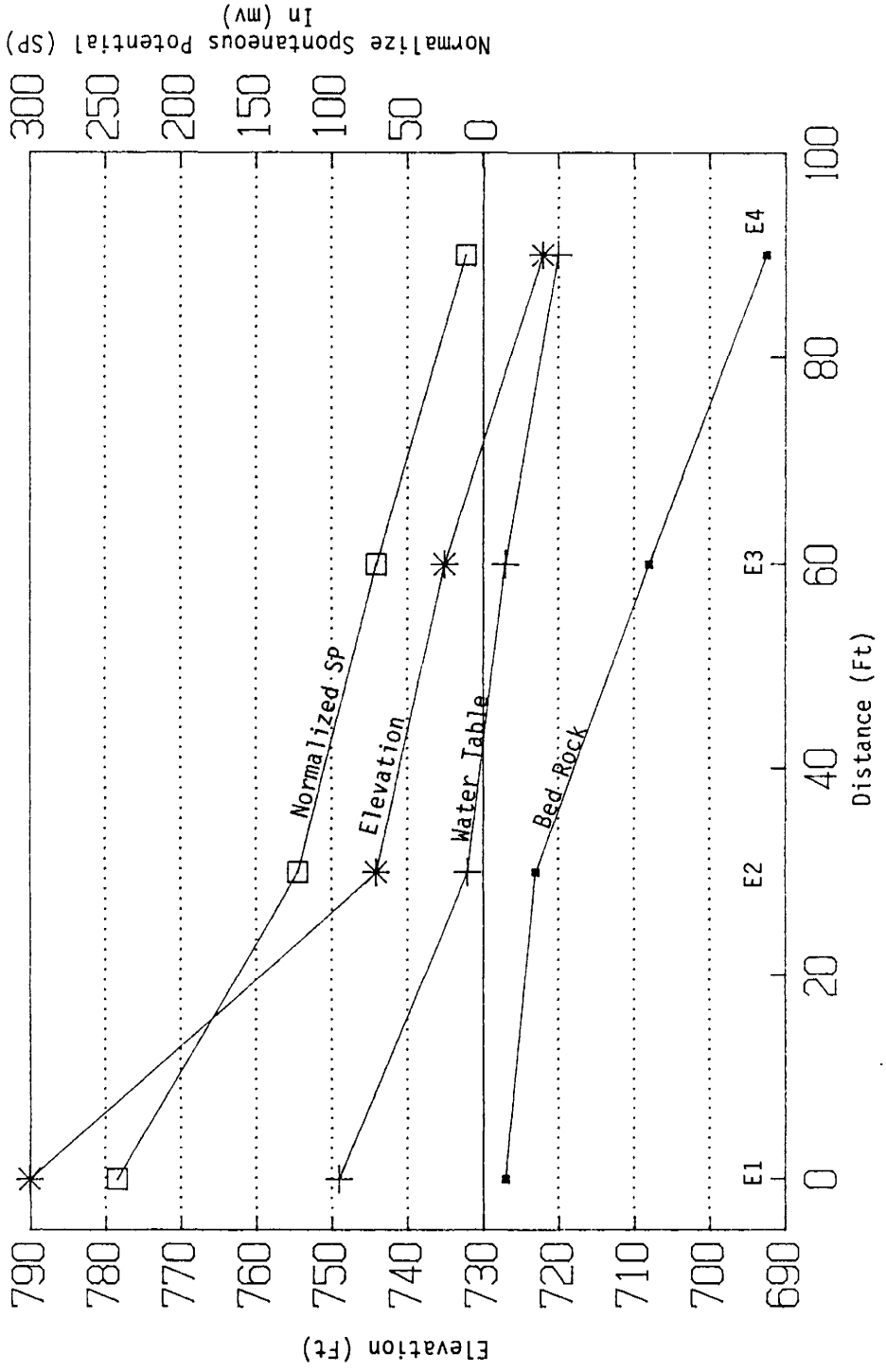

Figure 29. Cross-Sectional Profile of Elevation, Water Table, Depth of Bedrock, and Normalized Spontaneous Potential Values at Electrodes E1, E2, E3, and E4 at Site III.

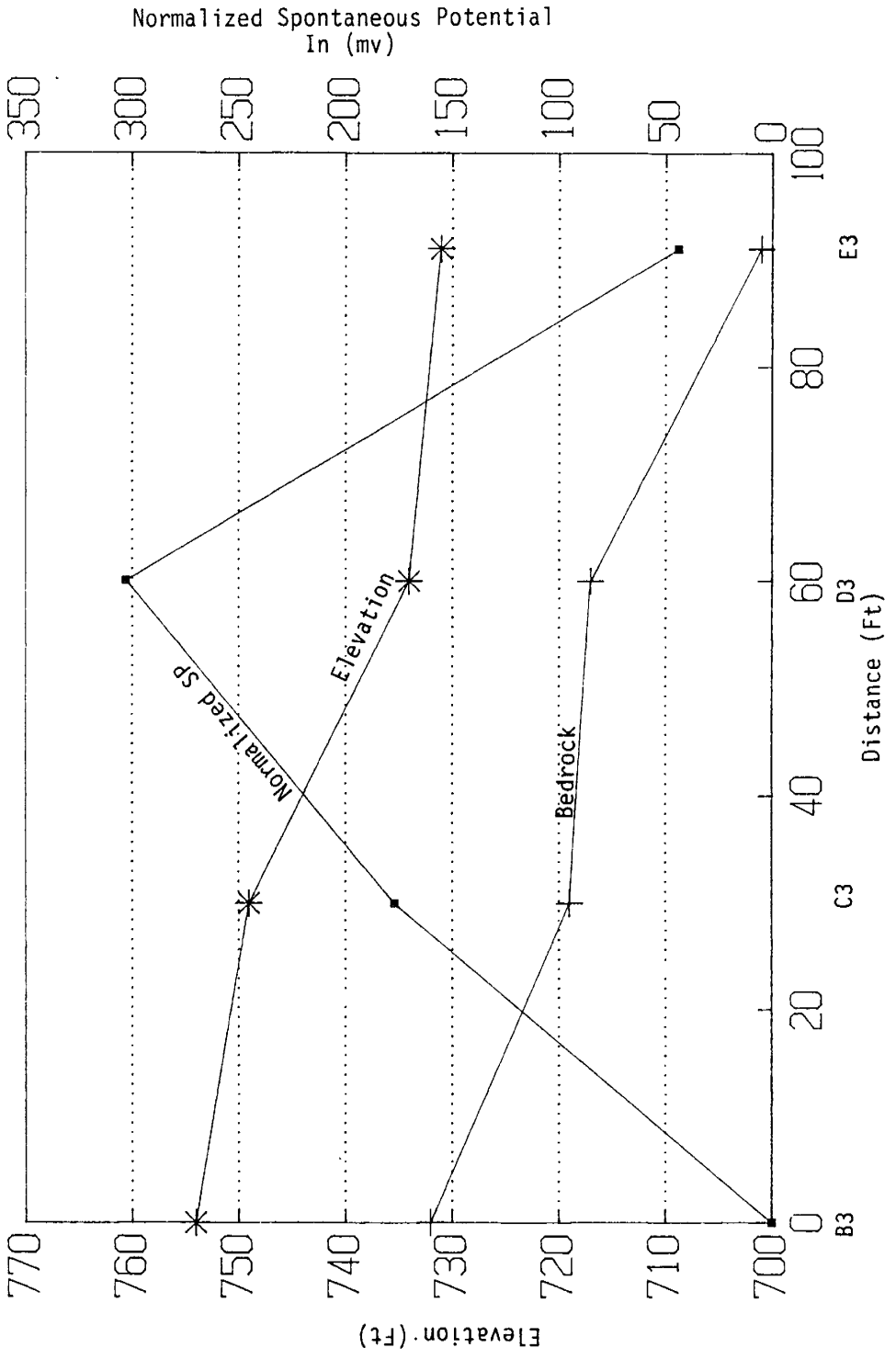

Figure 30. Cross-Sectional Profile of Elevation, Depth of Bedrock, and Normalized Spontaneous Potential Values at Electrodes E3, D3, C3, and B3 at Site III.

—well below the penetration depth.

The depth to the water table at sites E2, E3, and E4 was obtained by inserting plastic pipe into the penetrometer hole after the penetrometer was extracted. The pipes were then sounded after a 48-hr period to determine the depth to the water table. The two VDOT inclinometer casings on either side of Route 670 allowed the approximation of the depth of the water table at site E1.

If one normalizes the SP data, as previously explained, for any given day, a contour and surface projection map can be developed, as shown in Figure 28. These normalized maps show the lowest (negative) SP values as peaks and the highest (positive) SP values as low areas. Using the normalized data, a cross-sectional profile may be developed. Figures 29 and 30 are cross-sectional profiles along the slope's center line (column E including E1, E2, E3, and E4) and transversely (row 3 from the center line to the left flank, including E3, D3, C3, and B3), respectively. The elevations, approximate depth to bedrock, and normalized SP values are also shown. In Figure 29, the depth to the water table is also given. There is a direct relationship among the bedrock profile, topography, water table, and normalized SP values. For example, in Figure 29, as the hydraulic gradient changes along the water table, the normalized SP value also directly changes. The hydraulic gradient is greatest at the crown of the slope and is least at the quarry water line. Therefore, the flow rate will also be greatest where the normalized SP value and hydraulic gradient are the greatest. Figure 30 shows another factor causing the flow rate to increase. The profile water table was determined only at site E3, and therefore the hydraulic gradient cannot be directly determined; however, by noticing the depth to bedrock and the topographic profile, a constriction may be seen to exist at electrode D3. This constriction will result in an increase in the subsurface flow rate. As the flow rate increases, so should the normalized SP value, as indicated in Figure 30.

CONCLUSIONS

1. With changes in the physical factors that affect SP values, the expected changes in SP values were measured. Although the SP values that were recorded at any given electrode varied over a large range, the rankings of the values among different electrode sites were generally consistent. This was also true if the position of the reference electrode was changed. It appeared that precipitation and changes in surface ground temperature had the greatest affect on the variation of SP values over the testing period.

2. The SP technique used in this work was effective in detecting low SP anomalies from which areas of high subsurface flow paths could be inferred. These anomalous areas would have high hydraulic gradients and would be excellent locations at which to install horizontal drains to remediate these potential failure areas.

3. The SP technique in conjunction with the AMS at site I was effective in monitoring heavy rainfall (nearly 5 in) during the period August 23 to September 4, 1988. At 5 p.m. on August 29, all SP electrodes being monitored peaked simultaneously to a 400-mv reading. This was indicative of a saturated slope condition, although failure did not occur at this time. Had these high SP values continued or persisted, the slope's stability might have been in jeopardy. In addition, the continual monitoring of the slopes at sites I and III with the AMS allowed the visualization of these slopes expanding and contracting, saturating and draining, or heating and cooling, specifically with precipitation and temperature changes.

4. The development and implementation of a system that would warn of an incipient slope failure was accomplished by combining a real time recording system with the spontaneous potential measurement system. The monitoring and recording of the effect of the heavy rainfall at site I, as mentioned above, demonstrates that accomplishment. The only action required to provide a warning would be to arrange for the transmission of a signal to a centralized slope stability monitoring site. The warning signal would be transmitted if a spontaneous potential level that is considered to be dangerous is reached and maintained over a given period of time.

5. The TCM and ER tests were effective at these slope sites in western Virginia, specifically in determining the bedrock topography and consistency since the depth of bedrock was relatively close to the surface. The TCM data were compared with borings and penetrometer measurements at sites I and III to confirm this finding. The main advantages of the TCM are that it is portable, can provide rapid information to depths of 197 ft along steep slopes, and requires only two people for operation.

6. The VMI Dinastar penetrometer with the attached conductivity sensor was very effective in obtaining electrical and geotechnical depth profiles along the slope at site III. This small, lightweight penetrometer could obtain these data at locations where conventional penetrometers or boring rigs would be prohibited. The penetrometer with sensor provided data on soil strength, soil conductivity, and depth to bedrock along two slope profiles. Specifically noted were high-moisture layers, indicated by high conductivity values. These high-moisture layers correlated with low soil strength. This correlation provided insight into the location of weak layers that could delineate slip planes along which slope failure might occur. The knowledge of the location and thickness of these layers would provide valuable information in the slope remediation process.

RECOMMENDATIONS

To test the applicability of this work to a slope being considered for remediation, the following procedure is recommended:

1. Conduct a TCM survey to determine electrically anomalous conditions to a depth of 197 ft over the area of the slope to be remediated, and, if the bedrock is within this depth, determine the bedrock profile.

2. Install SP electrodes to determine the location of high surface flow paths and high hydraulic gradients.

3. Confirm these locations with the penetrometer conductivity sensor to determine the thickness of weak, high-moisture layers.

4. Install horizontal drains to dewater these layers, and monitor dewatering with the SP electrodes connected to the AMS.

This procedure could be conducted at minimal cost since all equipment is currently at VMI and only supplies (wires, electrodes, clips, etc.) would be required. Confirmation of the effectiveness of using these electrical measurement techniques could result in significantly better remediation success and significantly reduced maintenance costs. In addition, as more confidence is obtained in the monitoring system and the electrical measurement techniques, the feasibility of a cost-effective warning system may become a reality.

1912

REFERENCES

Anderson, L. A., & Johnson, G. R. (1975). Application of the SP Method to Geothermal Exploration in Long Valley, California. *Journal of Geophysical Research, 81*(8): 1527–1532.

Bartholomew, M. J. (1971). Geology of the Humpback Mountain Area of the Blue Ridge in Nelson County and Augusta County, Virginia. *Dissertation Abstracts International, 32*(5): 1–158.

Bogoslovsky, V. A., & Ogilvy, A. A. (1972). The Study of Streaming Potentials on Fissured Media Models. *Geophysical Prosp., 20*: 109–117.

Brown, W. R. (1958). *Geology and Mineral Resources of the Lynchburg Quadrangle, Virginia.* Bulletin No. 74. Charlottesville: Virginia Division of Mineral Resources.

Butler, D. K. (1984). Geophysical Methods for Seepage Detection, Mapping, and Monitoring. *Proceedings of the 54th Annual Meeting of the Society of Exploration Geophysicists.* Atlanta, Georgia.

Cooper, S. S. (1982). *Geophysical Investigation at Gathright Dam.* Technical Report No. GL-82-2. U.S. Army Corps of Engineers, Waterways Experiment Station, Vicksburg, Mississippi.

Cooper, S. S. (1983). *Acoustic Resonance and Self-Potential Applications: Medford Cave and Manatee Spring, Florida.* Technical Report No. GL-83-1. U.S. Army Corps of Engineers, Waterways Experiment Station, Vicksburg, Mississippi.

Cooper, S. S., & Koester, J. P. (1984). Detection and Delineation of Subsurface Seepage Using the Spontaneous-Potential Method. *Proceedings of the 54th Annual Meeting of the Society of Exploration Geophysicists.* Atlanta, Georgia.

Corwin, R. W., & Hoover, D. B. (1978). The Self-Potential Method in Geothermal Exploration. *Geophysics, 55*: 226–245.

Corwin, R. W. (1984). The Self-Potential Method and Its Engineering Applications: An Overview. *Proceedings of the 54th Annual Meeting of the Society of Exploration Geophysicists.* Atlanta, Georgia.

Corwin, R. W. (1989). *Development of Self-Potential Interpretation Techniques for Seepage Detection.* Technical Report No. REMG-GT-6. U.S. Army Corps of Engineers, Waterways Experiment Station, Vicksburg, Mississippi.

Ernston, K., & Scherer, H. U. (1986). Self-Potential Variations with Time and Their Relation to Hydrogeologic and Meteorological Parameters. *Geophysics, 51*: 5923–5928.

Fitterman, D. V. (1978). Electrokinetic and Magnetic Anomalies Associated with Dilatant Regions in a Layered Earth. *Journal of Geophysical Research, 83*(B12): 5923–5928.

Keefer, D. K.; Wilson, R. C.; Mark, R. K.; Brabb, E. E.; Brown, W .M. III; Ellen, S. E.; Harp, E. L.; Wieczorek, G. F.; Alger, C. S.; & Zatkin, R. S. (1987). Real-Time Landslide Warning During Heavy Rainfall. *Science, 238*: 921–925.

Keller, G. V., & Frischknecht, F. C. (1966). *Electrical Methods in Geophysical Prospecting*. New York: Pergamon Press.

Koester, J .P.; Butler, D. K.; Cooper, S. S.; & Llopis, J. L. (1984). *Geophysical Investigations in Support of Clearwater Dam Comprehensive Seepage Analysis.* Miscellaneous Paper No. GL-84-3. U.S. Army Corps of Engineers, Waterways Experiment Station, Vicksburg, Mississippi.

Ogilvy, A. A.; Ayed, M. A; & Bogoslovsky, V .A. (1969). Geophysical Studies of Water Leakages from Resevoirs. *Geophysical Prosp., 27*: 36–62.

Rodriquez, B. D. (1984). A Self-Potential Investigation of a Coal Mine Fire. *Proceedings of the 54th Annual Meeting of the Society of Exploration Geophysicists.* Atlanta, Georgia.

Triggs, J. F., Jr., & Liang, R. Y. K. (1988). Development of and Experiences from a Light-Weight, Portable Penetrometer Able To Combine Dynamic and Static Cone Tests. *Proceedings of the First International Symposium on Penetration Testing,* ISOPT-1, Orlando, Florida.

Varnes, D. J. (1978). Slope Movement Types and Processes. *Landslides: Analysis and Control,* R. L. Schuster and R. J. Krizek, eds. TRB Special Report No. 176. Washington, DC: Transportation Research Borad.

Wait, J. R. (1962). A Note on the Electromagnetic Response of a Stratified Earth. *Geophysics, 27*: 1130–1144.

APPENDIX A

Data from Site I

1916

DATA PRESENTED

1. The array pattern showing the position and labels of the 28 electrodes. This is also Figure 5 in the text but is presented again in this appendix to assist the reader in reading the other maps.

2. The spontaneous potential (SP) contour maps obtained from SP data collected on the following dates: May 4, 5, 6, 9, 11, 13, 20, 23, and 31; June 10, 16, and 29; and July 1, 1988.

3. Hourly SP values obtained using the automated measuring system (AMS) for electrodes C0, D0, F0, G0, A1, B1, C1, D1, E1, F1, G1, H1, E2, and F2. The measuring period presented is August 25 to September 4, 1988.

4. Daily precipitation and average temperature for the period August 25 to November 16, 1988. This was the period during which the AMS was activated at Site I.

5. Daily average SP values obtained using the AMS of electrodes C0, D0, F0, G0, A1, B1, C1, D1, E1, F1, G1, H1, E2, and F2 for the period August 25 to November 16, 1988.

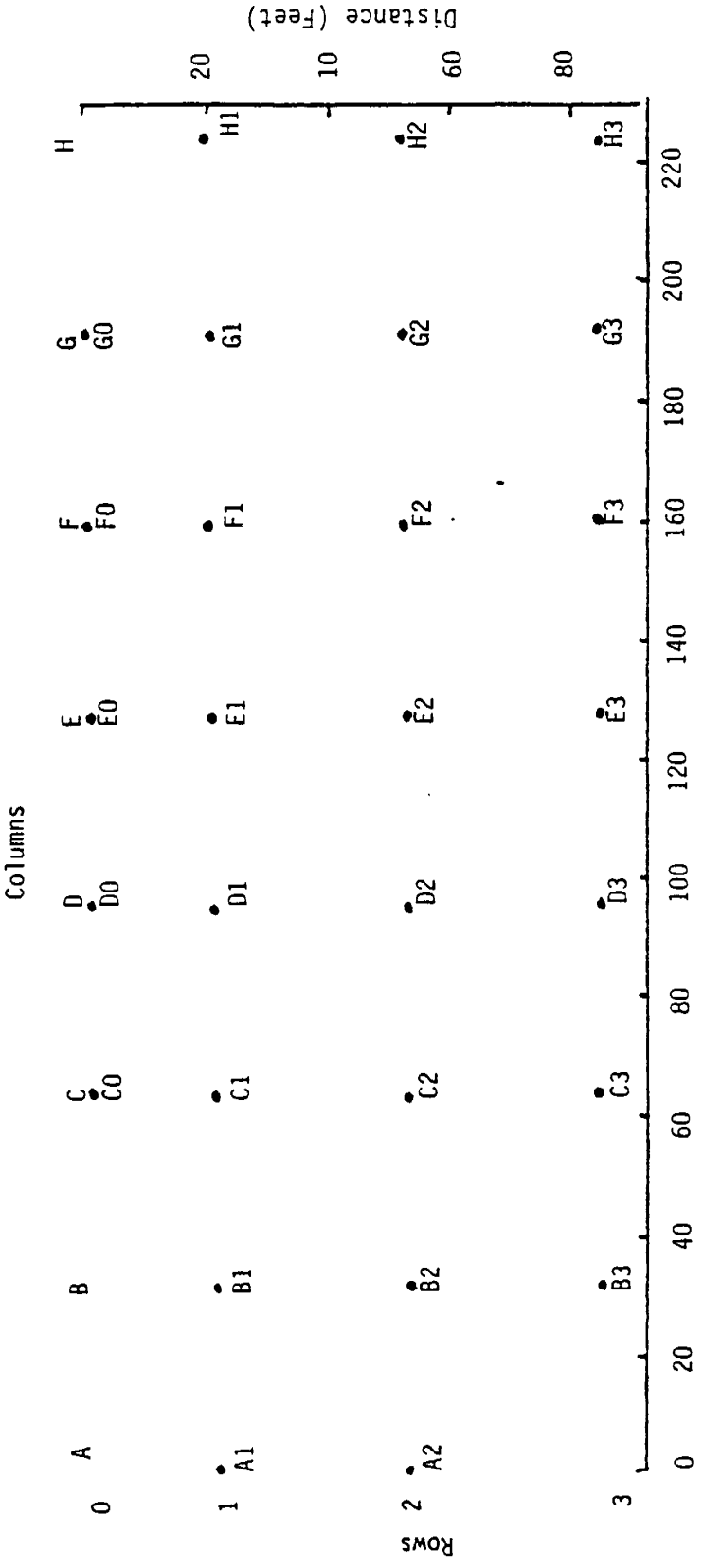

Figure 5: Spontaneous Potential Electrode Array Pattern at Site I.
The 28 Electrodes Installed Are Labeled C0 Through H3.

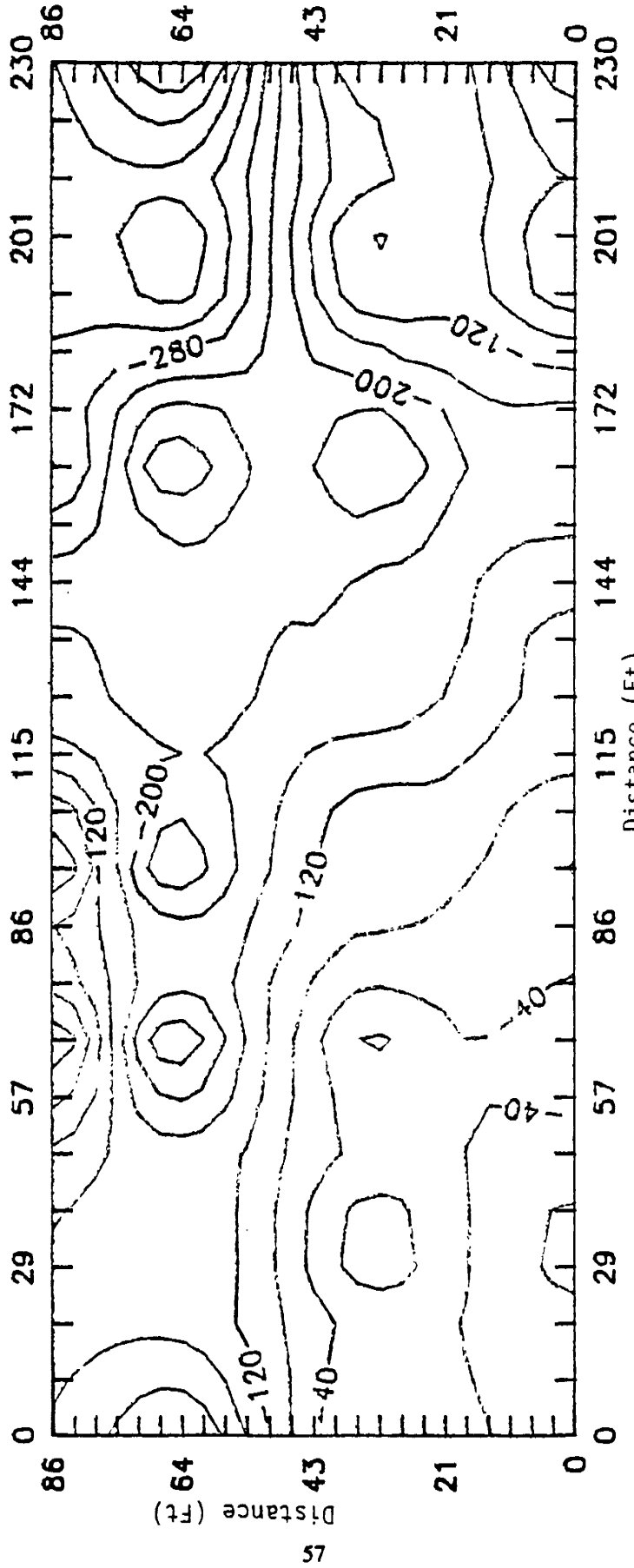

SP Contour Map for Site I on 4 May 1988.
Contour Interval is 40 mv.

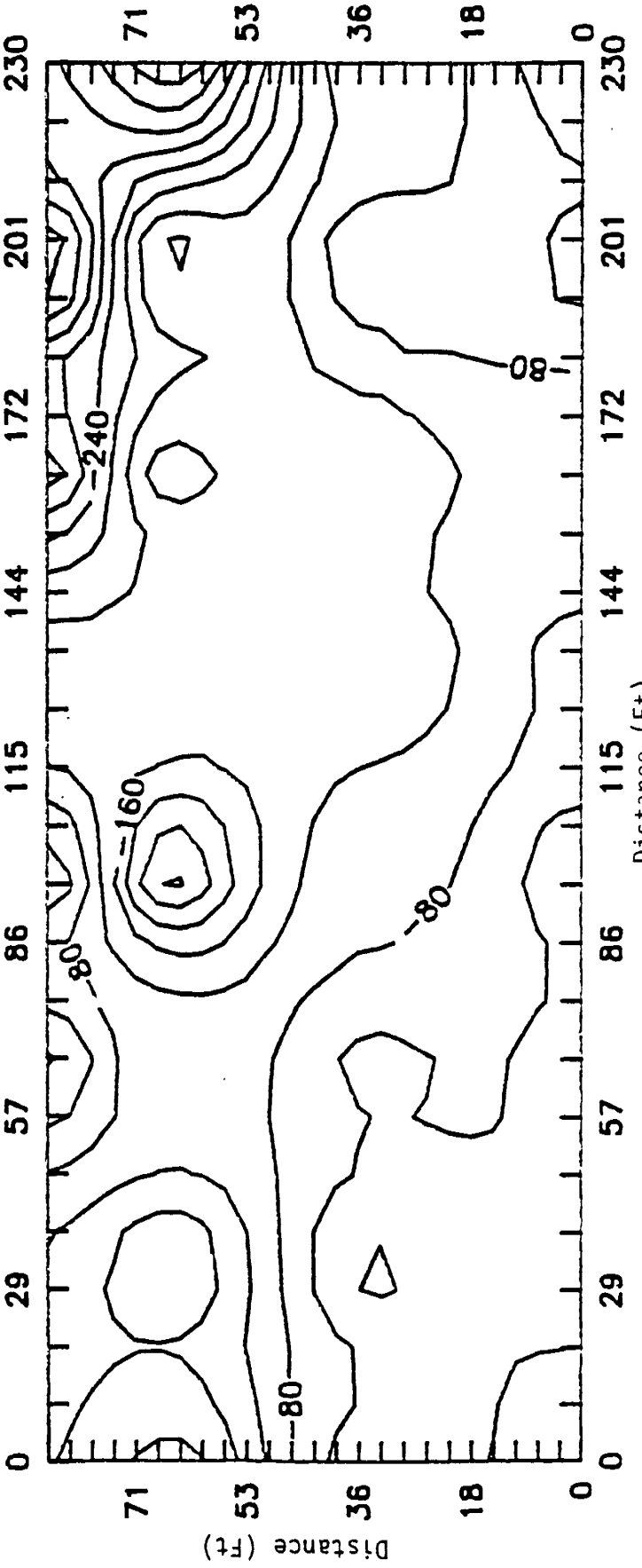
Distance (Ft)
0
29
57
86
115
144
172
201
230
71
53
36
18
0
-80
-160
-240
Distance (Ft)
SP Contour Map for Site I on 5 May 1988
Contour Interval is 40 mv.

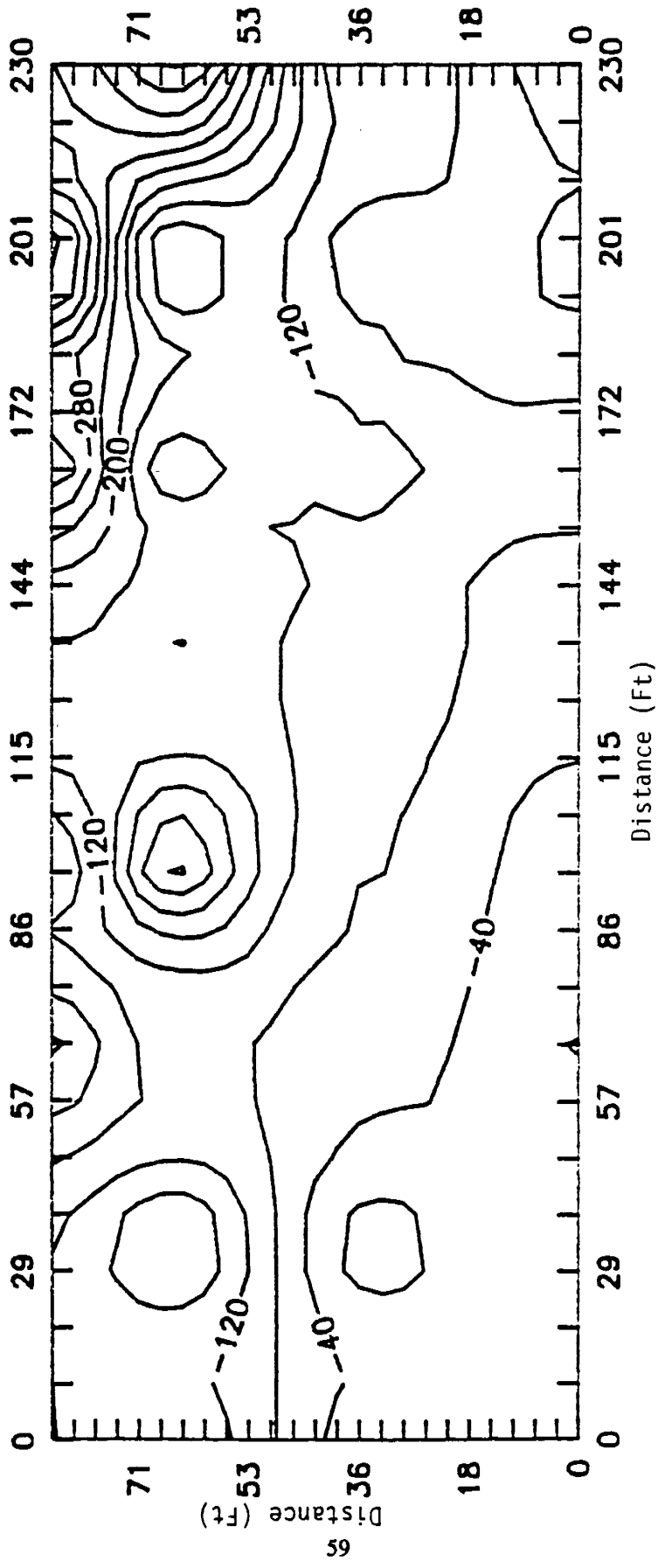

SP Contour Map for Site I on 6 May 1988
Contour Interval is 40 mv.

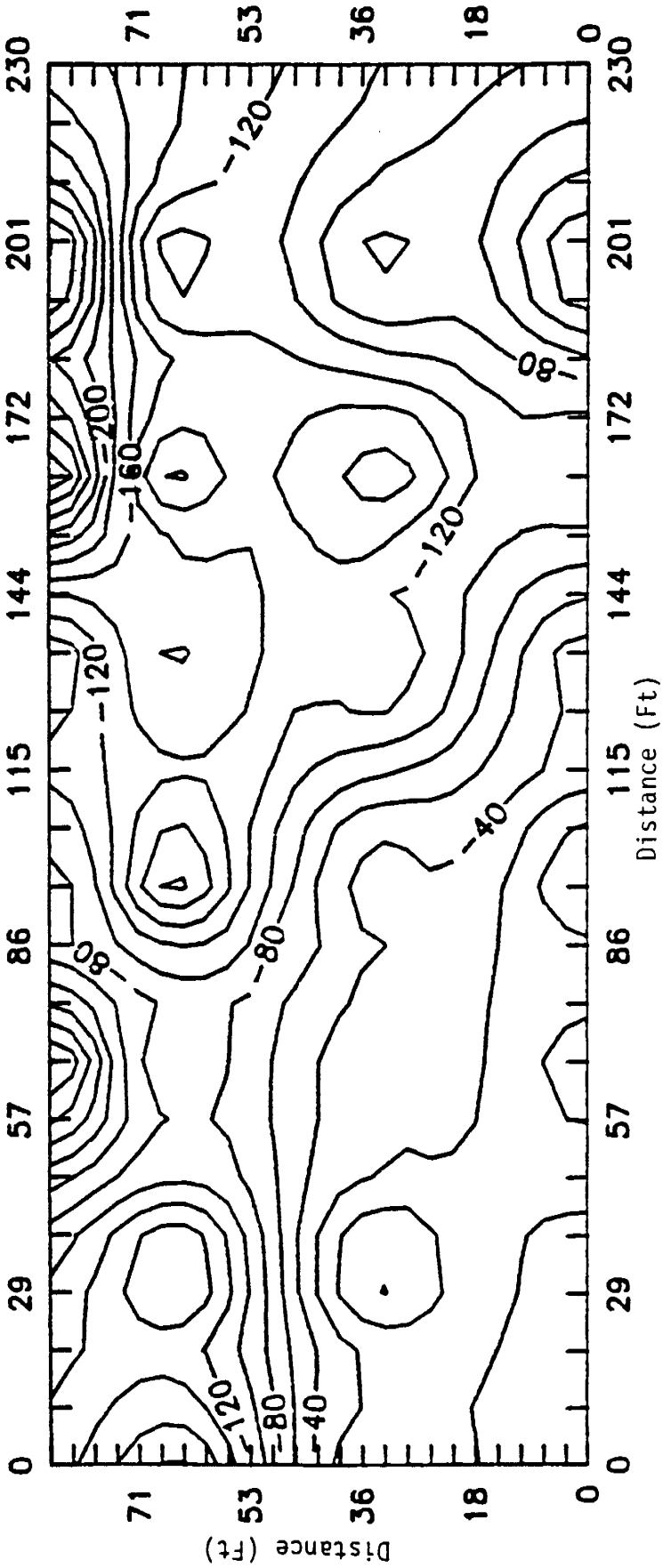

SP Contour Map for Site I on 9 May 1988
Contour Interval is 20 mv.

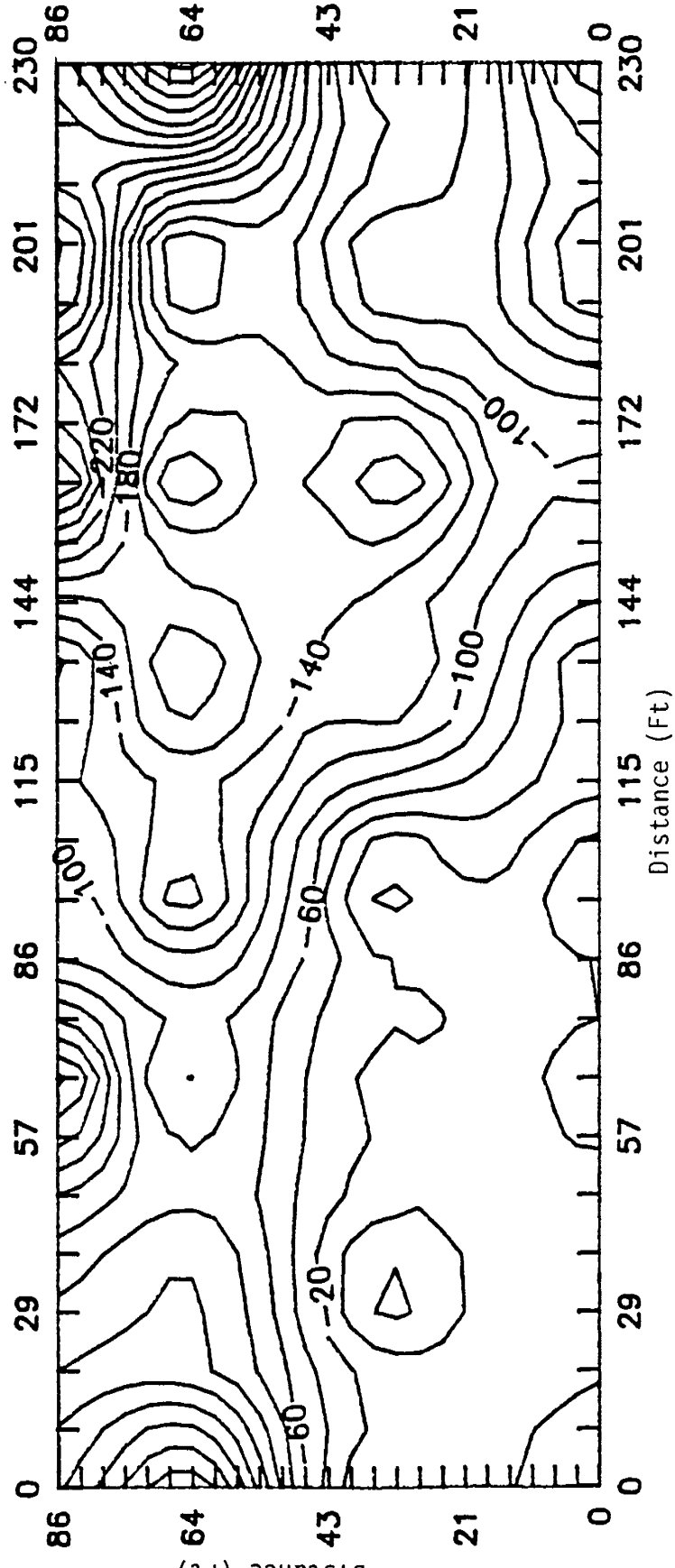

SP Contour Map for Site I on 11 May 1988.
Contour Interval is 20 mv.

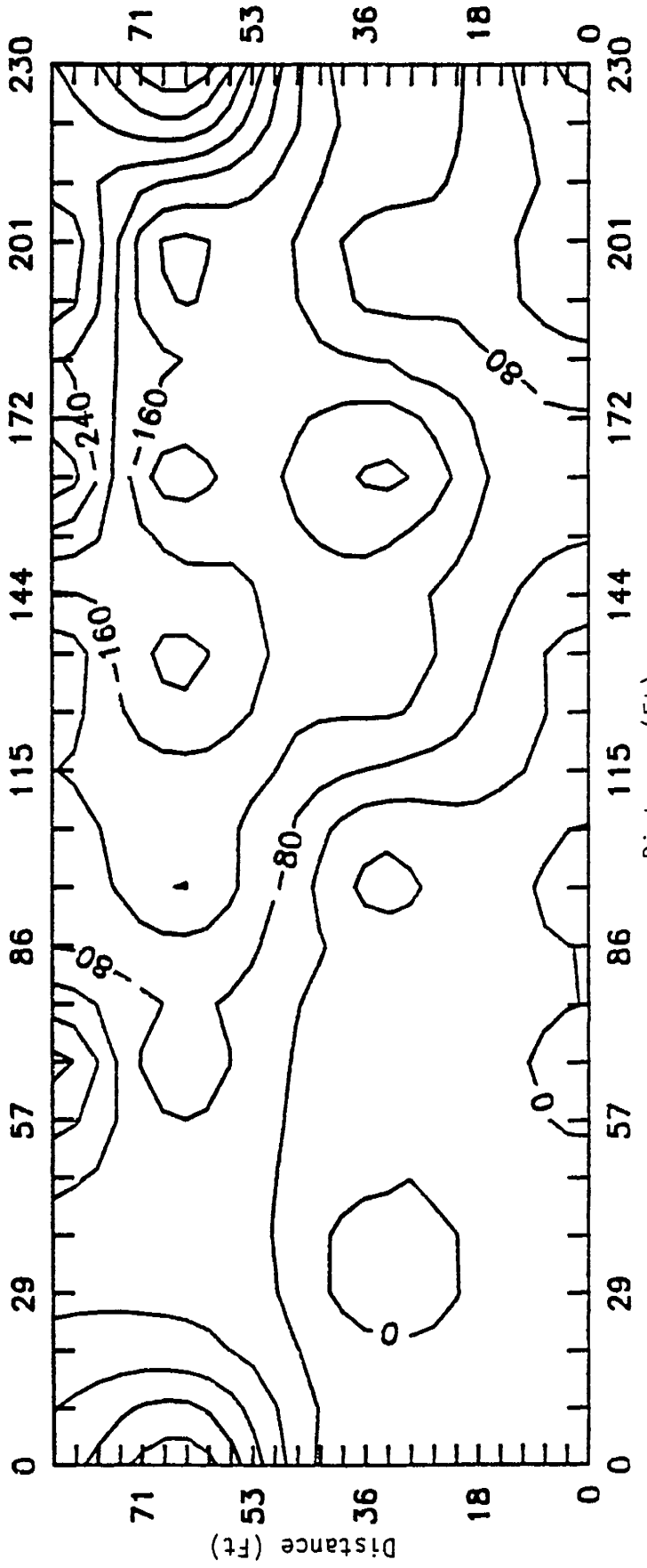

SP Contour Map for Site I on 13 May 1988
Contour Interval is 40 mv.

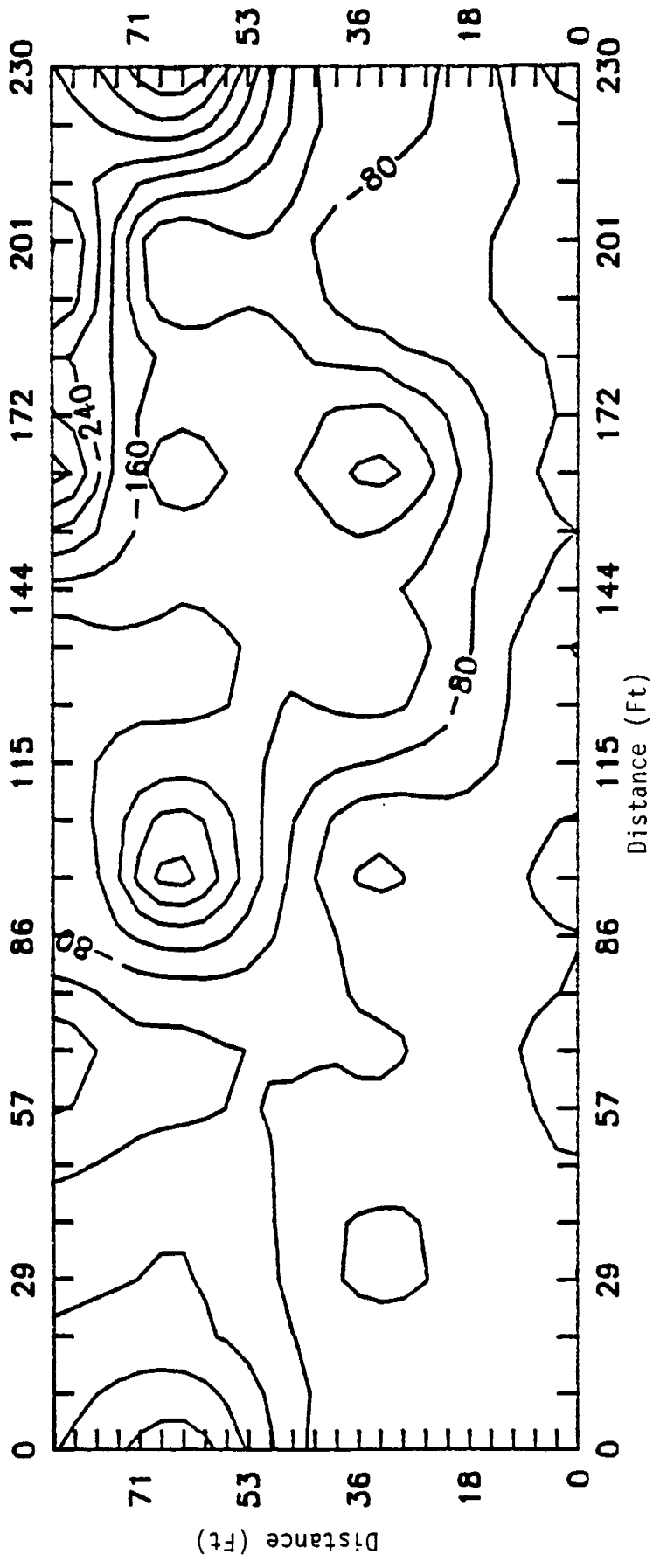

SP Contour Map for Site I on 20 May 1988
Contour Interval is 40 mv.

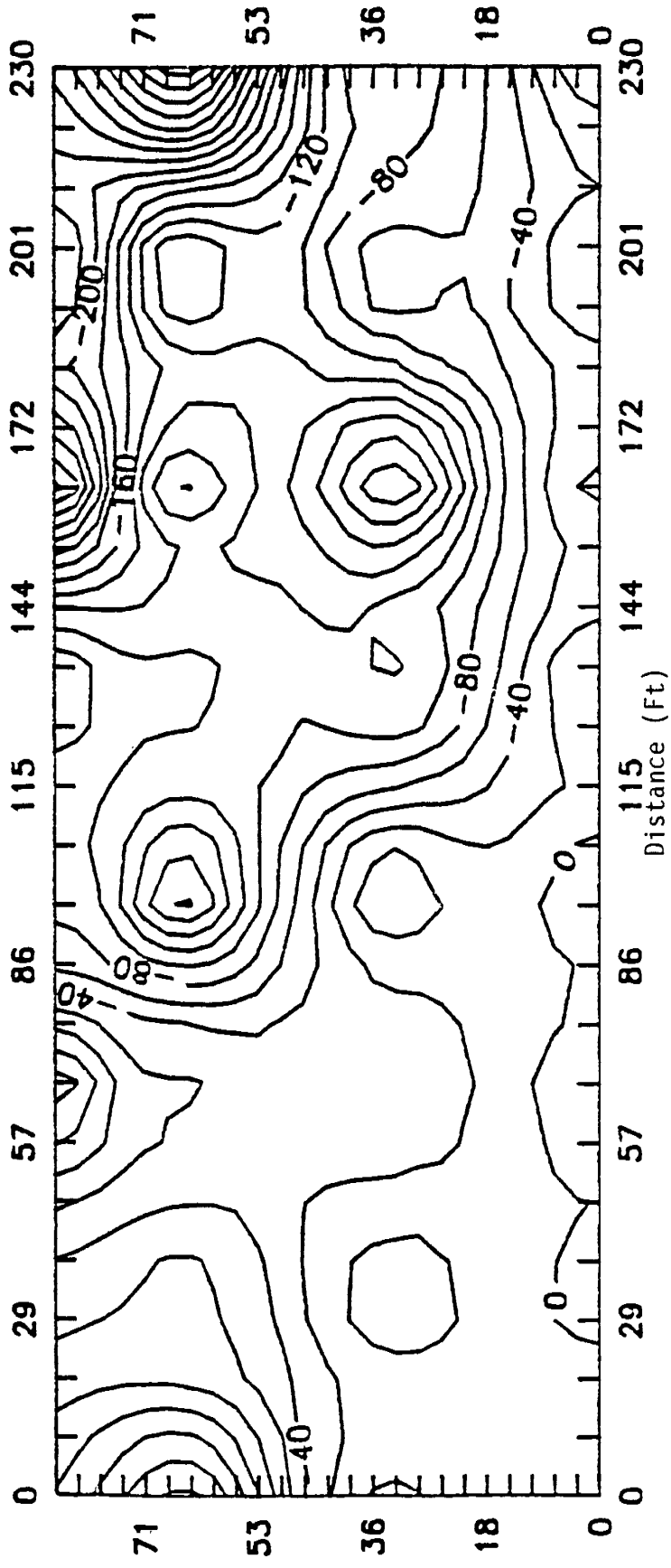

SP Contour Map for Site I on 23 May 1988.
Contour Interval is 40 mv.

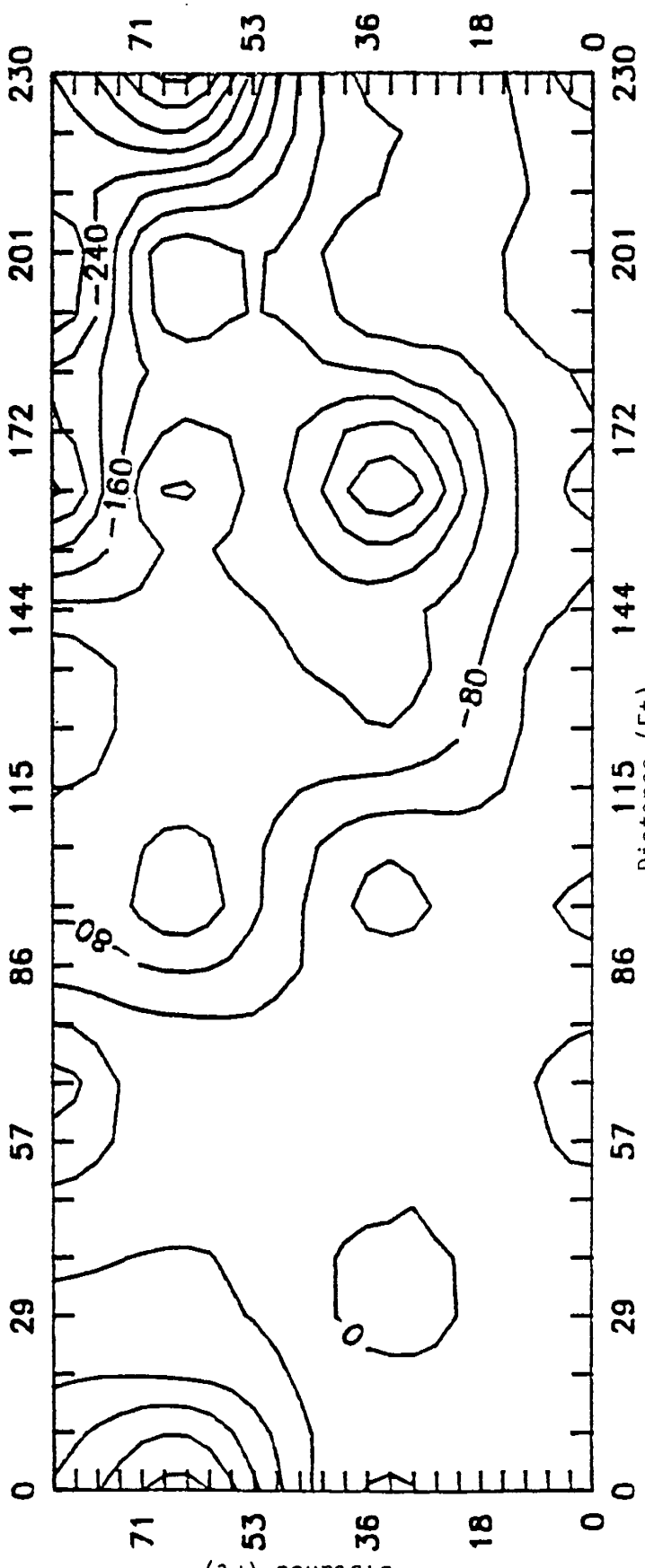

SP Contour Map for Site I on 31 May 1988.
Contour Interval is 40 mv.

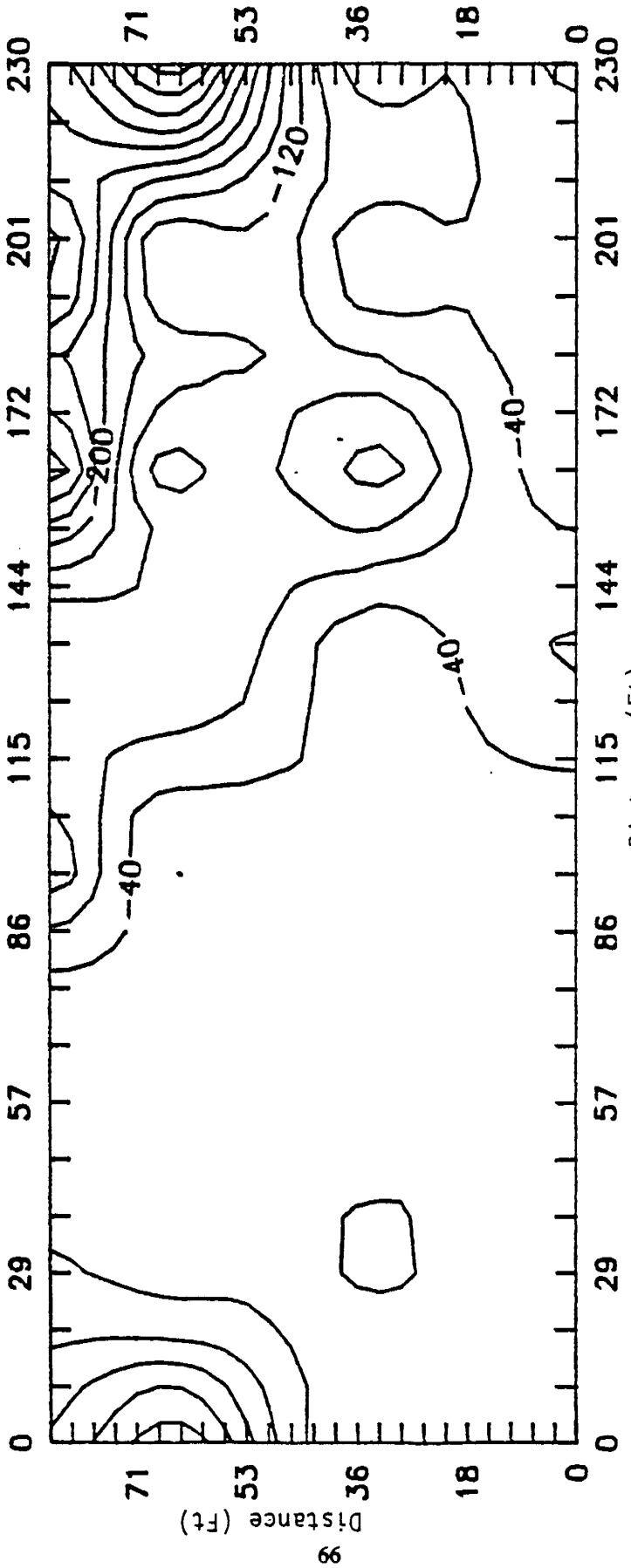

SP Contour Map for Site I on 10 June 1988.
Contour Interval is 40 mv.

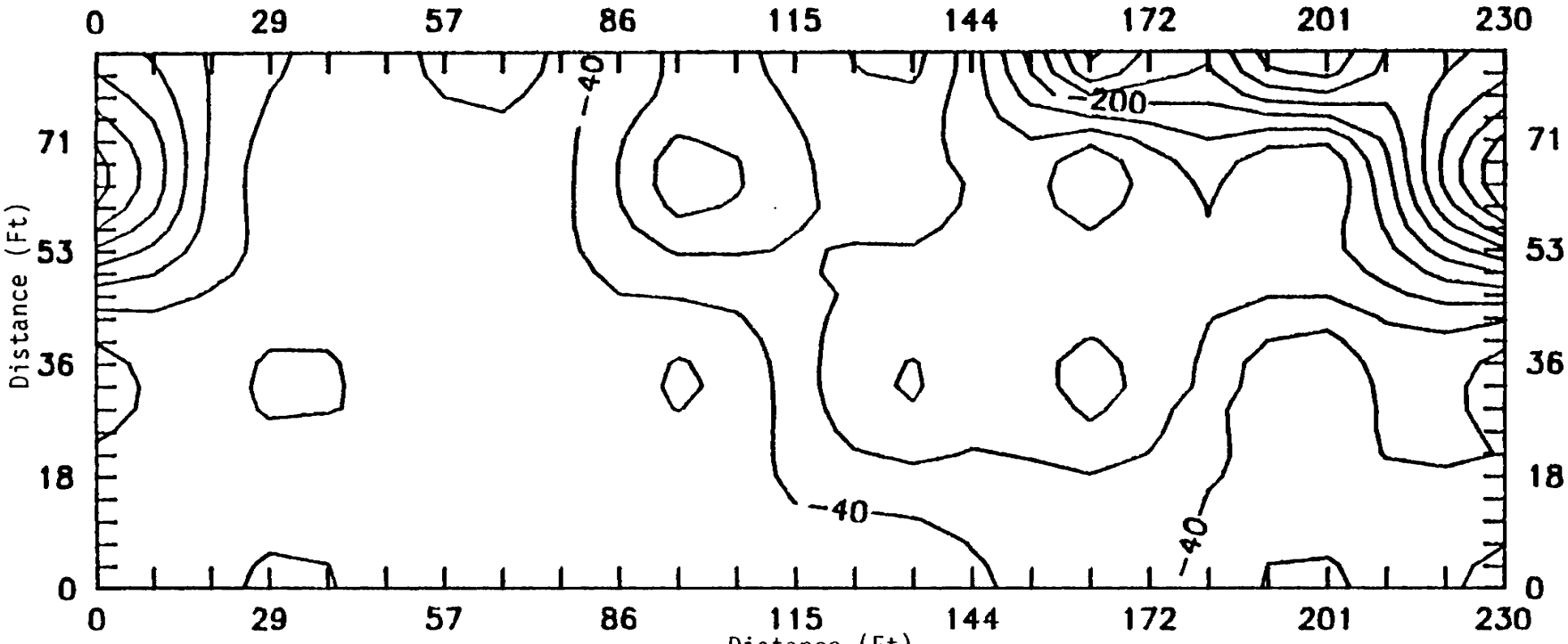

SP Contour Map for Site I on 16 June 1988.
Contour Interval is 40 mv.

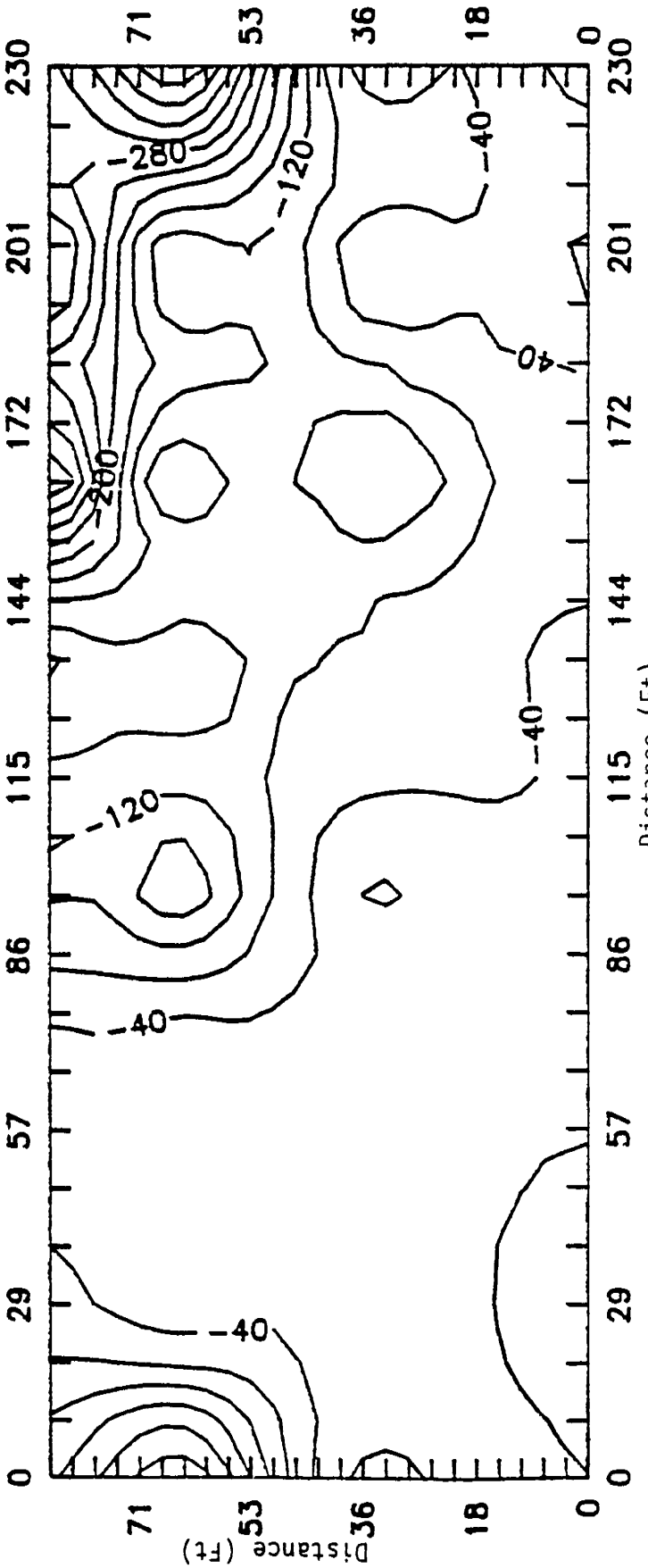

SP Contour Map for Site I on 29 June 1988.
Contour Interval is 40 mv.

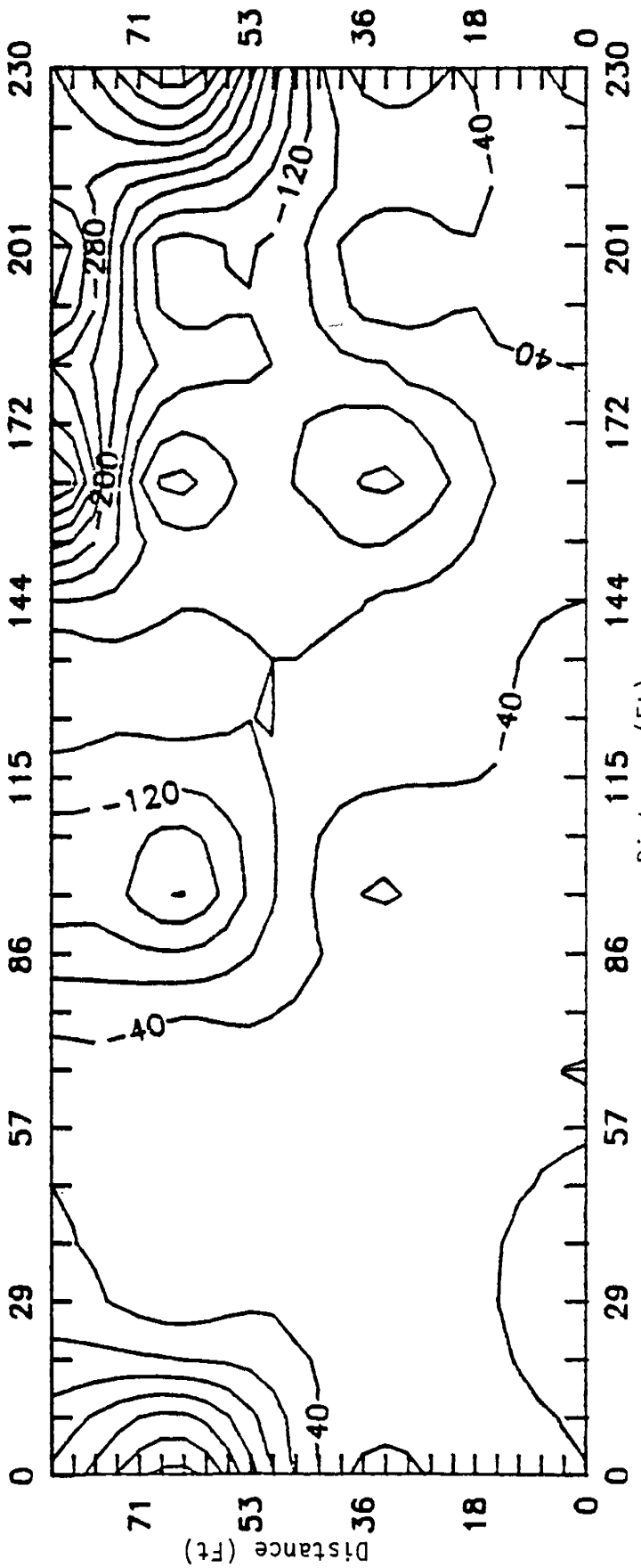

SP Contour Map for Site I on 1 July 1988.
Contour Interval is 40 mv.

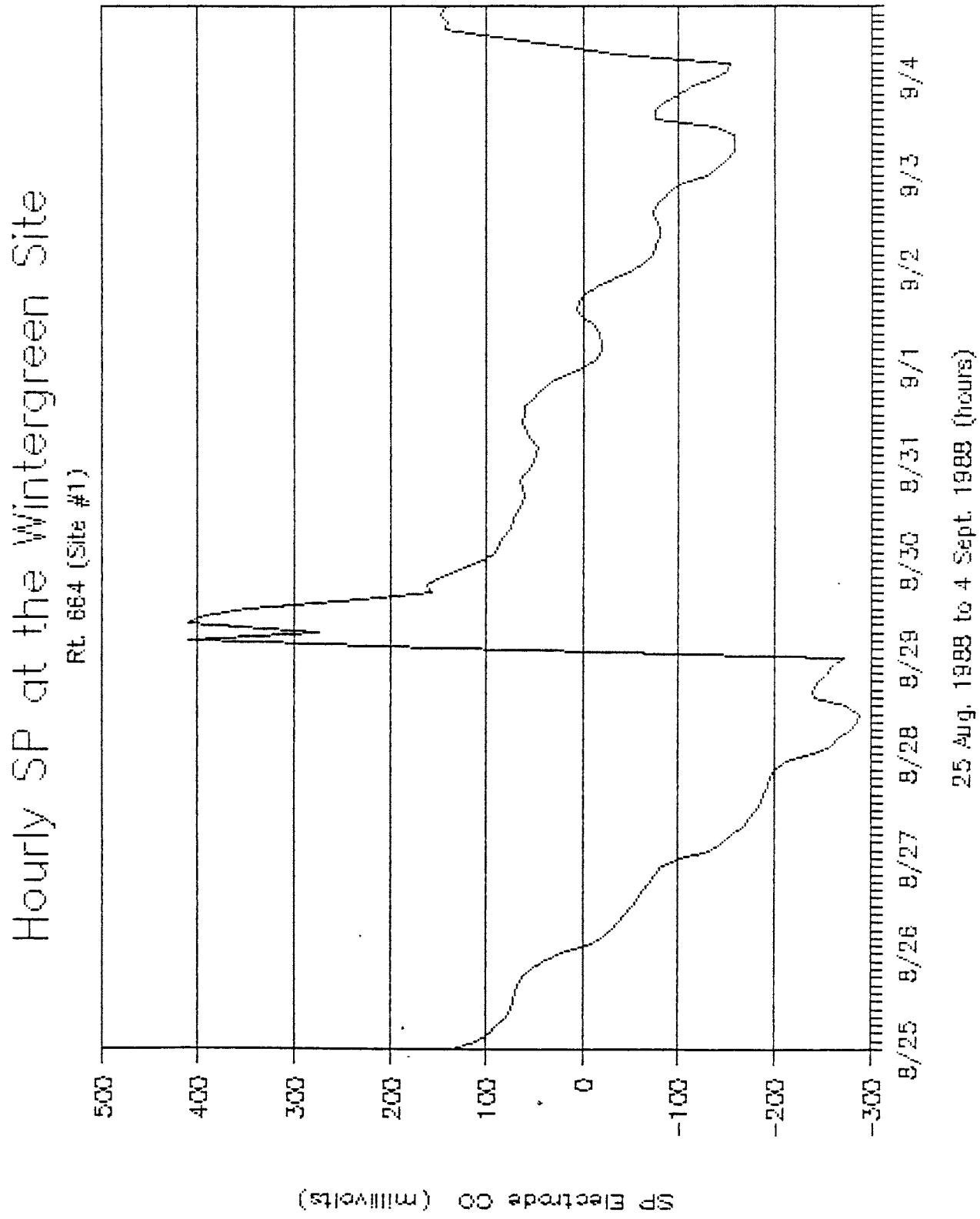
Hourly SP at the Wintergreen Site
Rt. 664 (Site #1)
SP Electrode CO (millivolts)
500
400
300
200
100
0
-100
-200
-300
8/25
8/26
8/27
8/28
8/29
8/30
8/31
9/1
9/2
9/3
9/4
25 Aug. 1988 to 4 Sept. 1988 (hours)

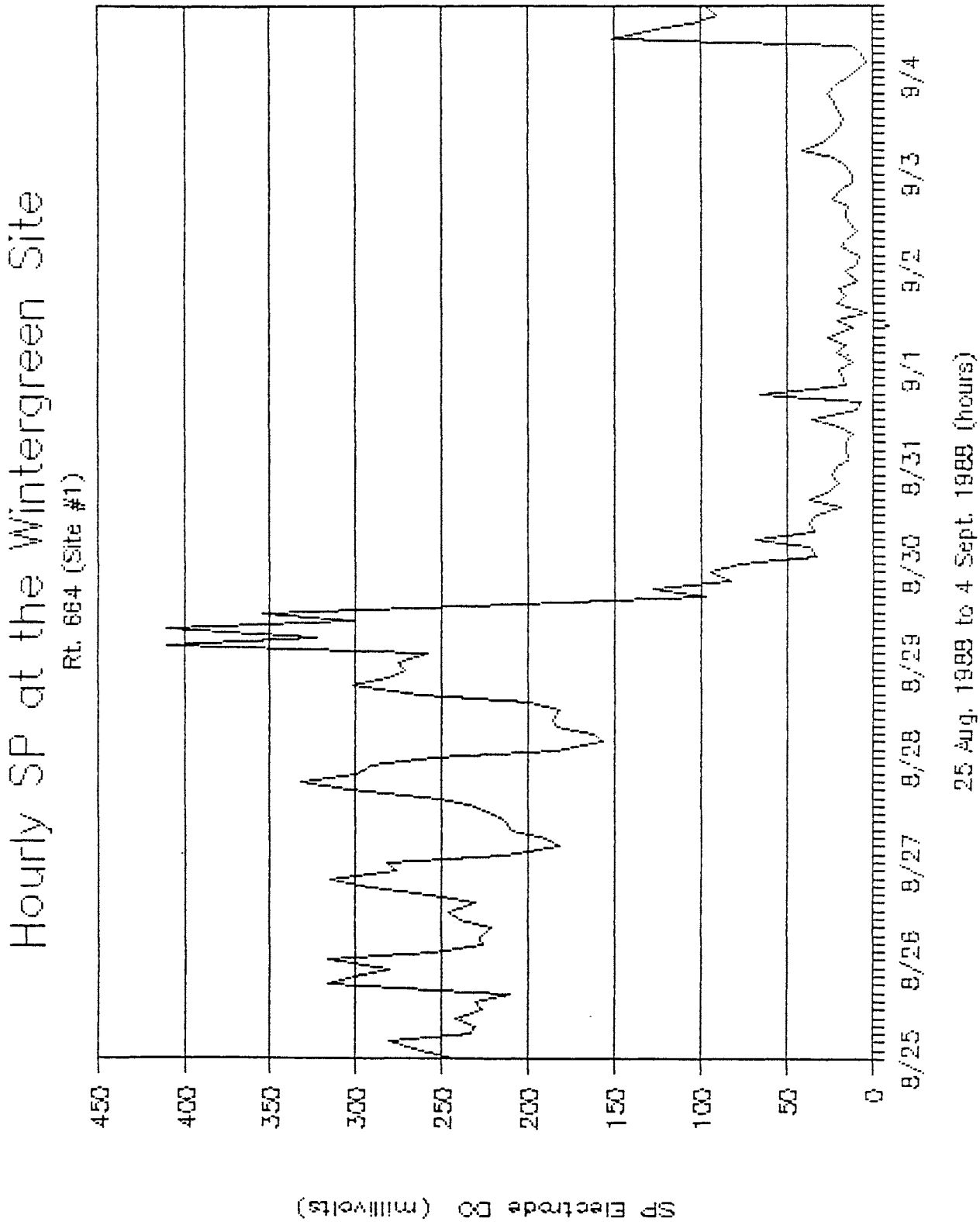
Hourly SP at the Wintergreen Site
Rt. 664 (Site #1)
SP Electrode DO (millivolts)
450
400
350
300
250
200
150
100
50
0
8/25
8/26
8/27
8/28
8/29
8/30
8/31
9/1
9/2
9/3
9/4
25 Aug. 1988 to 4 Sept. 1988 (hours)

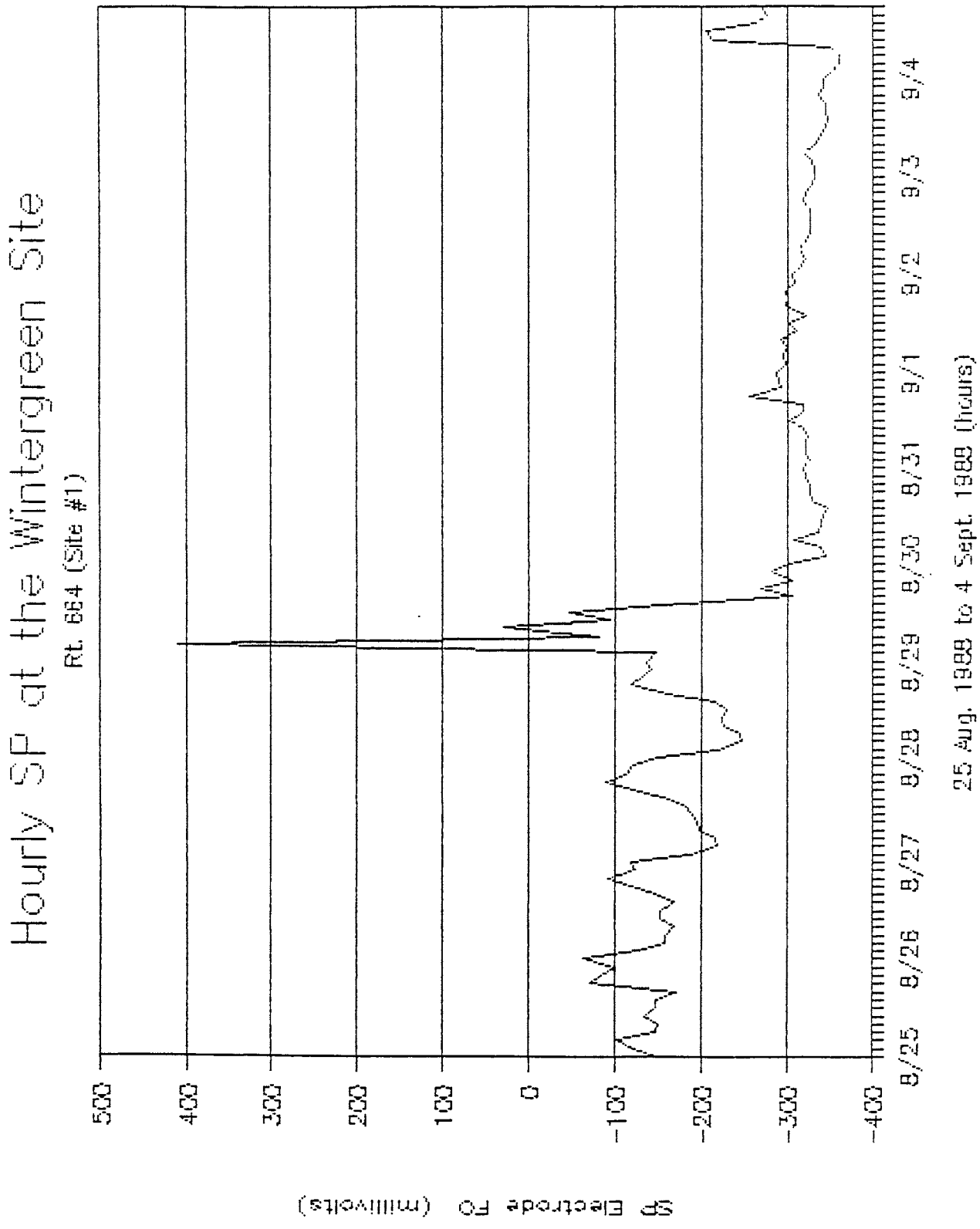
Hourly SP at the Wintergreen Site
Rt. 664 (Site #1)
SP Electrode FO (millivolts)
500
400
300
200
100
0
-100
-200
-300
-400
8/25
8/26
8/27
8/28
8/29
8/30
8/31
9/1
9/2
9/3
9/4
25 Aug. 1988 to 4 Sept. 1988 (hours)

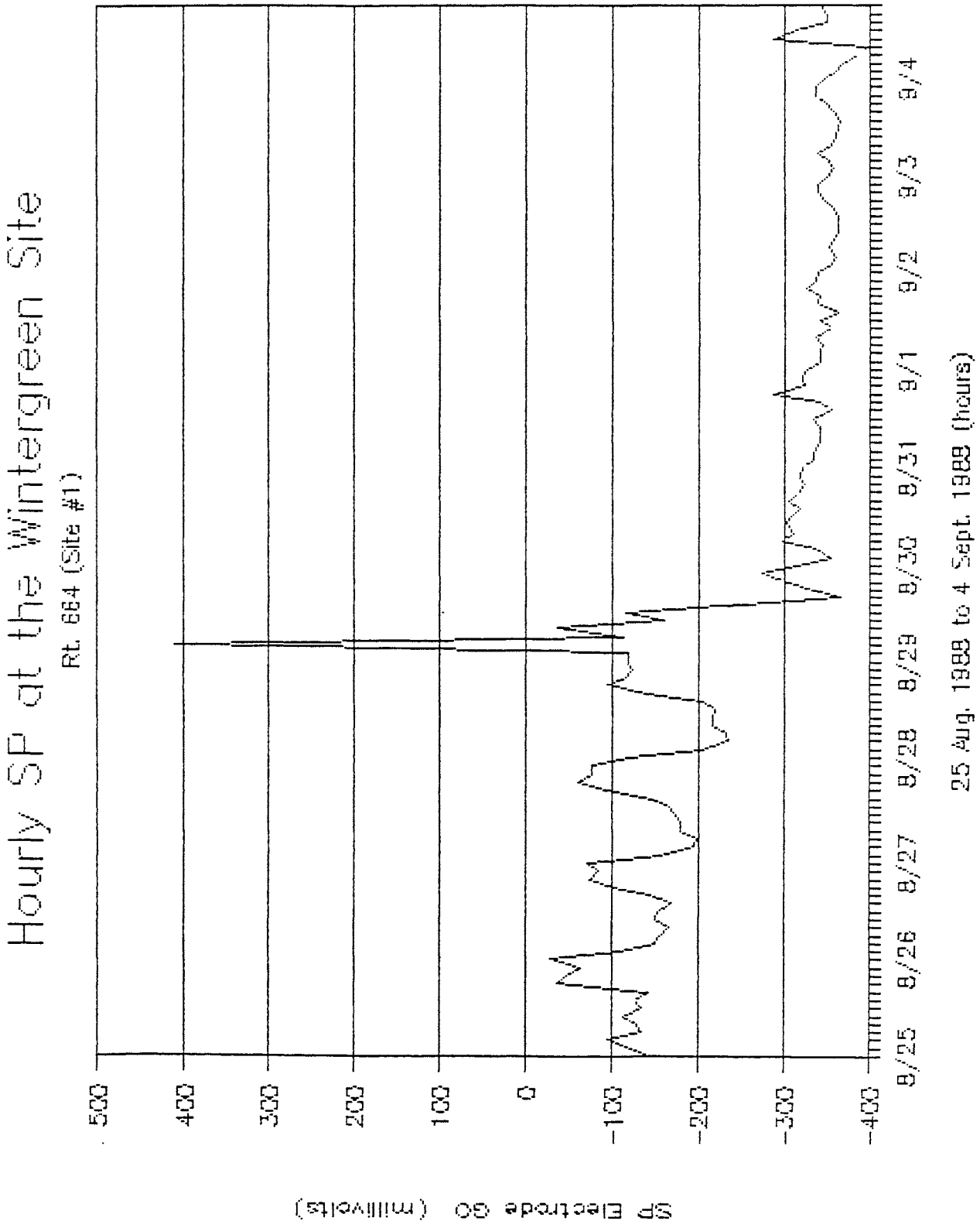
Hourly SP at the Wintergreen Site
Rt. 664 (Site #1)
SP Electrode GO (millivolts)
500
400
300
200
100
0
-100
-200
-300
-400
8/25
8/26
8/27
8/28
8/29
8/30
8/31
9/1
9/2
9/3
9/4
25 Aug. 1988 to 4 Sept. 1988 (hours)

1936

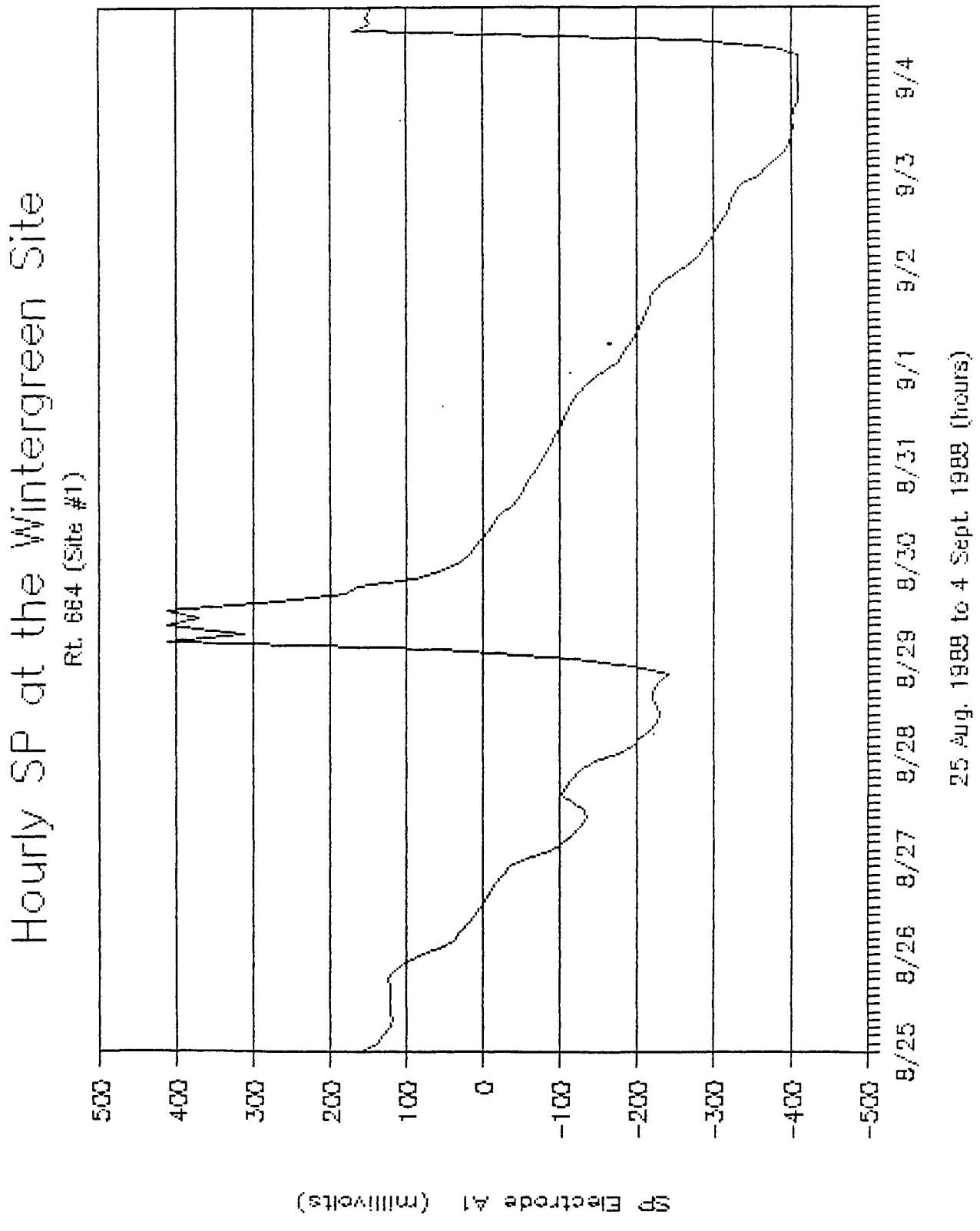
Hourly SP at the Wintergreen Site
Rt. 664 (Site #1)
SP Electrode A1 (millivolts)
500
400
300
200
100
0
-100
-200
-300
-400
-500
8/25
8/26
8/27
8/28
8/29
8/30
8/31
9/1
9/2
9/3
9/4
25 Aug. 1988 to 4 Sept. 1988 (hours)

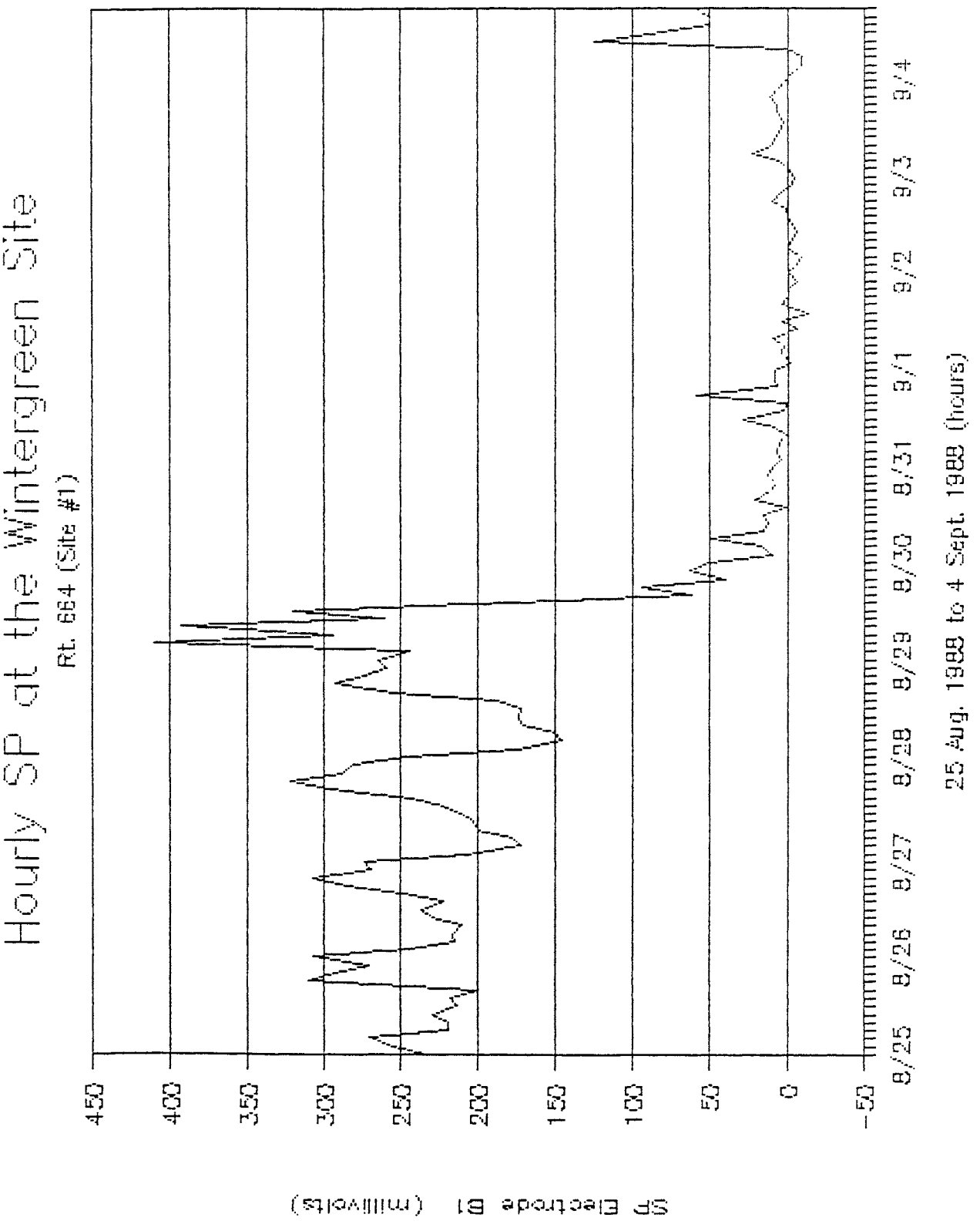
Hourly SP at the Wintergreen Site
Rt. 664 (Site #1)
SP Electrode B1 (millivolts)
450
400
350
300
250
200
150
100
50
0
-50
8/25
8/26
8/27
8/28
8/29
8/30
8/31
9/1
9/2
9/3
9/4
25 Aug. 1988 to 4 Sept. 1988 (hours)

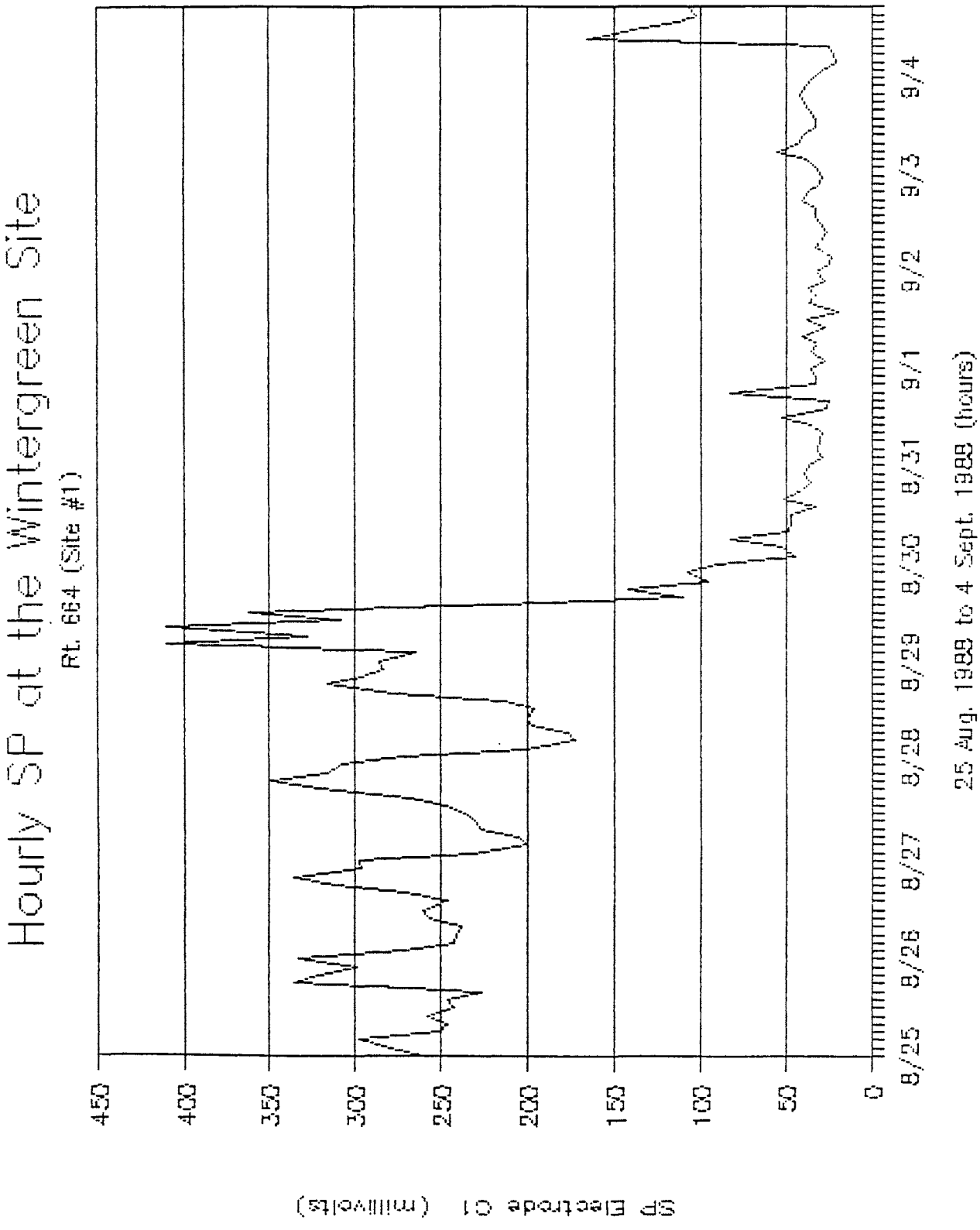
Hourly SP at the Wintergreen Site
Rt. 664 (Site #1)
SP Electrode 01 (millivolts)
450
400
350
300
250
200
150
100
50
0
8/25
8/26
8/27
8/28
8/29
8/30
8/31
9/1
9/2
9/3
9/4
25 Aug. 1988 to 4 Sept. 1988 (hours)

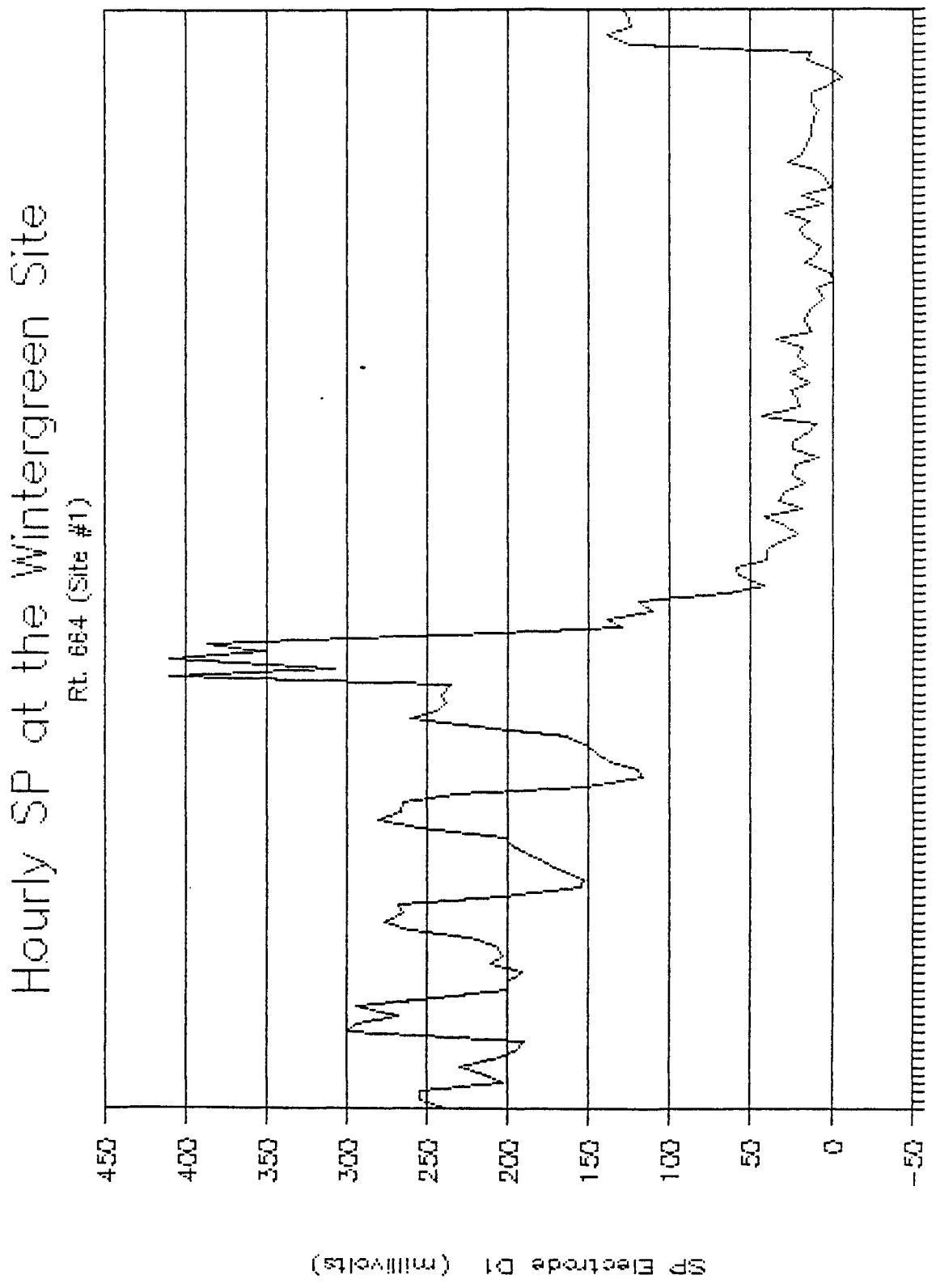
Hourly SP at the Wintergreen Site
Rt. 664 (Site #1)
SP Electrode D1 (millivolts)
450
400
350
300
250
200
150
100
50
0
-50
8/25
8/26
8/27
8/28
8/29
8/30
8/31
9/1
9/2
9/3
9/4
25 Aug. 1988 to 4 Sept. 1988 (hours)

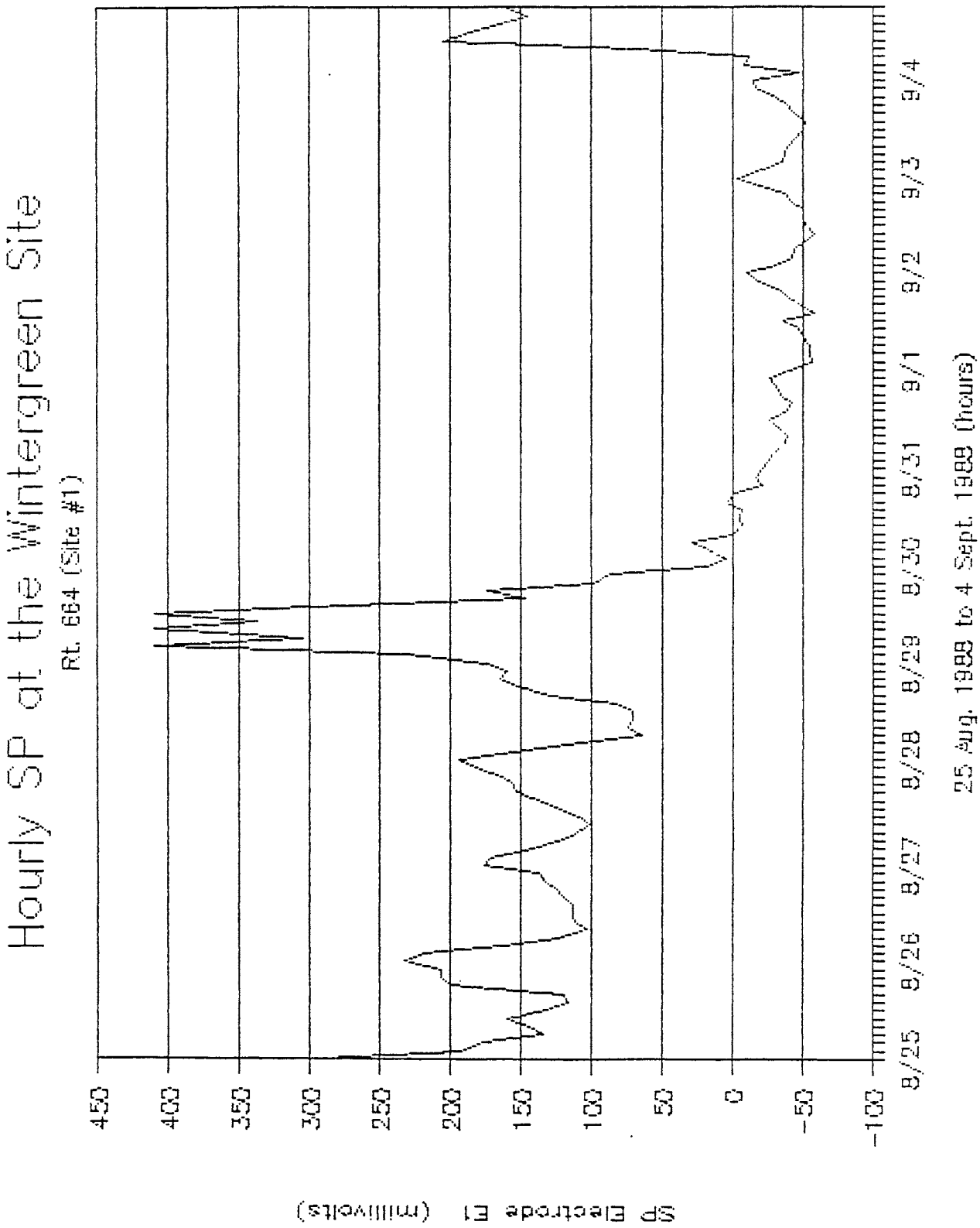
Hourly SP at the Wintergreen Site
Rt. 664 (Site #1)
SP Electrode E1 (millivolts)
450
400
350
300
250
200
150
100
50
0
-50
-100
8/25
8/26
8/27
8/28
8/29
8/30
8/31
9/1
9/2
9/3
9/4
25 Aug. 1988 to 4 Sept. 1988 (hours)

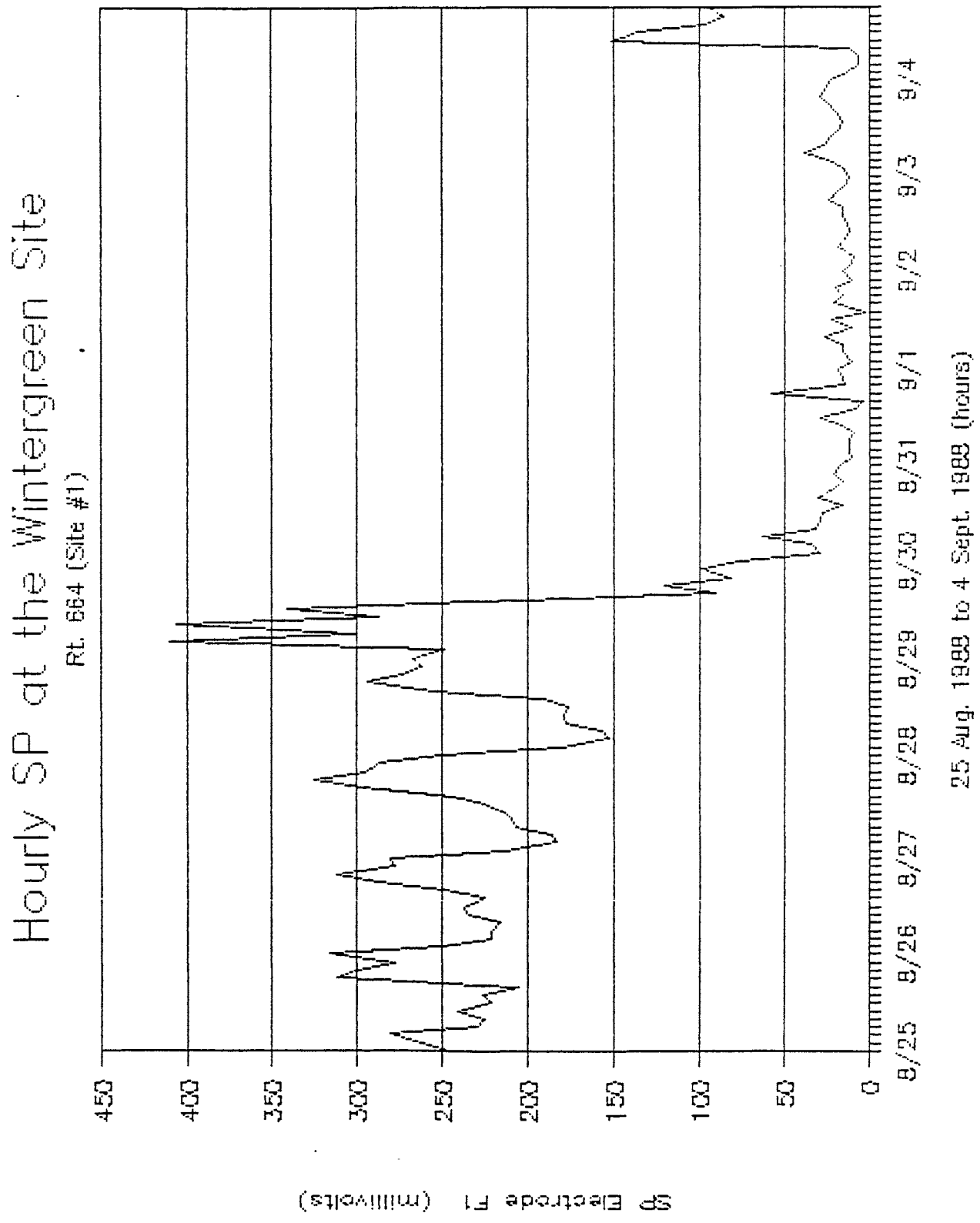
Hourly SP at the Wintergreen Site
Rt. 664 (Site #1)
SP Electrode F1 (millivolts)
450
400
350
300
250
200
150
100
50
0
8/25
8/26
8/27
8/28
8/29
8/30
8/31
9/1
9/2
9/3
9/4
25 Aug. 1988 to 4 Sept. 1988 (hours)

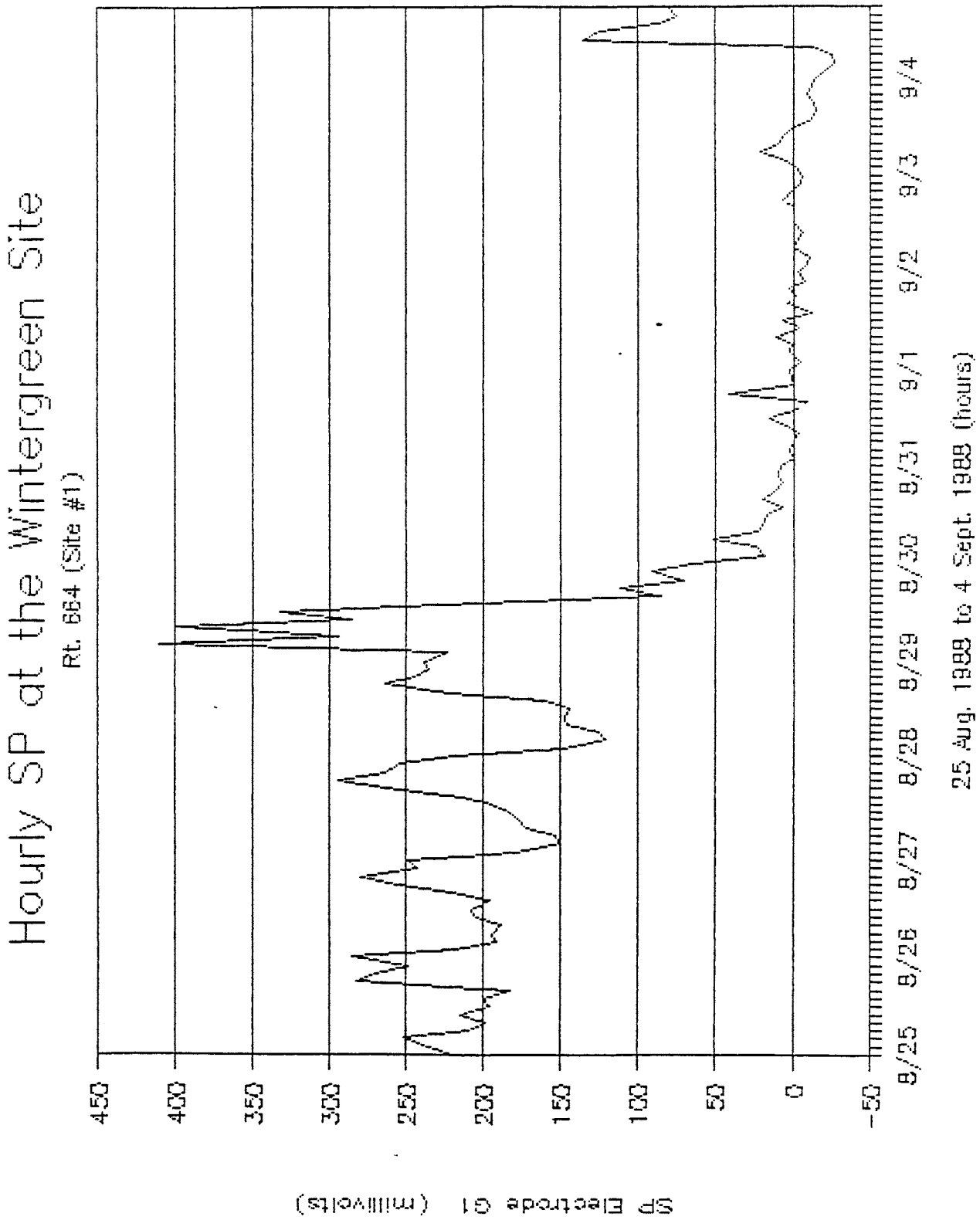
Hourly SP at the Wintergreen Site
Rt. 664 (Site #1)
SP Electrode G1 (millivolts)
450
400
350
300
250
200
150
100
50
0
-50
8/25
8/26
8/27
8/28
8/29
8/30
8/31
9/1
9/2
9/3
9/4
25 Aug. 1988 to 4 Sept. 1988 (hours)

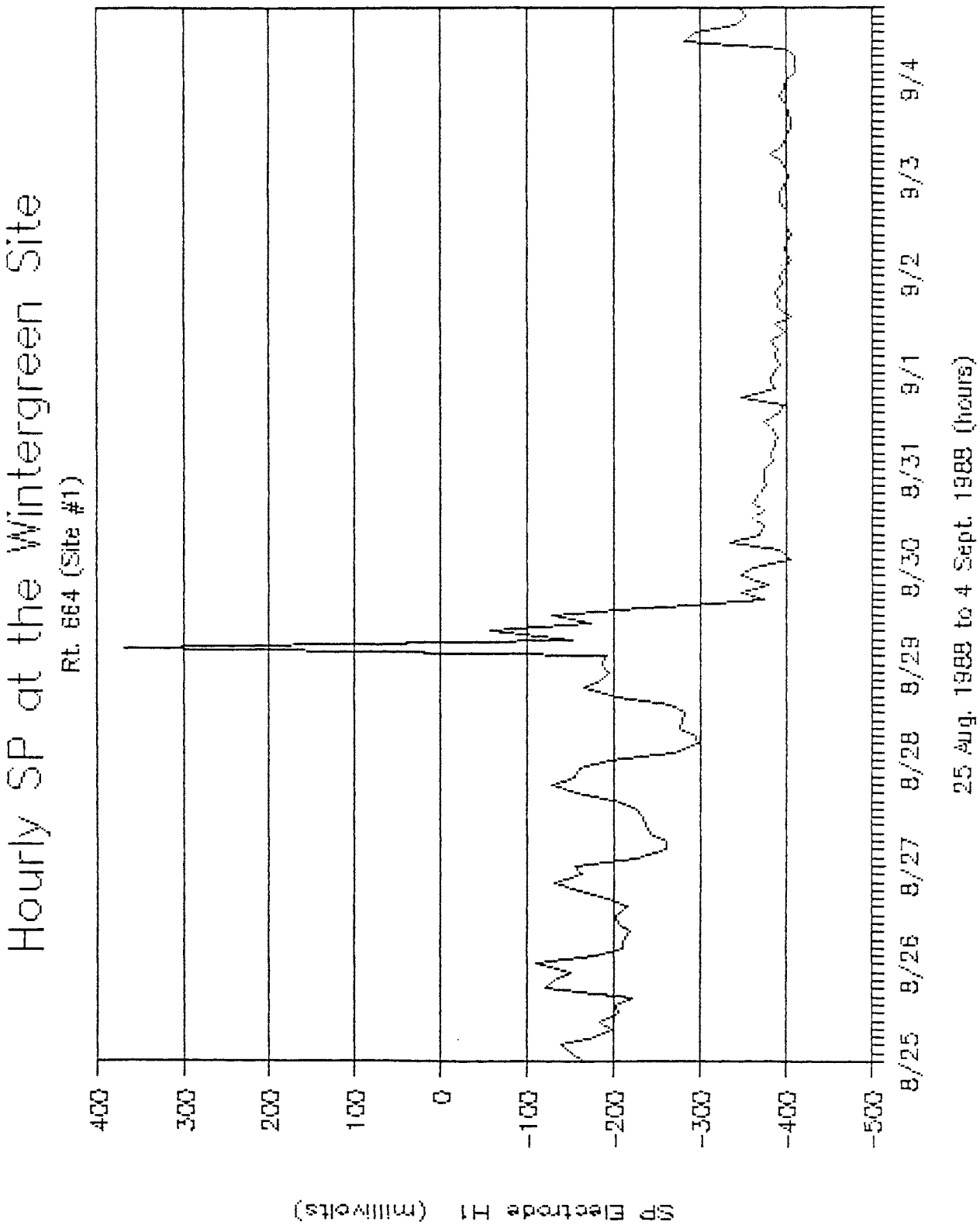
Hourly SP at the Wintergreen Site
Rt. 664 (Site #1)
SP Electrode H1 (millivolts)
400
300
200
100
0
-100
-200
-300
-400
-500
8/25
8/26
8/27
8/28
8/29
8/30
8/31
9/1
9/2
9/3
9/4
25 Aug. 1988 to 4 Sept. 1988 (hours)

1944

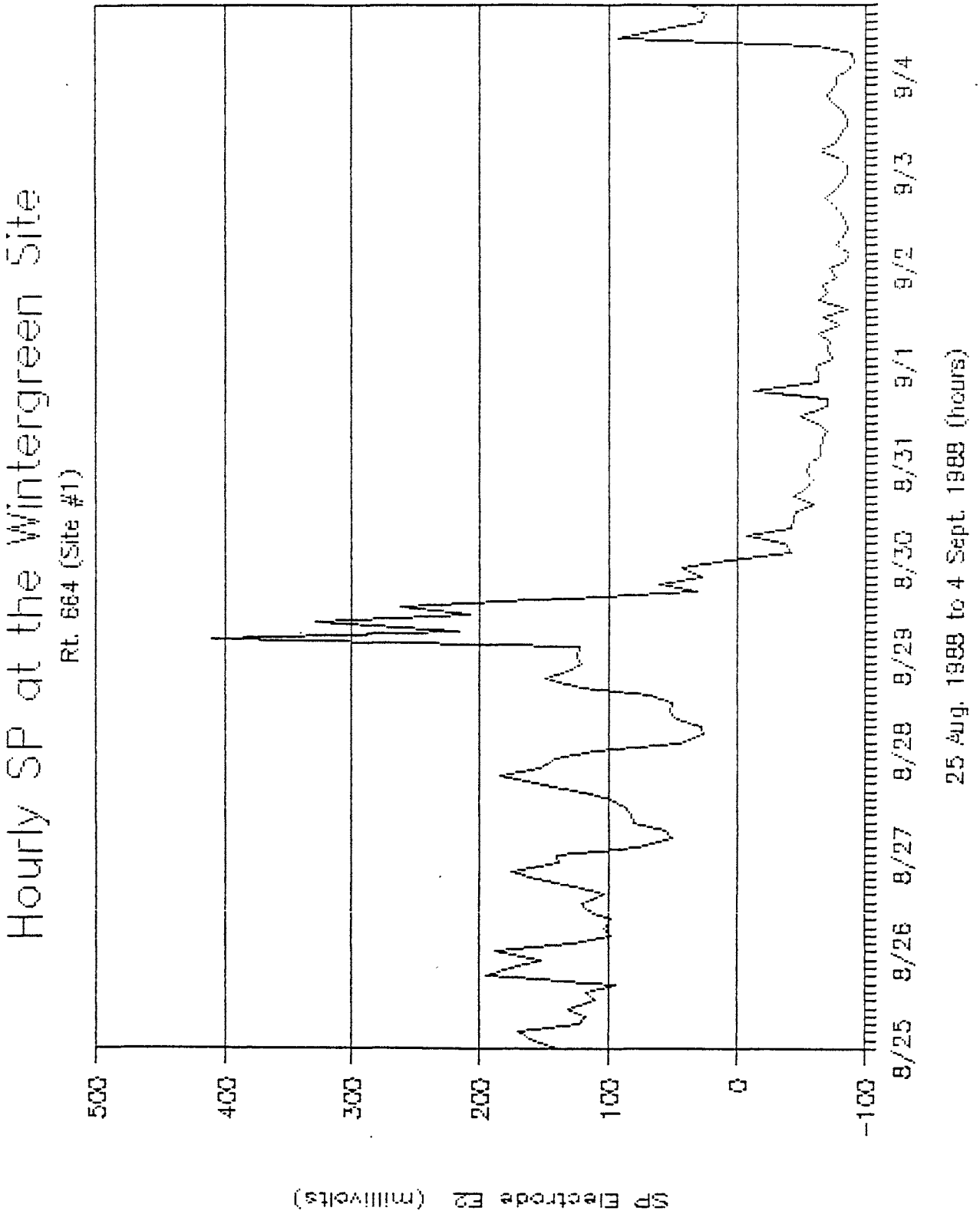
Hourly SP at the Wintergreen Site
Rt. 664 (Site #1)
SP Electrode E2 (millivolts)
500
400
300
200
100
0
-100
8/25
8/26
8/27
8/28
8/29
8/30
8/31
9/1
9/2
9/3
9/4
25 Aug. 1988 to 4 Sept. 1988 (hours)

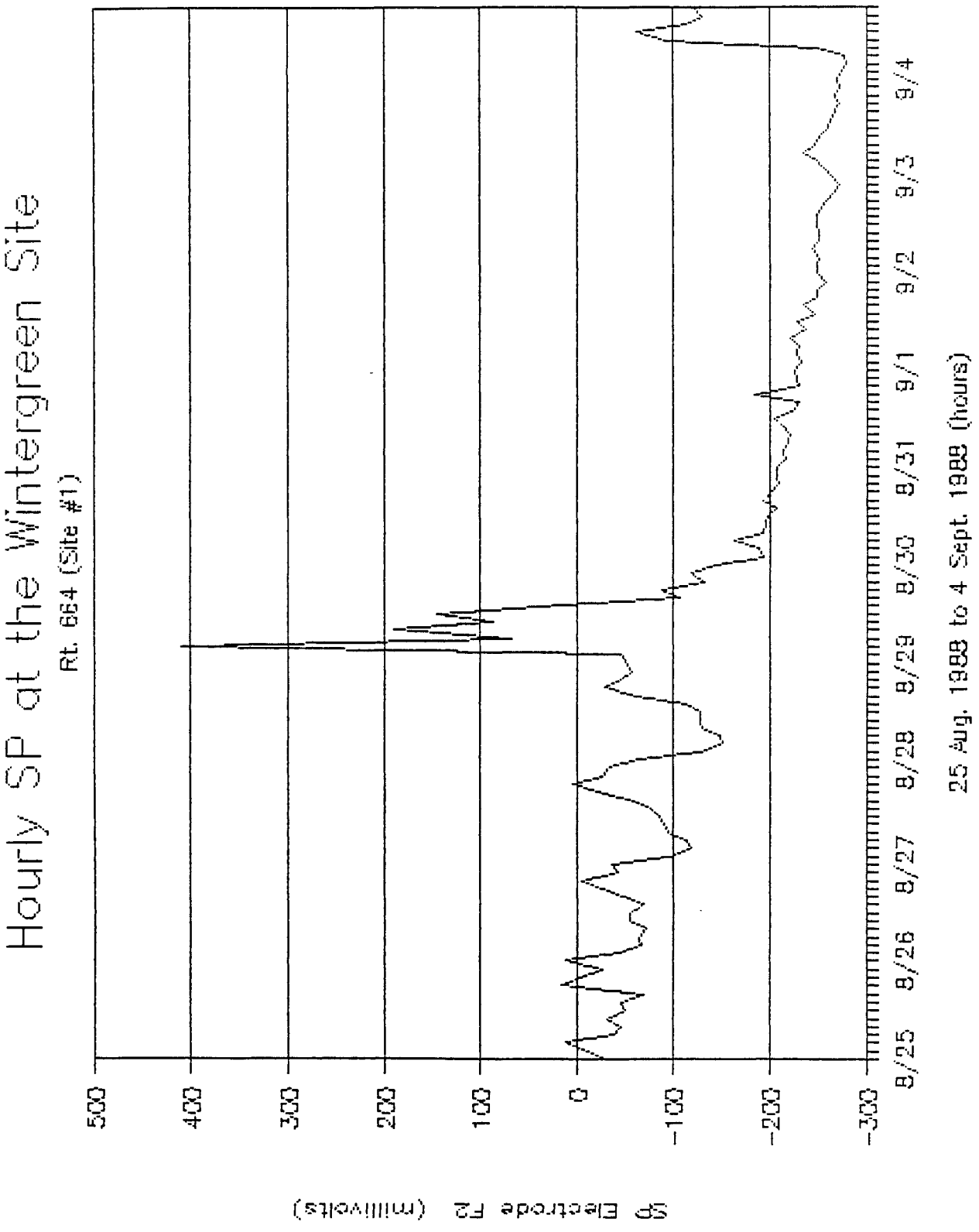
Hourly SP at the Wintergreen Site
Rt. 664 (Site #1)
SP Electrode F2 (millivolts)
500
400
300
200
100
0
-100
-200
-300
8/25
8/26
8/27
8/28
8/29
8/30
8/31
9/1
9/2
9/3
9/4
25 Aug. 1988 to 4 Sept. 1988 (hours)

1946

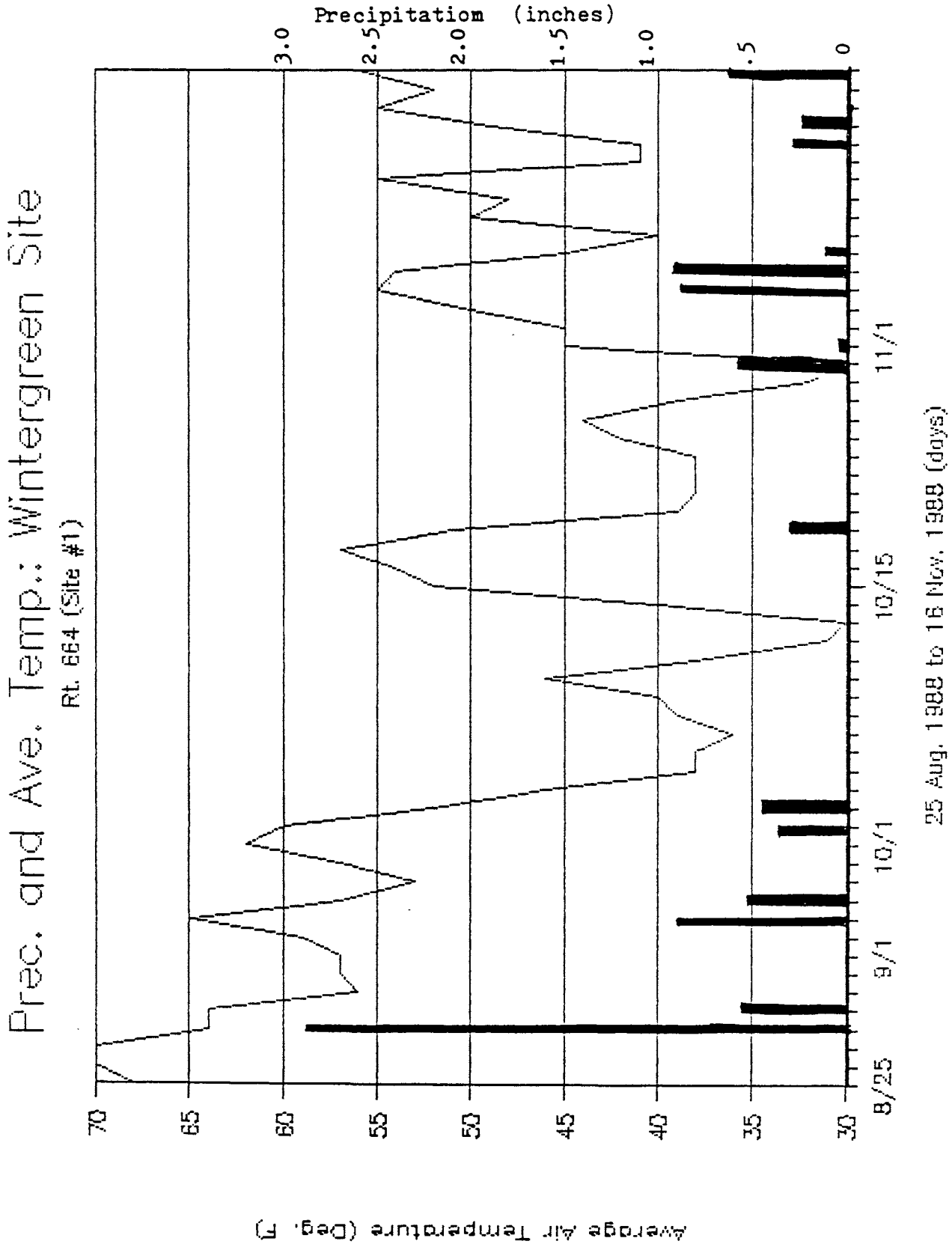
Prec. and Ave. Temp.: Wintergreen Site
Rt. 664 (Site #1)
Precipitation (inches)
3.0
2.5
2.0
1.5
1.0
.5
0
70
65
60
55
50
45
40
35
30
8/25
9/1
10/1
10/15
11/1
25 Aug. 1988 to 16 Nov. 1988 (days)
Average Air Temperature (Deg. F)

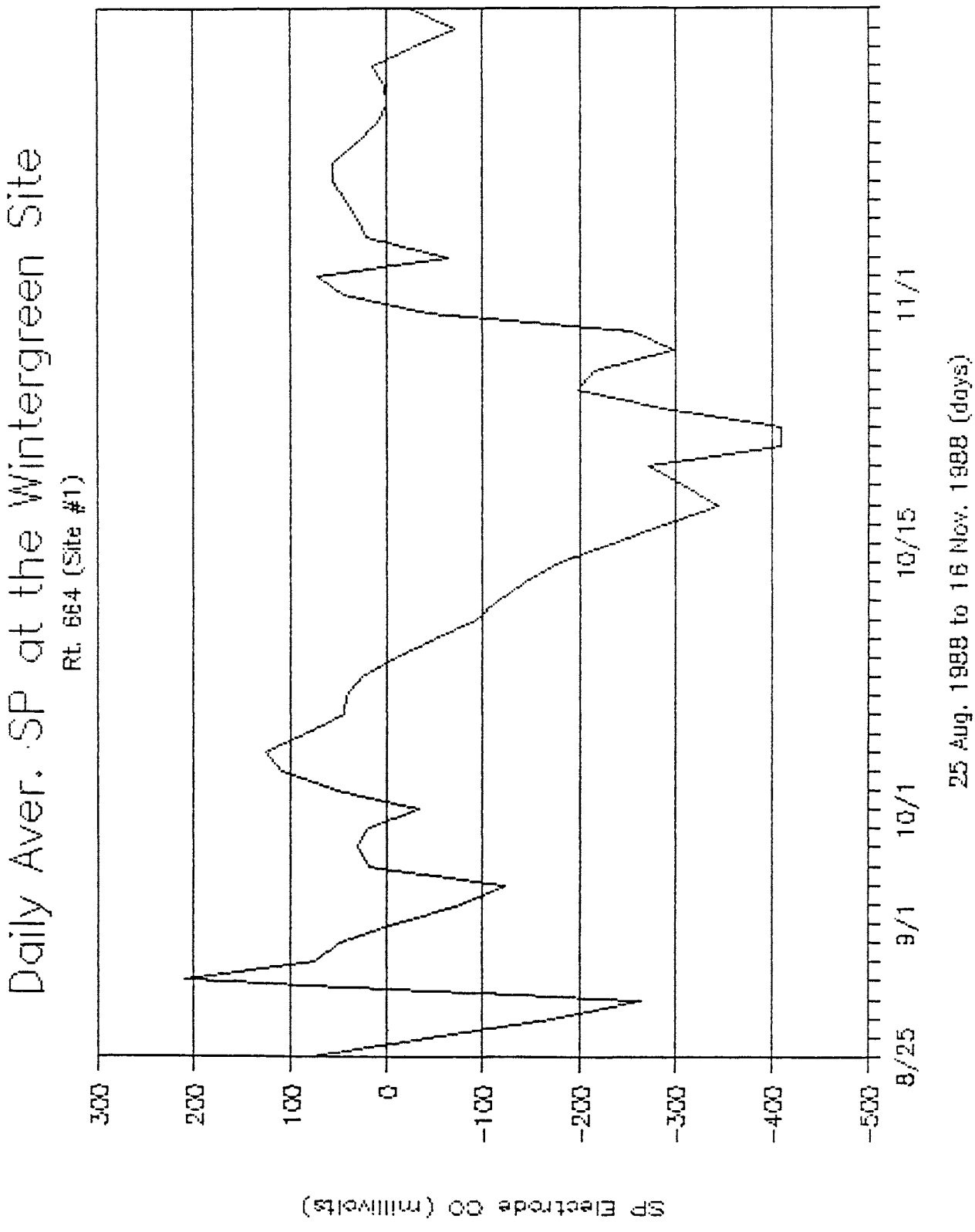
Daily Aver. SP at the Wintergreen Site
Rt. 664 (Site #1)
SP Electrode 00 (millivolts)
300
200
100
0
-100
-200
-300
-400
-500
8/25
9/1
10/1
10/15
11/1
25 Aug, 1988 to 16 Nov, 1988 (days)

194°

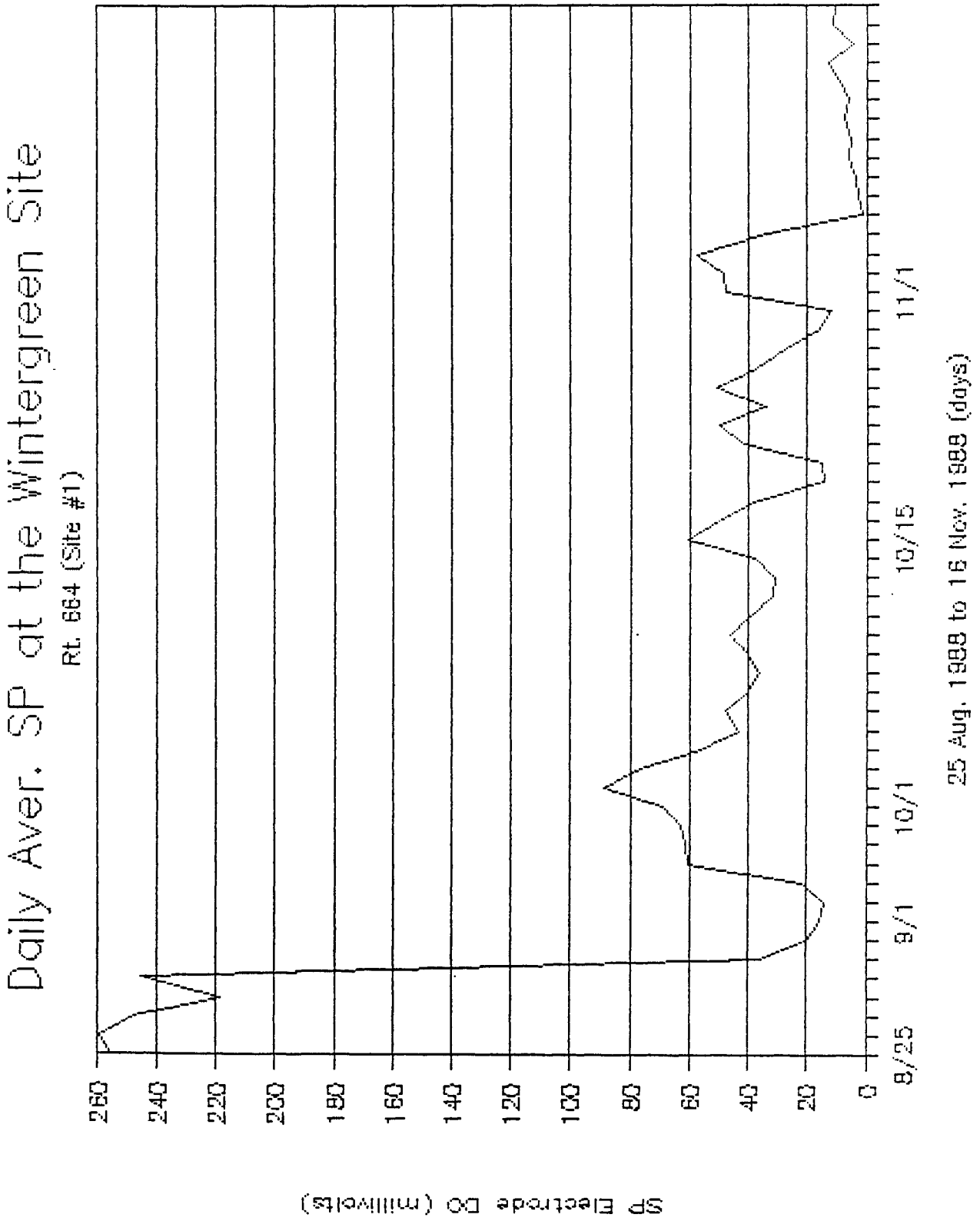
Daily Aver. SP at the Wintergreen Site
Rt. 664 (Site #1)
SP Electrode DO (millivolts)
260
240
220
200
180
160
140
120
100
80
60
40
20
0
8/25
9/1
10/1
10/15
11/1
25 Aug. 1988 to 16 Nov. 1988 (days)

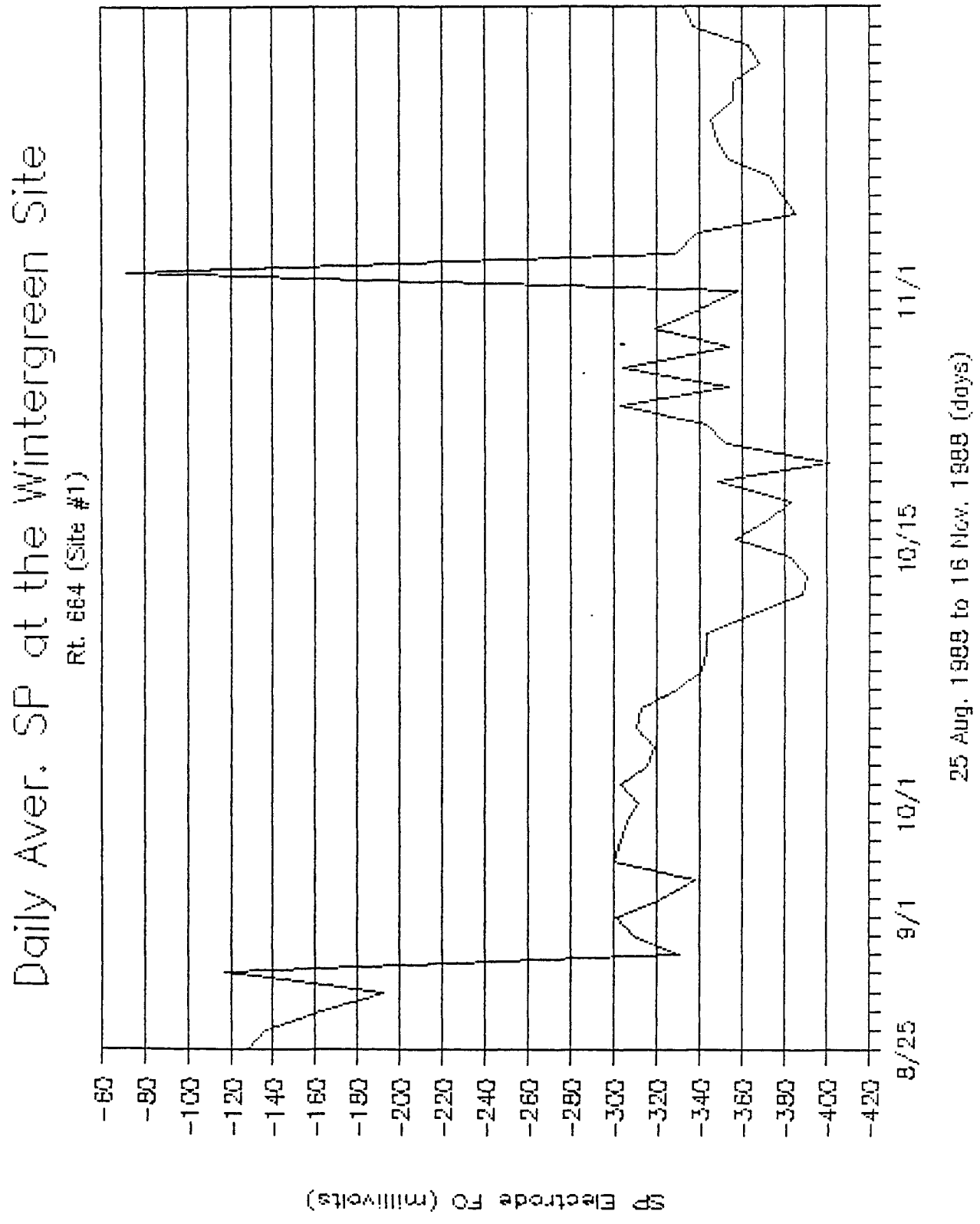
Daily Aver. SP at the Wintergreen Site
Rt. 664 (Site #1)
SP Electrode FO (millivolts)
-60
-80
-100
-120
-140
-160
-180
-200
-220
-240
-260
-280
-300
-320
-340
-360
-380
-400
-420
8/25
9/1
10/1
10/15
11/1
25 Aug. 1988 to 16 Nov. 1988 (days)

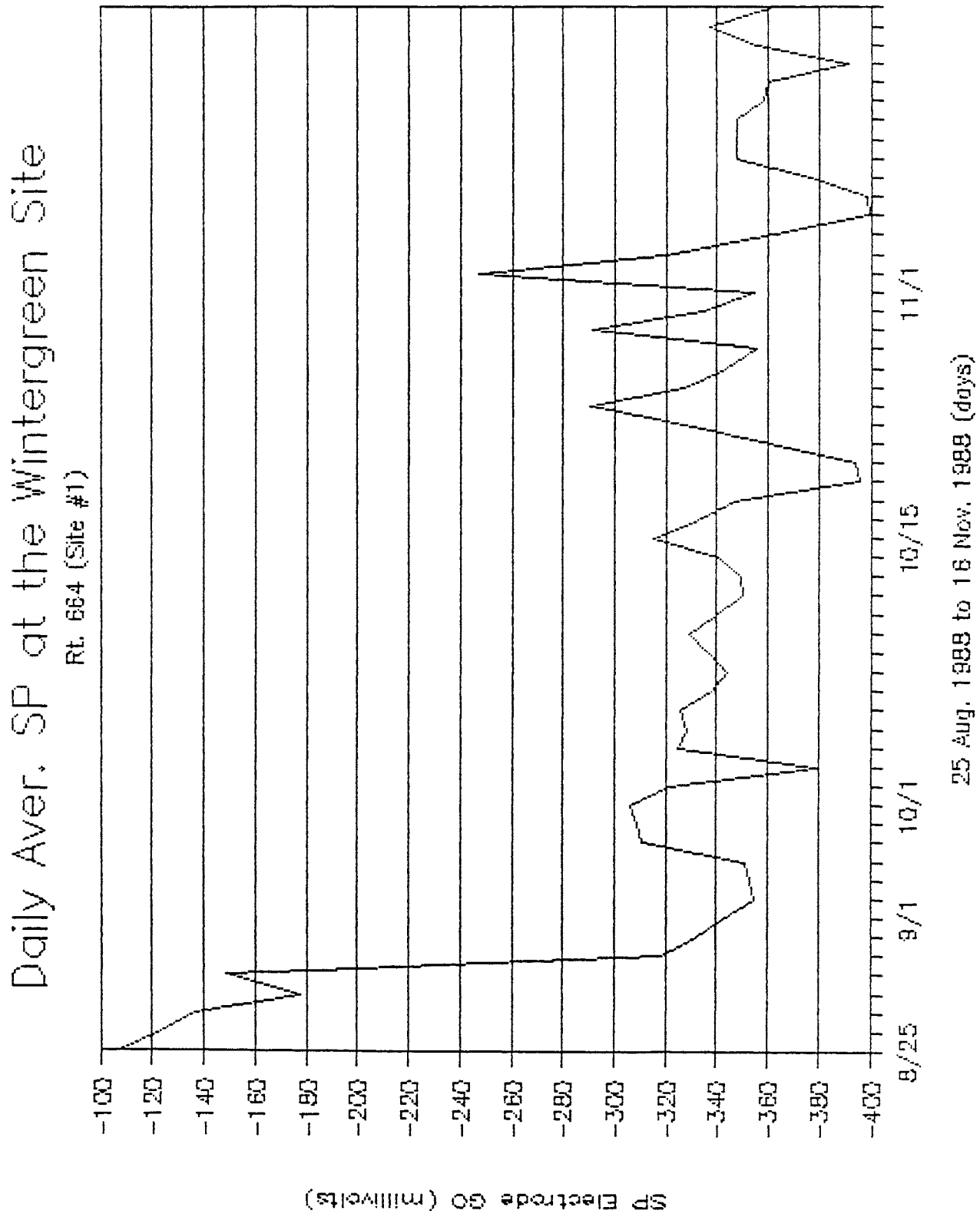
Daily Aver. SP at the Wintergreen Site
Rt. 664 (Site #1)
SP Electrode Go (millivolts)
-100
-120
-140
-160
-180
-200
-220
-240
-260
-280
-300
-320
-340
-360
-380
-400
8/25
9/1
10/1
10/15
11/1
25 Aug. 1988 to 16 Nov. 1988 (days)

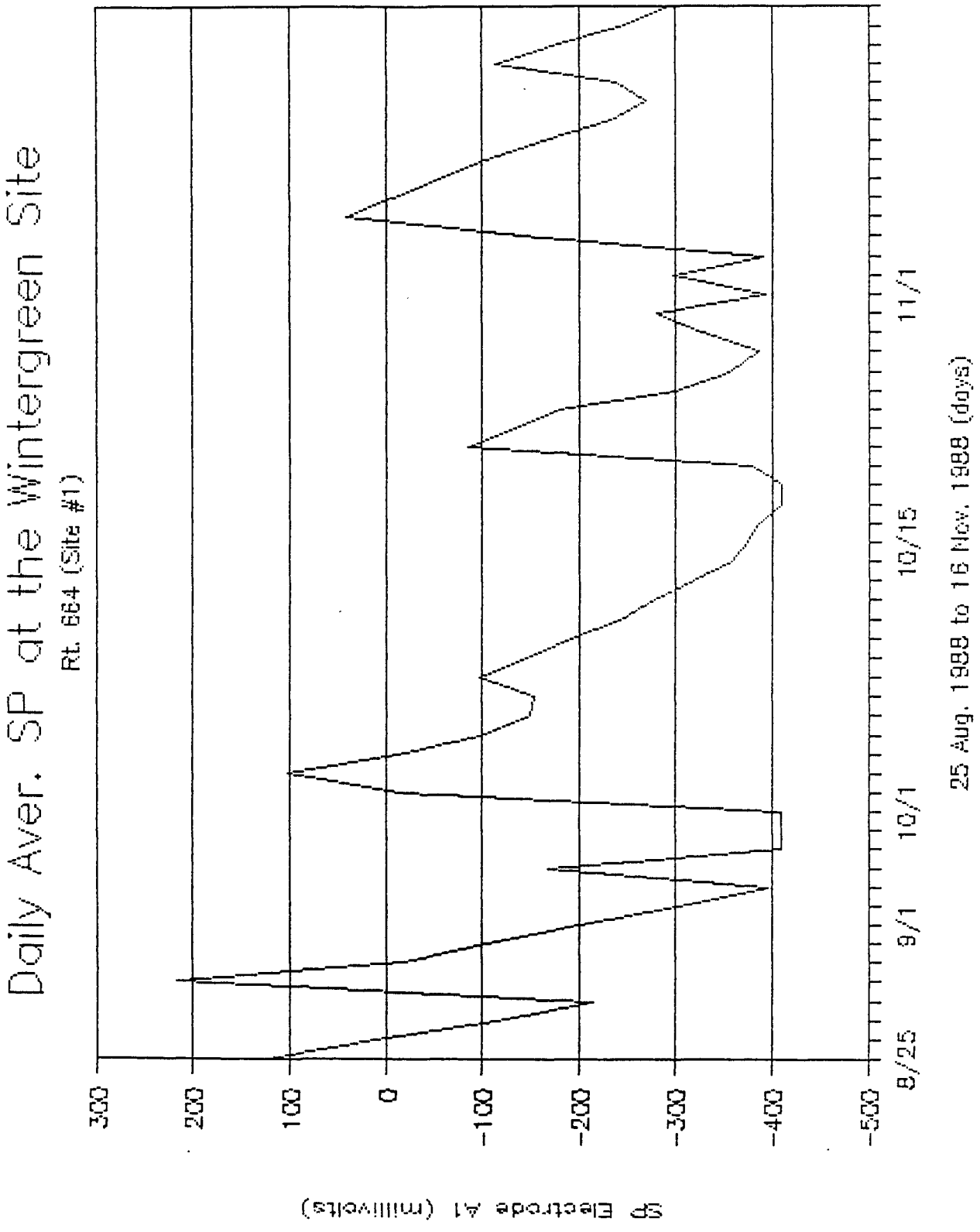
Daily Aver. SP at the Wintergreen Site
Rt. 664 (Site #1)
SP Electrode A1 (millivolts)
300
200
100
0
-100
-200
-300
-400
-500
8/25
9/1
10/1
10/15
11/1
25 Aug. 1988 to 16 Nov. 1988 (days)

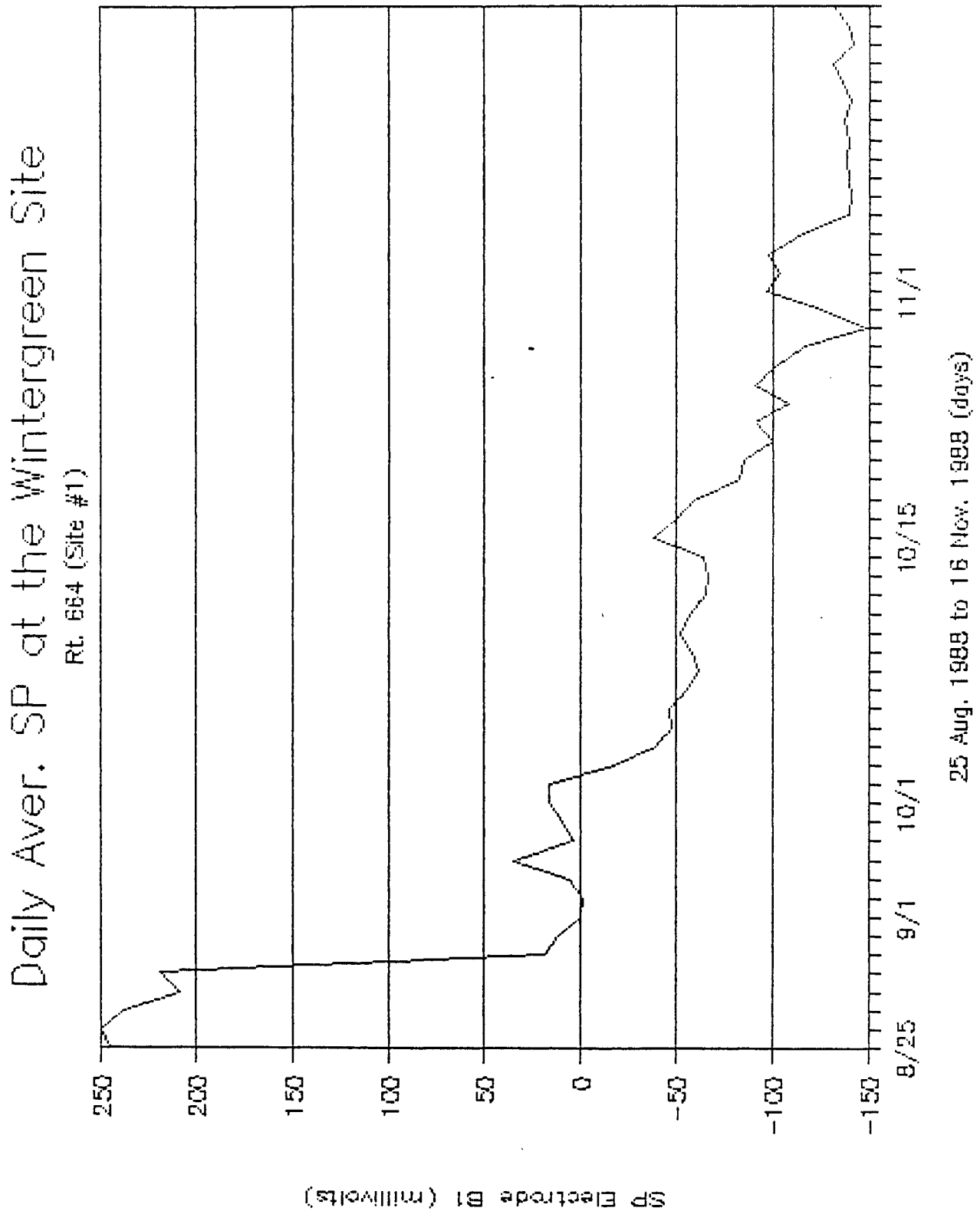
Daily Aver. SP at the Wintergreen Site
Rt. 664 (Site #1)
SP Electrode B1 (millivolts)
250
200
150
100
50
0
-50
-100
-150
8/25
9/1
10/1
10/15
11/1
25 Aug. 1988 to 16 Nov. 1988 (days)

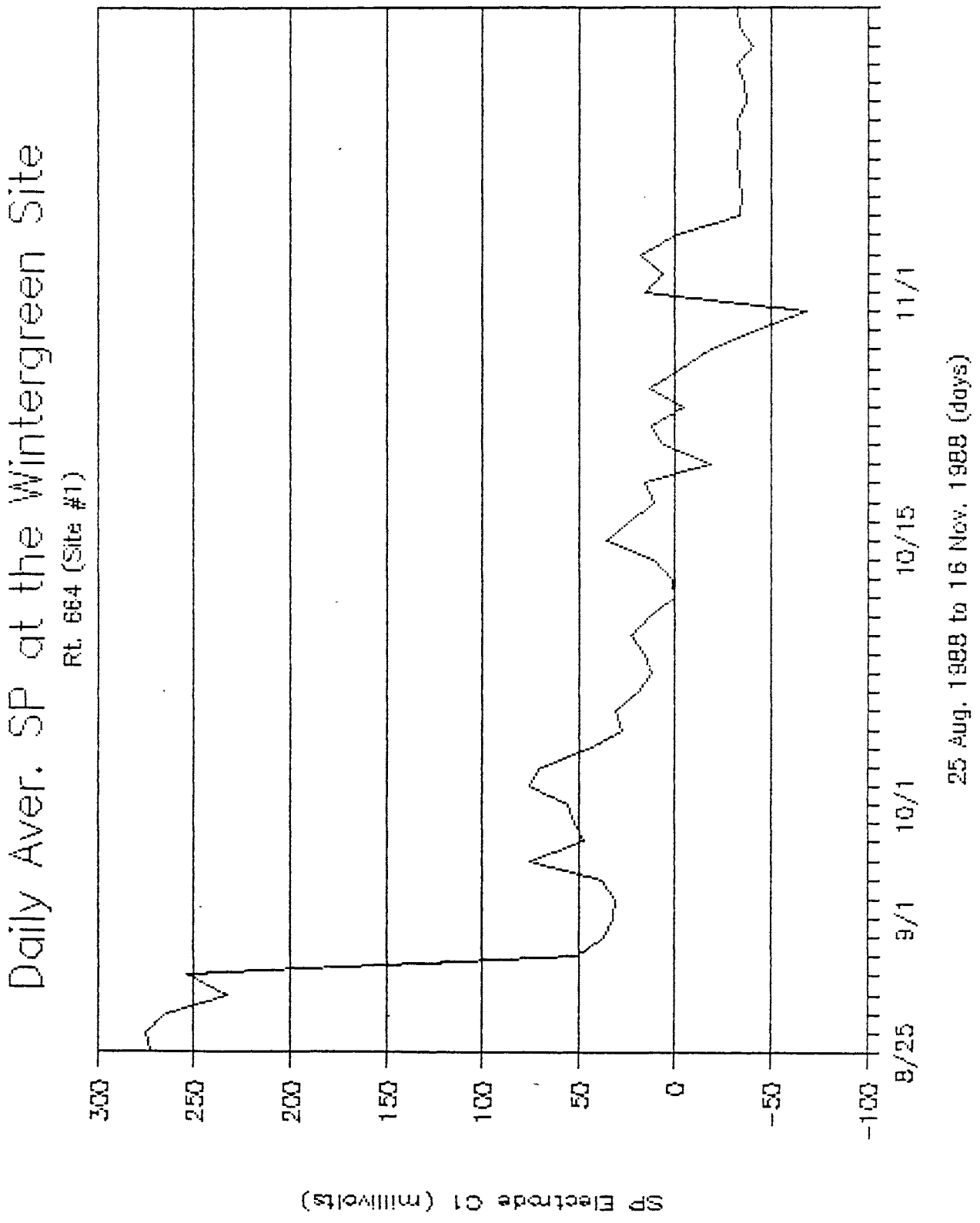
Daily Aver. SP at the Wintergreen Site
Rt. 664 (Site #1)
SP Electrode C1 (millivolts)
300
250
200
150
100
50
0
-50
-100
8/25
9/1
10/1
10/15
11/1
25 Aug. 1988 to 16 Nov. 1988 (days)

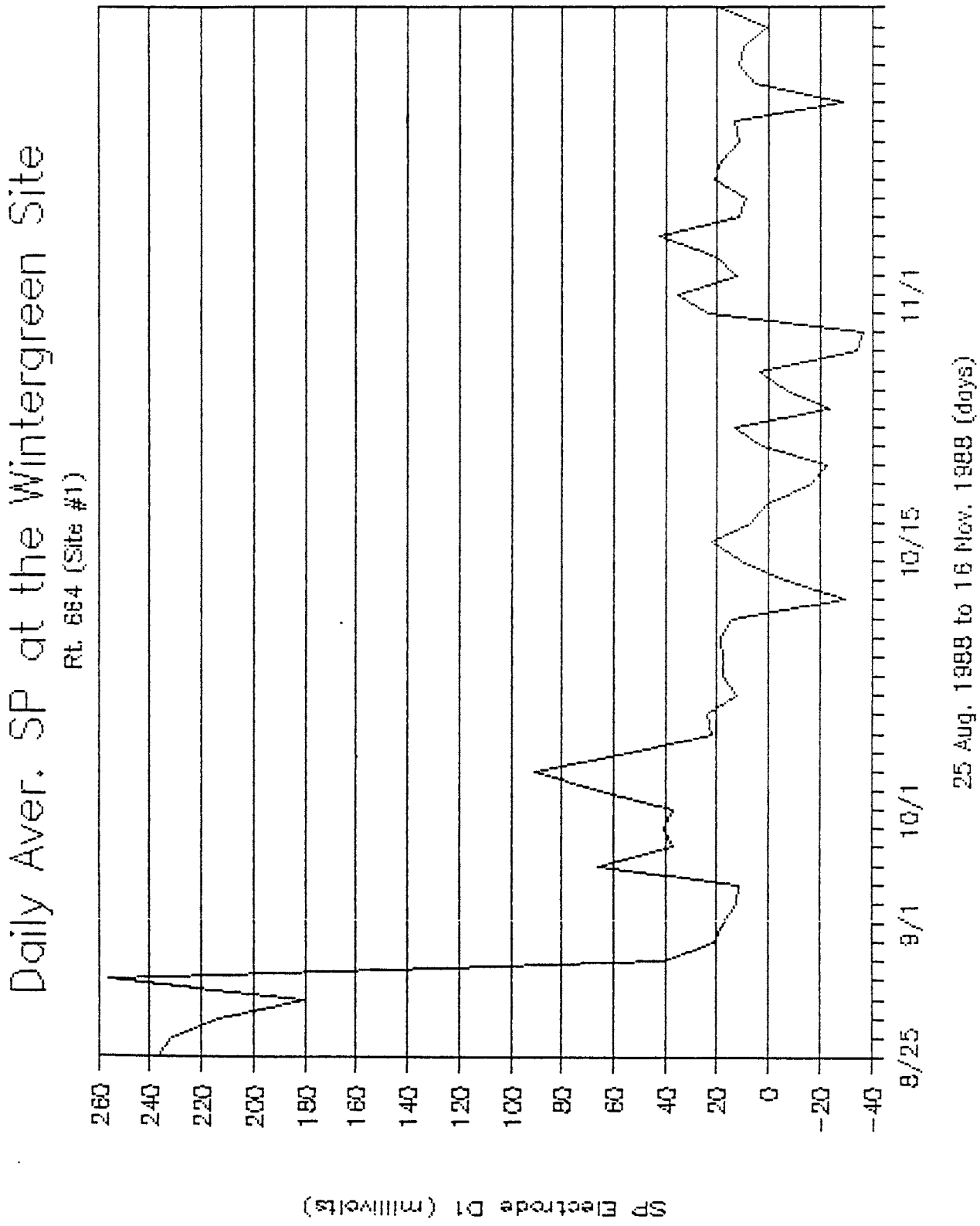
Daily Aver. SP at the Wintergreen Site
Rt. 664 (Site #1)
SP Electrode 01 (millivolts)
260
240
220
200
180
160
140
120
100
80
60
40
20
0
-20
-40
8/25
9/1
10/1
10/15
11/1
25 Aug. 1988 to 16 Nov. 1988 (days)

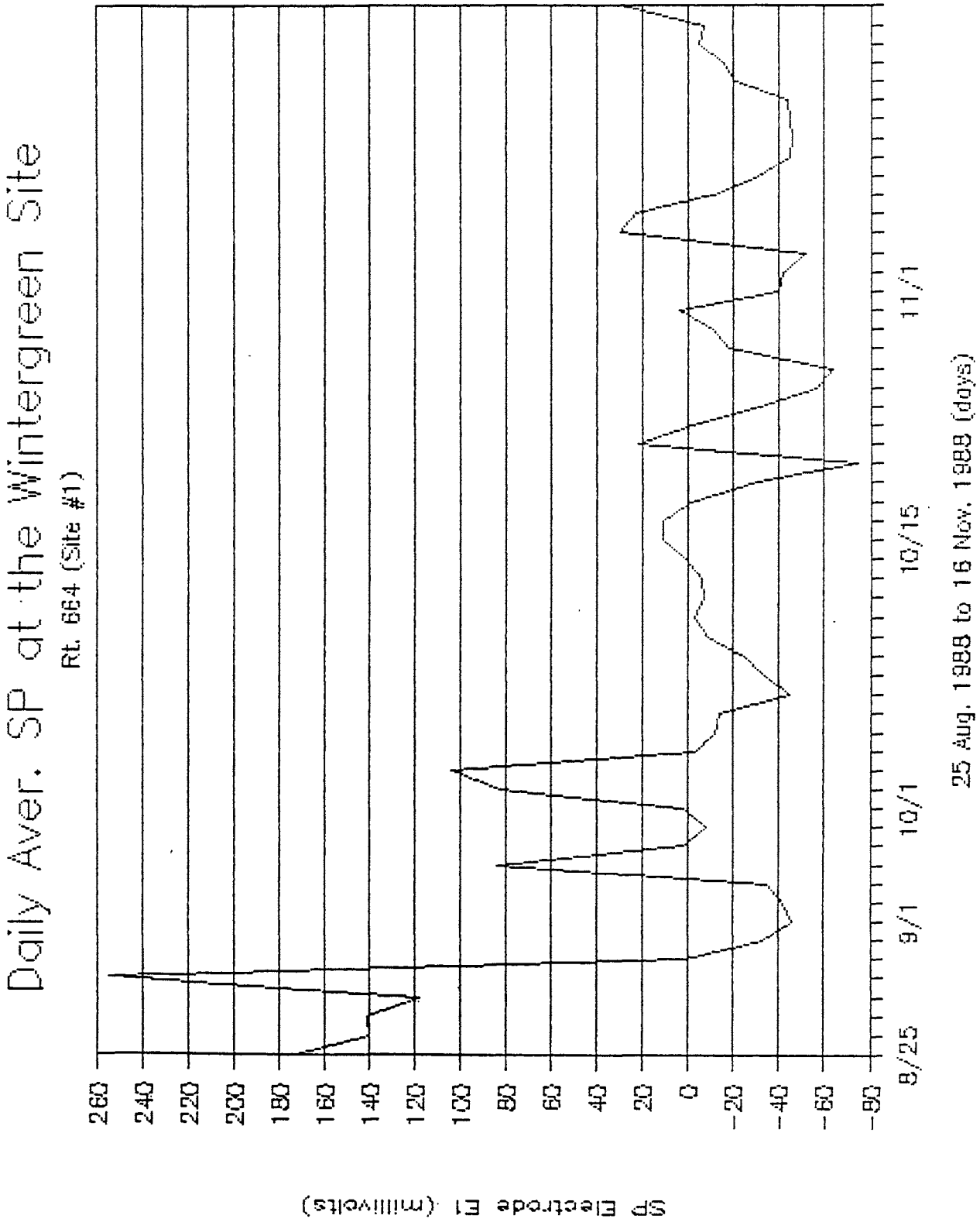
Daily Aver. SP at the Wintergreen Site
Rt. 664 (Site #1)
SP Electrode E1 (millivolts)
260
240
220
200
180
160
140
120
100
80
60
40
20
0
-20
-40
-60
-80
8/25
9/1
10/1
10/15
11/1
25 Aug. 1988 to 16 Nov. 1988 (days)

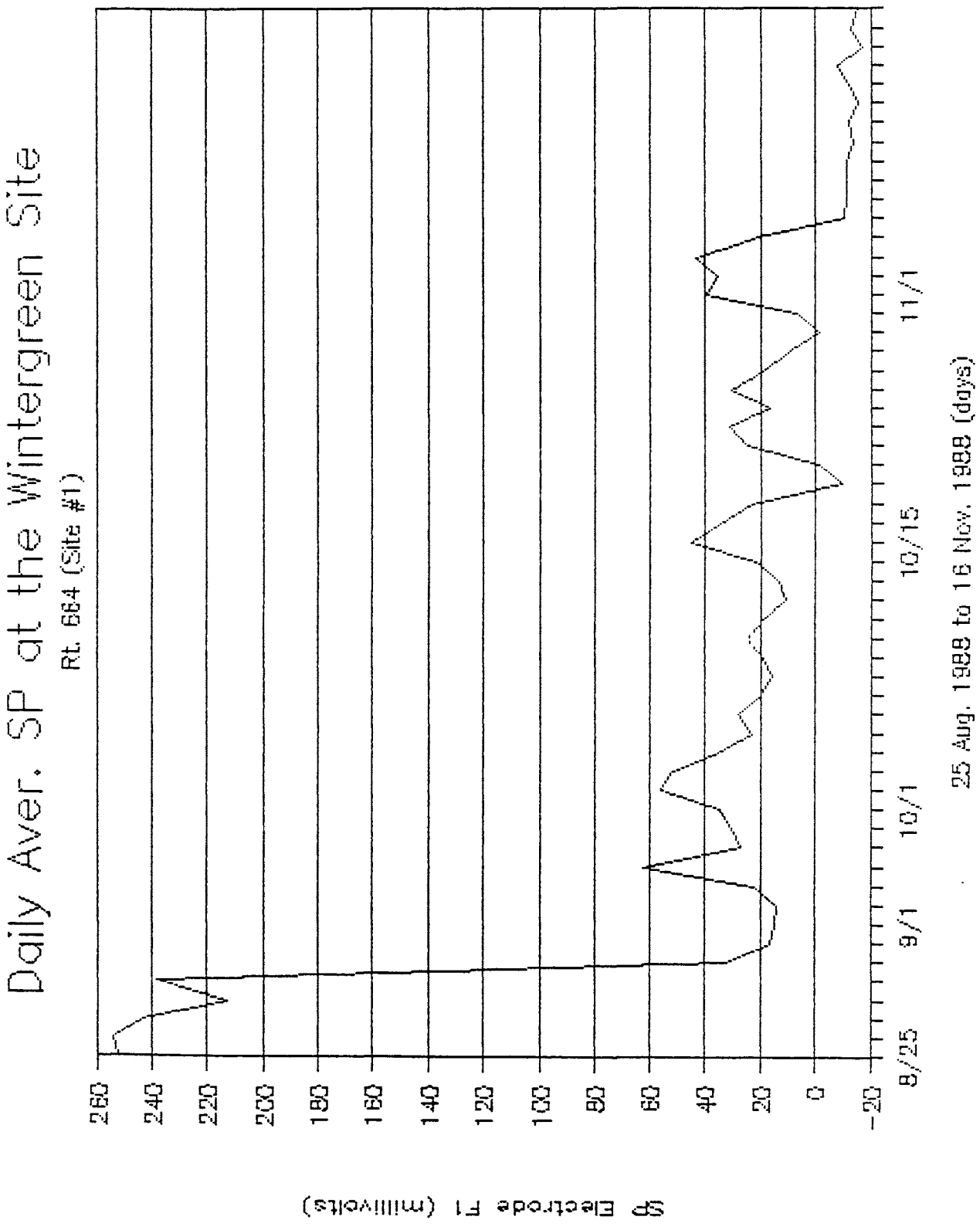
Daily Aver. SP at the Wintergreen Site
Rt. 664 (Site #1)
SP Electrode F1 (millivolts)
260
240
220
200
180
160
140
120
100
80
60
40
20
0
-20
8/25
9/1
10/1
10/15
11/1
25 Aug. 1988 to 16 Nov. 1988 (days)

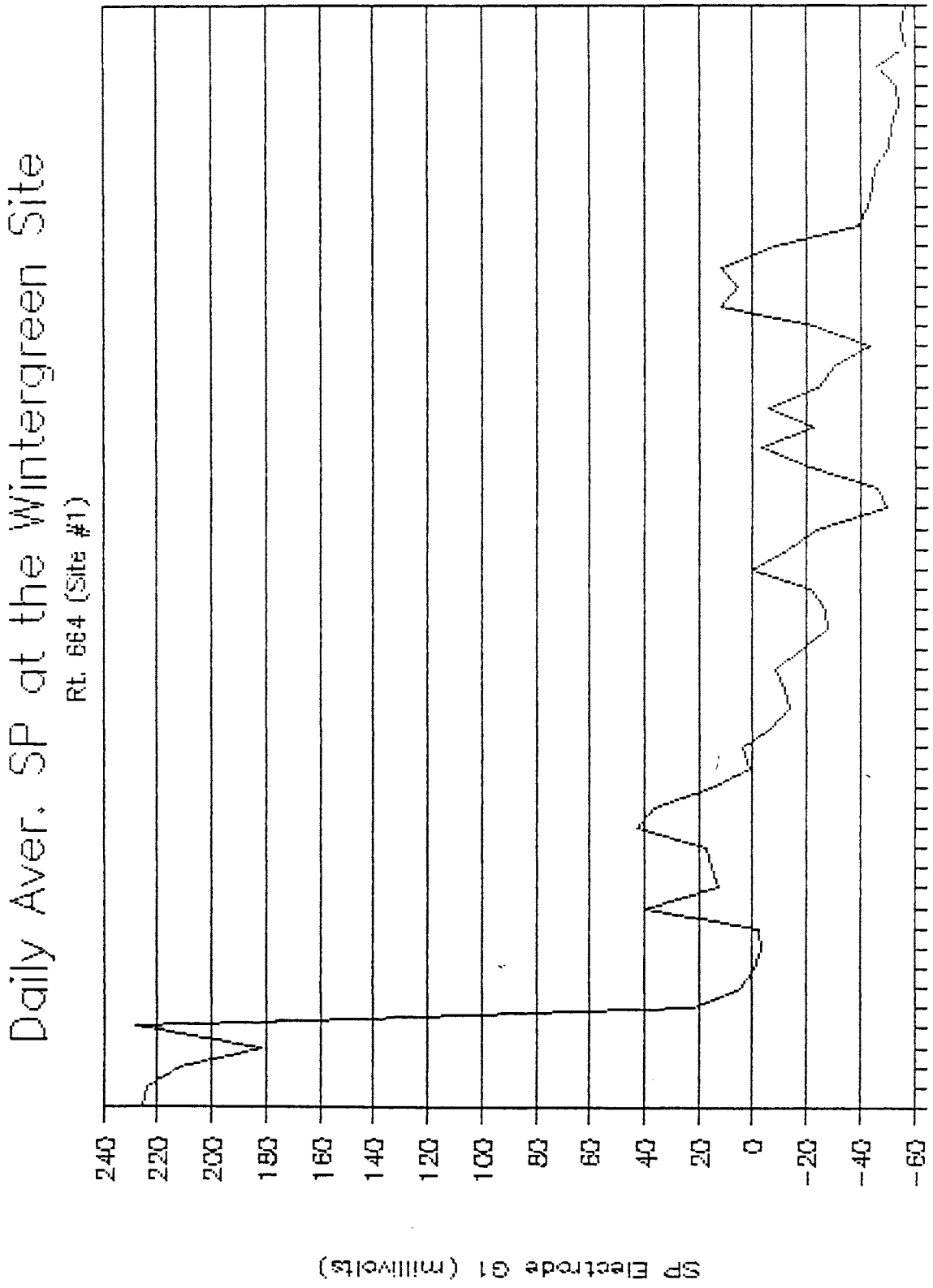
Daily Aver. SP at the Wintergreen Site
Rt. 664 (Site #1)
SP Electrode G1 (millivolts)
240
220
200
180
160
140
120
100
80
60
40
20
0
-20
-40
-60
8/25
9/1
10/1
10/15
11/1
25 Aug. 1988 to 16 Nov. 1988 (days)

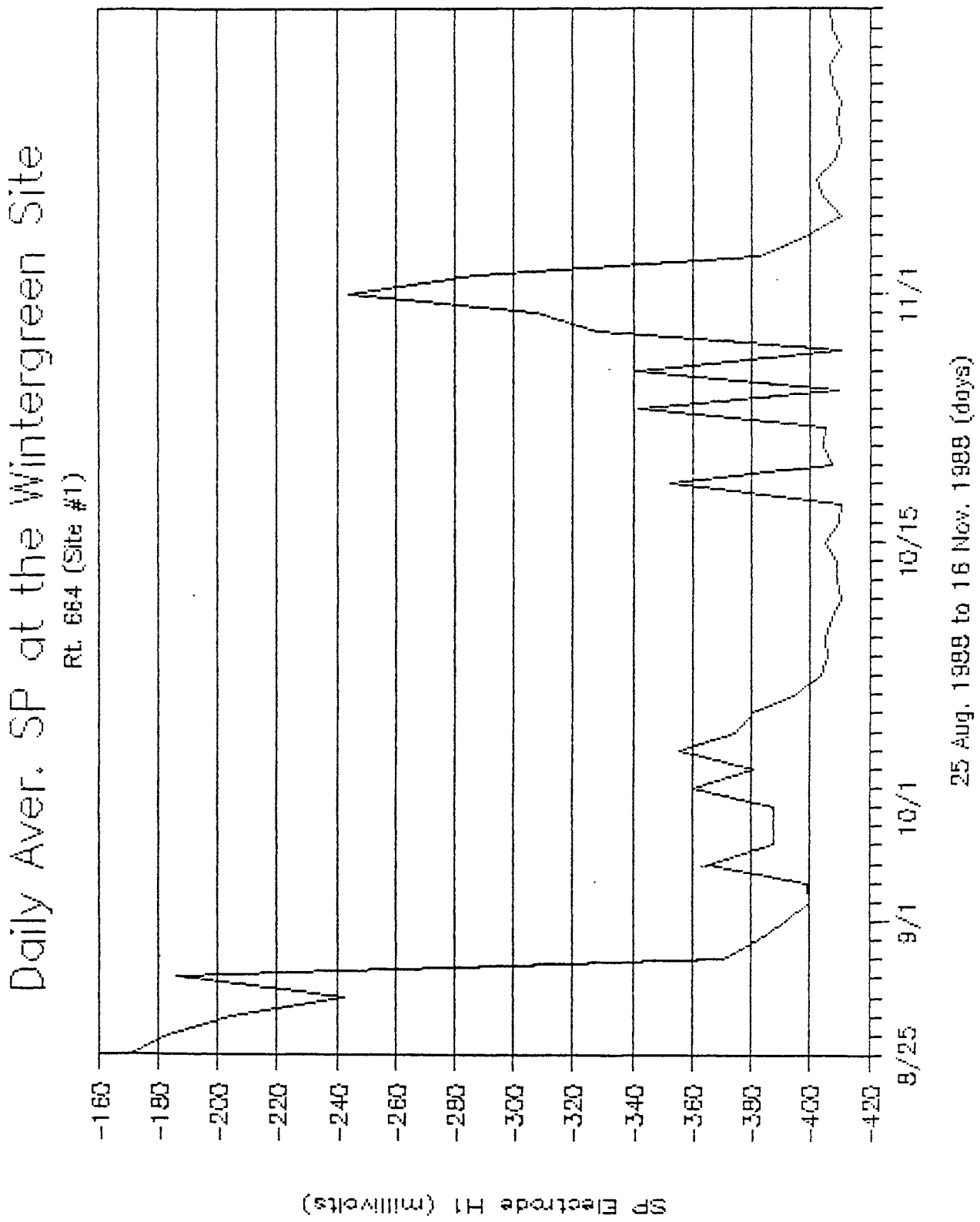
Daily Aver. SP at the Wintergreen Site
Rt. 664 (Site #1)
SP Electrode H1 (millivolts)
-160
-180
-200
-220
-240
-260
-280
-300
-320
-340
-360
-380
-400
-420
8/25
9/1
10/1
10/15
11/1
25 Aug. 1988 to 16 Nov. 1988 (days)

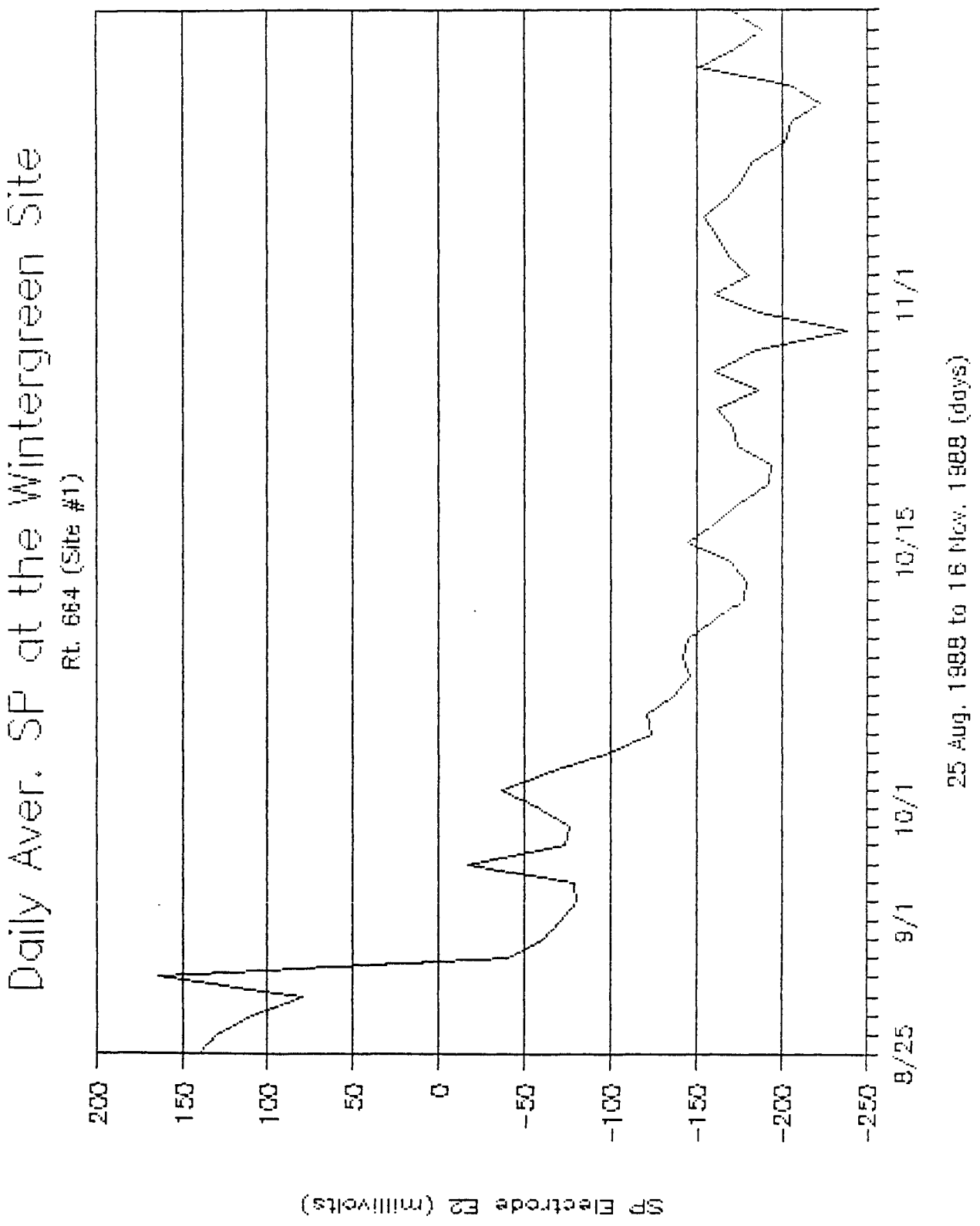
Daily Aver. SP at the Wintergreen Site
Rt. 664 (Site #1)
SP Electrode E2 (millivolts)
200
150
100
50
0
-50
-100
-150
-200
-250
8/25
9/1
10/1
10/15
11/1
25 Aug. 1988 to 16 Nov. 1988 (days)

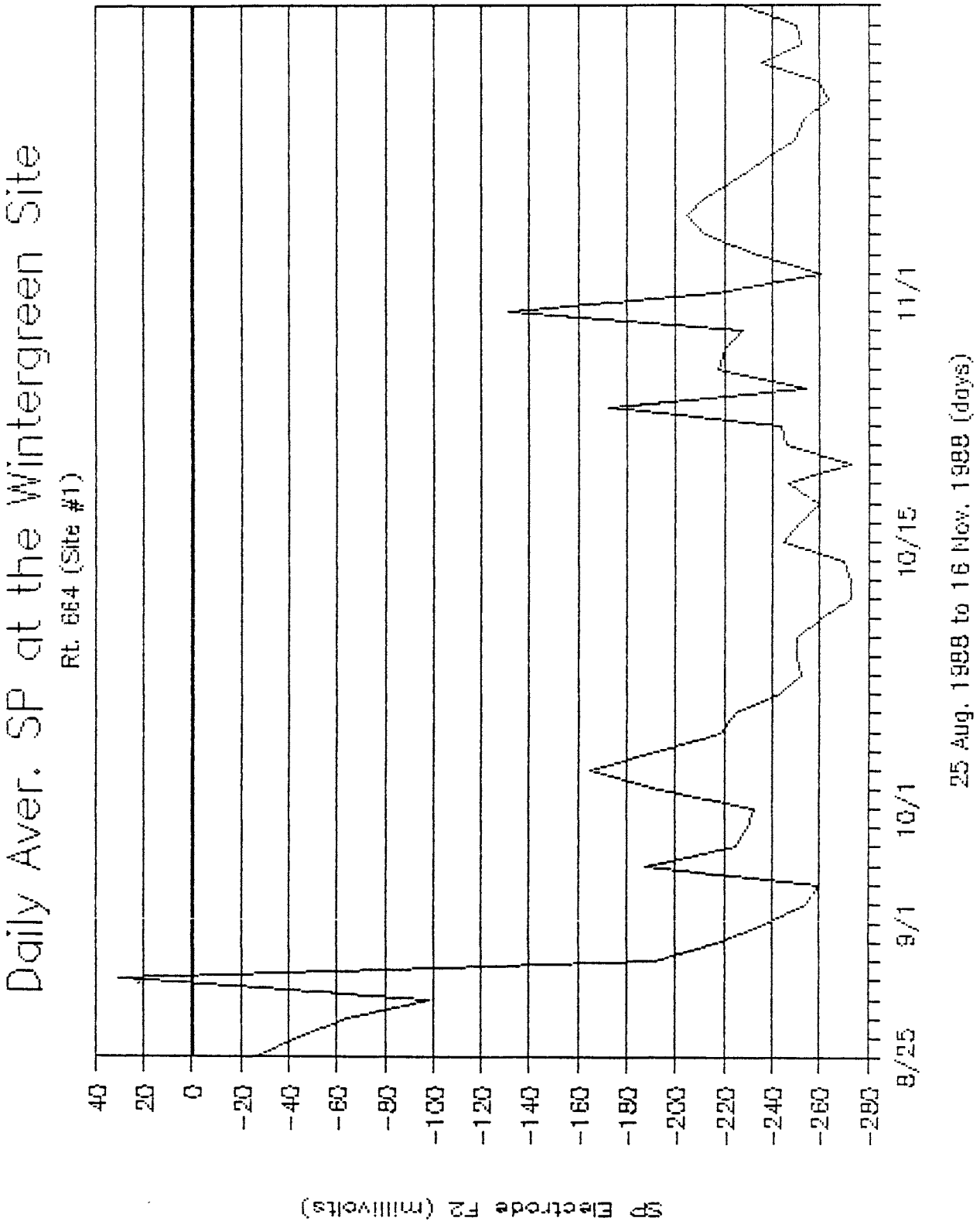
Daily Aver. SP at the Wintergreen Site
Rt. 664 (Site #1)
SP Electrode F2 (millivolts)
40
20
0
-20
-40
-60
-80
-100
-120
-140
-160
-180
-200
-220
-240
-260
-280
8/25
9/1
10/1
10/15
11/1
25 Aug. 1988 to 16 Nov. 1988 (days)

APPENDIX B

Data from Site II

1962

DATA PRESENTED

1. The array pattern showing the position and labels of the 11 electrodes. This is also Figure 13 in the text but is presented again in this appendix to assist the reader in reading the other maps.

2. The spontaneous potential (SP) contour maps obtained from SP data collected on the following dates: May 4, 5, 6, 9, 13, 20, 23, and 31; June 10, 16, and 29; and July 1 and 26, 1988.

3. The SP data collected on the following dates: September 20, 23, 26, and 29; October 7, 13, 18, 20, 24, 27, and 31; and November 3, 7, 10, and 14, 1988.

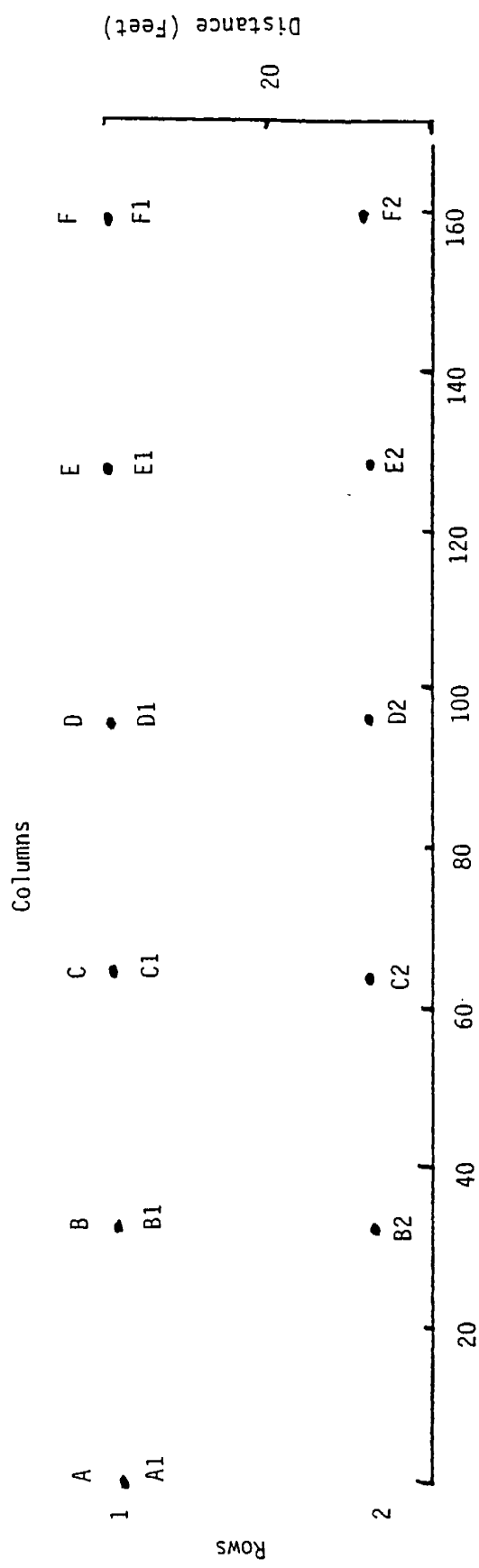

Figure 13: Spontaneous Potential Electrode Arry Pattern at Site II.

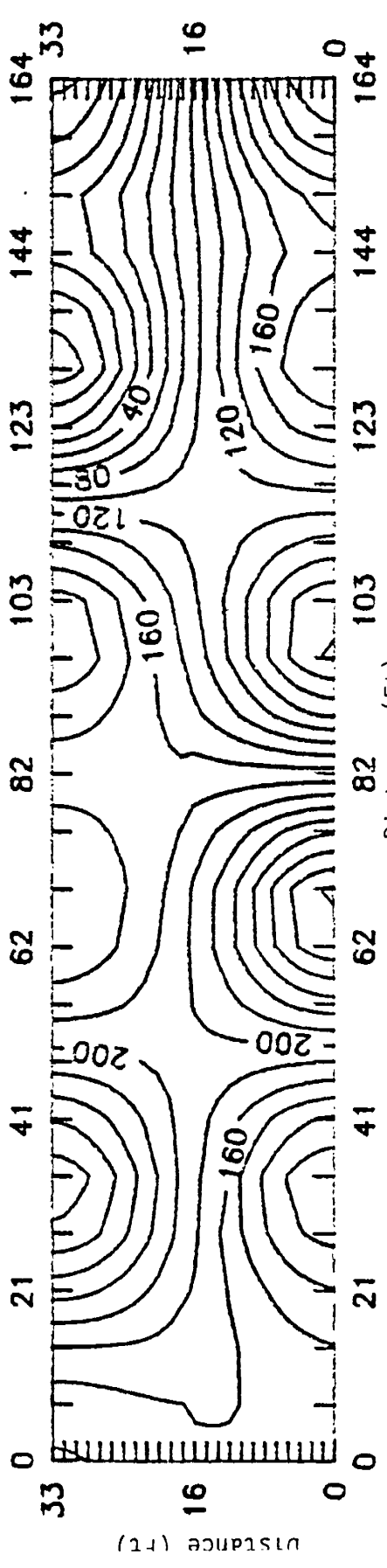

SP Contour Map for Site II on 4 May 1988.
Contour Interval is 40 mv.

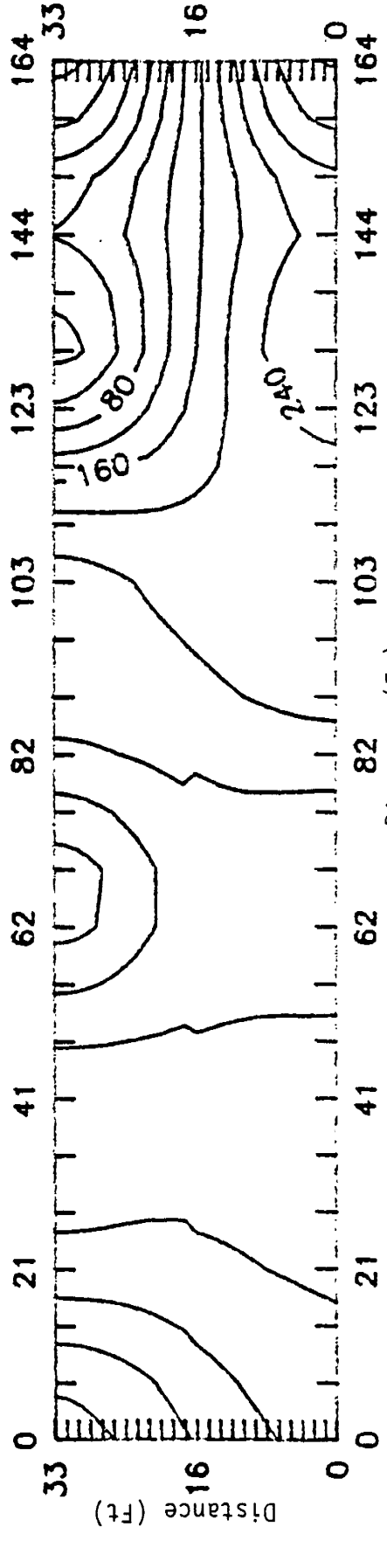

SP Contour Map for Site II on 5 May 1988.
Contour Interval is 40 mv.

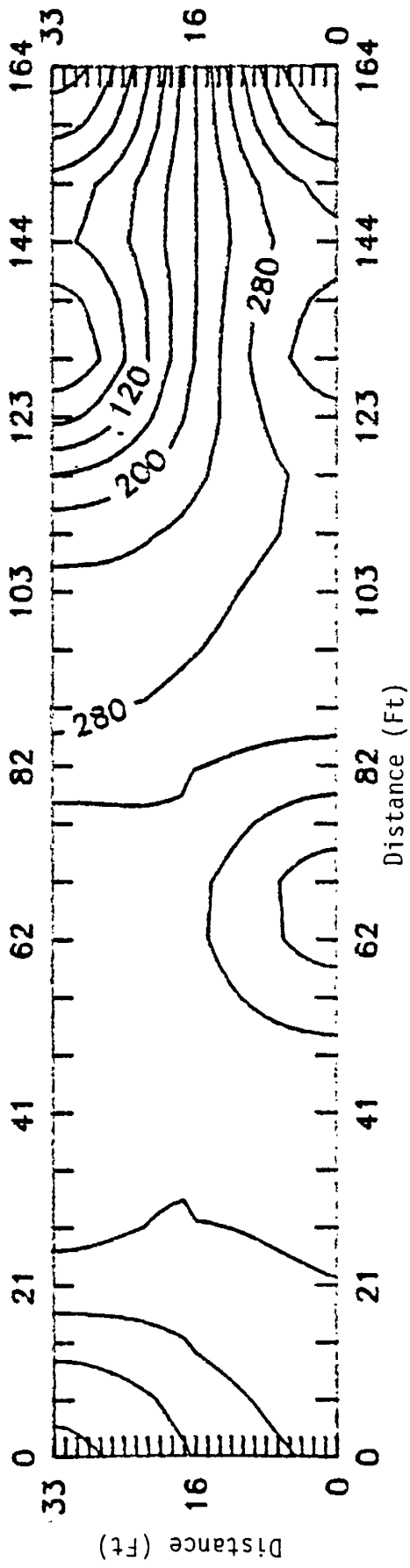

SP Contour Map for Site II on 6 May 1988.
Contour Interval is 40 mv.

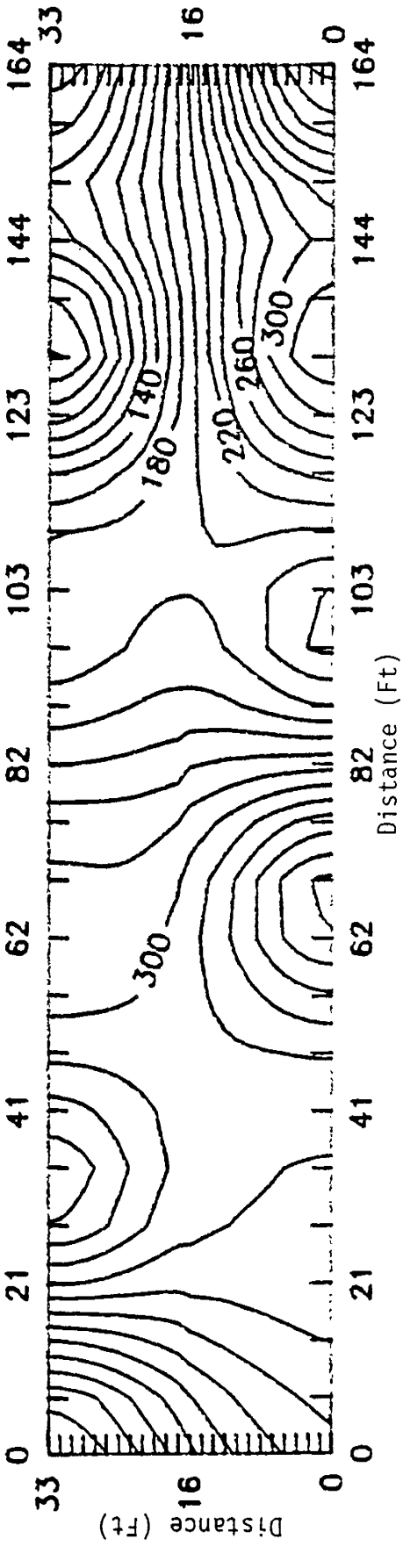

SP Contour Map for Site II on 9 May 1988.
Contour Interval is 40 mv.

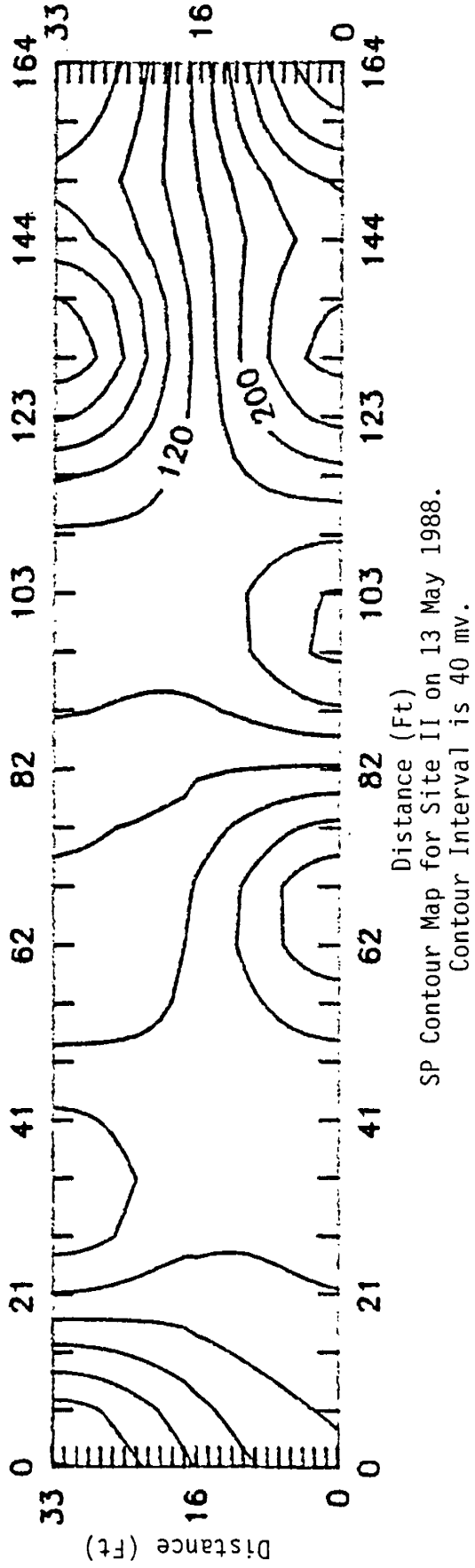

SP Contour Map for Site II on 13 May 1988.
Contour Interval is 40 mv.

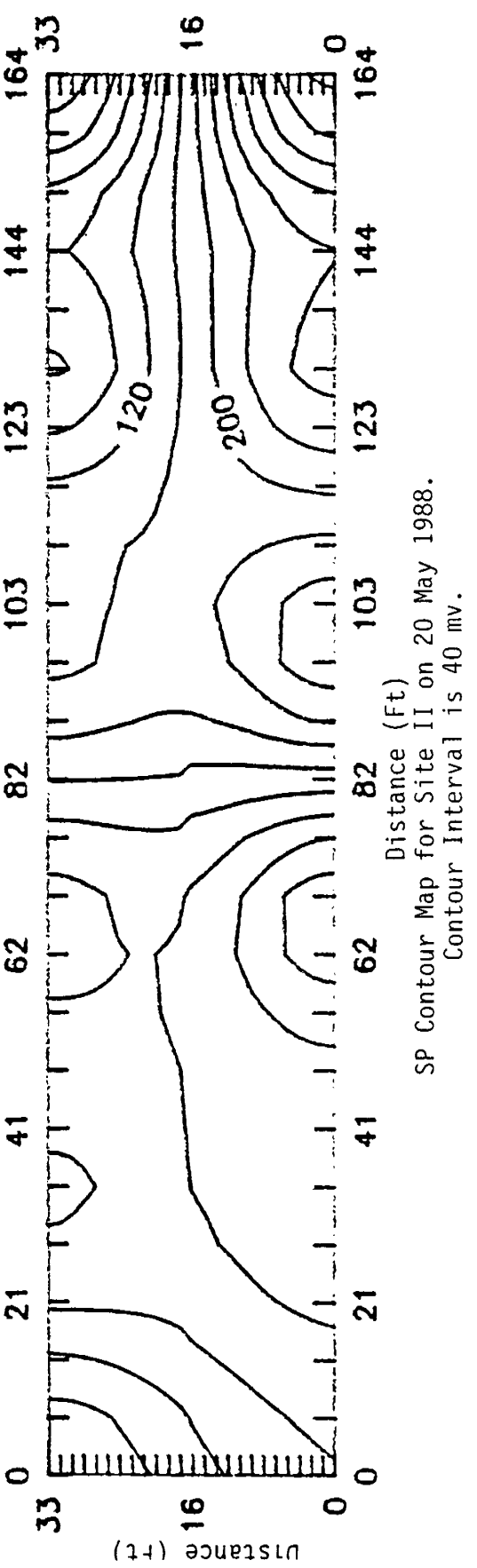

SP Contour Map for Site II on 20 May 1988.
Contour Interval is 40 mv.

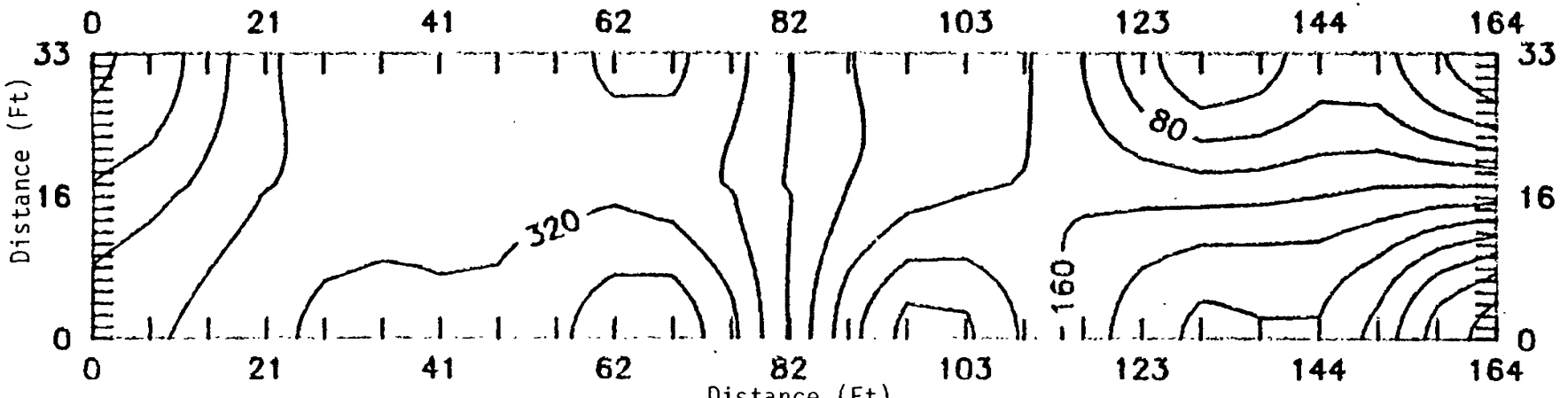

Distance (Ft)
SP Contour Map for Site II on 23 May 1988.
Contour Interval is 40 mv.

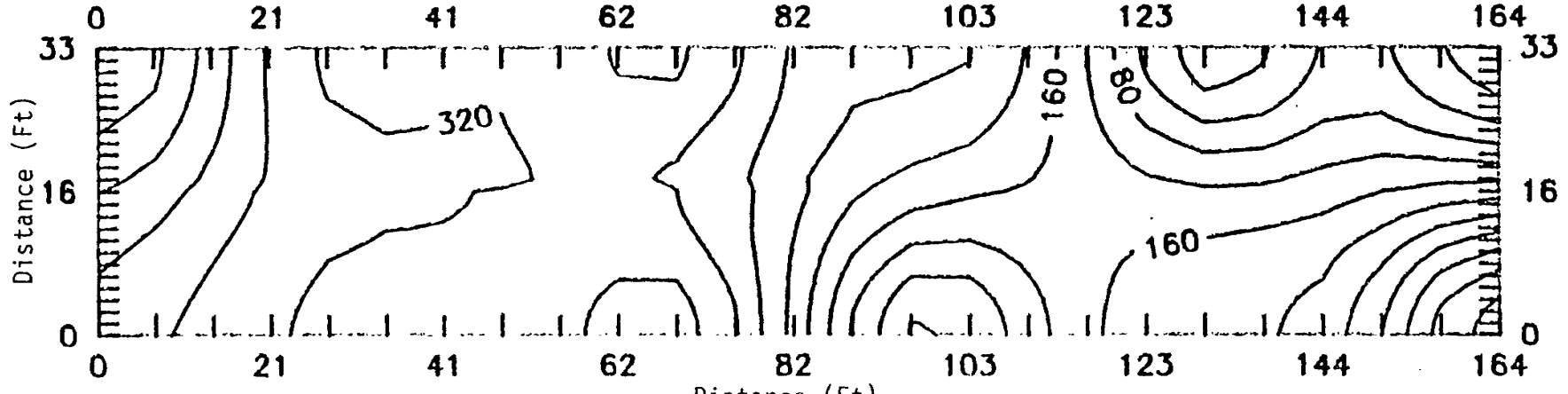

Distance (Ft)
SP Contour Map for Site II on 31 May 1988.
Contour Interval is 40 mv.

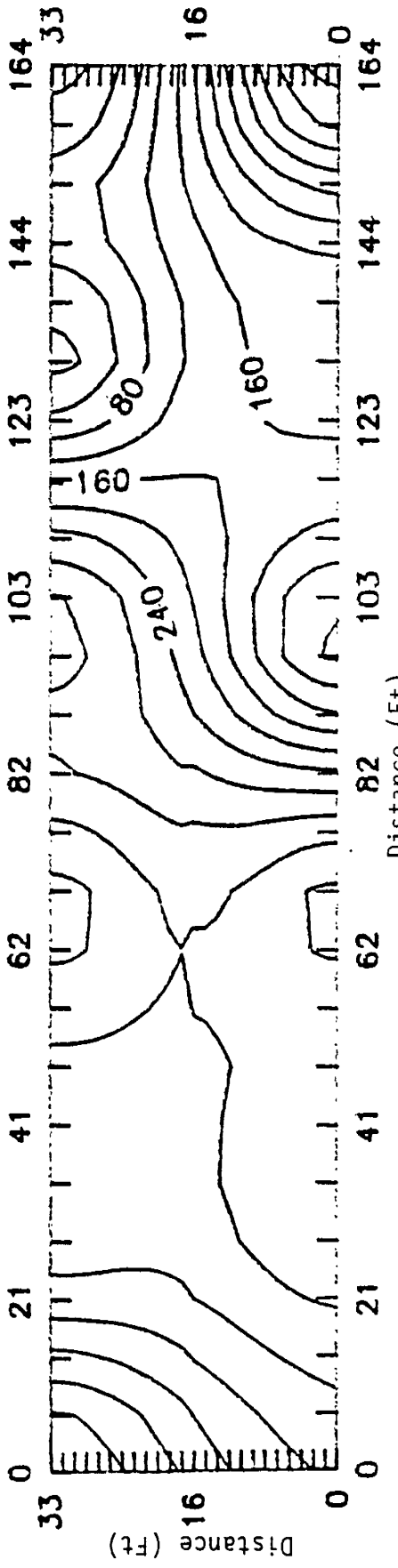

SP Contour Map for Site II on 10 June 1988.
Contour Interval is 40 mv.

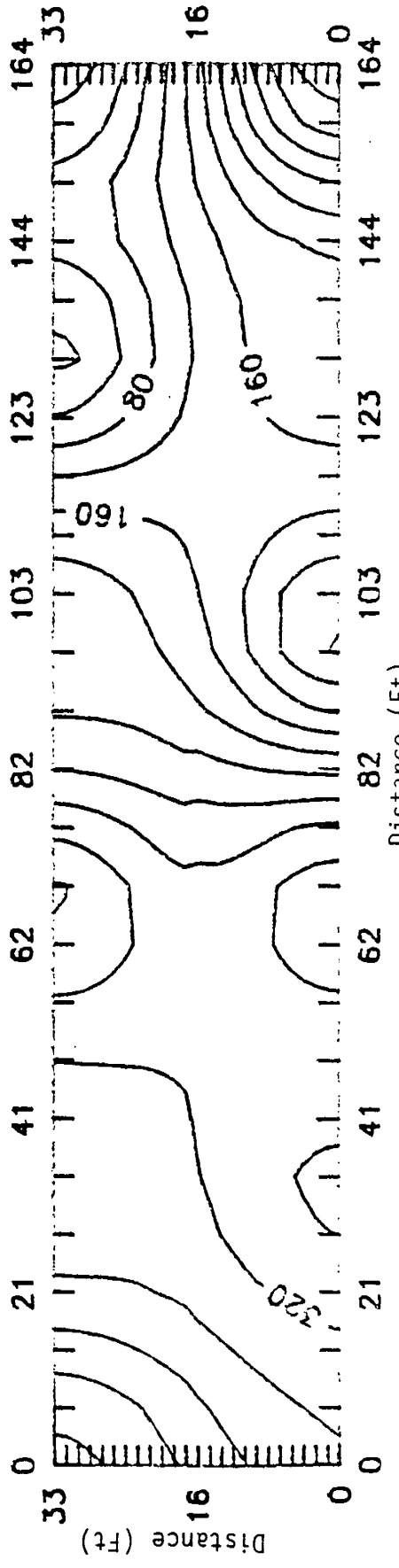

SP Contour Map for Site II on 16 June 1988.
Contour Interval is 40 mv.

1970

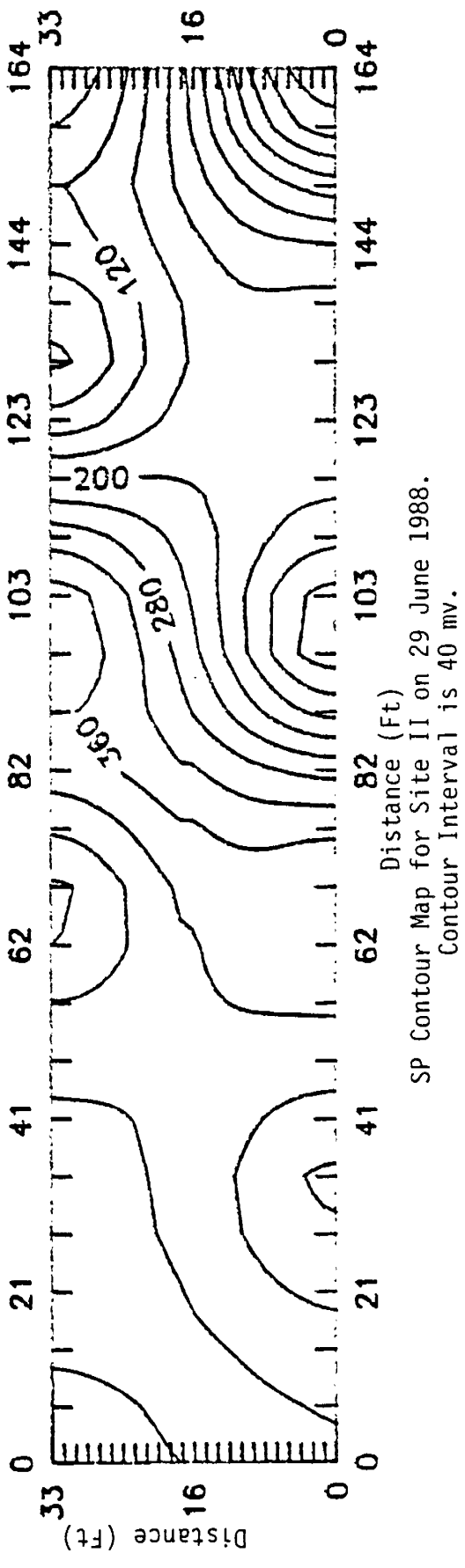

SP Contour Map for Site II on 29 June 1988.
Contour Interval is 40 mv.

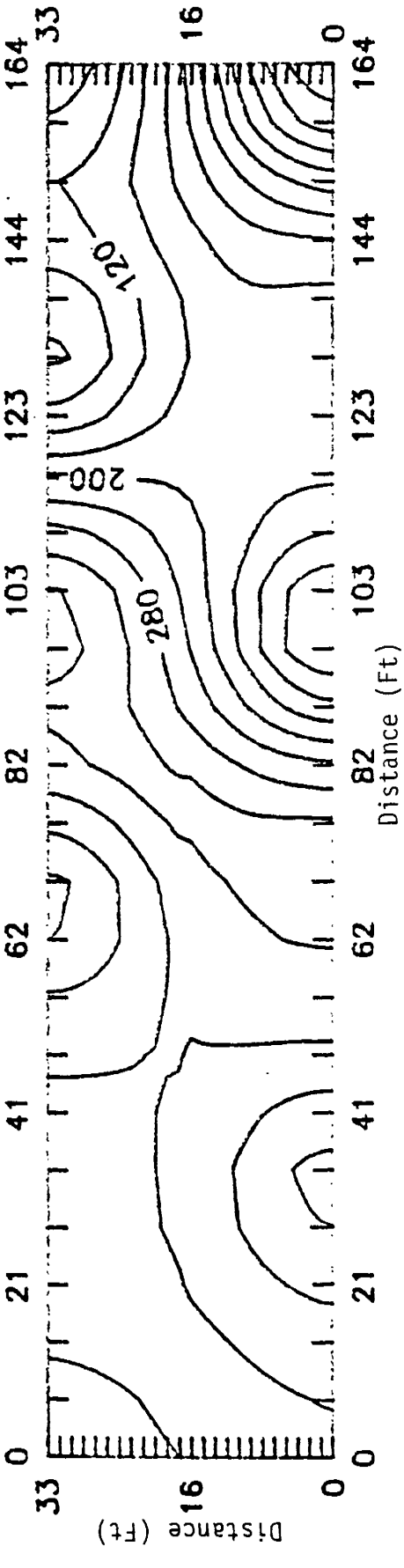

SP Contour Map for Site II on 1 July 1988.
Contour Interval is 40 mv.

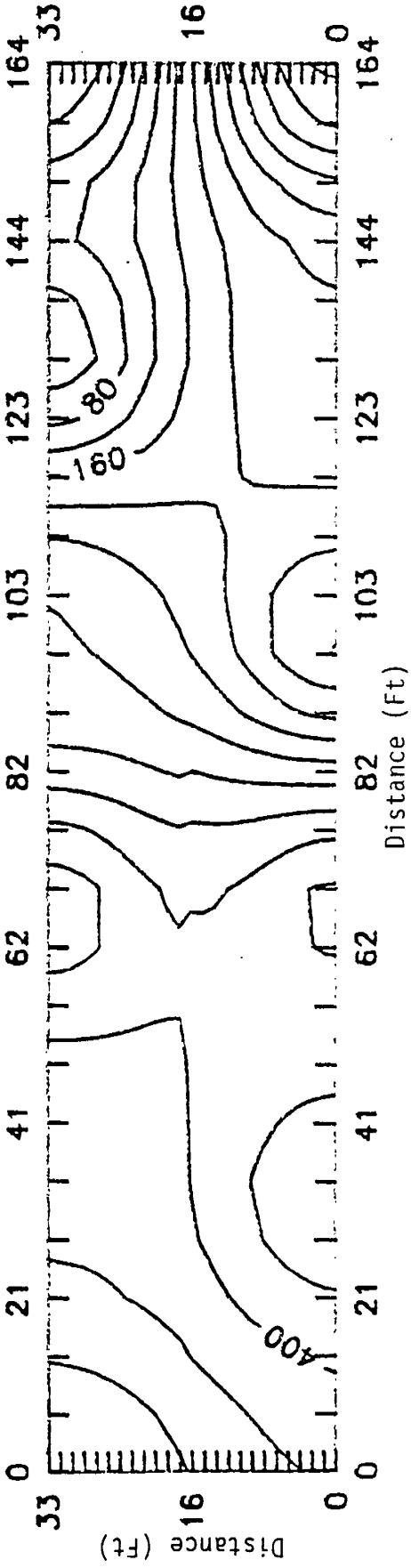

SP Contour Map for Site II on 26 July 1988.
Contour Interval is 40 mv.

1972

ELECTRODE VALUES FOR WINTERGREEN SLOPE TWO

DATE	A1	B1	B2	C1	C2	D1	D2	E1	E2
F1	F2	GTEMP							
20 SEPT	.168	.337	.439	.441	.386	.193	.070	-.067	.159
-.053	.430	20.5							
23 SEPT	.156	.315	.438	.439	.389	.194	.051	-.075	.156
-.050	.428	22.0							
26 SEPT	.108	.262	.385	.381	.334	.152	.047	-.103	.111
-.132	.368	17.0							
29 SEPT	.095	.247	.415	.418	.360	.142	.056	-.103	.131
-.070	.400	15.0							
07 OCT	.047	.143	.390	.404	.343	.100	.047	-.129	.111
-.088	.380	10.0							
13 OCT	.058	.161	.419	.420	.363	.131	.047	-.134	.133
-.074	.406	10.0							
18 OCT	.083	.208	.427	.425	.369	.146	.045	-.089	.135
-.093	.412	15.0							
20 OCT	.072	.208	.428	.431	.365	.137	.039	-.093	.132
-.066	.415	12.0							
24 OCT	.047	.174	.394	.398	.348	.115	.040	-.114	.114
-.087	.388	10.5							
27 OCT	.052	.168	.420	.428	.366	.125	.048	-.104	.132
-.071	.408	10.0							
31 OCT	.057	.144	.425	.439	.367	.122	.042	-.099	.126
-.065	.409	9.0							
03 NOV	.052	.174	.405	.387	.357	.120	.048	-.107	.121
-.077	.395	8.0							
07 NOV	.033	.263	.426	.414	.378	.103	.059	-.051	.140
-.039	.407	9.5							
10 NOV	.055	.230	.430	.411	.380	.104	.089	-.063	.142
-.034	.418	10.0							
14 NOV	.030	.219	.400	.387	.353	.087	.069	-.097	.124
-.073	.393	10.0							

APPENDIX C

Data from Site III

1974

DATA PRESENTED

1. The array pattern showing the position and labels of the 32 electrodes. This is also Figure 15 in the text but is presented again in this appendix to assist the reader in reading the other maps.

2. The spontaneous potential (SP) contour maps obtained from SP data collected on the following dates: using reference electrode 1 on May 4, 5, 6, 9, 13, 17, and 23, and August 25, 1988; using reference electrode 2 on May 17 and 23; June 10; July 11 and 19; August 25 and 30; September 13 and 20; and November 22, 1988, and on May 19 and June 8, 1989.

3. The SP values taken every 15 min for 6 days (September 1 to 6, 1989) for electrodes A3, A4, B2, B3, and D2. The first figure for each electrode is the graphical presentation of unfiltered data. The second figure for each electrode is the graphical presentation of filtered data. The data were filtered by determining corresponding high and low limits of data. These limits were determined by inspection. If a data value exceeded either the high or low limit, it was replaced by the preceding data point. This process was iterative to ensure that all values passed through the filter. The data were then averaged for a 1-hr increment and plotted versus time. To eliminate the diurnal temperature effects, daily averages of SP values for these five electrodes were plotted for the entire AMS measuring system and are also presented.

4. The penetration resistance (kg/cm^2) versus depth obtained using the VMI Dinastar penetrometer at electrodes B3, C3, D3, E1, E2, E3, and E4.

5. The conductivity (micro mhos/cm) versus depth obtained using the VMI Dinastar penetrometer at electrodes B3, C3, D3, E1, E2, E3, and E4.

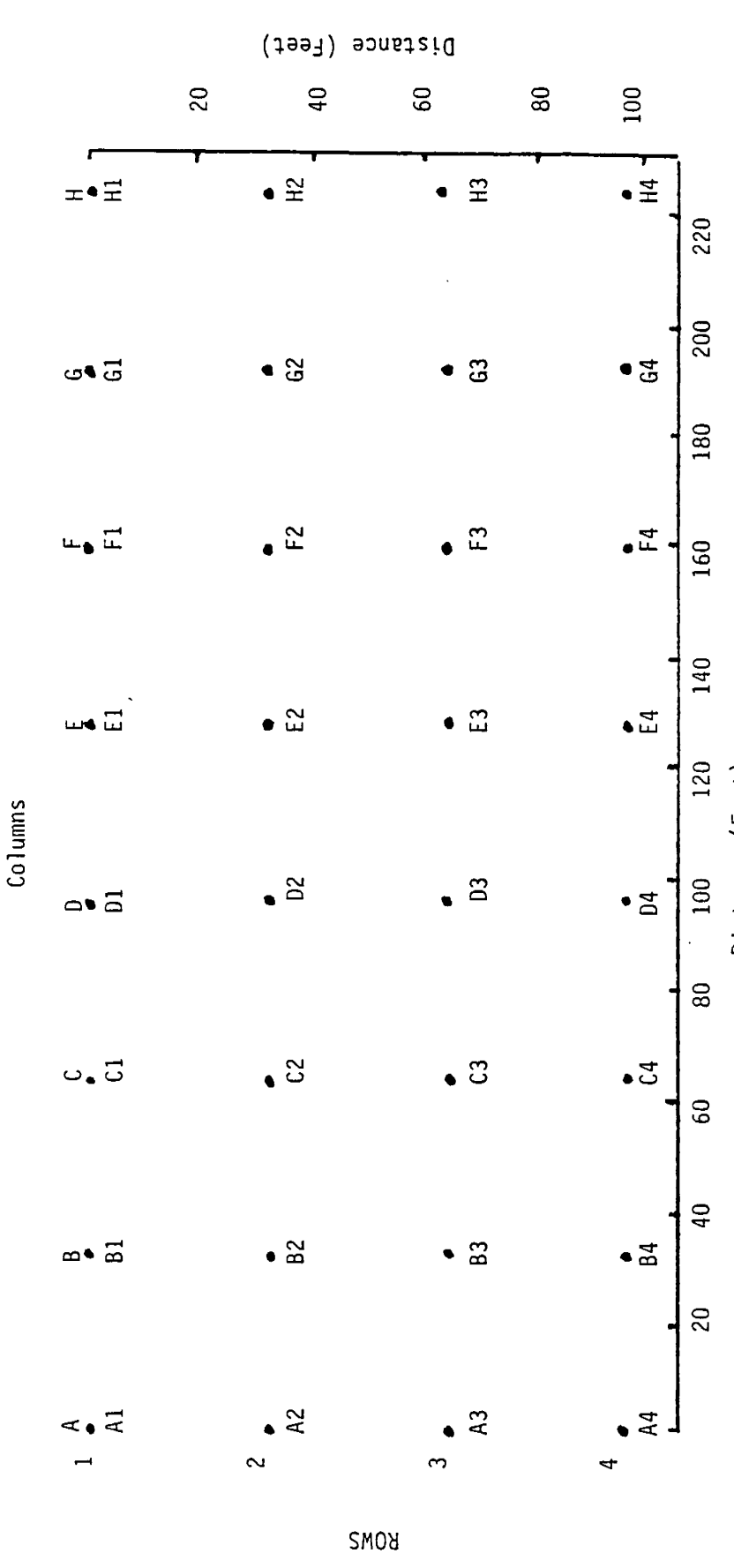

Figure 15: Spontaneous Potential Electrode Array Pattern at Site III

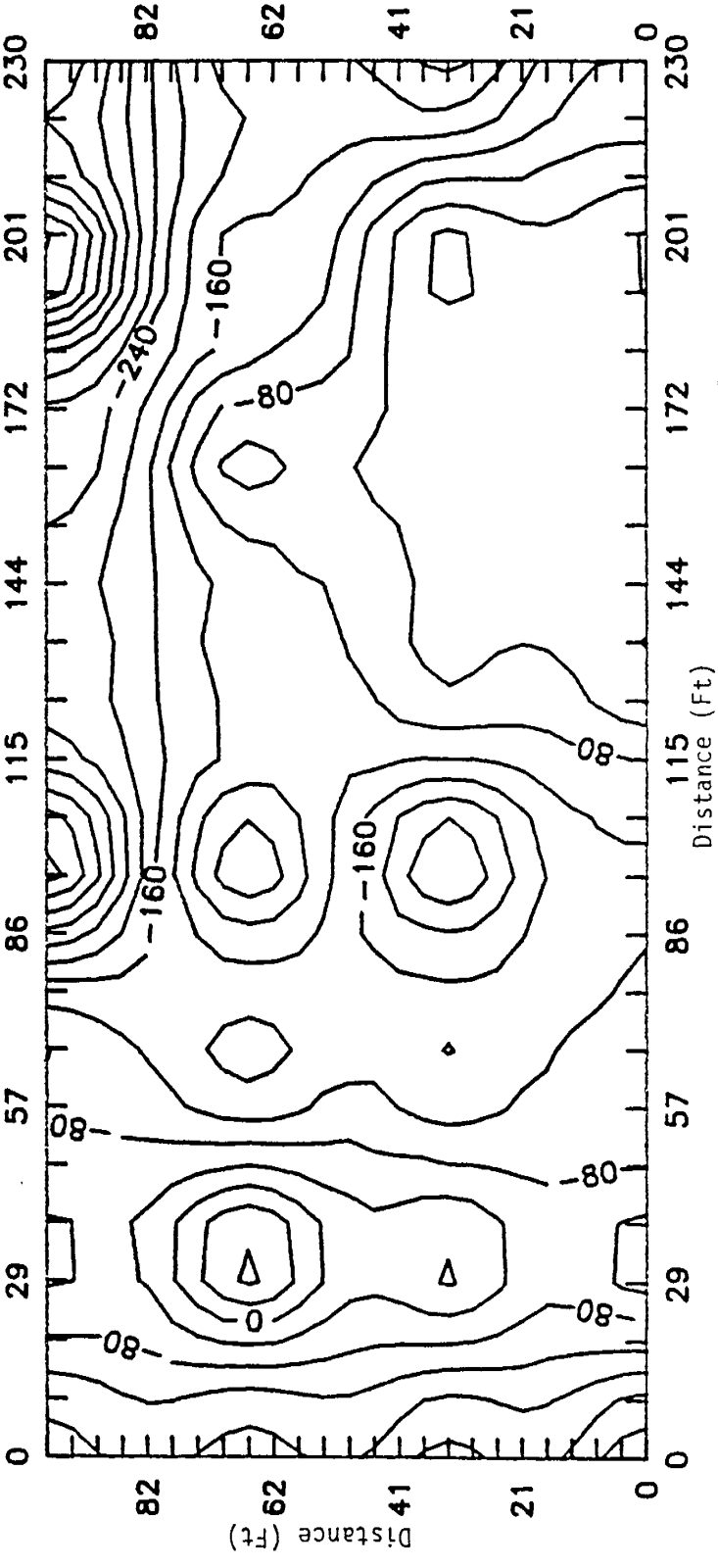

SP Contour Map Using Reference Electrode One at Site III
on 4 May 1988. Contour Interval is 40 mv.

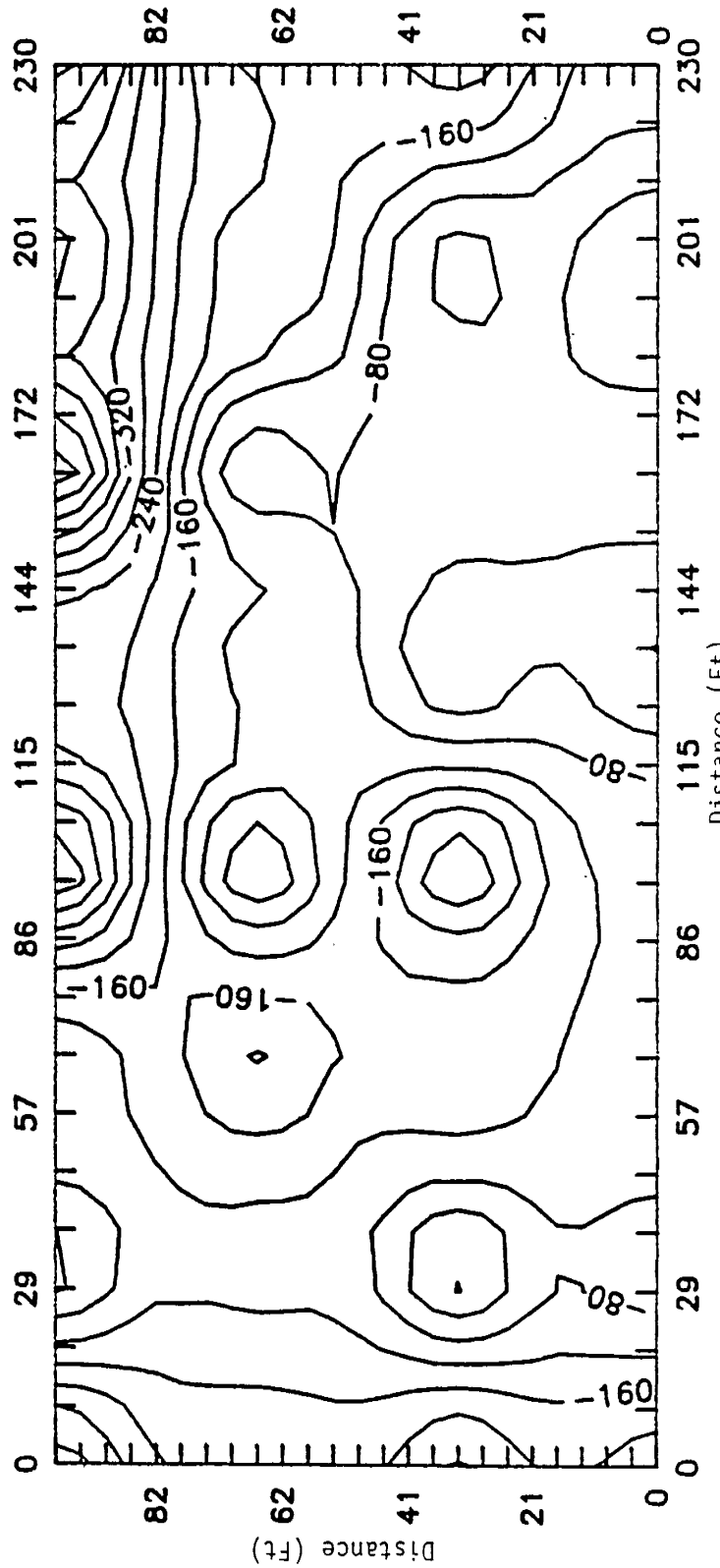

SP Contour Map Using Reference Electrode One at Site III
on 5 May 1988. Contour Interval is 40 mv.

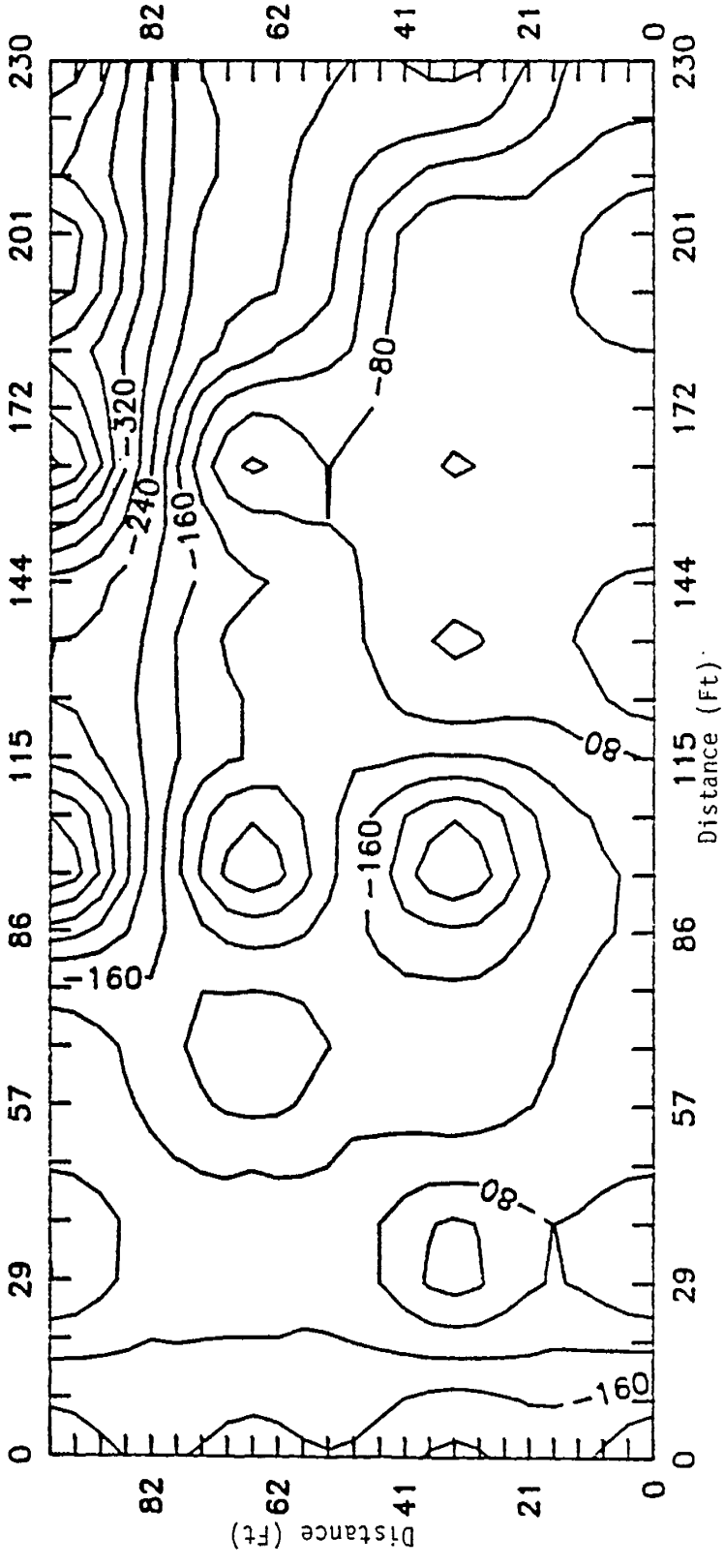

SP Contour Map Using Reference One at Site Site III
on 6 May 1988. Contour Interval is 40 mv.

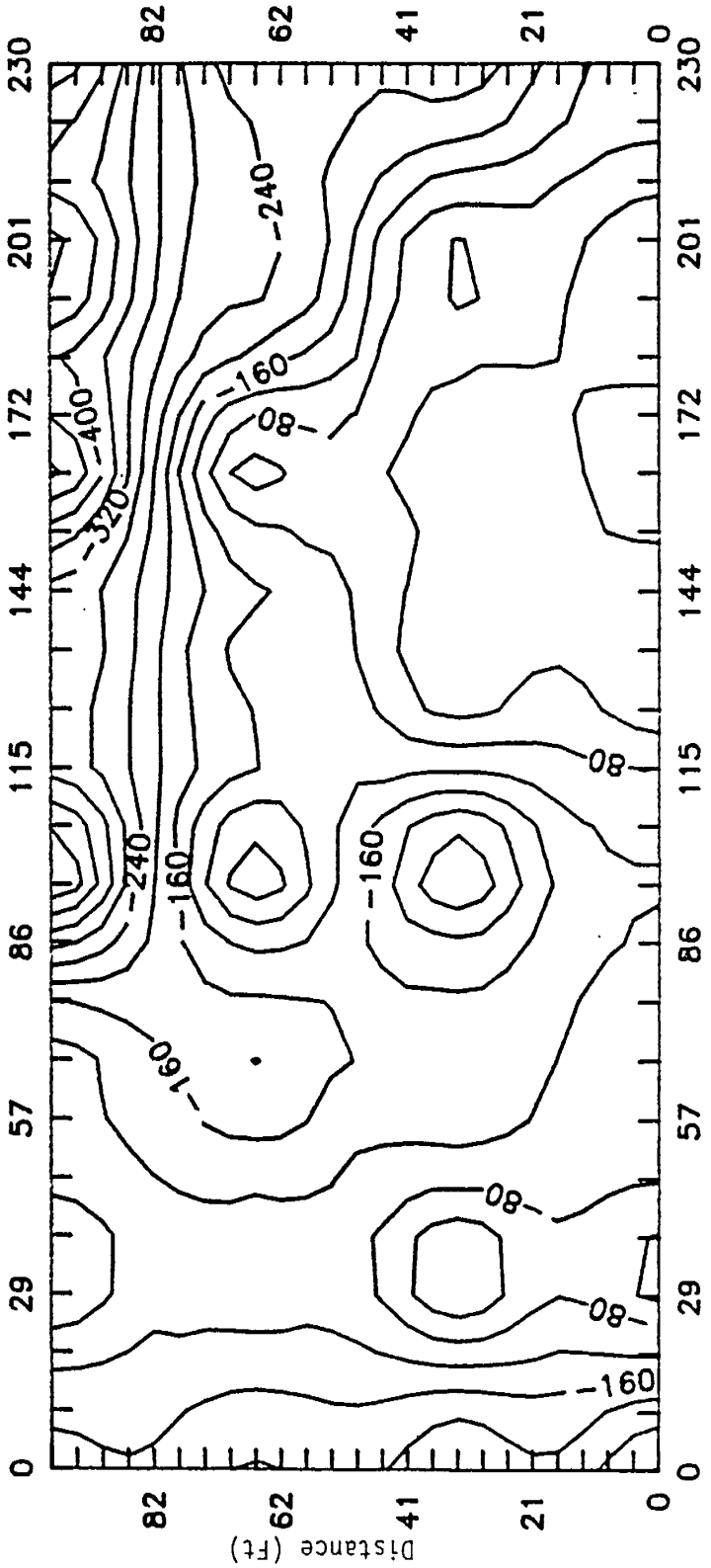

SP Contour Map Using Reference Electrode One at Site III
on 9 May 1988. Contour Interval is 40 mv.

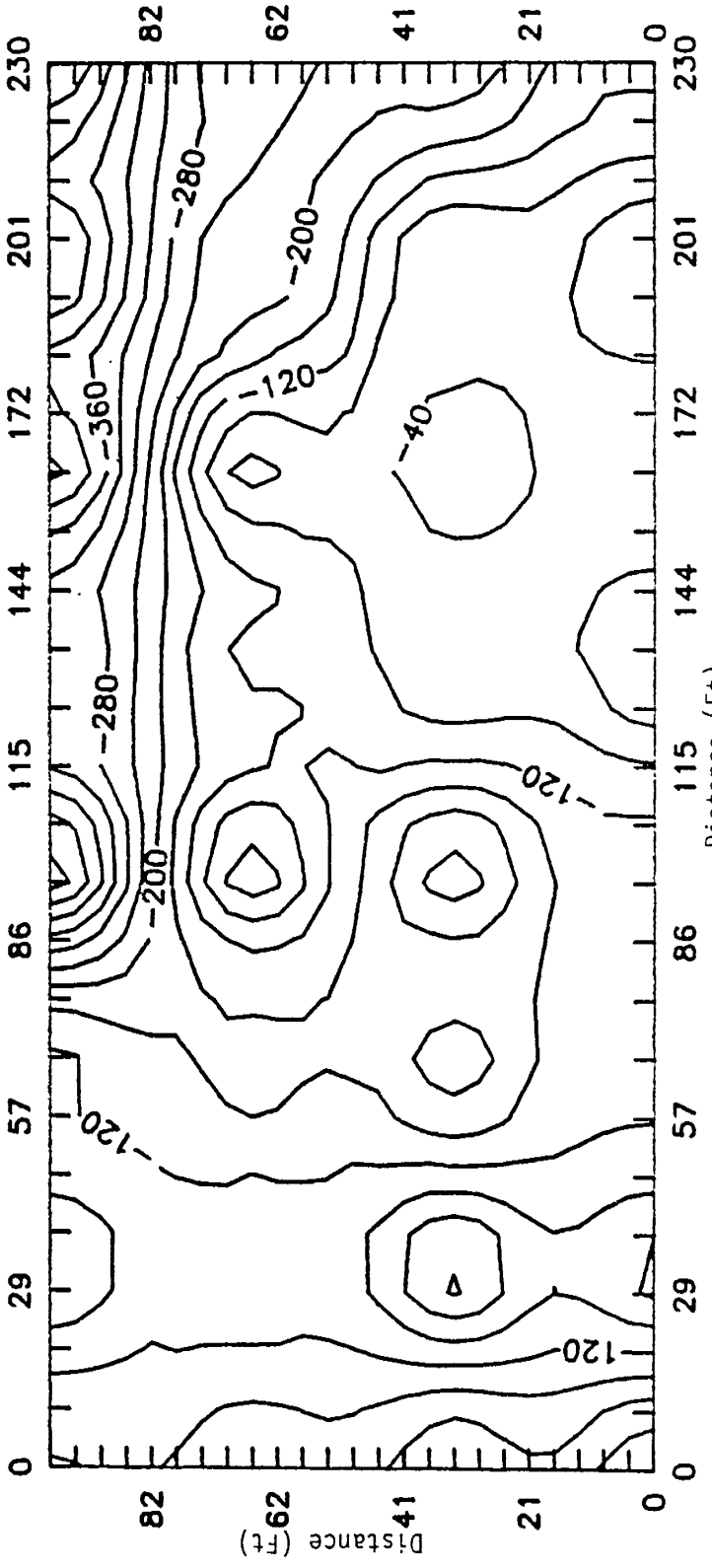

SP Contour Map Using Reference Electrode One at Site III
on 13 May 1988. Contour Interval is 40 mv.

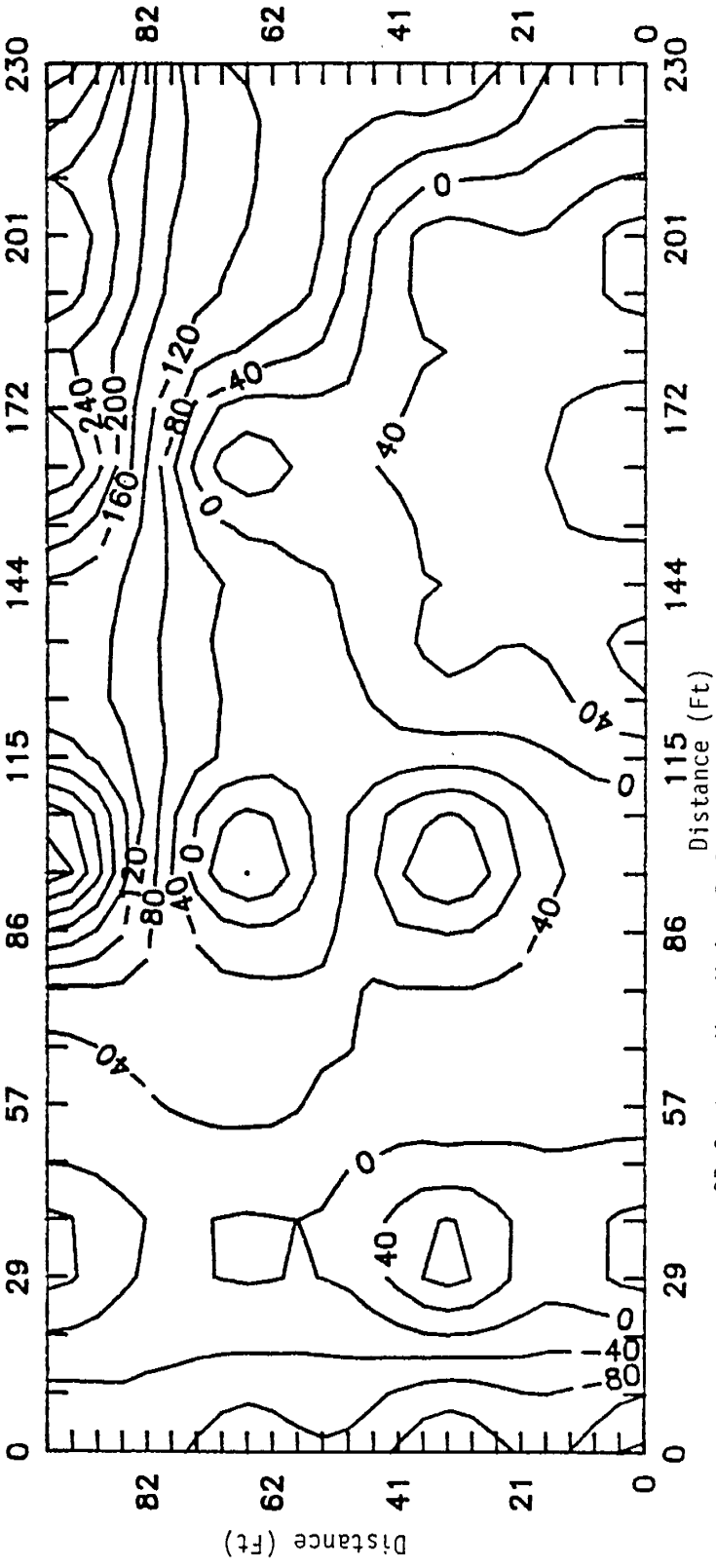

SP Contour Map Using Reference Electrode One at Site III
on 17 May 1988. Contour Interval is 40 mv.

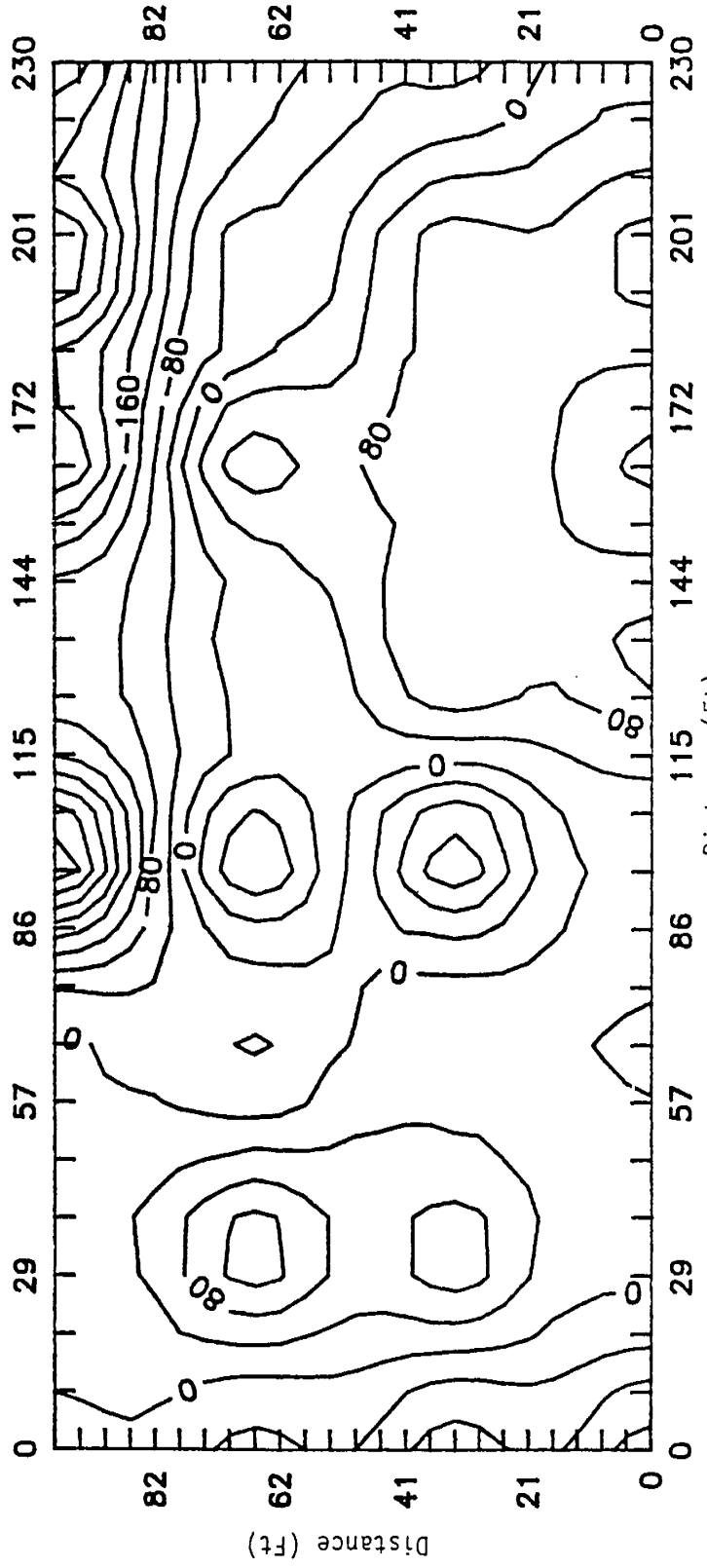

SP Contour Map Using Reference Electrode One at Site III
on 23 May 1988. Contour Interval is 40 mv.

1984

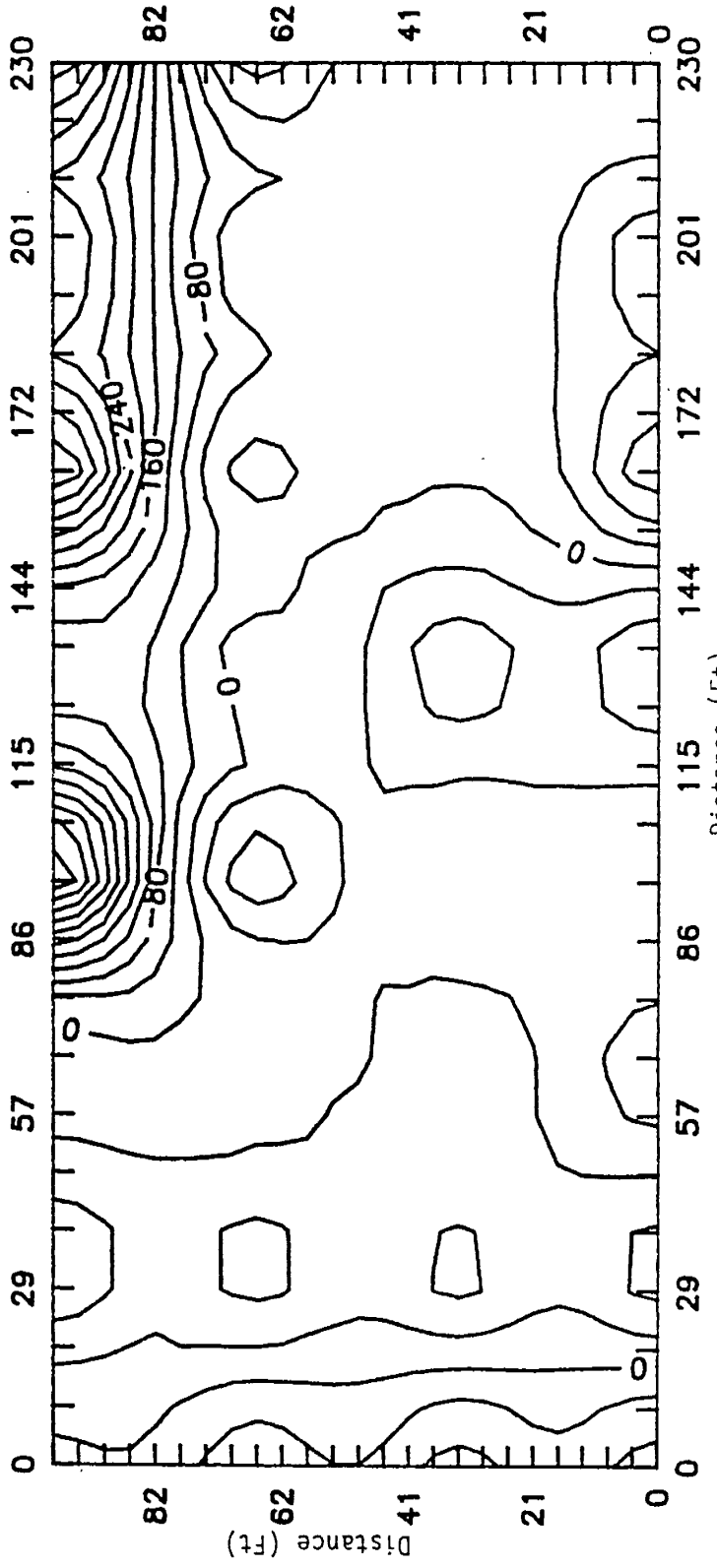

SP Contour Map Using Reference Electrode One at Site III
on 25 August 1988. Contour Interval is 40 mv.

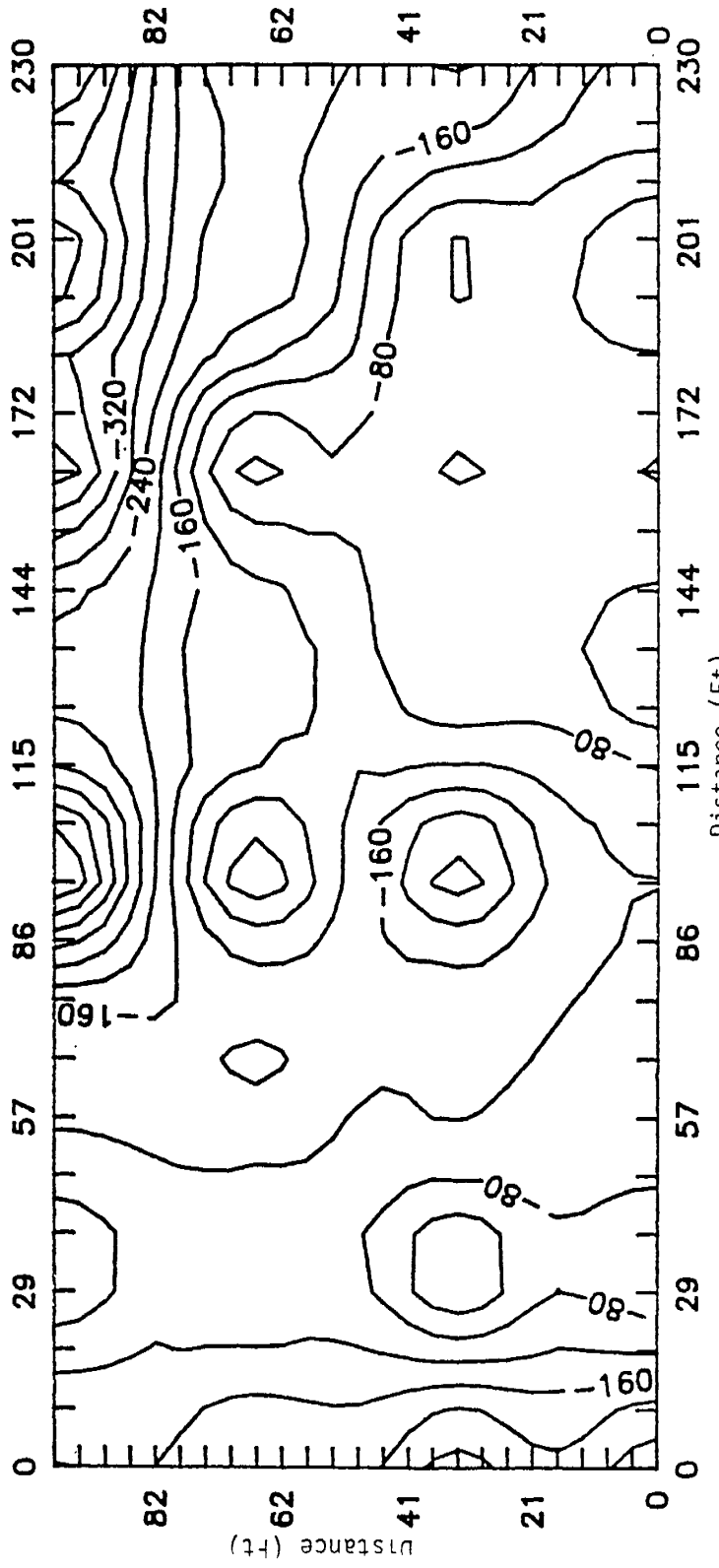

SP Contour Map Using Reference Electrode Two at Site III
on 17 May 1988. Contour Interval is 40 mv.

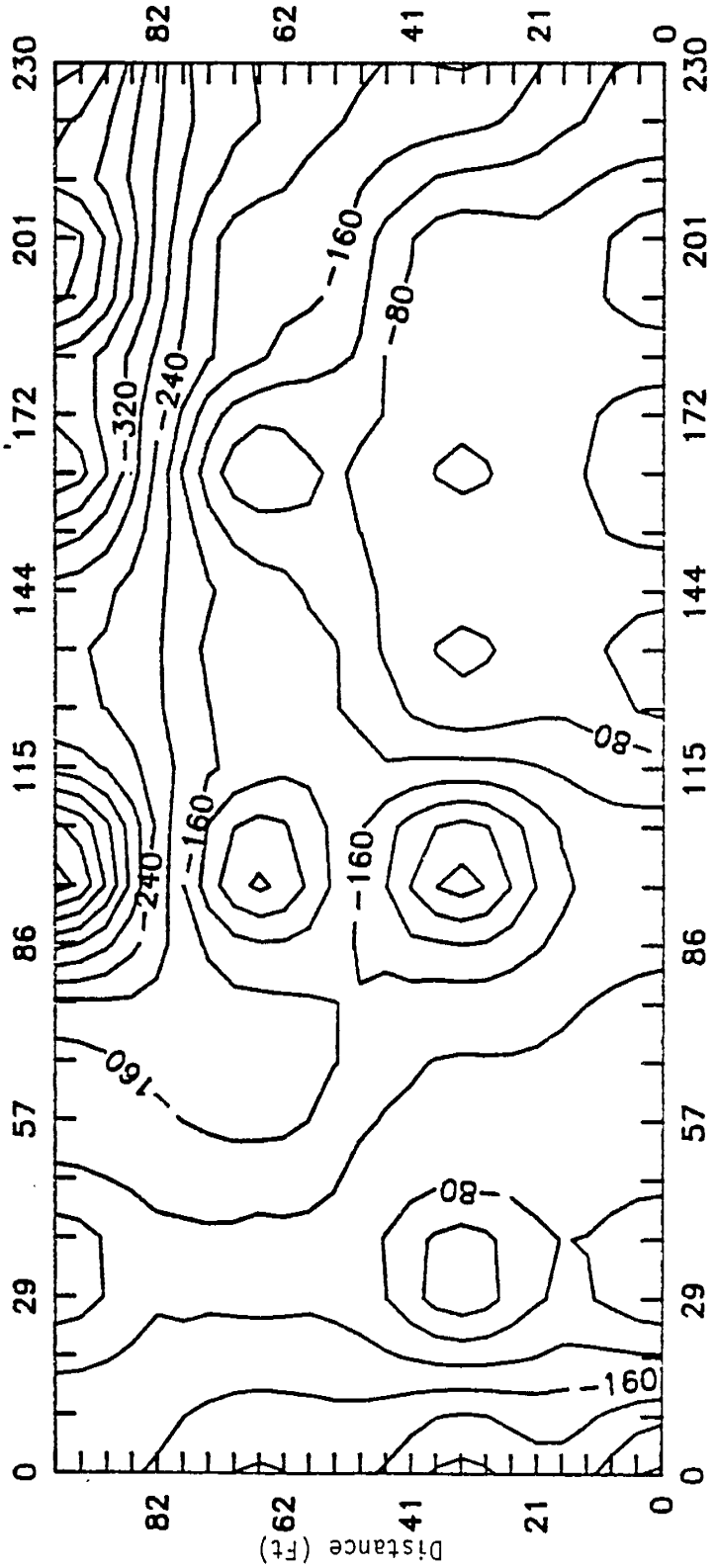

SP Contour Map Using Reference Electrode Two at Site III
on 23 May 1988. Contour Interval is 40 mv.

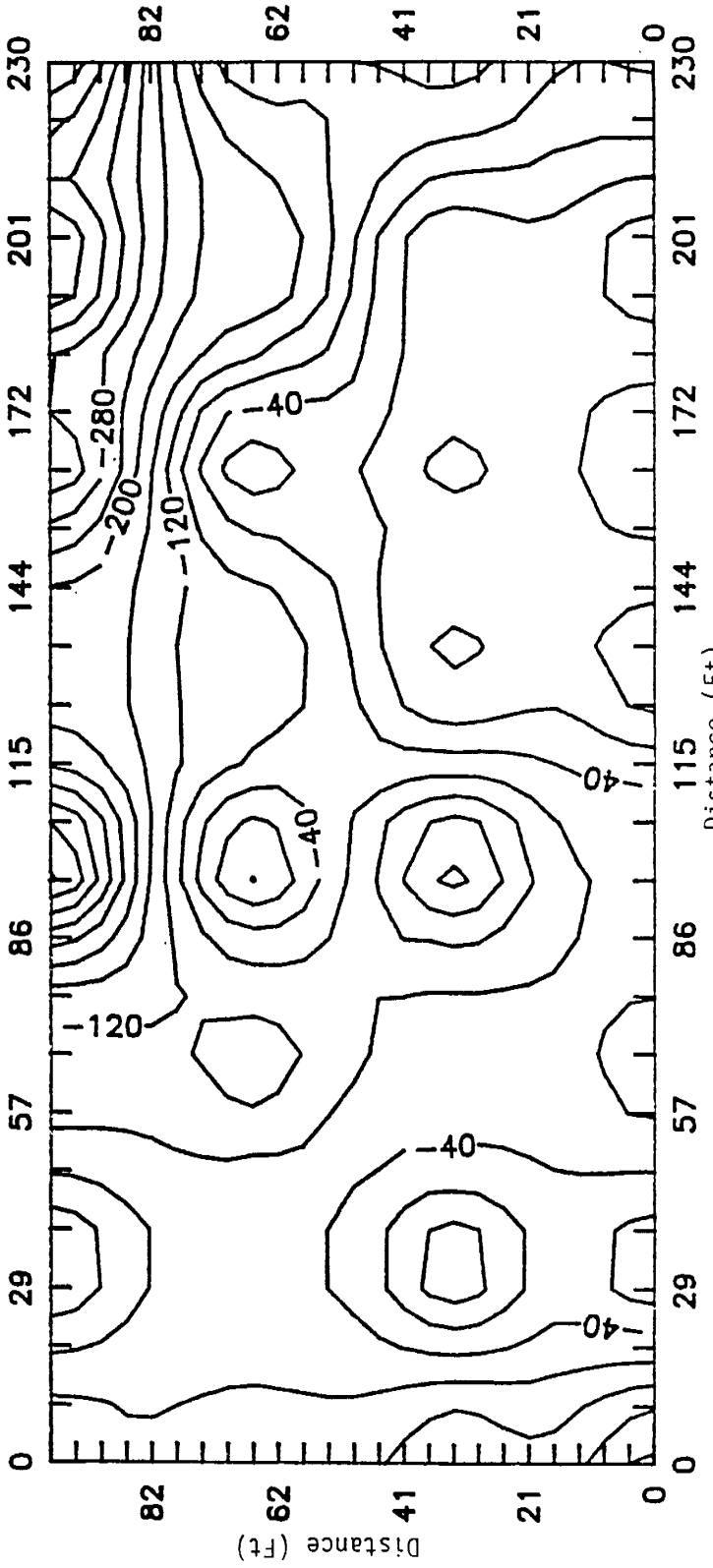

SP Contour Map Using Reference Electrode Two at Site III
on 10 June 1988. Contour Interval is 40 mv.

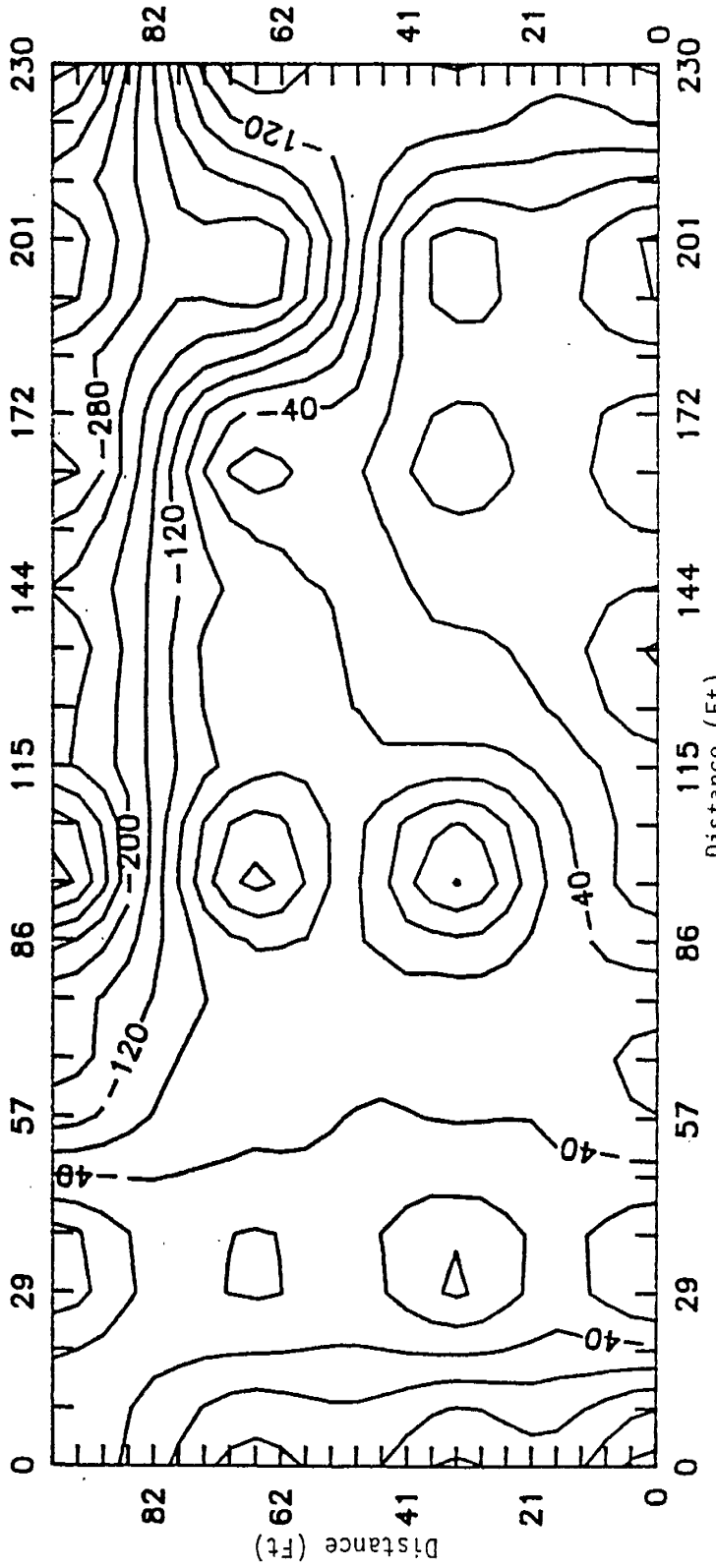

SP Contour Map Using Reference Electrode Two at Site III
on 11 July 1988. Contour Interval is 40 mv.

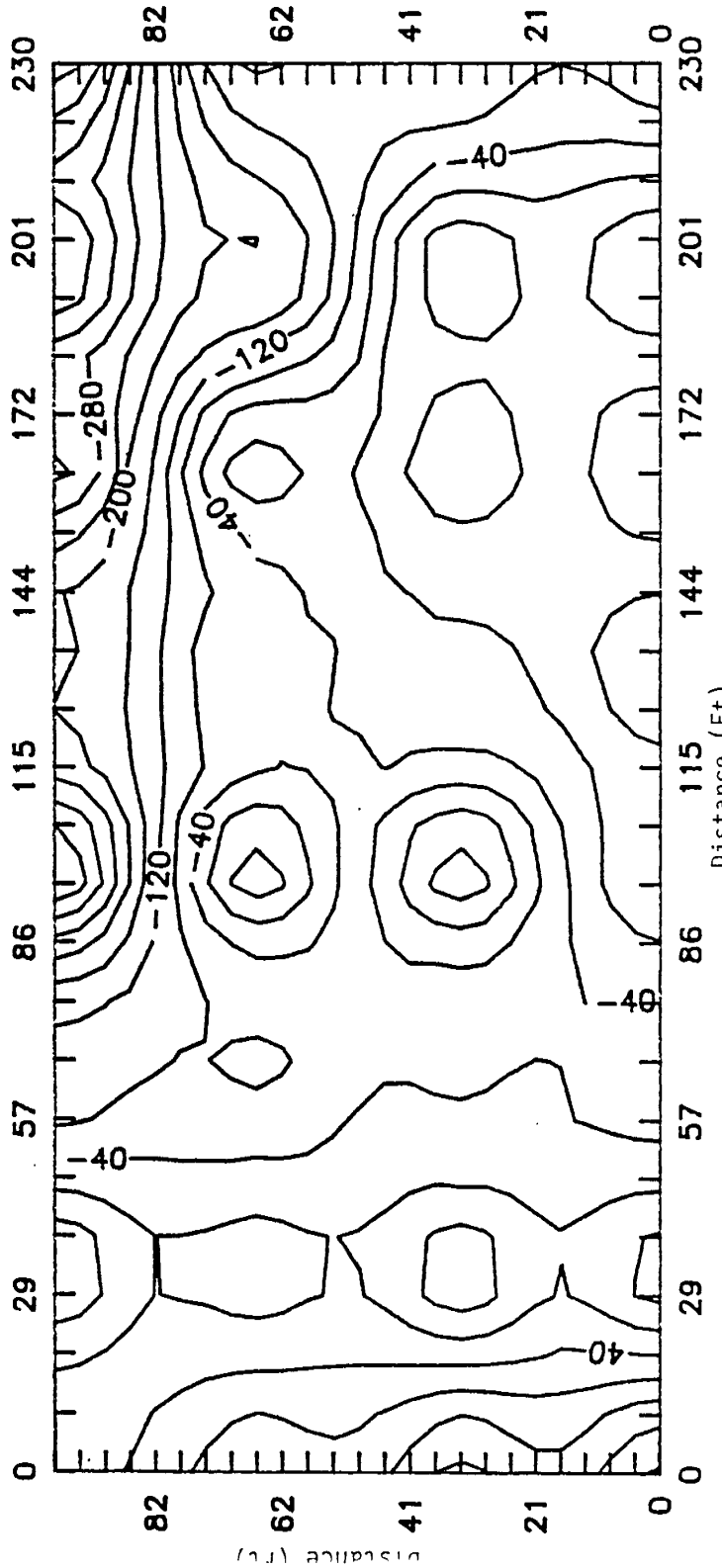

SP Contour Map Using Reference Electrode Two at Site III
on 19 July 1988. Contour Interval is 40 mv.

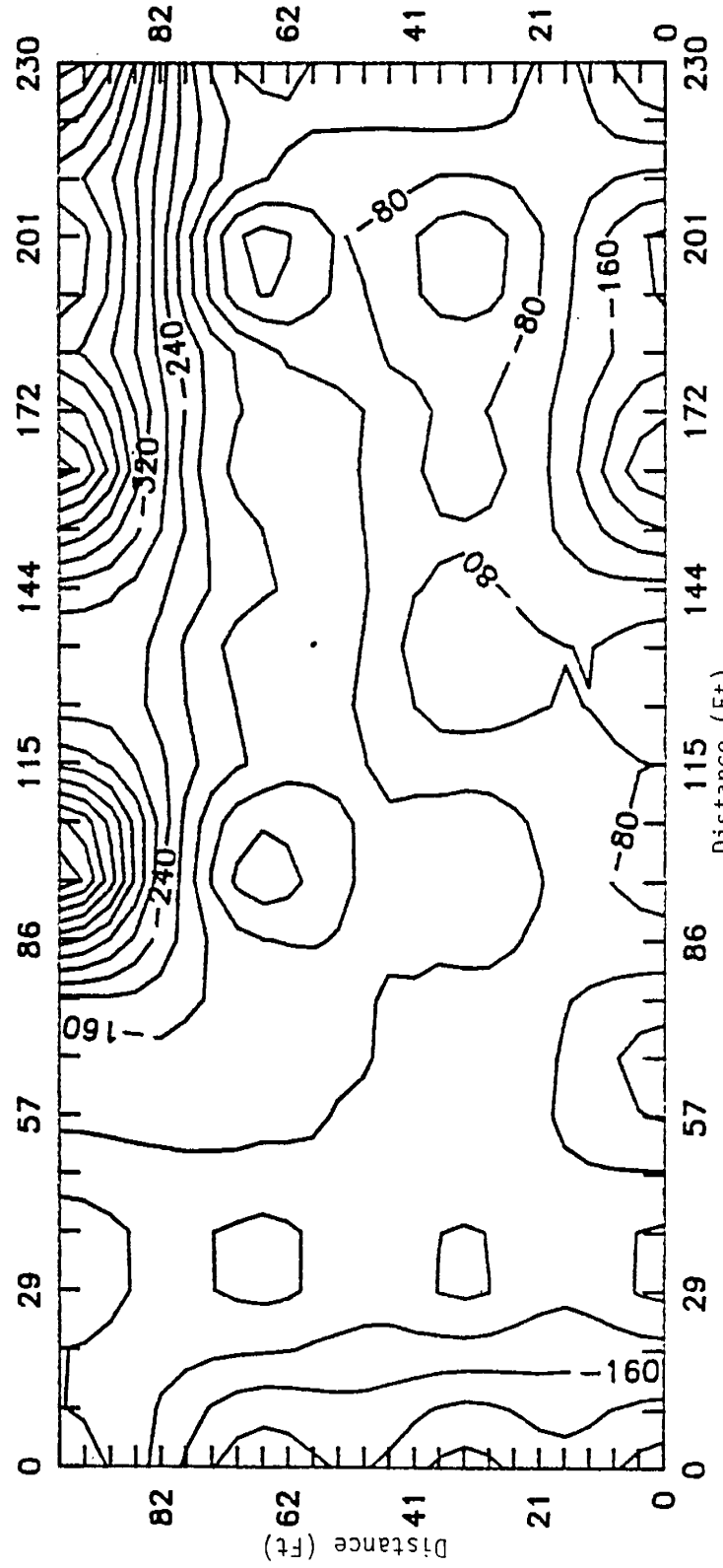

SP Contour Map Using Reference Electrode Two at Site III
on 25 August 1988. Contour Interval is 40 mv.

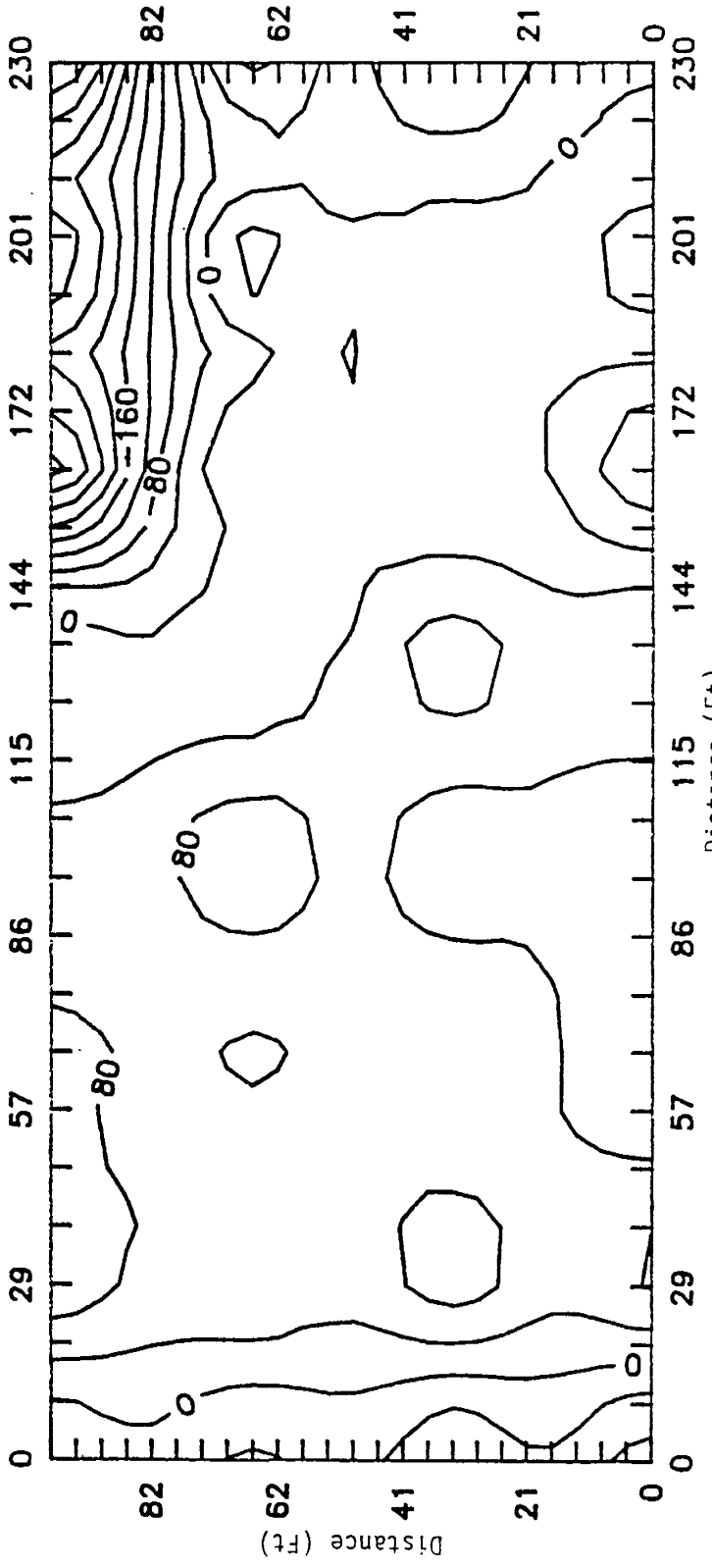

SP Contour Map Using Reference Electrode Two at Site III
on 30 August 1988. Contour Interval is 40 mv.

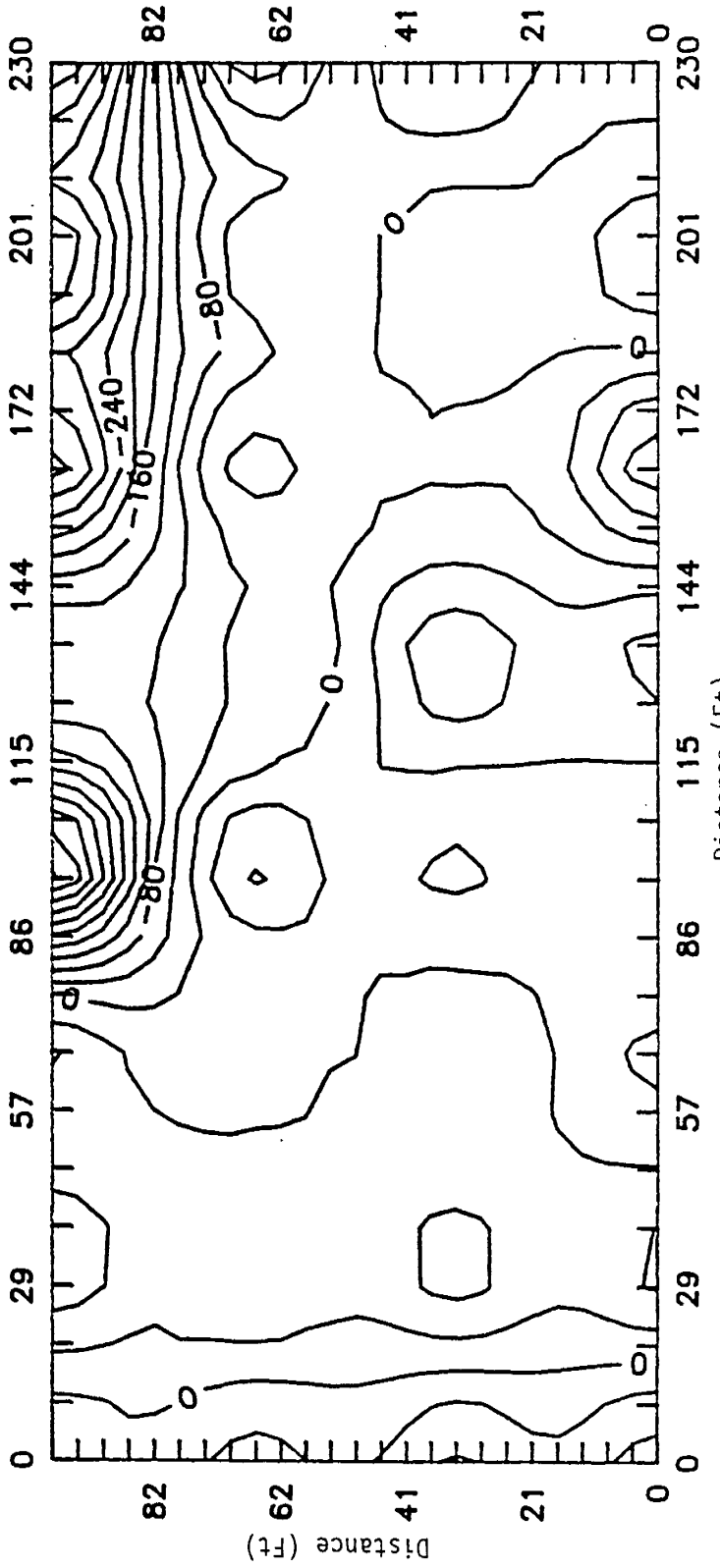

SP COntour Map Using Reference Electrode Two at Site III
on 13 September 1988. Contour Interval is 40 mv.

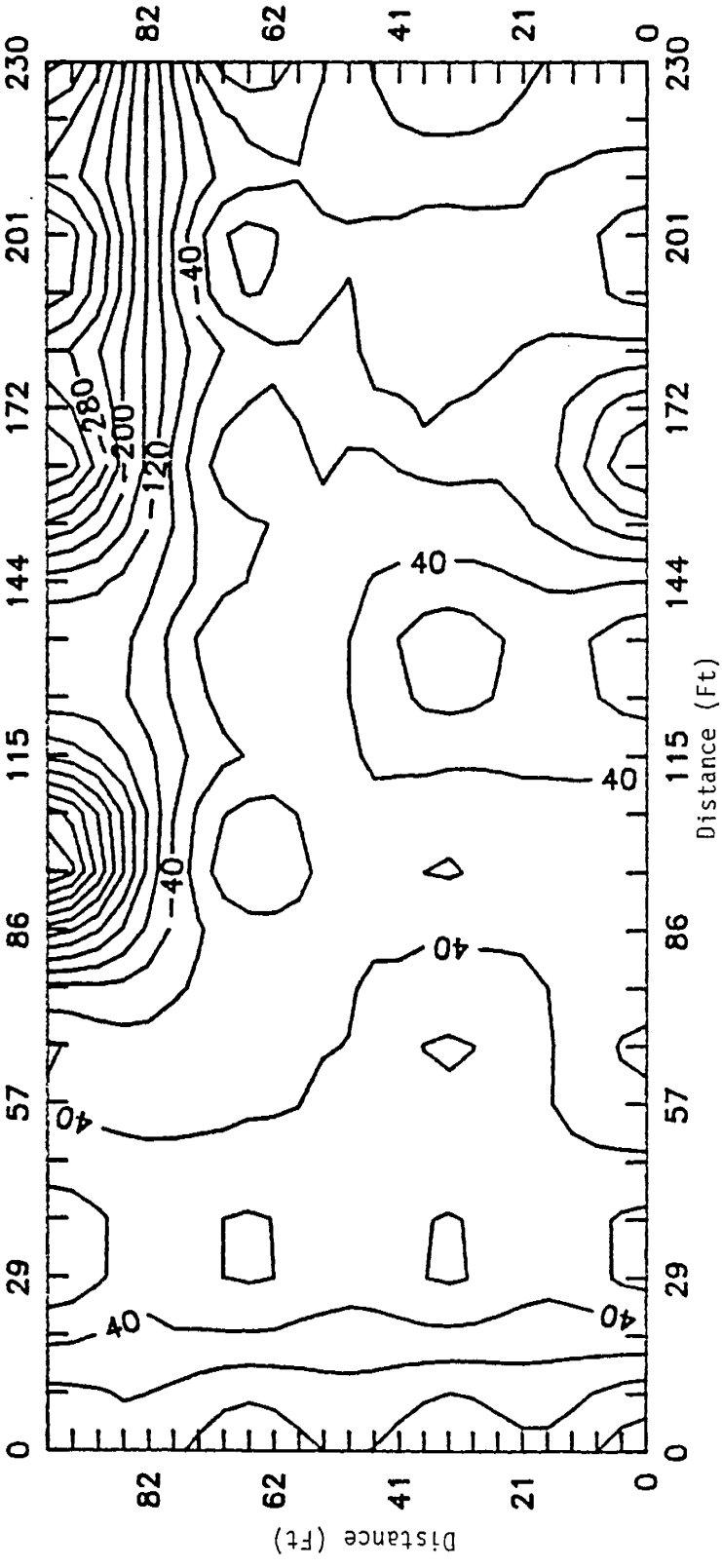

SP Contour Map Using Reference Electrode Two at Site III
on 20 September 1988. Contour Interval is 40 mv.

1994

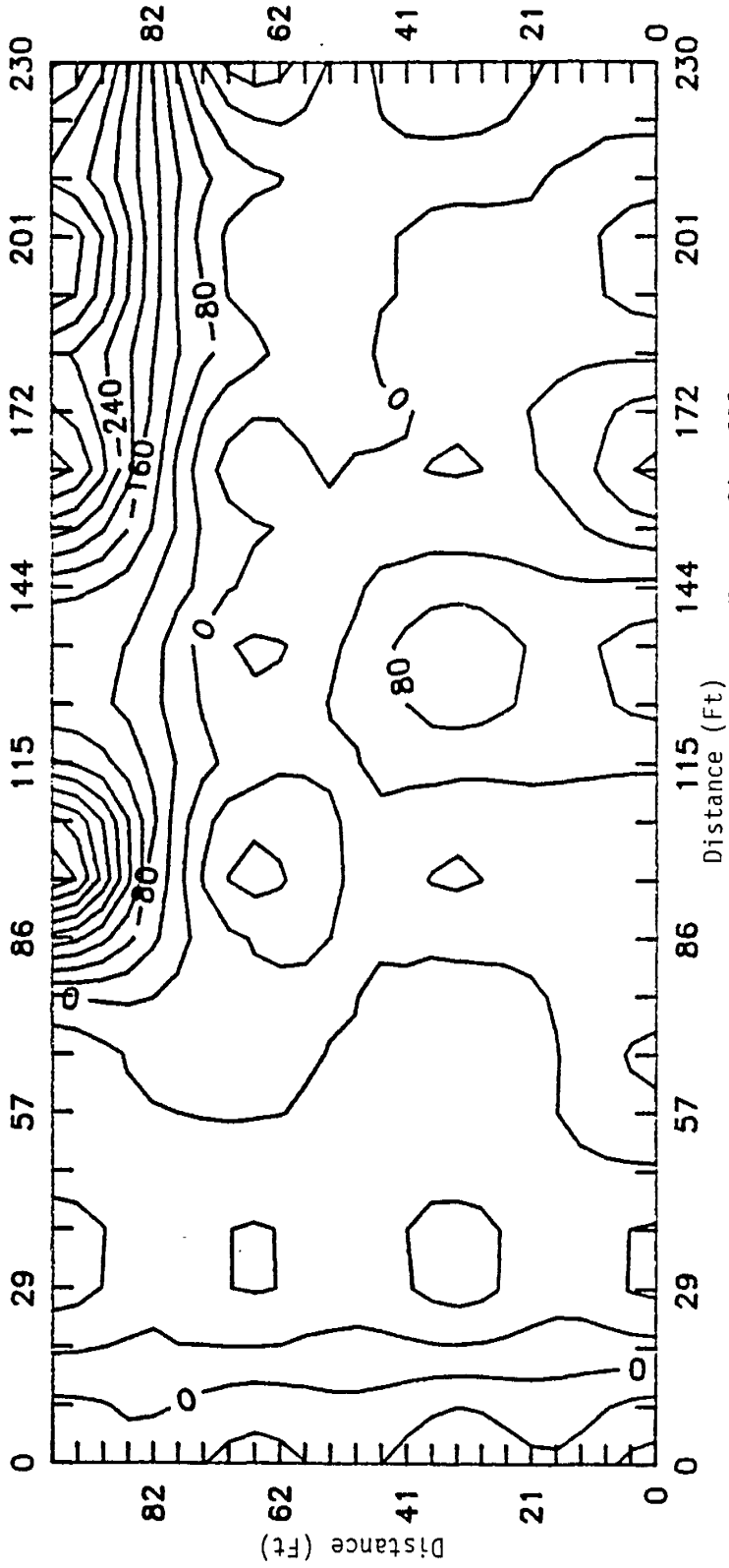

SP Contour Map Using Reference Electrode Two at Site III
on 22 November 1988. Contour Interval is 40 mv.

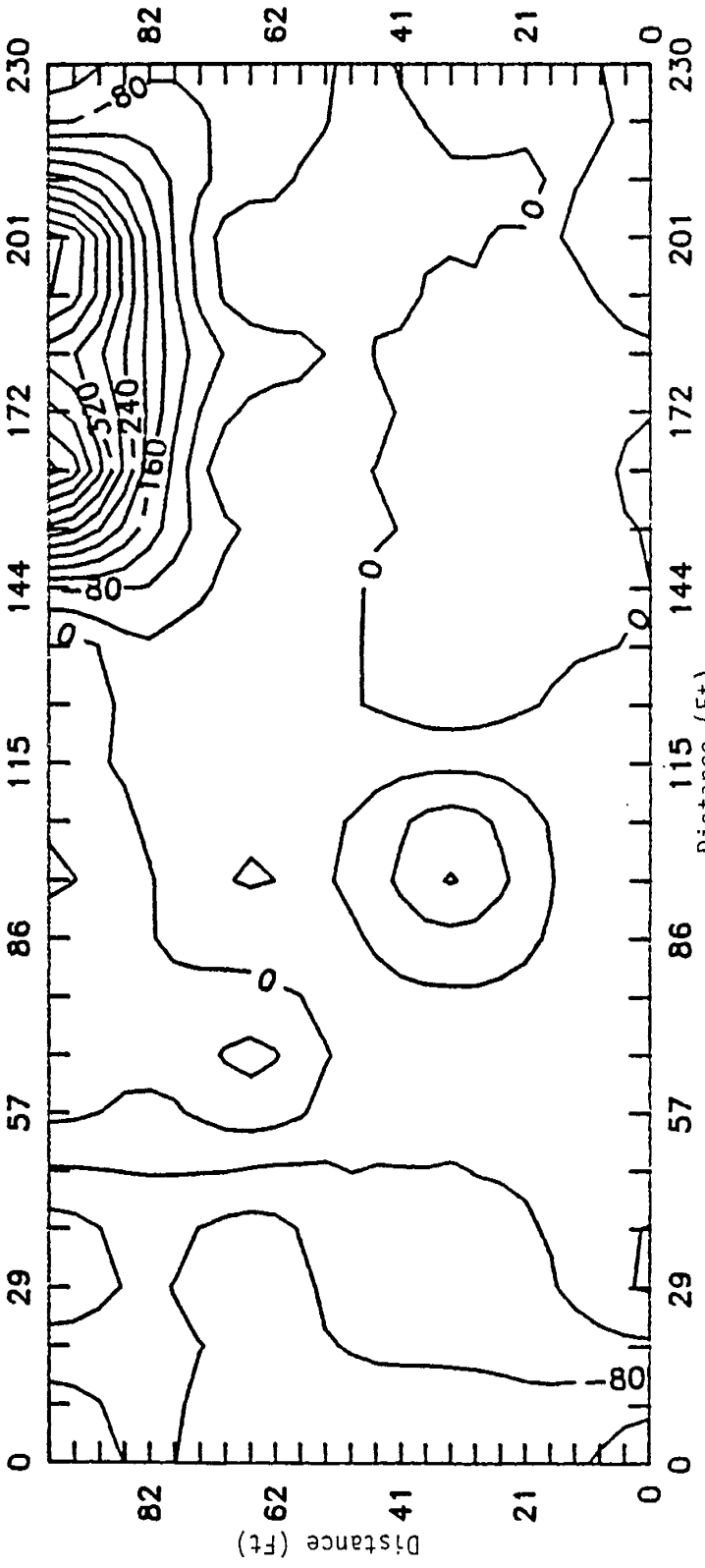

SP Contour Map Using Reference Electrode Two at Site III
on 19 May 1989. Contour Interval is 40 mv.

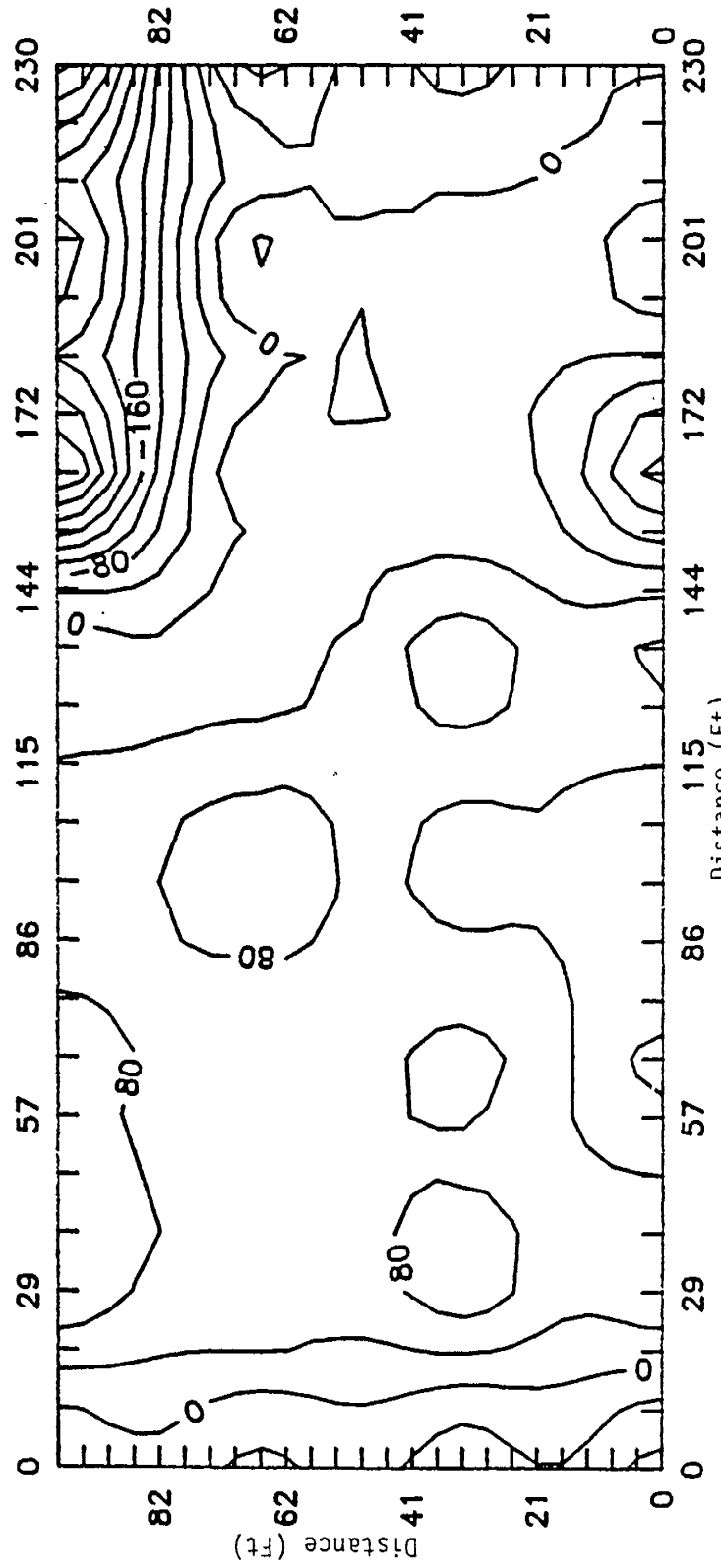

SP Contour Map Using Reference Electrode Two at Site III
on 8 June 1989. Contour Interval is 40 mv.

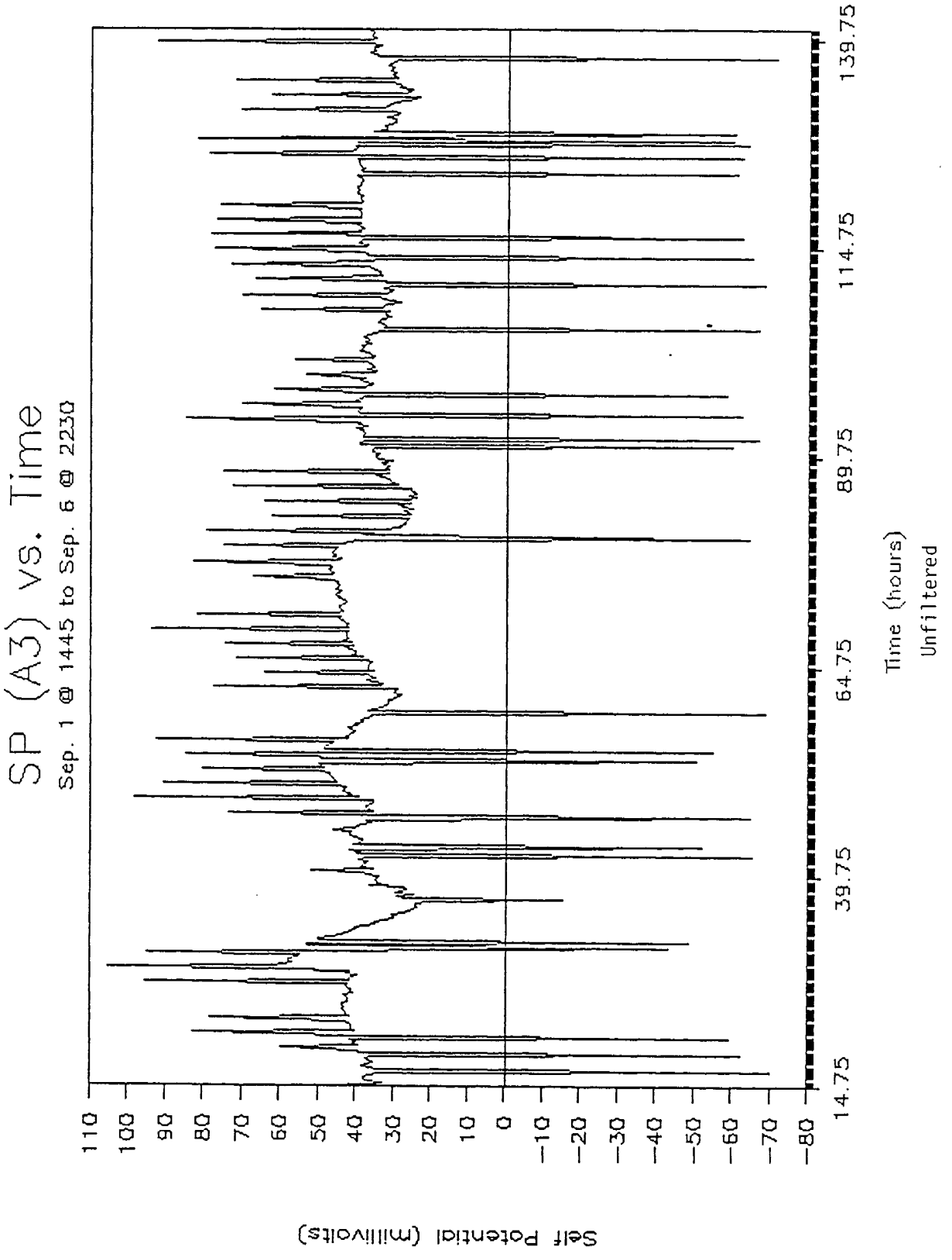
SP (A3) vs. Time
Sep. 1 @ 1445 to Sep. 6 @ 2230
Self Potential (millivolts)
110
100
90
80
70
60
50
40
30
20
10
0
-10
-20
-30
-40
-50
-60
-70
-80
14.75
39.75
64.75
89.75
114.75
139.75
Time (hours)
Unfiltered

1998

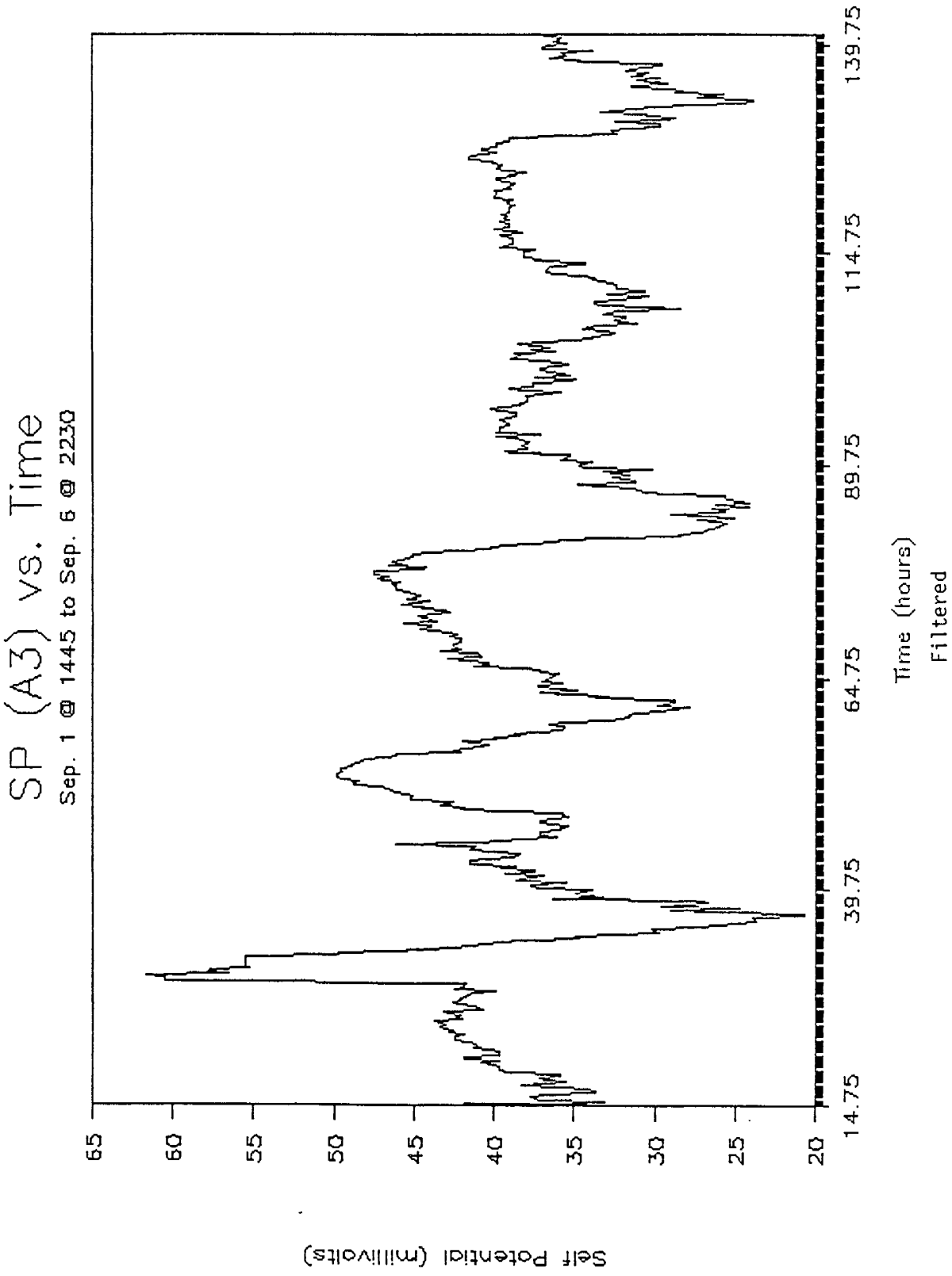
SP (A3) vs. Time
Sep. 1 @ 1445 to Sep. 6 @ 2230
Self Potential (millivolts)
65
60
55
50
45
40
35
30
25
20
14.75
39.75
64.75
89.75
114.75
139.75
Time (hours)
Filtered

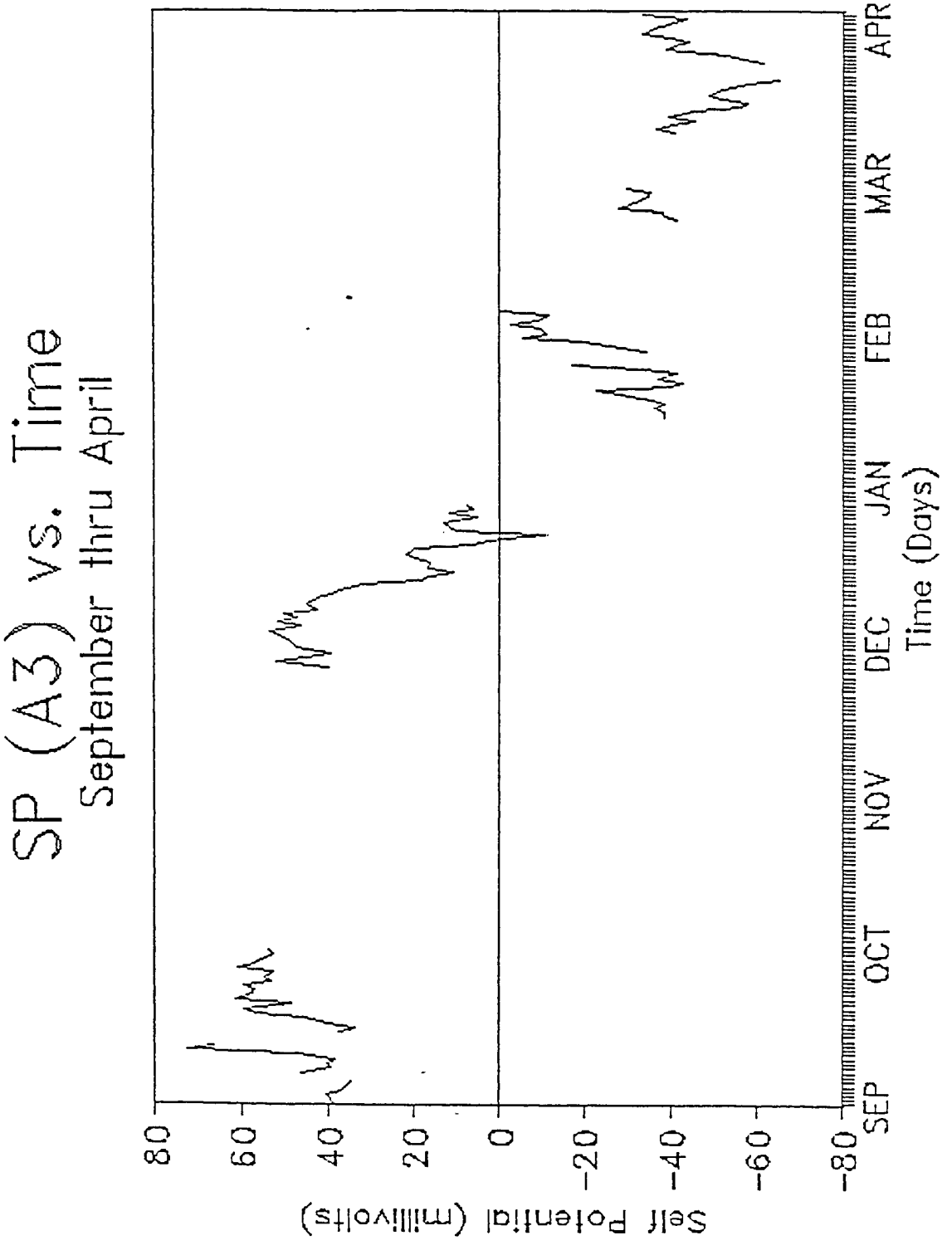
SP (A3) vs. Time
September thru April
Self Potential (millivolts)
80
60
40
20
0
-20
-40
-60
-80
SEP
OCT
NOV
DEC
JAN
FEB
MAR
APR
Time (Days)

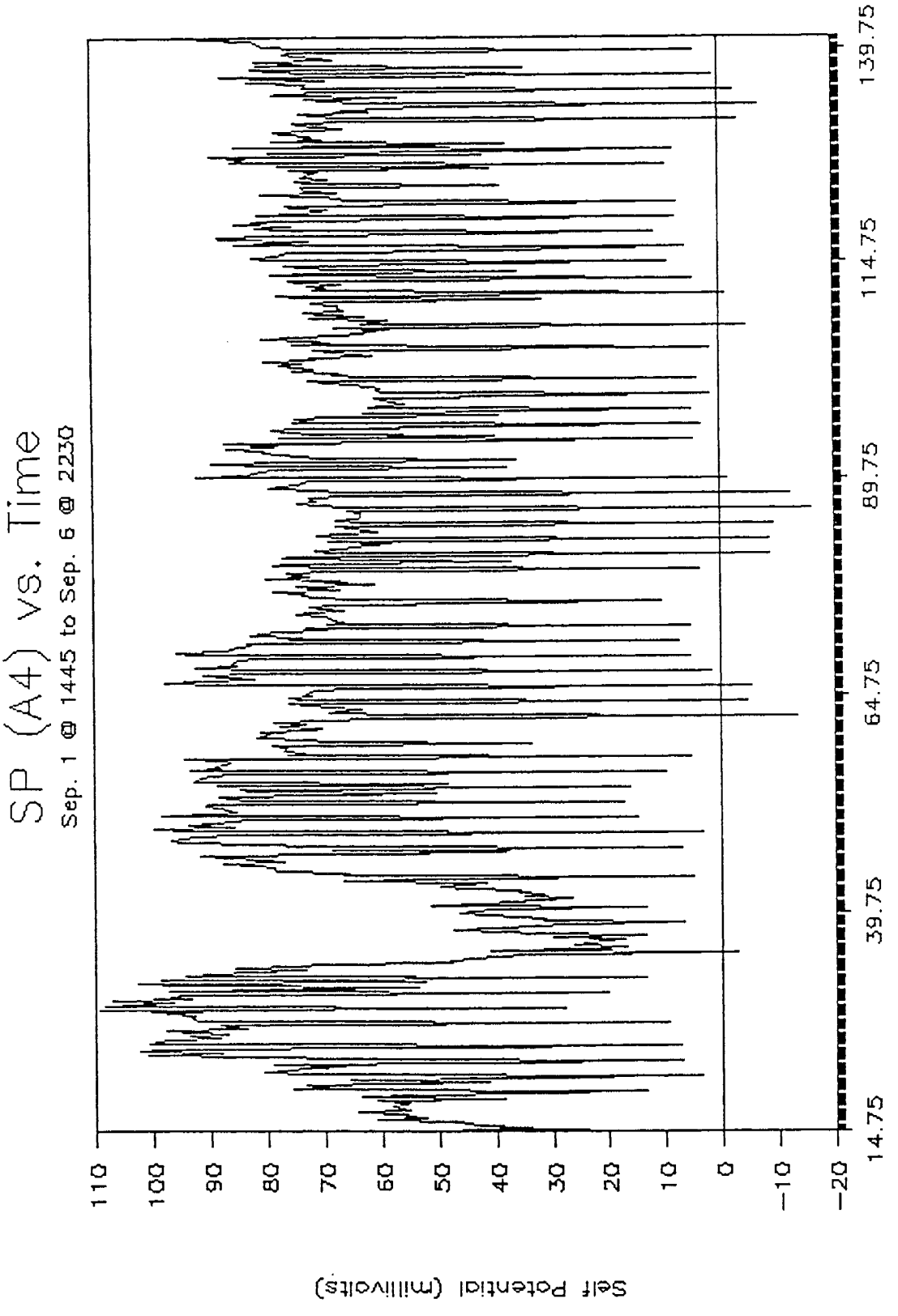
SP (A4) vs. Time
Sep. 1 @ 1445 to Sep. 6 @ 2230
Self Potential (millivolts)
110
100
90
80
70
60
50
40
30
20
10
0
-10
-20
14.75
39.75
64.75
89.75
114.75
139.75
Time (hours)
Unfiltered

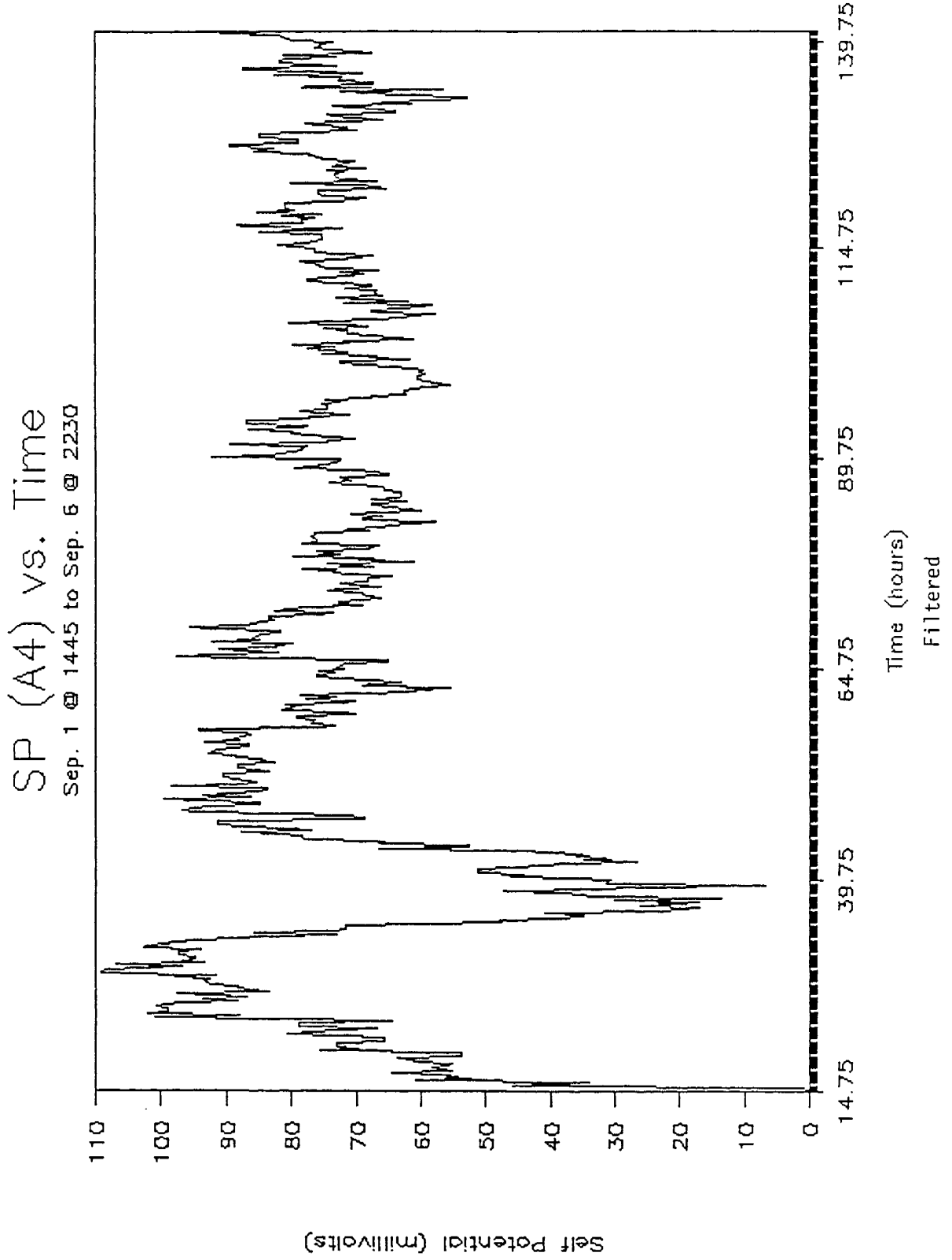
SP (A4) vs. Time
Sep. 1 @ 1445 to Sep. 6 @ 2230
Self Potential (millivolts)
110
100
90
80
70
60
50
40
30
20
10
0
14.75
39.75
64.75
89.75
114.75
139.75
Time (hours)
Filtered

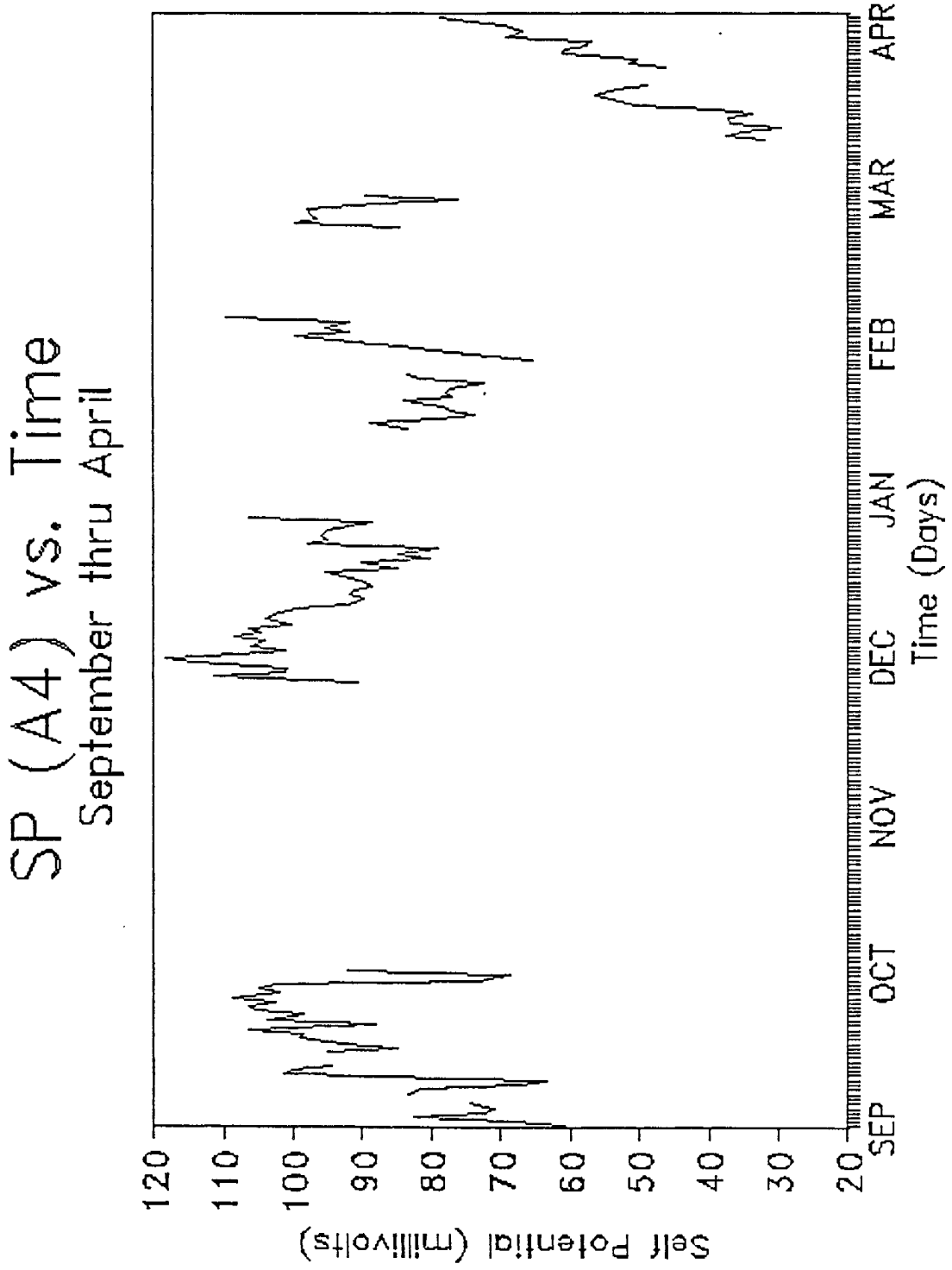
SP (A4) vs. Time
September thru April
Self Potential (millivolts)
120
110
100
90
80
70
60
50
40
30
20
SEP
OCT
NOV
DEC
JAN
FEB
MAR
APR
Time (Days)

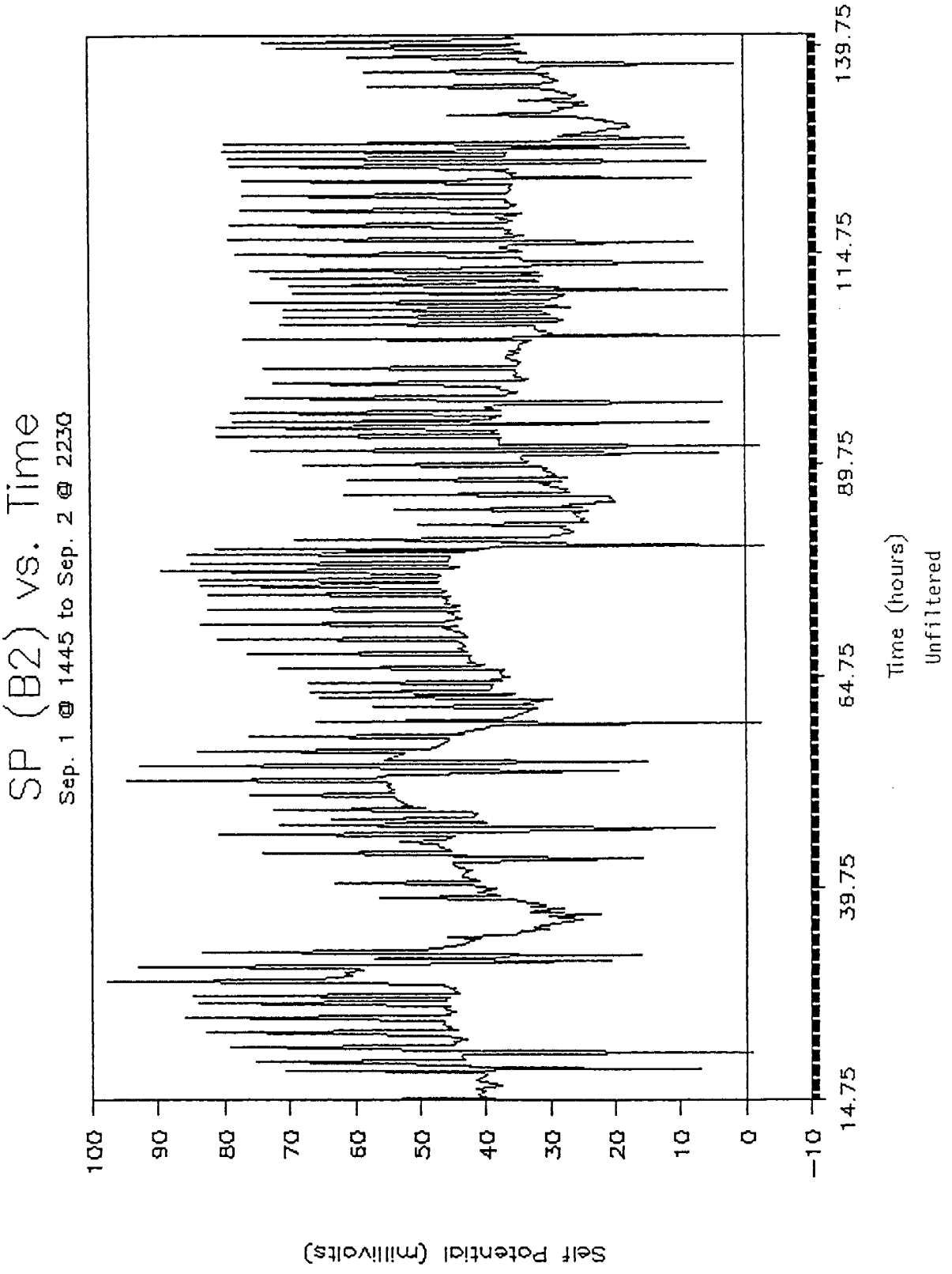
SP (B2) vs. Time
Sep. 1 @ 1445 to Sep. 2 @ 2230
Self Potential (millivolts)
100
90
80
70
60
50
40
30
20
10
0
-10
14.75
39.75
64.75
89.75
114.75
139.75
Time (hours)
Unfiltered

2004

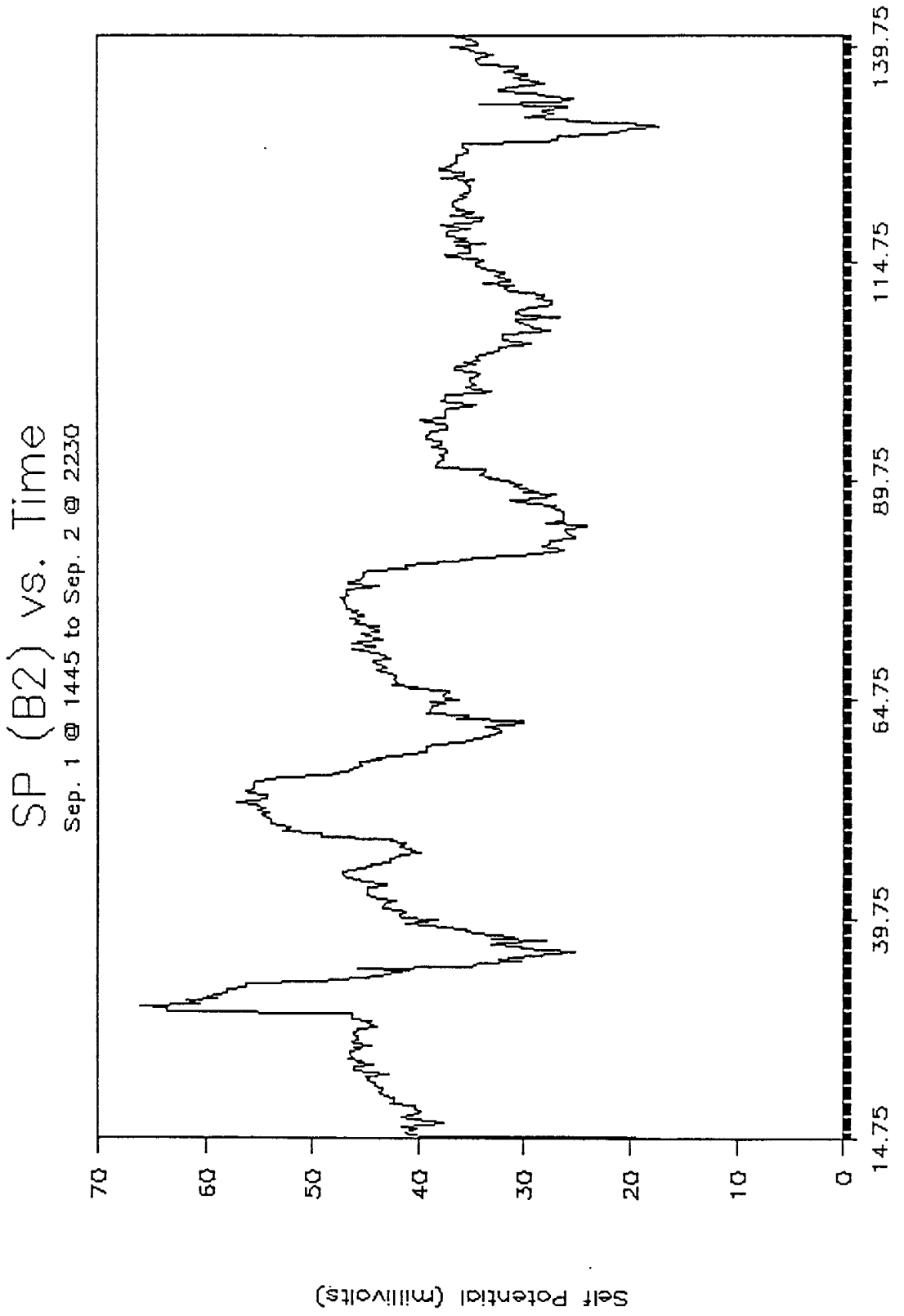
SP (B2) vs. Time
Sep. 1 @ 1445 to Sep. 2 @ 2230
Self Potential (millivolts)
70
60
50
40
30
20
10
0
14.75
39.75
64.75
89.75
114.75
139.75
Time (hours)
Filtered

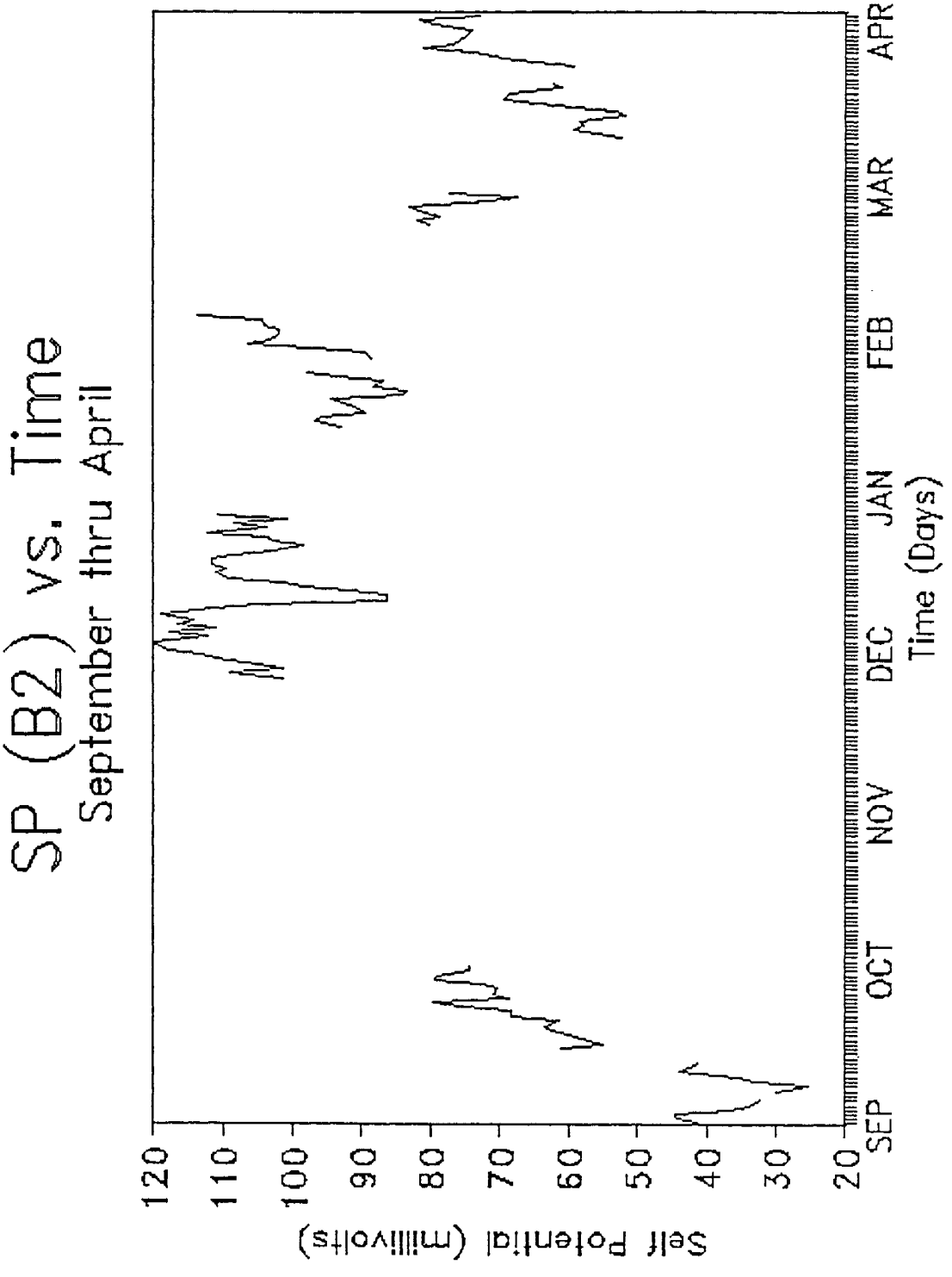
SP (B2) vs. Time
September thru April
Self Potential (millivolts)
120
110
100
90
80
70
60
50
40
30
20
SEP
OCT
NOV
DEC
JAN
FEB
MAR
APR
Time (Days)

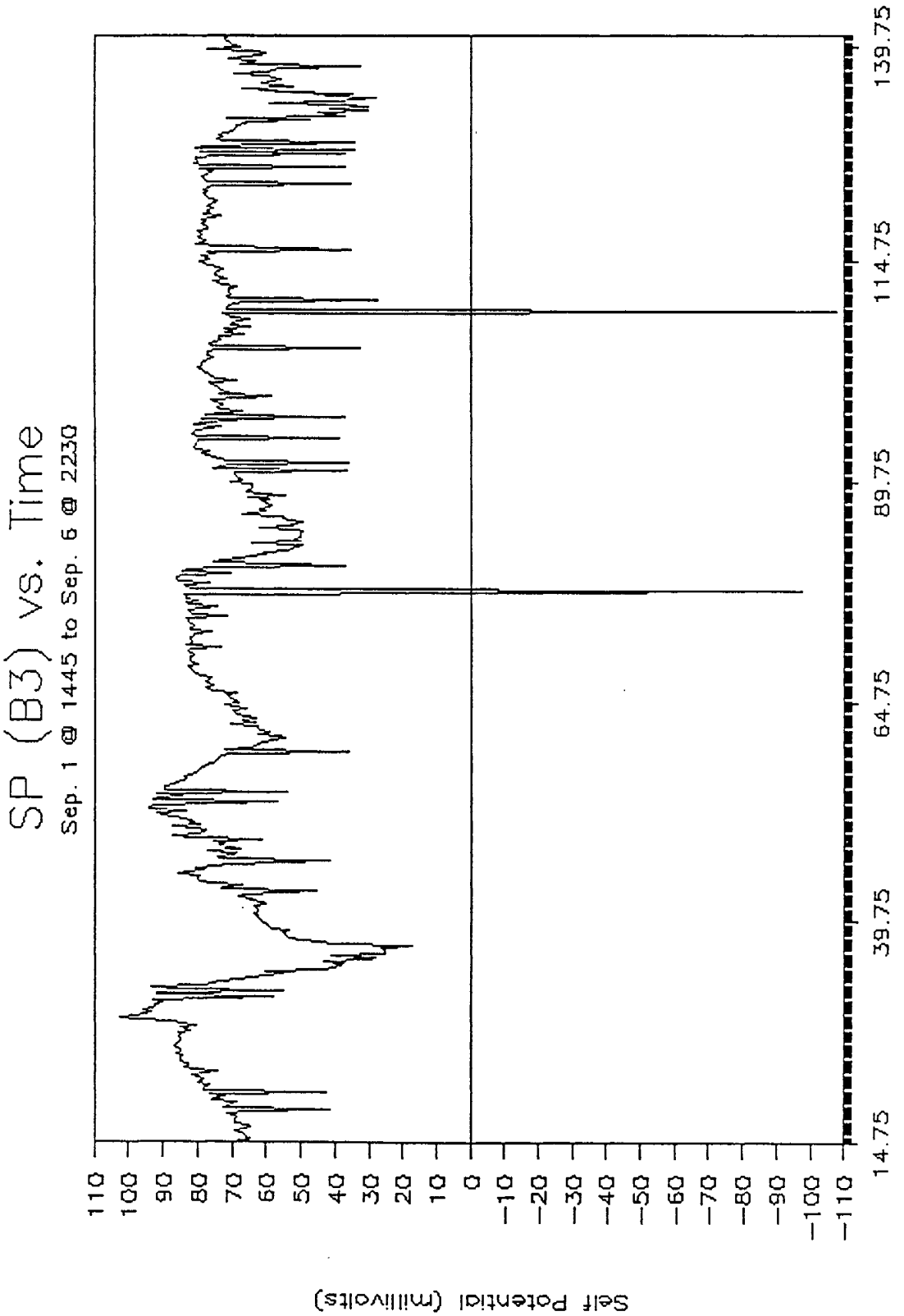
SP (B3) vs. Time
Sep. 1 @ 1445 to Sep. 6 @ 2230
Self Potential (millivolts)
110
100
90
80
70
60
50
40
30
20
10
0
-10
-20
-30
-40
-50
-60
-70
-80
-90
-100
-110
14.75
39.75
64.75
89.75
114.75
139.75
Time (hours)
Unfiltered

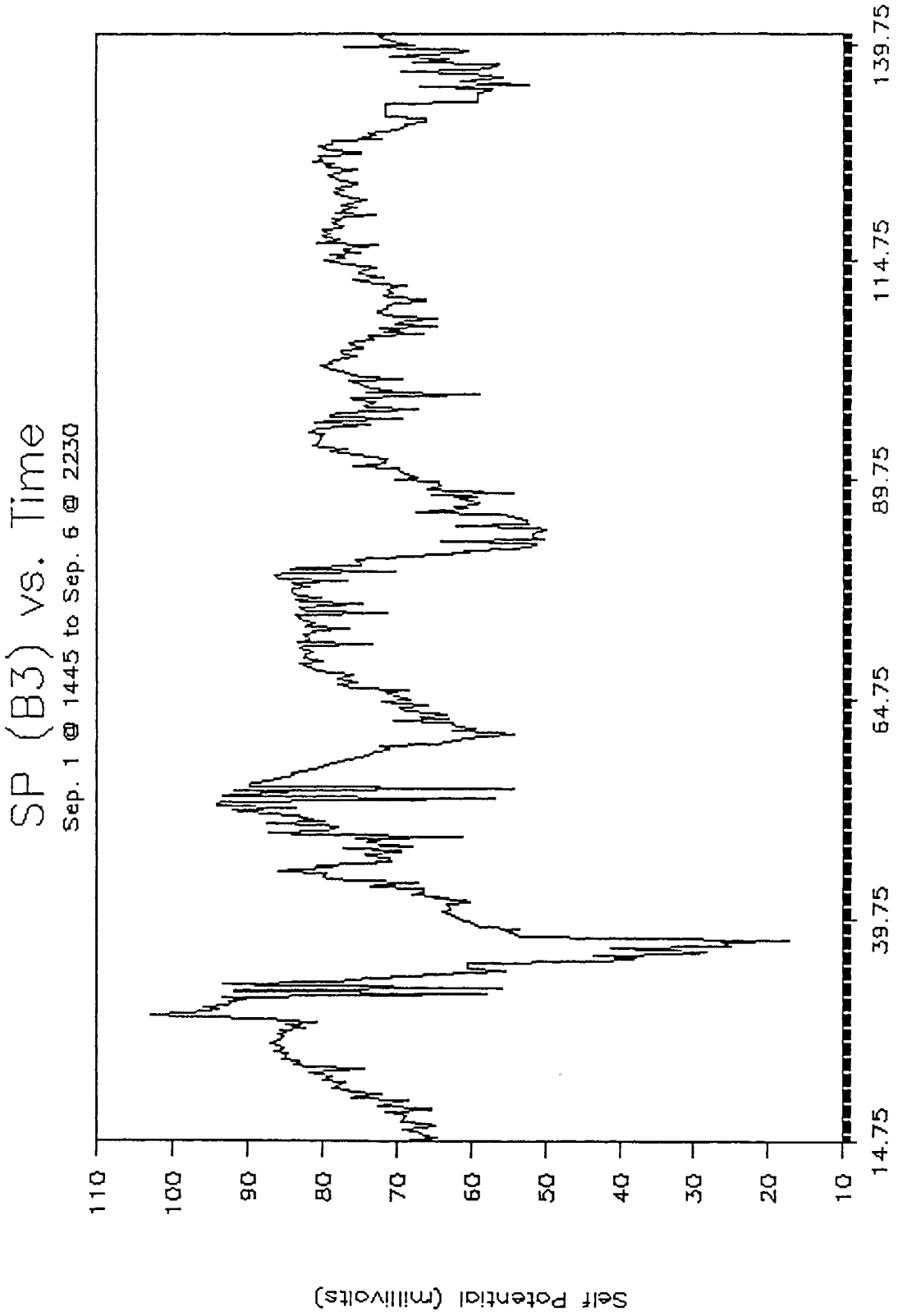
SP (B3) vs. Time
Sep. 1 @ 1445 to Sep. 6 @ 2230
Self Potential (millivolts)
110
100
90
80
70
60
50
40
30
20
10
14.75
39.75
64.75
89.75
114.75
139.75
Time (hours)
Filtered

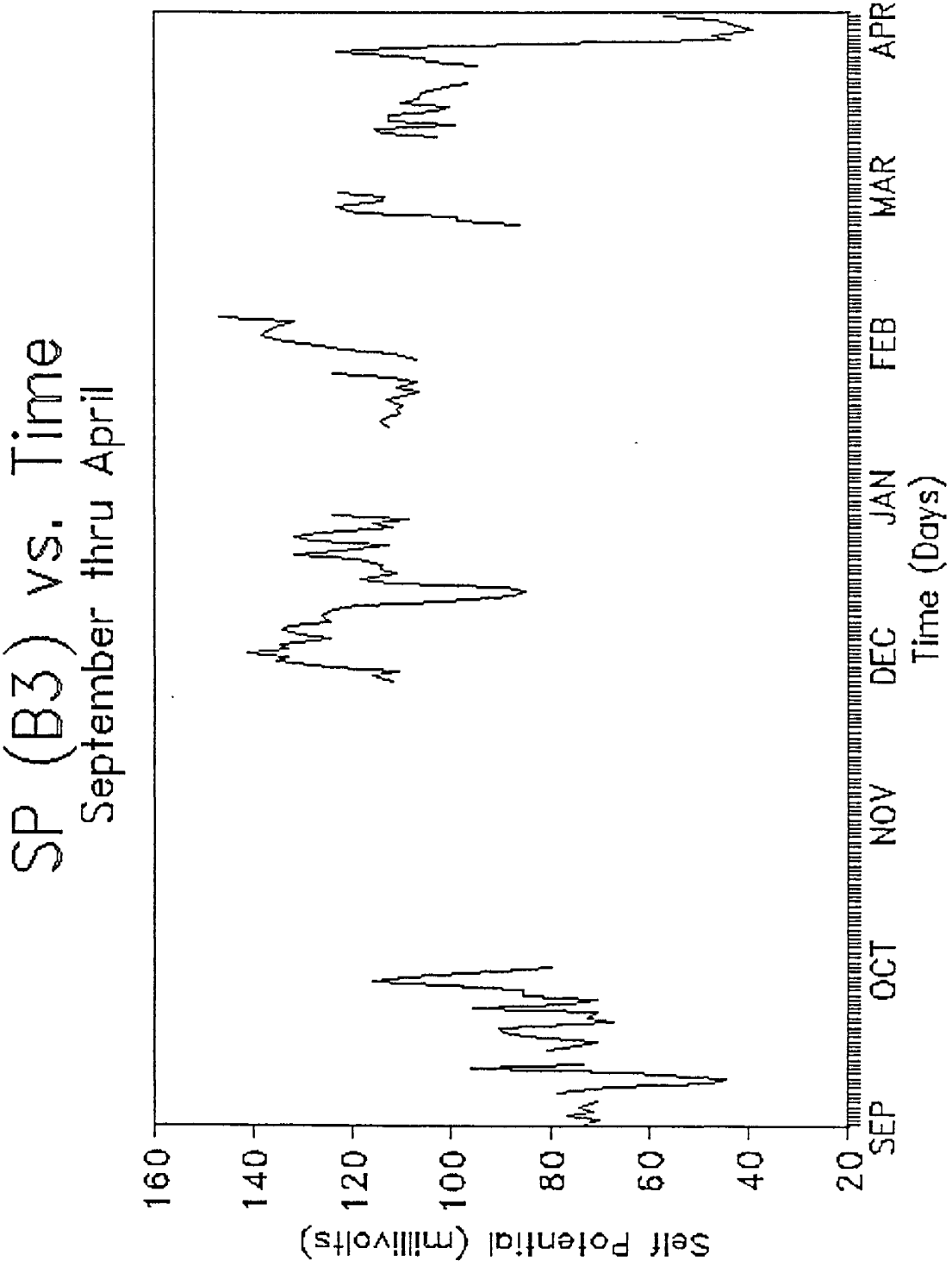
SP (B3) vs. Time
September thru April
Self Potential (millivolts)
160
140
120
100
80
60
40
20
SEP
OCT
NOV
DEC
JAN
FEB
MAR
APR
Time (Days)

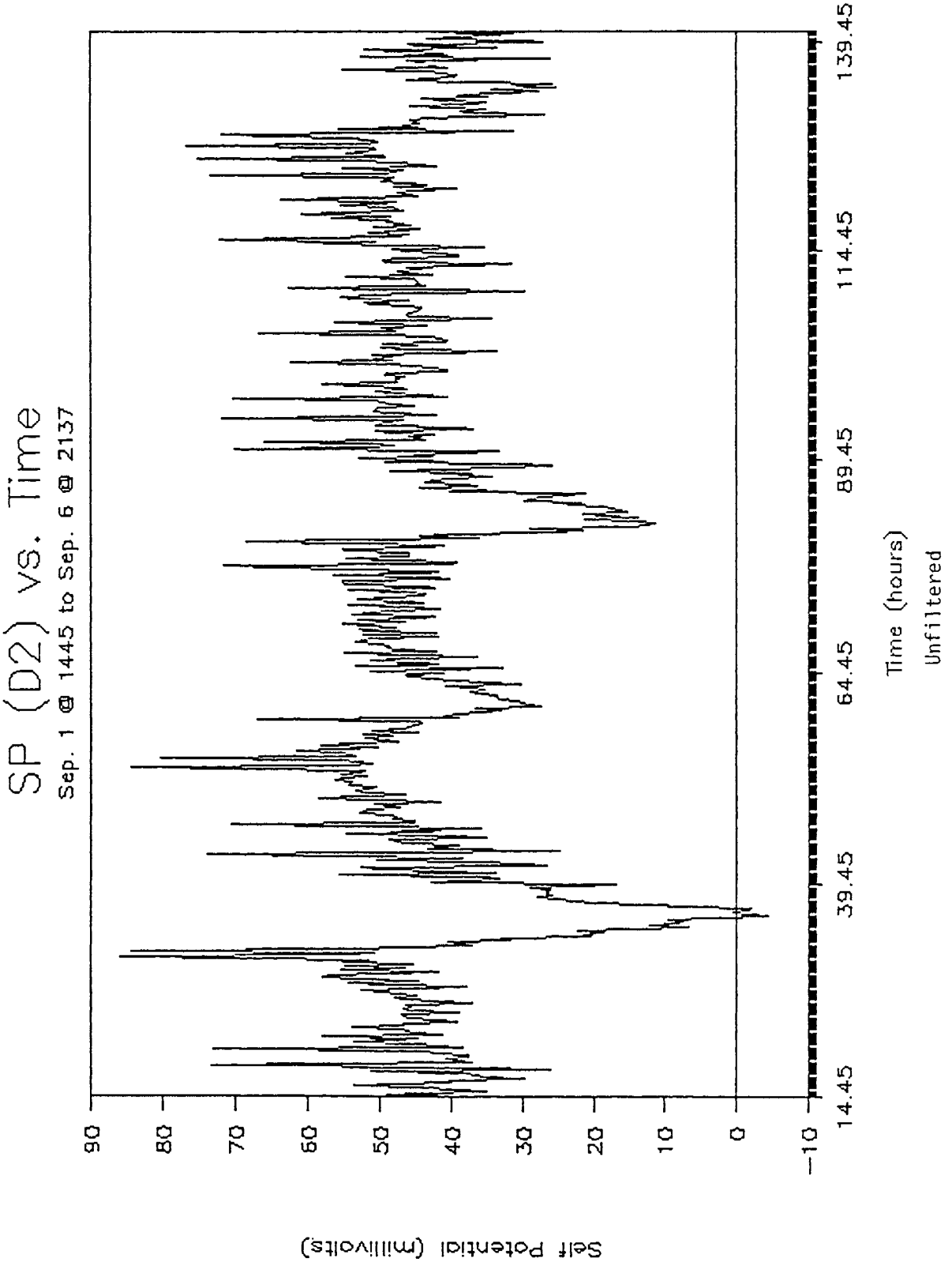
SP (D2) vs. Time
Sep. 1 @ 1445 to Sep. 6 @ 2137
Self Potential (millivolts)
90
80
70
60
50
40
30
20
10
0
-10
14.45
39.45
64.45
89.45
114.45
139.45
Time (hours)
Unfiltered

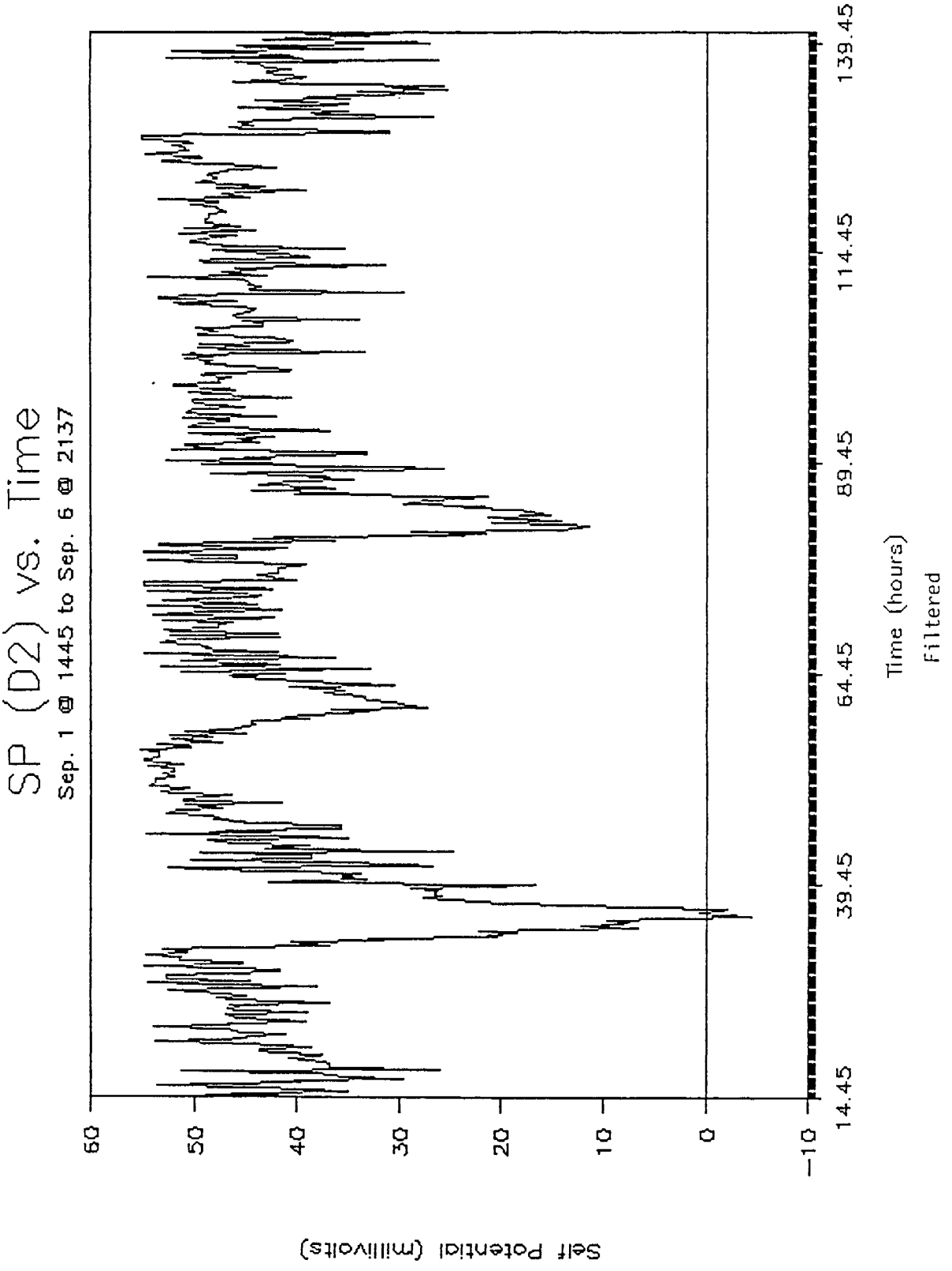
SP (D2) vs. Time
Sep. 1 @ 1445 to Sep. 6 @ 2137
Self Potential (millivolts)
60
50
40
30
20
10
0
-10
14.45
39.45
64.45
89.45
114.45
139.45
Time (hours)
Filtered

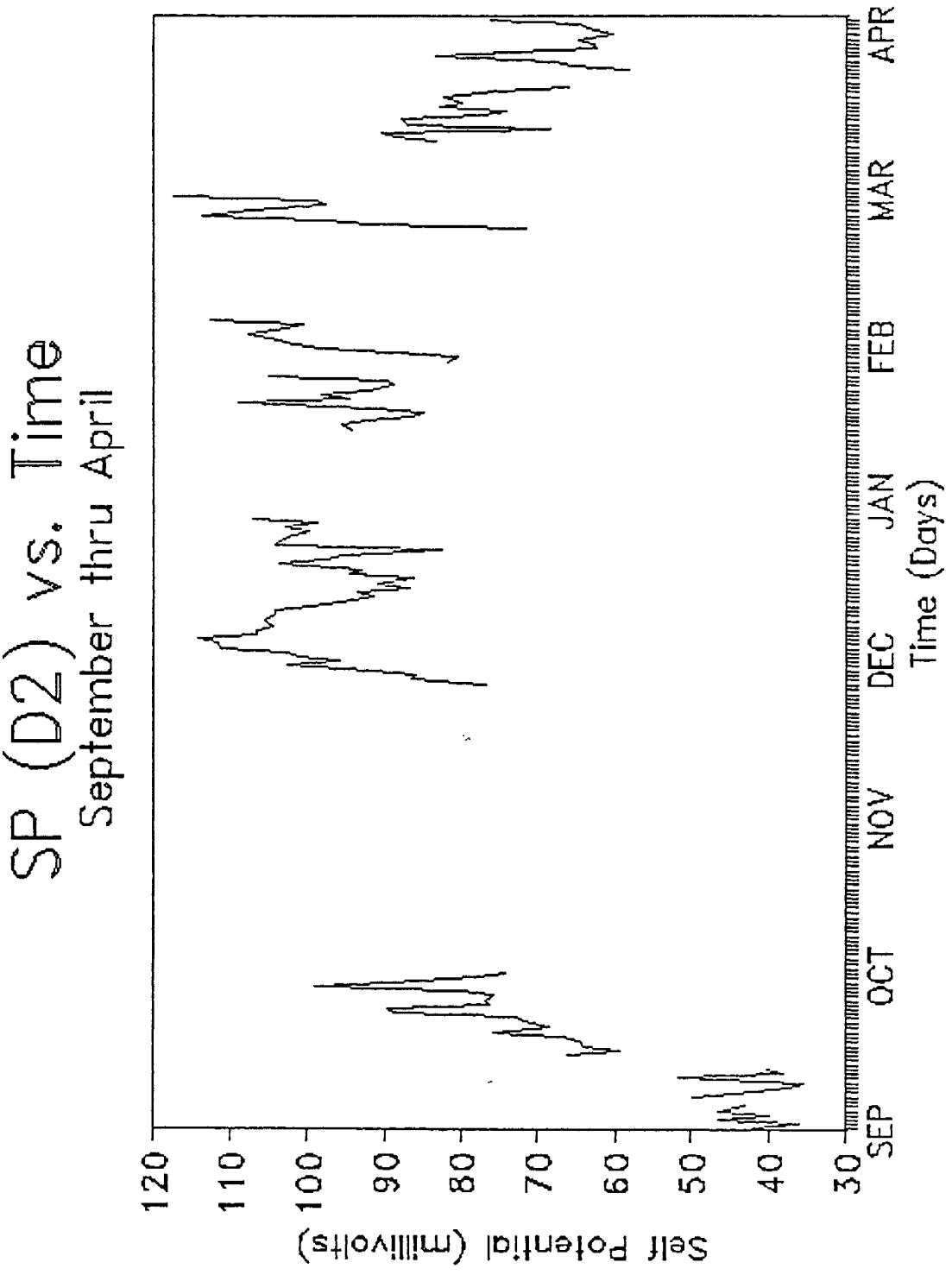
SP (D2) vs. Time
September thru April
Self Potential (millivolts)
120
110
100
90
80
70
60
50
40
30
SEP
OCT
NOV
DEC
JAN
FEB
MAR
APR
Time (Days)

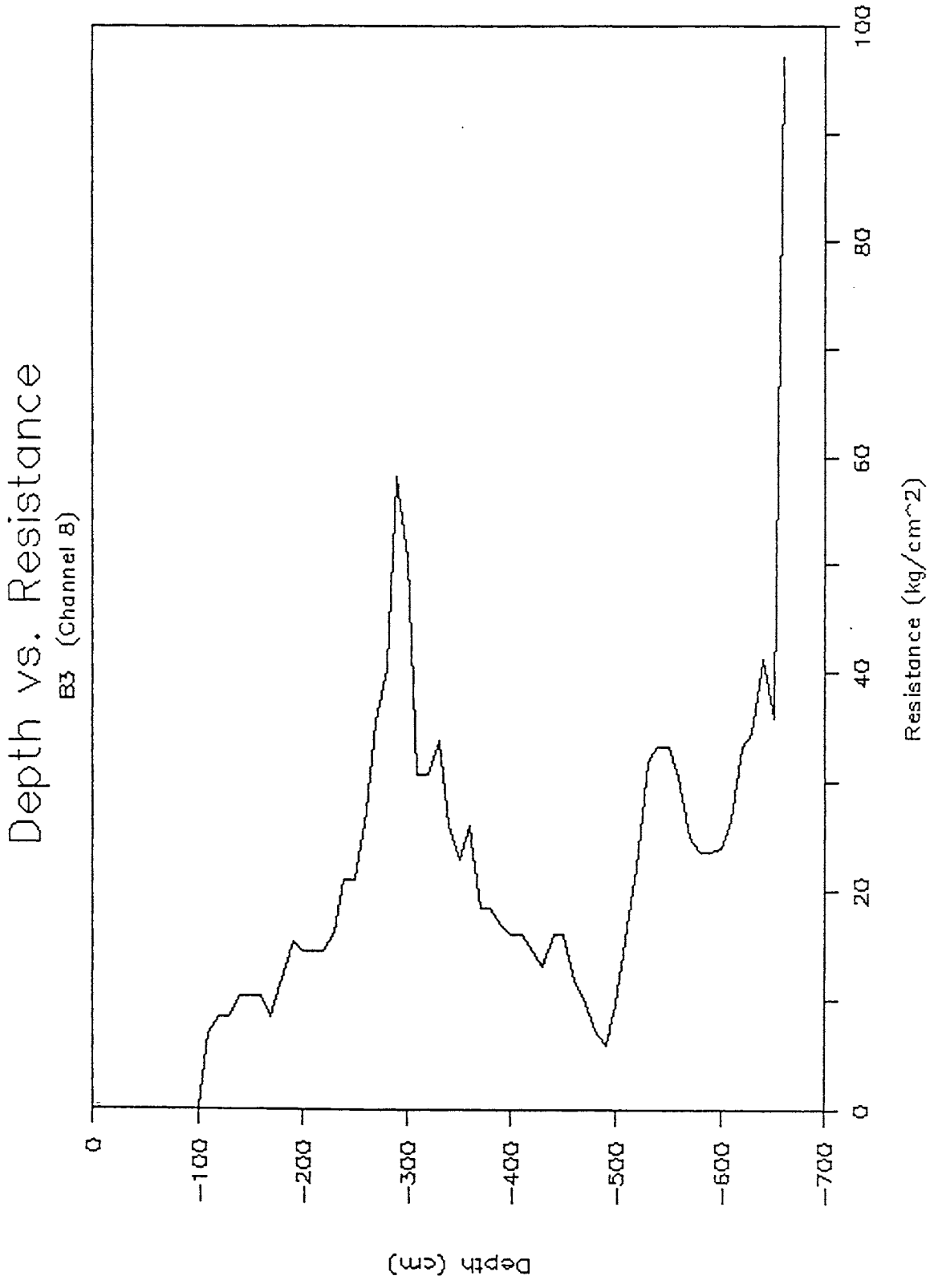
Depth vs. Resistance
B3 (Channel 8)
Depth (cm)
0
-100
-200
-300
-400
-500
-600
-700
Resistance (kg/cm^2)
0
20
40
60
80
100

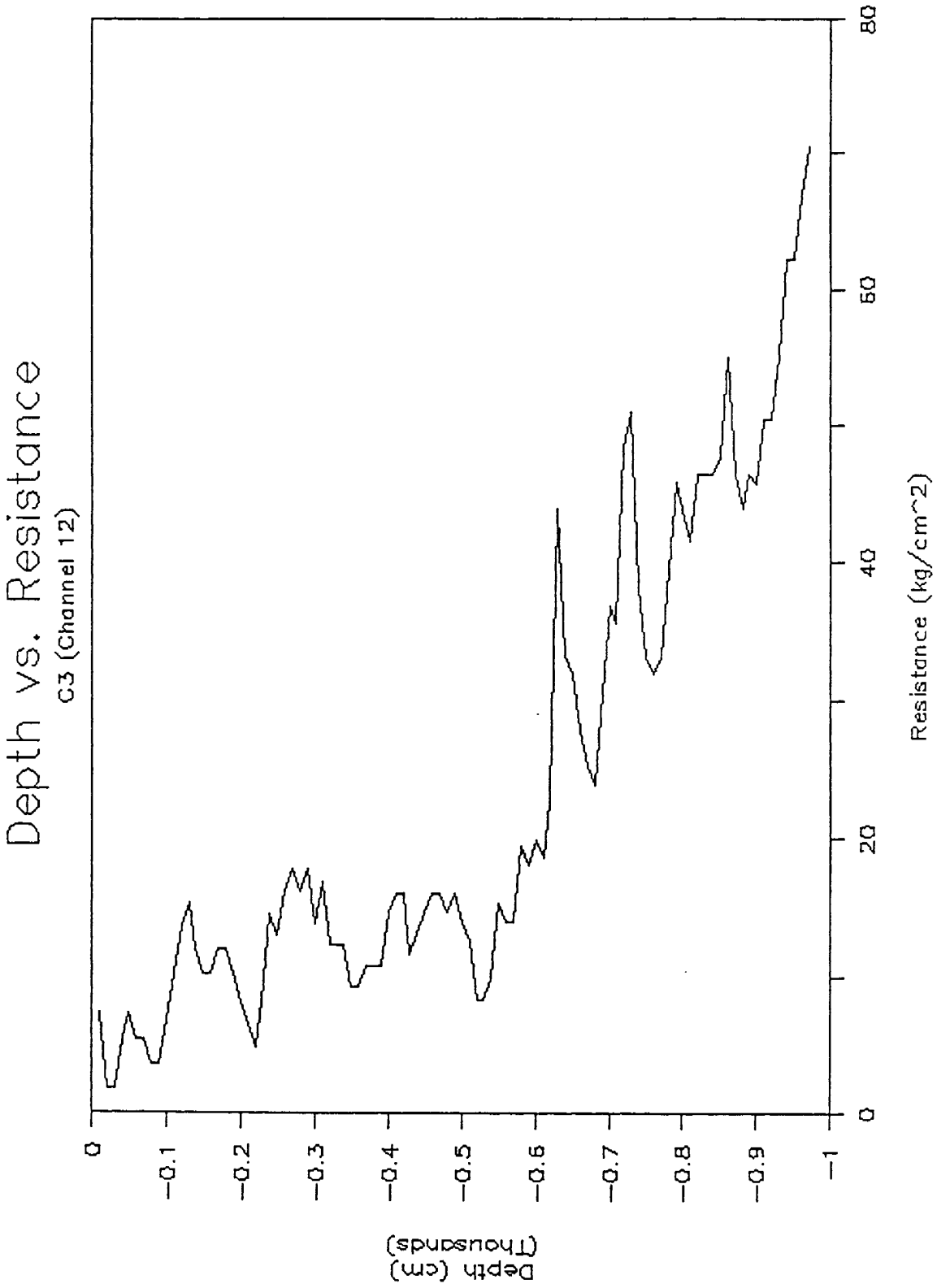
Depth vs. Resistance
C3 (Channel 12)
Depth (cm)
(Thousands)
0
-0.1
-0.2
-0.3
-0.4
-0.5
-0.6
-0.7
-0.8
-0.9
-1
Resistance (kg/cm^2)
0
20
40
60
80

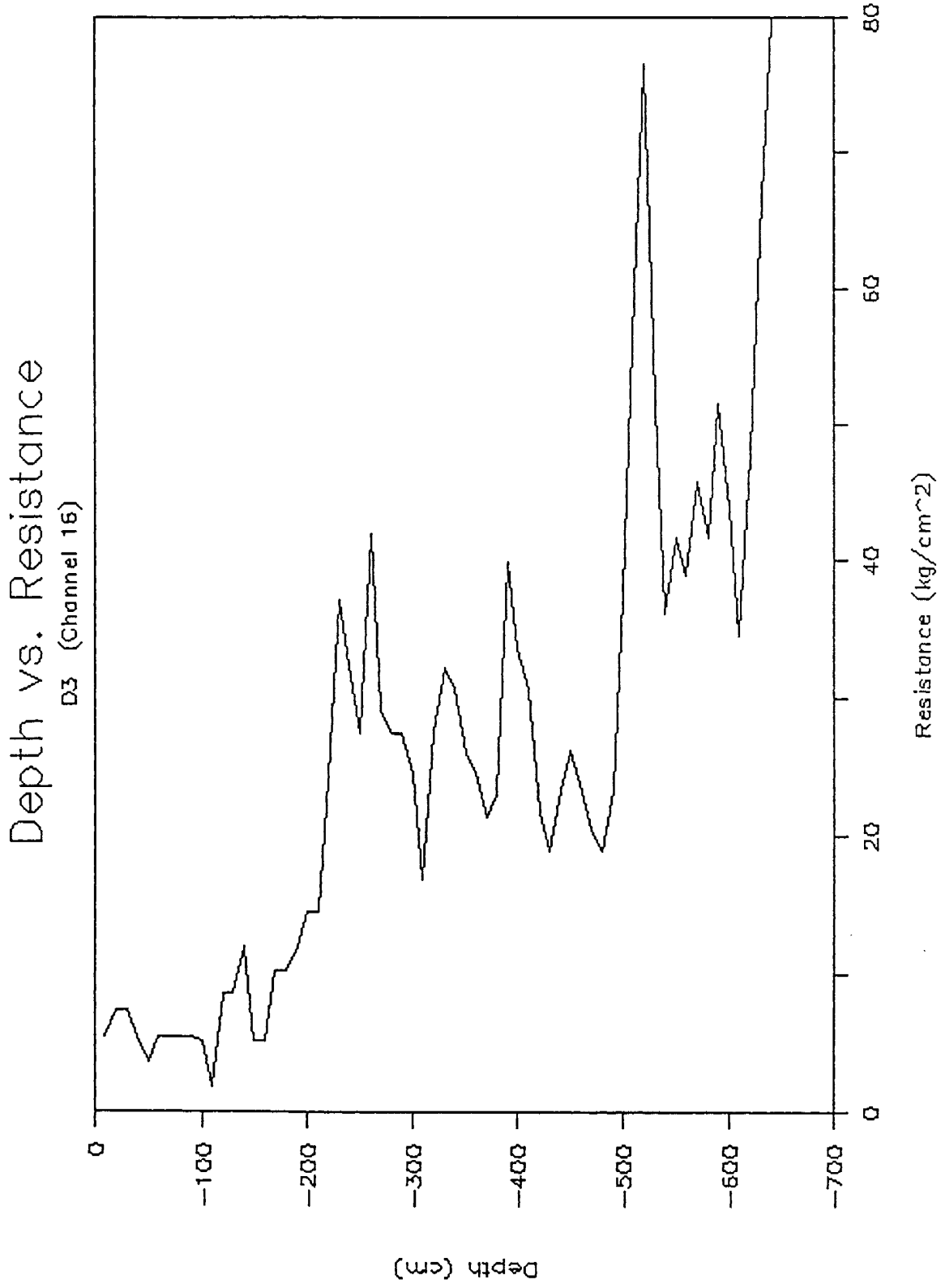
Depth vs. Resistance
D3 (Channel 16)
Depth (cm)
0
-100
-200
-300
-400
-500
-600
-700
Resistance (kg/cm^2)
0
20
40
60
80

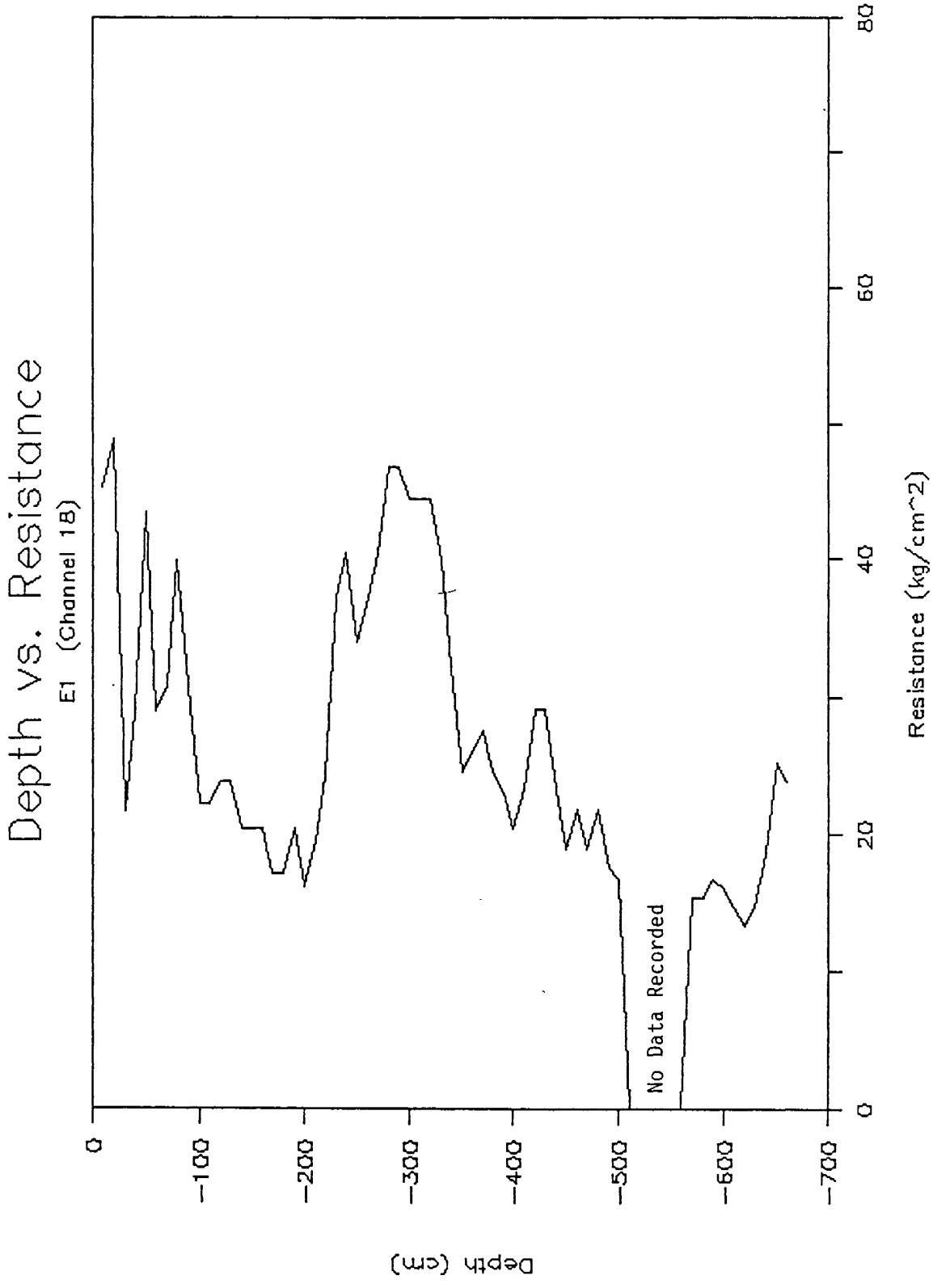
Depth vs. Resistance
E1 (Channel 18)
No Data Recorded
Depth (cm)
0
-100
-200
-300
-400
-500
-600
-700
Resistance (kg/cm^2)
0
20
40
60
80

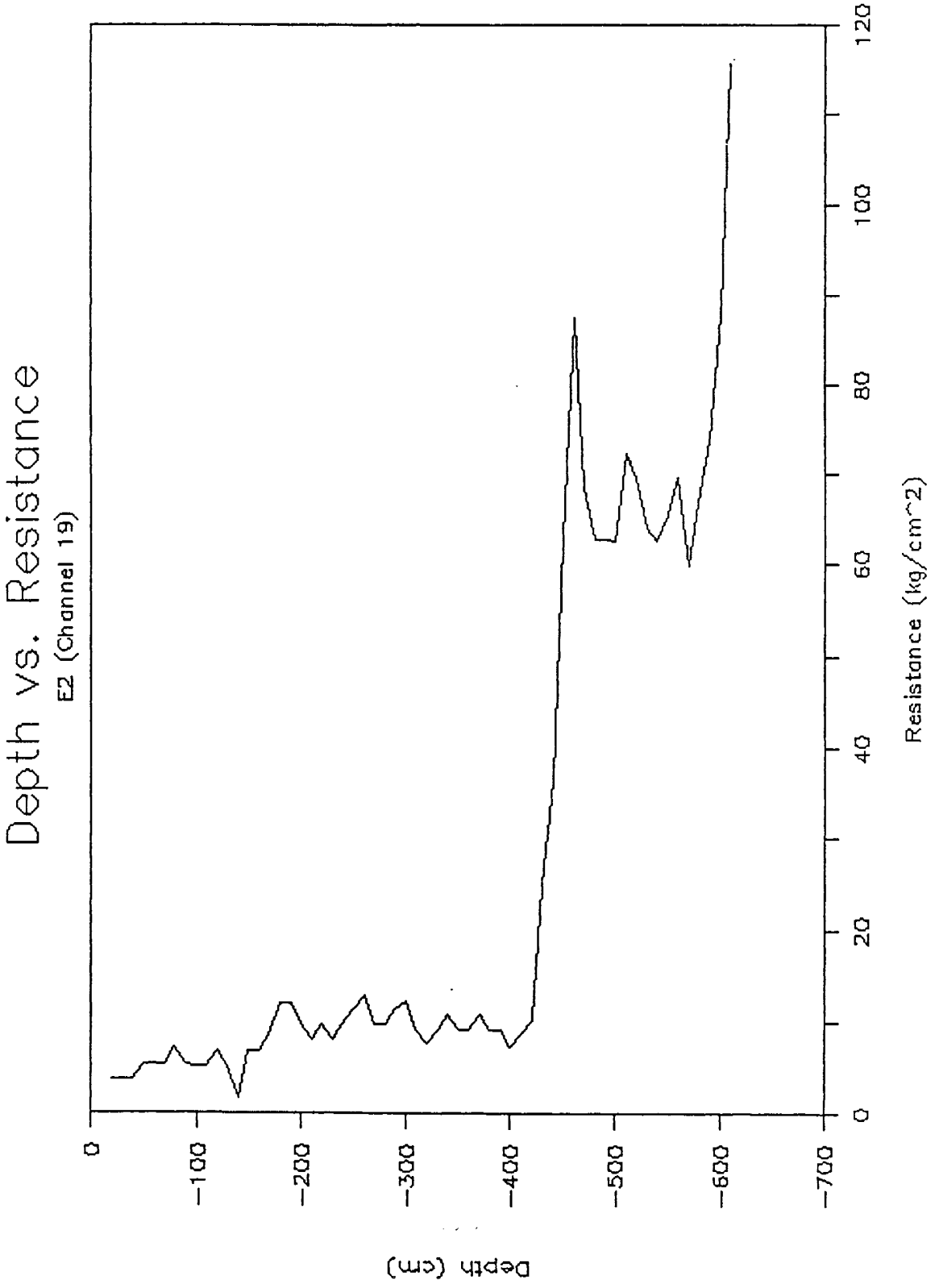
Depth vs. Resistance
E2 (Channel 19)
Depth (cm)
0
-100
-200
-300
-400
-500
-600
-700
Resistance (kg/cm^2)
0
20
40
60
80
100
120

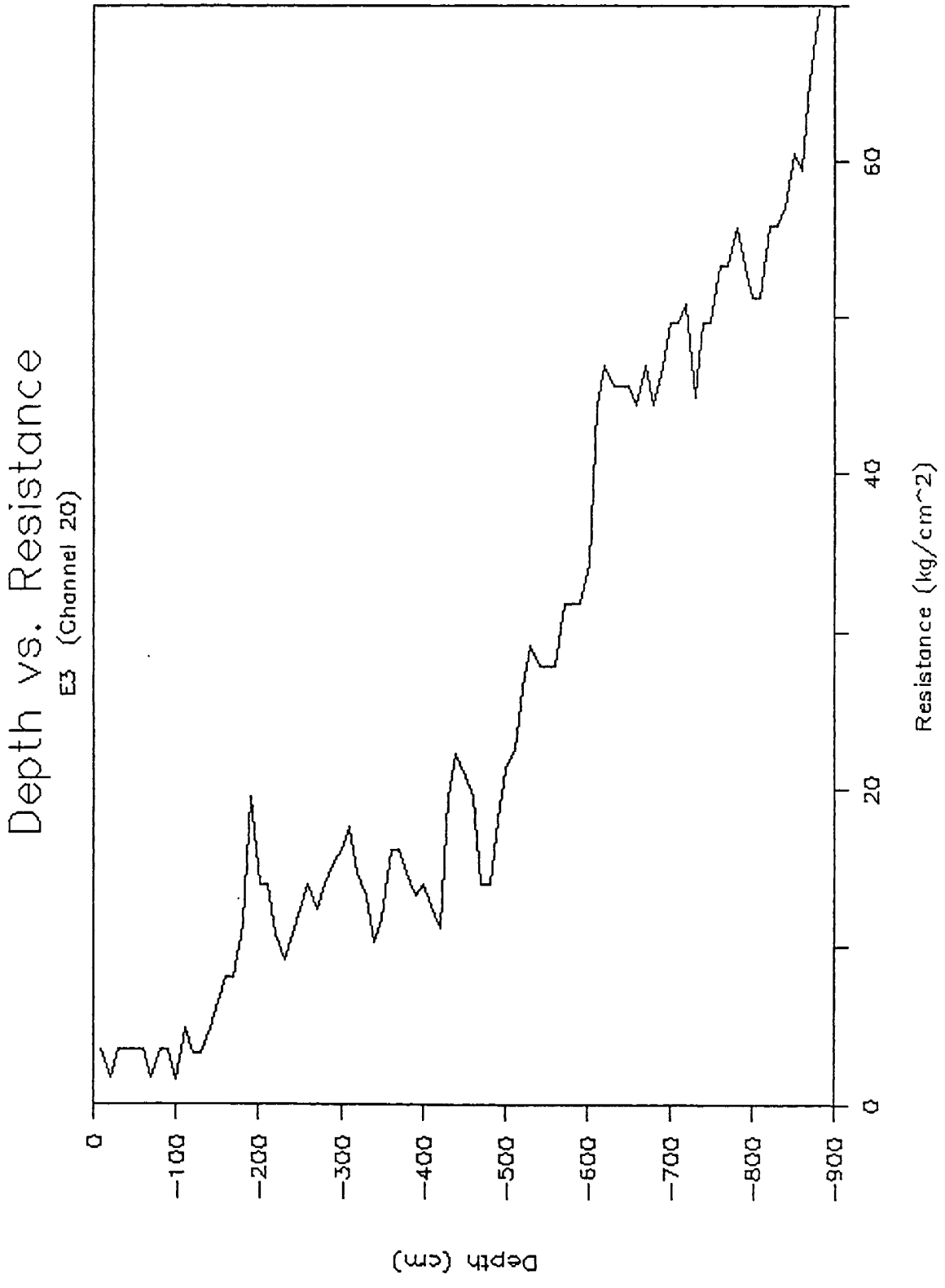
Depth vs. Resistance
E3 (Channel 20)
Depth (cm)
0
-100
-200
-300
-400
-500
-600
-700
-800
-900
Resistance (kg/cm^2)
0
20
40
60

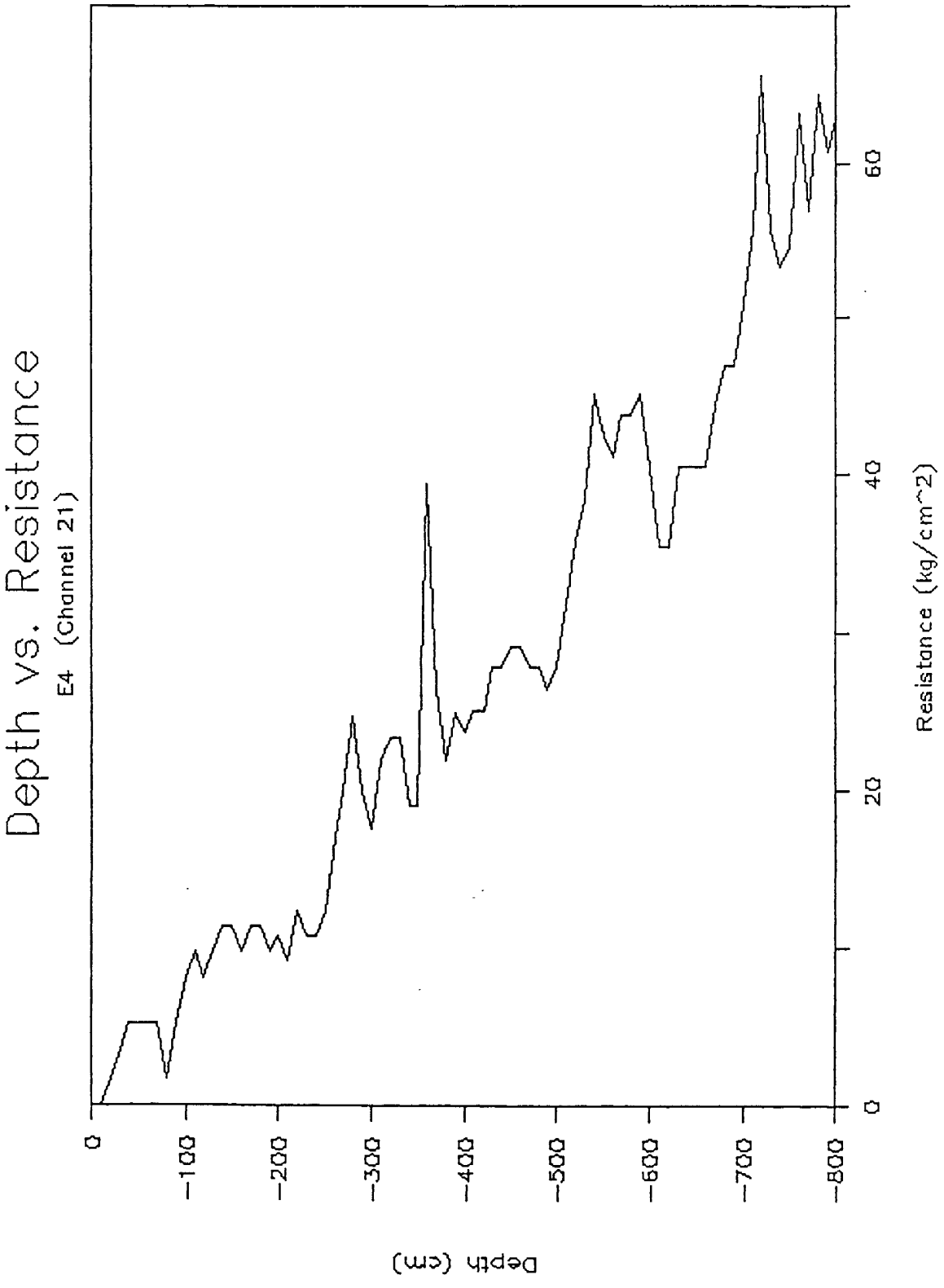
Depth vs. Resistance
E4 (Channel 21)
Depth (cm)
0
-100
-200
-300
-400
-500
-600
-700
-800
Resistance (kg/cm^2)
0
20
40
60

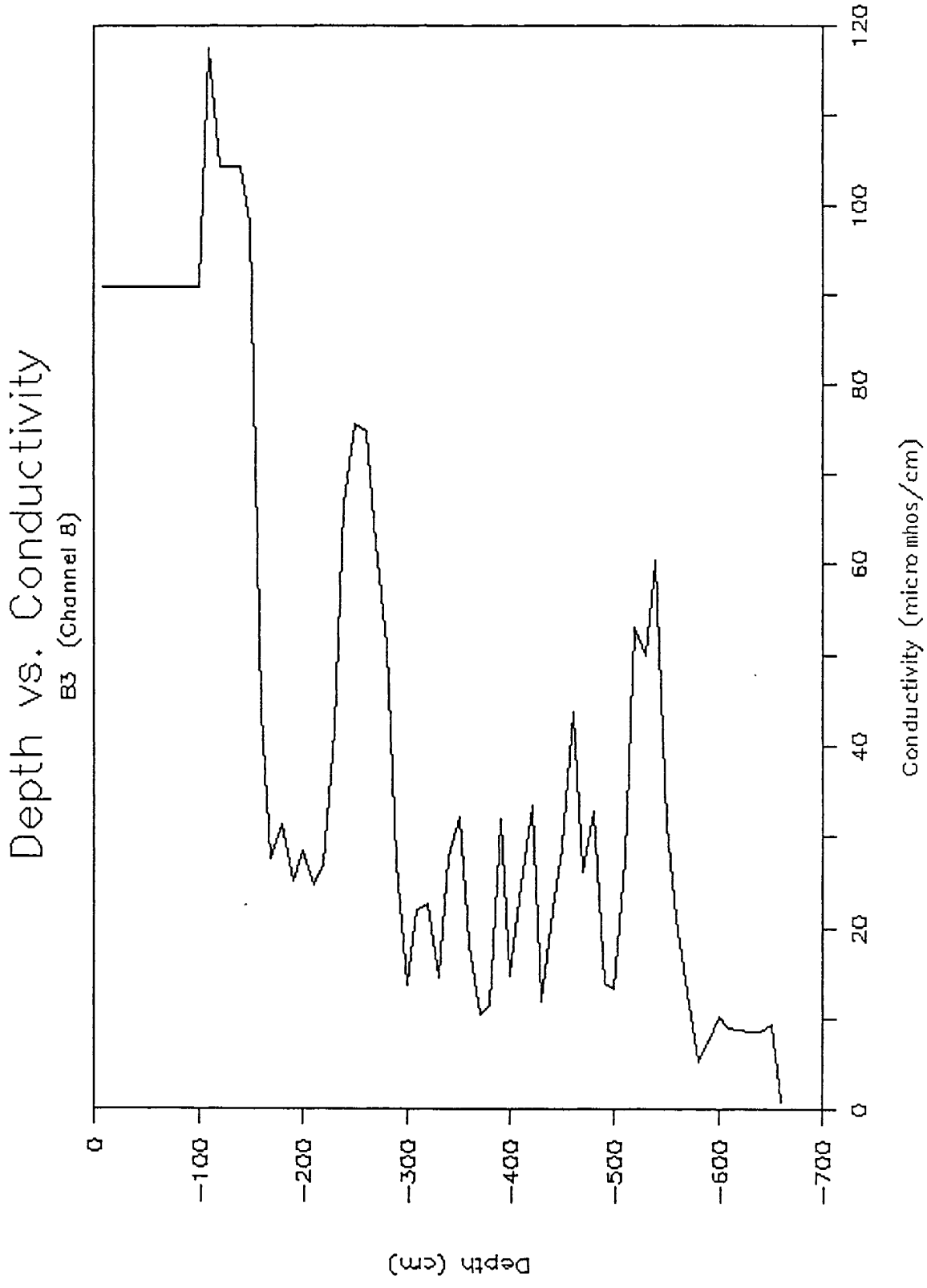
Depth vs. Conductivity
B3 (Channel B)
0
-100
-200
-300
-400
-500
-600
-700
Depth (cm)
0
20
40
60
80
100
120
Conductivity (micro mhos/cm)

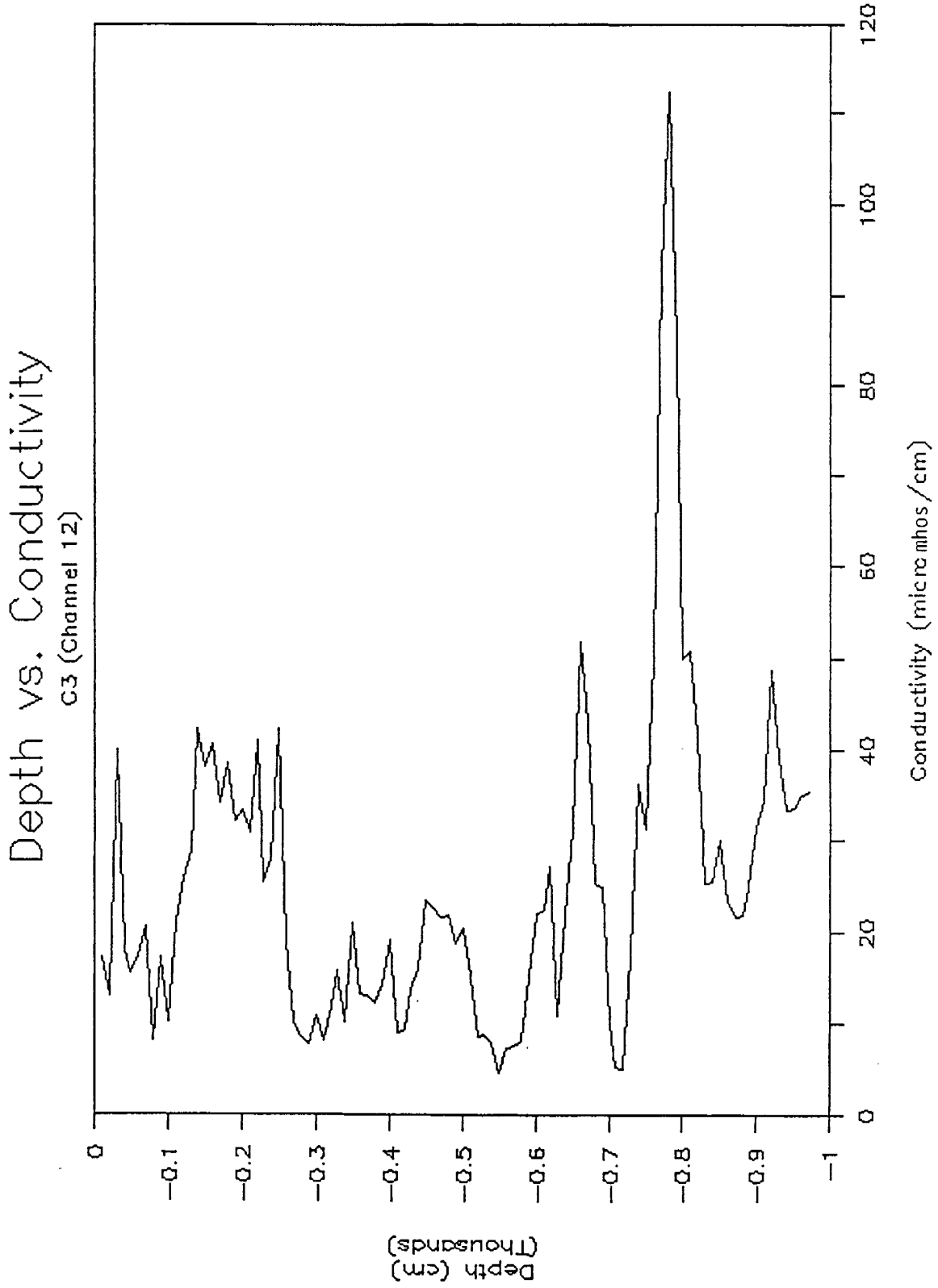
Depth vs. Conductivity
C3 (Channel 12)
Depth (cm)
(Thousands)
0
-0.1
-0.2
-0.3
-0.4
-0.5
-0.6
-0.7
-0.8
-0.9
-1
Conductivity (micromhos/cm)
0
20
40
60
80
100
120

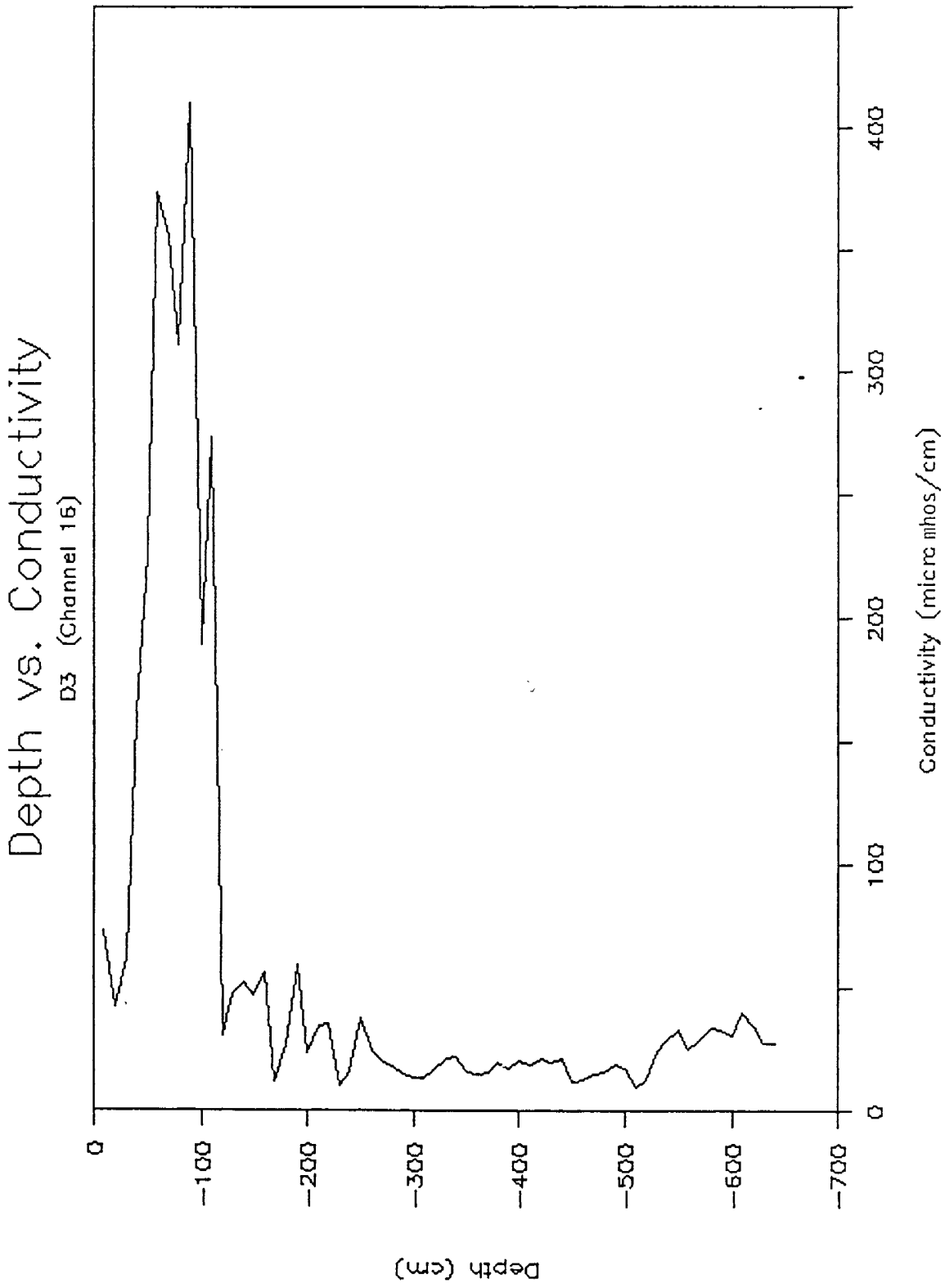
Depth vs. Conductivity
D3 (Channel 16)
Depth (cm)
0
-100
-200
-300
-400
-500
-600
-700
Conductivity (micro mhos/cm)
0
100
200
300
400

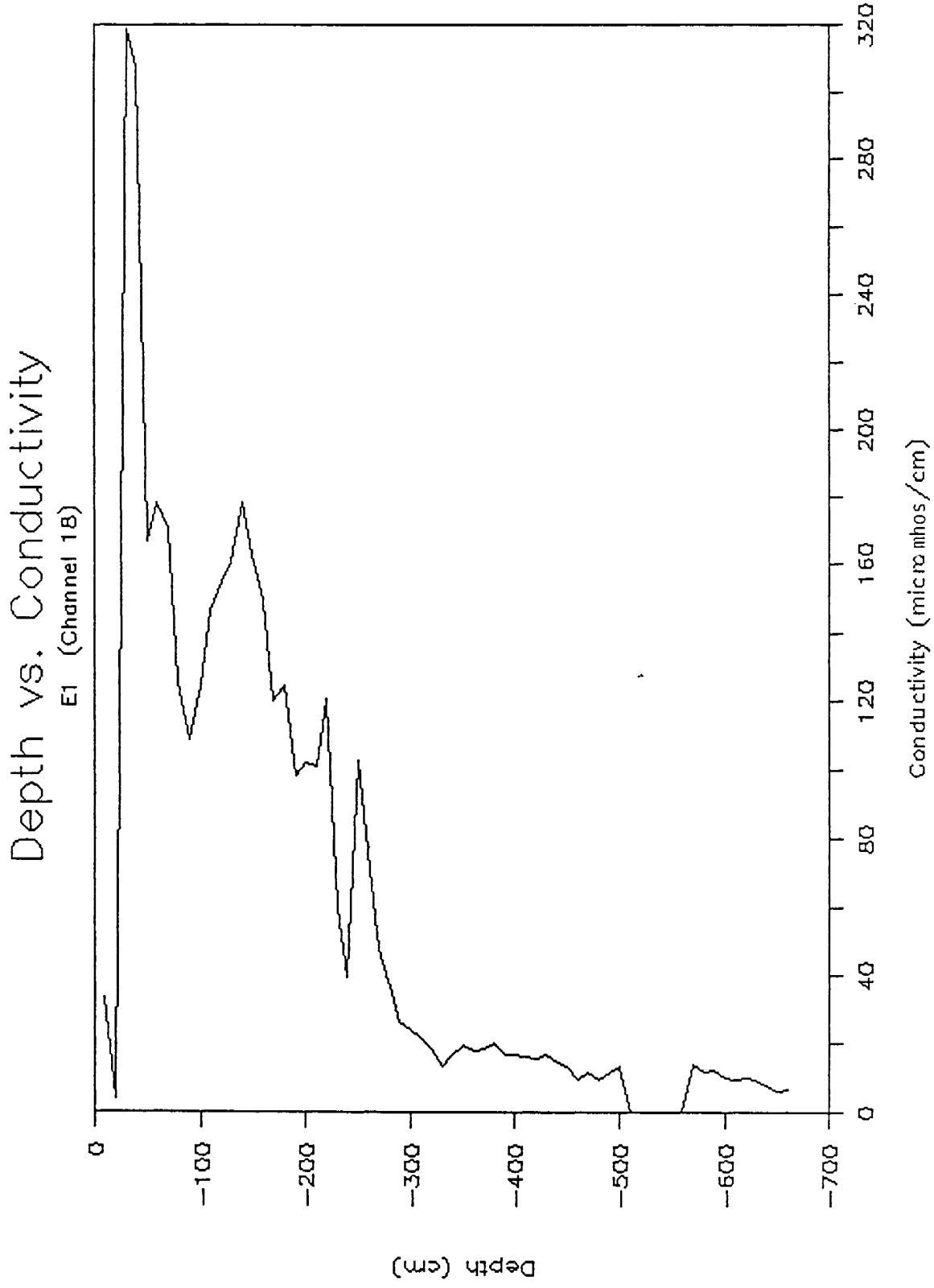
Depth vs. Conductivity
E1 (Channel 18)
Depth (cm)
0
-100
-200
-300
-400
-500
-600
-700
Conductivity (micromhos/cm)
0
40
80
120
160
200
240
280
320

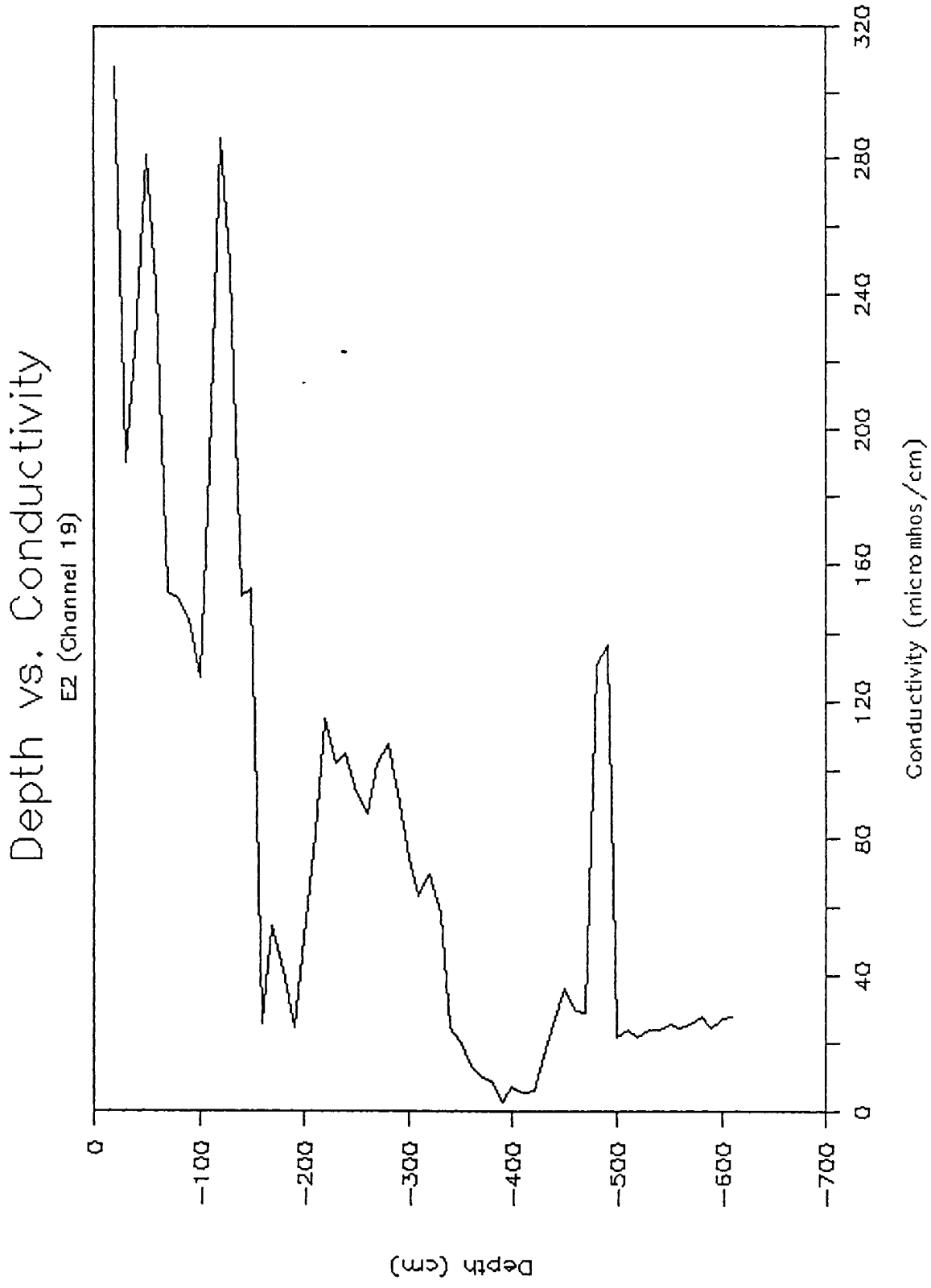
Depth vs. Conductivity
E2 (Channel 19)
Depth (cm)
0
-100
-200
-300
-400
-500
-600
-700
Conductivity (micromhos/cm)
0
40
80
120
160
200
240
280
320

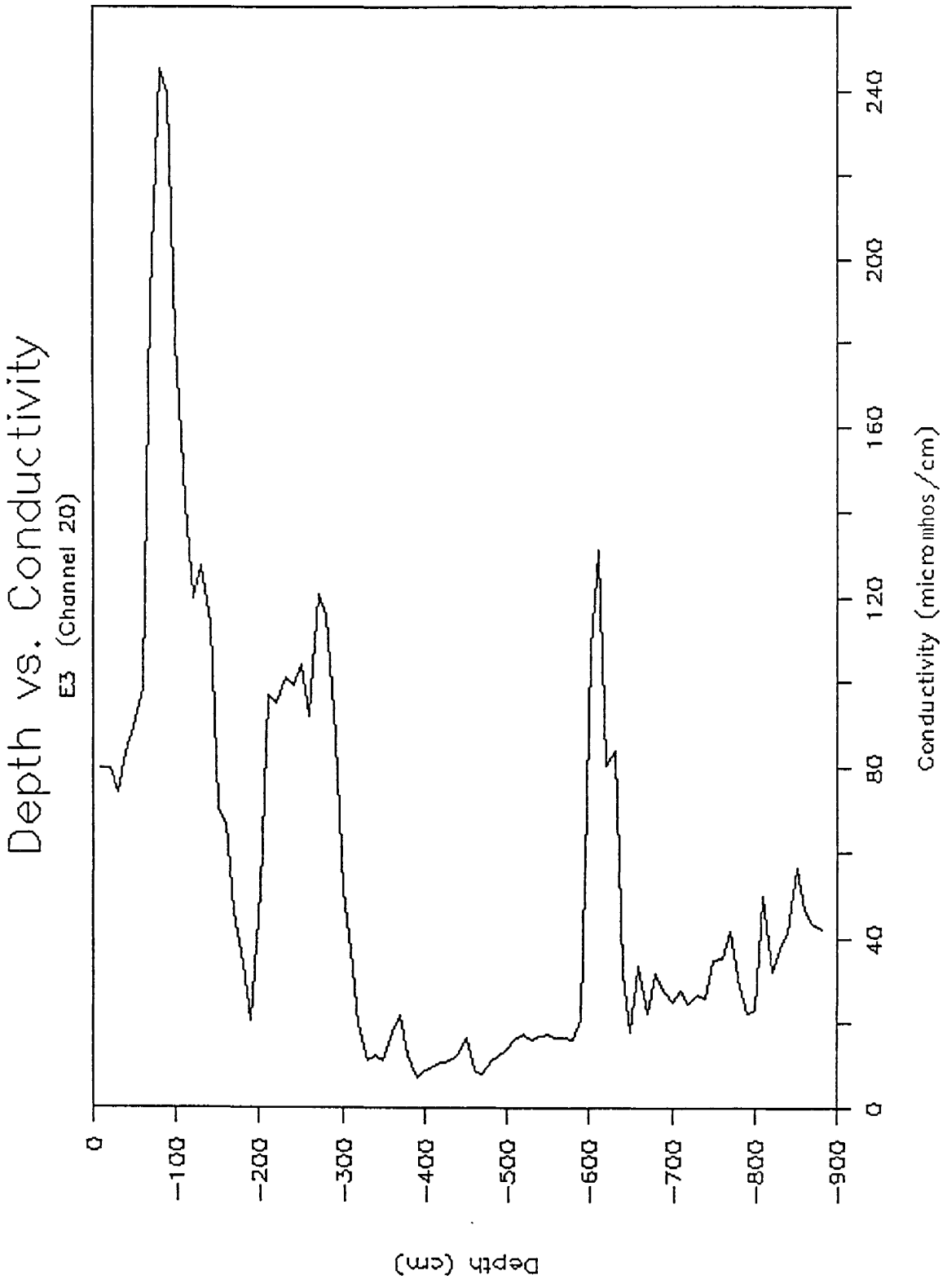
Depth vs. Conductivity
E3 (Channel 20)
Depth (cm)
0
-100
-200
-300
-400
-500
-600
-700
-800
-900
Conductivity (micromhos/cm)
0
40
80
120
160
200
240

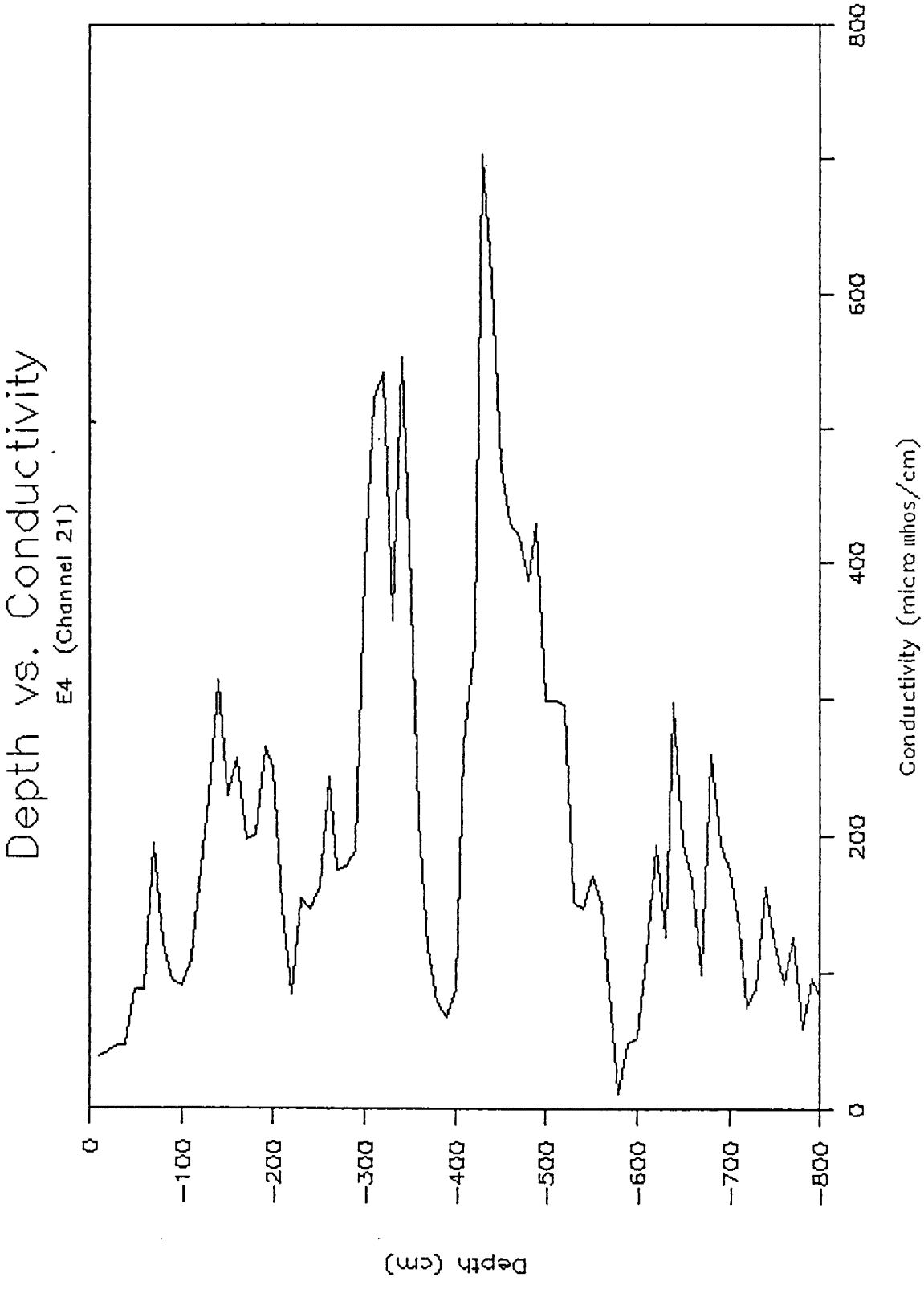
Depth vs. Conductivity
E4 (Channel 21)
Depth (cm)
0
-100
-200
-300
-400
-500
-600
-700
-800
Conductivity (micro mhos/cm)
0
200
400
600
800

2026